

An AREVA and Siemens company

BAW-10247NPA
Revision 0

**Realistic Thermal-Mechanical Fuel Rod
Methodology for Boiling Water Reactors**

April 2008



AREVA NP Inc.

BAW-10247NPA
Revision 0

**Realistic Thermal-Mechanical Fuel Rod
Methodology for Boiling Water Reactors**

April 2008

AREVA NP Inc.

BAW-10247NPA
Revision 0

Copyright © 2008

AREVA NP Inc.
All Rights Reserved



UNITED STATES
NUCLEAR REGULATORY COMMISSION
WASHINGTON, D.C. 20555-0001

February 12, 2008

Mr. Ronnie L. Gardner, Manager
Site Operations and Regulatory Affairs
AREVA NP Inc.
3315 Old Forest Road
Lynchburg, VA 24501

SUBJECT: FINAL SAFETY EVALUATION FOR AREVA NP, INC. (AREVA) TOPICAL
REPORT (TR) BAW-10247(P), REVISION 0, "REALISTIC THERMAL-
MECHANICAL FUEL ROD METHODOLOGY FOR BOILING WATER
REACTORS" (TAC NO. MC4261)

Dear Mr. Gardner:

By letter dated August 19, 2004 (Agencywide Documents Access and Management System (ADAMS) Accession No. ML042810356), Framatome ANP, now known as AREVA, submitted TR BAW-10247(P), Revision 0, "Realistic Thermal-Mechanical Fuel Rod Methodology for Boiling Water Reactors," to the U.S. Nuclear Regulatory Commission (NRC) staff for review. By letter dated January 18, 2008, an NRC draft safety evaluation (SE) regarding our approval of TR BAW-10247(P), Revision 0, was provided for your review and comments. By letter dated January 30, 2008, AREVA commented on the draft SE. The NRC staff's disposition of AREVA comments on the draft SE are discussed in the attachment to the final SE enclosed with this letter.

The NRC staff has found that TR BAW-10247(P), Revision 0, is acceptable for referencing in licensing applications for boiling water reactors to the extent specified and under the limitations delineated in the TR and in the enclosed final SE. The final SE defines the basis for acceptance of the TR.

Our acceptance applies only to material provided in the subject TR. We do not intend to repeat our review of the acceptable material described in the TR. When the TR appears as a reference in license applications, our review will ensure that the material presented applies to the specific plant involved. License amendment requests that deviate from this TR will be subject to a plant-specific review in accordance with applicable review standards.

In accordance with the guidance provided on the NRC website, we request that AREVA publish accepted proprietary and non-proprietary versions of this TR within three months of receipt of this letter. The accepted versions shall incorporate this letter and the enclosed final SE after the title page. Also, they must contain historical review information, including NRC requests for additional information and your responses. The accepted versions shall include a "-A" (designating accepted) following the TR identification symbol.

R. Gardner

-2-

If future changes to the NRC's regulatory requirements affect the acceptability of this TR, AREVA and/or licensees referencing it will be expected to revise the TR appropriately, or justify its continued applicability for subsequent referencing.

Sincerely,



Ho K. Nieh, Deputy Director
Division of Policy and Rulemaking
Office of Nuclear Reactor Regulation

Project No. 728

Enclosures: 1. Non-Proprietary Final SE
2. Proprietary Final SE



UNITED STATES
NUCLEAR REGULATORY COMMISSION
WASHINGTON, D.C. 20555-0001

SAFETY EVALUATION BY THE OFFICE OF NUCLEAR REACTOR REGULATION

TOPICAL REPORT BAW-10247(P), REVISION 0

"REALISTIC THERMAL-MECHANICAL FUEL ROD METHODOLOGY
FOR BOILING WATER REACTORS"

AREVA NP, INC. (AREVA)

PROJECT NO. 728

1.0 INTRODUCTION AND BACKGROUND

By letter dated August 19, 2004, Framatome ANP, now known as AREVA, submitted to the U.S. Nuclear Regulatory Commission (NRC) Topical Report (TR) BAW-10247(P), Revision 0 (Reference 1), entitled "Realistic Thermal-Mechanical Fuel Rod Methodology for Boiling Water Reactors," for review and approval. The TR describes a fuel performance code, RODEX4, for best-estimate thermal-mechanical evaluation for fuel rods of boiling water reactors (BWRs).

Two additional reports, EMF-2994(P), Revision 0 (Reference 2) and EMF-3014, Revision 0 (Reference 3), were provided to support the review. The NRC staff notes the additional reports were not submitted for review and approval, and as such, the approval of BAW-10247(P), Revision 0, will not automatically extend to cover these two supporting reports. The report EMF-2994(P), Revision 0, entitled "RODEX4: Thermal-Mechanical Fuel Rod Performance Code Theory Manual," describes the theory basis, structure, thermal and mechanical models, and material properties in the code. The report EMF-3014, Revision 0, entitled "RODEX4: Thermal-Mechanical Fuel Rod Performance Code Verification and Validation Report," describes the analytical results to validate the code. Due to the empirical nature of the RODEX4 calibration and validation process, the specific values of the equation constants and tuning parameters derived in TR BAW-10247(P), Revision 0 (as updated by RAI responses) become inherently part of the approved models. Thus, these values may not be updated without necessitating further NRC review.

Pacific Northwest National Laboratory (PNNL) acted as a consultant to the NRC staff in this review. As a result of the NRC staff and PNNL review of the TR, a request for additional information (RAI) dated November 25, 2005, was sent to AREVA. AREVA provided a response to these RAIs in References 4 and 5 dated July 7, 2006, and November 7, 2006, respectively. The NRC staff sent a second RAI dated January 3, 2007, and AREVA responded in References 6 and 7 dated December 11, 2006, and August 31, 2007, respectively.

To support licensees referencing TR BAW-10247(P), Revision 0, in license amendment requests, AREVA will use the RODEX4 code to determine fuel rod internal pressure, cladding strain, and fuel melting analyses. The NRC audit code, FRAPCON-3 (References 8 and 9), was used to support the review in evaluating models and calculation results from RODEX4.

ENCLOSURE 1

2.0 REGULATORY EVALUATION

The fuel system consists of arrays of fuel rods, including fuel pellets and tubular cladding, spacer grids, end plates, and reactivity control rods. The objectives of the fuel system safety review are to provide assurance that (1) the fuel system is not damaged as a result of normal operation and anticipated operational occurrences (AOOs), (2) fuel system damage is never so severe as to prevent control rod insertion when it is required, (3) the number of fuel rod failures is not underestimated for postulated accidents, and (4) coolability is always maintained. The NRC staff acceptance criteria are based on the NUREG-0800, Standard Review Plan (SRP), Section 4.2, "Fuel System Design." These criteria include three parts: (1) design bases that describe specified acceptable fuel design limits as depicted in General Design Criterion 10 to Appendix A of Title 10 of the *Code of Federal Regulations* (10 CFR) Part 50, (2) design evaluation that demonstrates that the design bases are met, and (3) testing, inspection, and surveillance plans that show that there are adequate monitoring and surveillance of irradiated fuel. The design bases include fuel system damage, fuel rod failure, and fuel coolability. Fuel performance codes provide analytical evaluation to verify design bases and criteria.

3.0 TECHNICAL EVALUATION

3.1 THERMAL MODELS

3.1.1 Fuel Thermal Conductivity

The RODEX4 thermal conductivity model is a function of temperature, burnup, gadolinia, and plutonium content similar to the thermal conductivity model in FRAPCON-3. The NRC audit code, FRAPCON-3, currently utilizes a urania (UO_2) fuel thermal conductivity model proposed by Nuclear Fuel Industries (NFI) of Japan that has been modified by PNNL to better fit the current data. The modified NFI model is based on recent high burnup and high temperature thermal conductivity data and provides a good comparison to both in-reactor fuel temperature and ex-reactor diffusivity data at high burnups (References 10 and 11). The RODEX4 model is based on the thermal conductivity data at intermediate to high temperatures of unirradiated UO_2 using measurements of thermal diffusivity and heat capacity by a specialized laser-flash method. Comparison of these two models for unirradiated UO_2 shows that the RODEX4 model predicts slightly higher thermal conductivity than the FRAPCON-3 model with increasing temperature. Based on the consistent results with FRAPCON-3, the NRC staff considers the RODEX4 model acceptable.

For urania-gadolinia ($\text{UO}_2\text{-Gd}_2\text{O}_3$) fuel, the RODEX4 thermal conductivity model contains a degradation function that is proportional to the weight fraction of Gd_2O_3 contained in burnable absorber rods. To assess the thermal conductivity penalty applied in RODEX4 for gadolinia additions, the RODEX4 model was compared to the similar correction for gadolinia addition in FRAPCON-3. At high temperature, the FRAPCON-3 thermal conductivity model underpredicts these data while the RODEX4 model provides a best-estimate prediction of these data. Based on the best-estimate predictions, the NRC staff finds that the RODEX4 gadolinia modification to fuel thermal conductivity is acceptable.

Based on the consistent results and predictions with the FRAPCON-3 models, the NRC staff concludes that the RODEX4 thermal conductivity models are acceptable for UO_2 and $\text{UO}_2\text{-Gd}_2\text{O}_3$ fuel pellets.

3.1.2 Cladding Thermal Conductivity

The cladding thermal conductivity in RODEX4 is the same as in both MATPRO (NUREG/CR-0497) and FRAPCON-3. MATPRO is an NRC-developed material handbook for fuel rod design from which many FRAPCON-3 models are based. Based on the same model, the NRC staff concludes that the cladding thermal conductivity model in RODEX4 is acceptable.

3.1.3 Gap Conductance

The pellet-cladding gap heat transfer model in RODEX4 includes three modes: (1) conduction through the interface gas, (2) conduction through points of contact when pellet-cladding interference is predicted, and (3) radiation heat transfer from the fuel surface to the cladding inner surface. The equations for these modes are standard.

The uncertainty in the gap heat transfer is dominated by the uncertainty of the effective gap size in RODEX4. The effective gap size is determined by the sum of mechanical gap, surface roughness, and extrapolation distance. FRAPCON-3 has similar terms with the exception that the latter is termed a temperature jump distance rather than an extrapolation distance.

Based on the similar features between the two codes, the NRC staff concludes that the gap conductance model in RODEX4 is acceptable.

3.1.4 Fuel Thermal Expansion

The fuel thermal expansion model in RODEX4 predicts identical results to the FRAPCON-3 model except in high temperature range. In high temperature range, the RODEX4 model predicts slightly higher expansion than the FRAPCON-3 model. The expansion of the pellet is found by calculating the expansion of each radial ring based on the temperature at that ring and adding up the expansion from each ring to find the expansion of the entire pellet.

Based on the similar features between the two codes, the NRC staff concludes that the RODEX4 fuel thermal expansion model is acceptable.

3.2 FISSION GAS RELEASE MODEL

The fission gas release (FGR) model in RODEX4 assumes a two-stage process of high temperature and low temperature diffusion. The model has certain empirical parameters which are adjusted to predict steady-state and power-ramped gas release data. Different empirical parameters are applied during rapid power changes in order to adequately fit fission gas release data from ramp tests. AREVA provided a large database of gas release measurements from fuel rods operating at steady-state and transient conditions.

Examination of the RODEX4 predictions suggest that the code may have underprediction at high release. AREVA provided predicted-minus-measured versus burnup plots along with mean and

standard deviations. AREVA also provided a histogram to demonstrate whether the data was skewed towards underprediction. AREVA stated that some of the FGR data were known to have high experimental uncertainties and possible biases such that these were eliminated in their optimized database. A small underpredictive bias is still observed in the optimized database. However, a closer examination demonstrates that these underpredictions are from power-ramped rods and not from rods with steady-state operation. AREVA stated that some of the FGR data also had high uncertainties but demonstrated that the upper 95/95 confidence predictions bounded all the power-ramped data. AREVA also provided predictions of a typical BWR 4 fuel rod design with a nominal grain size and typical power ramps. The FRAPCON-3 predictions were performed against a similar database. The results show that the RODEX4 predictions are consistent with the FRAPCON-3 results.

Due to limitations within the FGR model, the analytical fuel pellet grain size shall not exceed 20 microns 3-D when the as-manufactured fuel pellet grain size could exceed 20 microns 3-D.

Based on the audit comparison calculations done with FRAPCON-3, the NRC staff concludes that the fission gas release model in RODEX4 is acceptable for steady-state and transient analyses.

3.3 CLADDING CORROSION MODEL

Cladding waterside corrosion presents added resistance to heat transfer from the cladding to the coolant. There are nodular corrosion and diffusion-controlled uniform corrosion in the BWR environment. Nodular corrosion is athermal, and the diffusion-controlled corrosion is temperature-driven. RODEX4 does not have a nodular corrosion model. The diffusion-controlled corrosion in RODEX4 is a function of time (exposure), an enhancement factor depending on reactor water chemistry, and temperature at the metal-oxide interface.

The oxidation rate is exponentially dependent on temperature with high activation energy. This leads to a situation where the crud buildup on the cladding surface and the resulting increase in surface temperature will substantially increase the oxidation rate. Hence, oxide layer development and crud buildup are intimately connected. For the purpose of this evaluation, an abnormal crud/corrosion layer is defined by a formation that increases the calculated fuel average temperature by more than 25 °C beyond the design basis calculation. There is no crud deposition model in RODEX4. AREVA stated that crud was a plant-specific problem, and as such, was not included in the modeling. Due to the potential impact of crud formation on heat transfer, fuel temperature, and related calculations, RODEX4 calculations must account for a design basis crud thickness. The level of deposited crud on the fuel rod surface should be based upon an upper bound of expected crud and may be based on plant-specific history. Specific analyses would be required if an abnormal crud or corrosion layer (beyond the design basis) is observed at any given plant.

The RODEX4 corrosion model shows that there is considerable scatter in the model predictions and underpredictions against data. AREVA suggested that the underpredictions could be due to the fact that even though the rods were scraped to remove crud there could still have residual crud left on the rods. AREVA provided additional data and added a small multiplier to the best-estimate corrosion model to bound the corrosion data with greater than 95/95 confidence. The

NRC staff agrees with the approach. Comparisons between the codes and the results show that RODEX4 predicts about the same as FRAPCON-3.

Based on the good comparison and improvement in the model, the NRC staff concludes that the corrosion model is acceptable. However, the NRC staff notes the hydrogen pickup model within RODEX4 is not approved for use.

3.4 IRRADIATION ROD GROWTH MODEL

The fuel rod axial growth model is a function of cladding temperature and fast fluence. There are two rod growth correlations for cold-worked stress-relieved (CWSR) Zr-2 fuel rods of 9x9 and 10x10 arrays. The correlation coefficients for CWSR Zr-2 cladding are calibrated against growth data from full length rods with various burnups. The RODEX4 model predicts better results for the 9x9 than the 10x10 arrays.

The FRAPCON-3 model is based on the Electric Power Research Institute (EPRI) model (Reference 12) and is validated up to a local burnup of 65 GWd/MTU. Comparing between the two models, the results shows that the RODEX4 model is in reasonable agreement with the FRAPCON-3 model.

Based on the reasonable agreement comparison, the NRC staff concludes that the RODEX4 rod growth model for CWSR Zr-2 cladding is acceptable.

3.5 CLADDING CREEP MODEL

The cladding creep model has two components, thermal creep and irradiation creep. The thermal creep is a function of temperature and stress, and is responsible for the cladding stress and the fuel-cladding contact pressure and gap closure. The irradiation creep is responsible for the cladding creepdown mechanism.

The irradiation cladding creep model in RODEX4 is a function of fast neutron flux, stress, and time. AREVA provided in-reactor creepdown data to verify this model. The in-reactor creepdown data consists of measurements of cladding outer diameter at different axial locations from the 9x9 and 10x10 fuel arrays with CWSR Zr-2 cladding. AREVA utilized only the creepdown data from the first or second cycles if the cladding was found not to have contacted the fuel. There are also measurements from a very small number of fuel rods with recrystallized annealed (RXA) Zr-2 cladding.

Examination of the comparisons to the CWSR Zr-2 data for in-reactor 9x9 fuel shows a very large uncertainty in the predictions. A comparison to a second data set of CWSR Zr-2 cladding from in-reactor 9x9 fuel shows an even larger uncertainty. A third data set of CWSR Zr-2 data from 10x10 fuel shows that the code underpredicts the creep strains. The comparison of predictions to irradiated creep data suggests that the uncertainty of the irradiation creep model is significantly higher than the uncertainty assumed by AREVA. The creep model in RODEX4 for CWSR Zr-4 and Zr-2 cladding is compared to the creep model in FRAPCON-3 for the same cladding type. Initially the creep strain in RODEX4 is lower than FRAPCON-3 in the early life

because the RODEX4 creep model does not model primary creep (early-in-life creep). Once the creep rate reaches steady-state condition, the RODEX4 creep model predicts a higher creep rate than FRAPCON-3.

AREVA provided additional comparisons to in-reactor creep data from commercial rods that quantitatively demonstrated that the uncertainties bounded the in-reactor data at a 95/95 confidence level. AREVA increased uncertainties of creep model, solid swelling model, and measurements to provide a bounding prediction for creep data at a 95/95 confidence bounding level. AREVA also provided a comparison between liner and non-liner cladding. The results showed that both cladding types had similar trend and distribution for in-reactor creep data. In RODEX4, the liner cladding will be modeled as non-liner cladding because of the extra thin liner film. Since AREVA continues collecting both liner and non-liner cladding creep data to verify the performance, the NRC staff finds this approach acceptable.

Based on the code comparison, increased uncertainty, and cladding comparison, the NRC staff concludes that the creep correlation and the liner cladding design are acceptable for RODEX4.

3.6 MECHANICAL MODEL

The modeling of fuel rod mechanical behavior in RODEX4 assumes that the pellet is non-rigid such that the fuel and cladding are allowed to strain when hard contact between the fuel and cladding is achieved. The fuel strains are calculated from fission product (solid and gaseous) swelling, densification, thermal expansion, fuel cracking, and fuel creep models. When hard contact between the fuel and cladding is established, the two are locked together, i.e., there is no axial slippage.

The cladding mechanical model assumes a plane strain, i.e., cladding deformation in the radial and azimuthal directions are independent of the axial direction, i.e., shear stress and strain are assumed to be zero. The code utilizes anisotropic properties for the cladding. Based upon its review of the cladding models including creep, the NRC staff concludes that the cladding models are acceptable in the RODEX4 code.

Additionally, based on the data and code comparisons, the NRC staff concludes that the mechanical model is acceptable for RODEX4.

3.7 LICENSING APPLICATIONS

3.7.1 Fuel Melting

RODEX4 assumes the melting temperature to be constant with burnups, while FRAPCON-3 has a burnup dependence for UO_2 fuel. The comparison between the two codes shows that the RODEX4 predictions are more conservative than the FRAPCON-3 predictions for the fuel melting analysis for UO_2 fuel. For $\text{UO}_2\text{-Gd}_2\text{O}_3$ fuel, the RODEX4 code shows a larger decrease in melting temperature with increasing Gd_2O_3 concentration than the FRAPCON-3 code. Thus, the RODEX4 code is more conservative than the FRAPCON-3 code.

The NRC staff notes that RODEX4 shall not be used to model fuel above incipient fuel melting temperatures. Based on the conservative results, the NRC staff concludes that the fuel melting analysis is acceptable for UO_2 and $UO_2-Gd_2O_3$ fuel for RODEX4.

3.7.2 Fuel Rod Internal Pressure

Fuel rods usually have upper and lower plenum regions. AREVA provided analyses including fuel rods with and without lower plenum. The results showed that both fuel rod types had similar results for rod pressure calculations. AREVA indicated that RODEX4 will model the lower plenum as part of the upper plenum during the calculation. The NRC staff agrees with this approach.

AREVA provided maximum rod internal pressure calculations for Atrium 10 rod design in different core conditions (e.g., BWR 4 and BWR 6 equilibrium cores and transition cores). The NRC staff made comparisons using the FRAPCON-3 code. The results showed that RODEX4 predicts greater rod pressures than FRAPCON-3. This is due to a greater FGR in RODEX4 than FRAPCON-3 on a best-estimate basis.

Based on the conservative predictions, the NRC staff concludes that the fuel rod internal pressure analysis is acceptable for RODEX4.

3.7.3 Clad Strain

AREVA provided a clad strain analysis for normal operation and incremental strain during a transient. The NRC staff made a comparison using the FRAPCON-3 code. The results showed that two codes provided similar results of permanent hoop strain during normal operation including an AOO.

To maximize the incremental strain, certain AOOs are applied to the power histories depending on the type of limiting transients. [

] The NRC staff made a comparison using the FRAPCON-3 code and found that the results were agreeable with the RODEX4 code.

Based on the consistent results, the NRC staff concludes that the RODEX4 prediction of cladding strain is acceptable.

3.7.4 Power Histories

To determine the steady-state power histories, AREVA [

]

To determine the AOO transient power histories, AREVA selected a set of power histories that contains AOO transients from [

]

calculated batch of power histories containing AOO transients. Then, AREVA applied similar uncertainties randomly the same way as in the steady-state case to determine the transient power histories. The NRC staff reviewed the power histories and determined them to be conservative.

Based on the adequate conservatism, the NRC staff concludes that the RODEX4 application of power histories for licensing analyses is acceptable.

3.7.5 Statistical Approach

The RODEX4 statistical approach is based on randomly selected uncertainties of fuel rod fabrication, operation (rod powers), and models to produce a distribution from which an estimate can be made [

]

In order to demonstrate that the new statistical approach [

]

Based on the rod pressure analysis, the NRC staff concludes that the RODEX4 statistical approach of [] is acceptable.

4.0 LIMITATIONS AND CONDITIONS

Compliance with the following conditions and limitations must be ensured when referencing TR BAW-10247(P), Revision 0:

1. Due to limitations within the FGR model, the analytical fuel pellet grain size shall not exceed 20 microns 3-D when the as-manufactured fuel pellet grain size could exceed 20 microns 3-D. (Section 3.2)

2. RODEX4 shall not be used to model fuel above incipient fuel melting temperatures. (Section 3.7.1)
3. The hydrogen pickup model within RODEX4 is not approved for use. (Section 3.3)
4. Due to the empirical nature of the RODEX4 calibration and validation process, the specific values of the equation constants and tuning parameters derived in TR BAW-10247(P), Revision 0 (as updated by RAI responses) become inherently part of the approved models. Thus, these values may not be updated without necessitating further NRC review. (Section 1.0)
5. RODEX4 has no crud deposition model. Due to the potential impact of crud formation on heat transfer, fuel temperature, and related calculations, RODEX4 calculations must account for a design basis crud thickness. The level of deposited crud on the fuel rod surface should be based upon an upper bound of expected crud and may be based on plant-specific history. Specific analyses would be required if an abnormal crud or corrosion layer (beyond the design basis) is observed at any given plant. For the purpose of this evaluation, an abnormal crud/corrosion layer is defined by a formation that increases the calculated fuel average temperature by more than 25°C beyond the design basis calculation. (Section 3.3)

5.0 CONCLUSION

As specified in TR BAW-10247(P), Revision 0, RODEX4 is approved for modeling BWR fuel rods with the following conditions:

- a. Peak rod average burnup limit of 62 GWd/MTU.
- b. Solid UO₂ fuel pellet with a maximum gadolinia content of 10.0 weight percent.
- c. CWSR Zr-2 fuel clad material.

The NRC staff has reviewed the AREVA submittal of the RODEX4 fuel performance code as described in TR BAW-10247(P), Revision 0. Based on the NRC staff's evaluation, the NRC staff concludes that the TR is acceptable for referencing in licensing applications for BWRs to the extent specified and under the Limitations and Conditions delineated in Section 4.0 of this Safety Evaluation.

6.0 REFERENCES

1. J. F. Mallay, AREVA letter to Document Control Desk, NRC, "Request for Review and Approval of BAW-10247(P), 'Realistic Thermal-Mechanical Fuel Rod Methodology for Boiling Water Reactors,'" August 19, 2004, ADAMS Accession No. ML042810356.
2. M. R. Billaux and V. I. Arimescu, RODEX4: Thermal-Mechanical Fuel Rod Performance Code Theory Manual, EMF-2994(P), Revision 0, August 2004.

3. M. R. Billaux and V. I. Arimescu, RODEX4: Thermal-Mechanical Fuel Rod Performance Code Verification and Validation Report, EMF-3014(P), Revision 0, August 2004.
4. R. L. Gardner, AREVA letter to Document Control Desk, NRC, "Additional Information for the Review of BAW-10247P, Revision 0, 'Realistic Thermal-Mechanical Fuel Rod Methodology for Boiling Water Reactors,'" July 7, 2006, ADAMS Accession No. ML061920542.
5. R. L. Gardner, AREVA letter to Document Control Desk, NRC, "Response to a Request for Additional Information Regarding BAW-10247(P), Revision 0, 'Realistic Thermal-Mechanical Fuel Rod Methodology for Boiling Water Reactors,'" November 7, 2006, ADAMS Accession No. ML063190127.
6. R. L. Gardner, AREVA letter to Document Control Desk, NRC, "Additional Information for the Review of BAW-10247P Revision 0, 'Realistic Thermal-Mechanical Fuel Rod Design Methodology for Boiling Water Reactors,'" December 11, 2006, ADAMS Accession No. ML063490135.
7. R. L. Gardner, AREVA letter to Document Control Desk, NRC, "Response to a Second Request for Additional Information for the Review of BAW-10247P, Revision 0, 'Realistic Thermal-Mechanical Fuel Rod Design Methodology for Boiling Water Reactors,'" August 31, 2007, ADAMS Accession No. ML072490415.
8. G. A. Berna, C. E. Beyer, K. L. Davis, and D. D. Lanning, FRAPCON-3: A Computer Code for the Calculation of Steady-State, Thermal-Mechanical Behavior of Oxide Fuel Rods for High Burnup, NUREG/CR-6534 (PNNL-11513) Vol. 2. NRC, 1997.
9. D. D. Lanning, C. E. Beyer, and C. L. Painter, FRAPCON-3: Modifications to Fuel Rod Material Properties and Performance Models for High-Burnup Applications. NUREG/CR-6534 (PNNL-11513) Vol. 1. NRC, 1997.
10. D. D. Lanning, and C. E. Beyer, "Assessment of Recent Data and Correlations for Fuel Pellet Thermal Conductivity," Presented at Enlarged Halden Program Meeting, March 11-16, 2001, HPR-356, 2001.
11. D. D. Lanning, and C. E. Beyer, "Revised UO₂ Thermal Conductivity for NRC Fuel Performance Codes," Transactions of the American Nuclear Society Annual Meeting, 2002.
12. Franklin, D. G., "Zircaloy-4 Cladding Deformation During Power Reactor Irradiation," Zirconium in the Nuclear Industry, ASTM STP 754, pp. 235-267, 1982.

Attachment: Resolution of Comments

Principal Contributor: Shih-Liang Wu

Date: February 12, 2008

RESOLUTION OF COMMENTS ON DRAFT SAFETY EVALUATION FOR

AREVA NP, INC. (AREVA)

TOPICAL REPORT BAW-10247(P), REVISION 0

"REALISTIC THERMAL-MECHANICAL FUEL ROD METHODOLOGY

FOR BOILING WATER REACTORS"

PROJECT NO. 728

By letter dated August 19, 2004, AREVA submitted to the U.S. Nuclear Regulatory Commission (NRC) Topical Report (TR) BAW-10247(P), Revision 0, entitled "Realistic Thermal-Mechanical Fuel Rod Methodology for Boiling Water Reactors," for review and approval. This Attachment provides the NRC staff's review and disposition of the comments made by AREVA in its January 30, 2008, letter.

AREVA General Comment

On Page 7, Lines 9-10, Omit "AREVA indicated that RODEX4 will model the lower plenum as part of the upper plenum during the calculation." This sentence was added by the NRC staff as a result of an initial response, by AREVA, to a restriction which indicated AREVA modeled the creep in the upper plenum, but not the lower plenum. This was incorrect since creep is not modeled in either plenum, and a different criteria was used to remove the restriction on the lower plenum.

NRC Response

In an email dated, November 2, 2007 (ADAMS Accession No. ML080370383), AREVA proposed that for fuel designs with lower plenums, RODEX4 be required to model the lower plenum free volume in the upper plenum where both thermal and irradiation induced creep would be modeled using the upper plenum conditions. This email contradicts the AREVA statement that the lower plenum modeling was "incorrect." On February 6, 2008, the lower plenum modeling approach was confirmed to be correct via teleconference with Gayle Elliott, AREVA Product Licensing Manager. As such, the NRC staff did not modify the SE.

ATTACHMENT



FRAMATOME ANP

An AREVA and Siemens Company

FRAMATOME ANP, Inc.

August 19, 2004
NRC:04:047

Document Control Desk
U.S. Nuclear Regulatory Commission
Washington, D.C. 20555-0001

Request for Review and Approval of BAW-10247(P), "Realistic Thermal-Mechanical Fuel Rod Methodology for Boiling Water Reactors"

Framatome ANP requests the NRC's review and approval of the topical report BAW-10247(P), "Realistic Thermal-Mechanical Fuel Rod Methodology for boiling water reactors." One CD containing a proprietary version of the report and one CD containing a non-proprietary version are enclosed.

This report presents a methodology for the realistic evaluation of the thermal-mechanical performance of fuel rods for Boiling Water Reactors (BWRs), which complies with the requirements of Section 4.2 of NUREG-800.

The methodology consists of the best-estimate fuel performance code RODEX4 that models the thermal-mechanical behavior of the fuel rods, and an application methodology for determining the behavior of rods in a BWR core during normal operation and anticipated operational occurrences. The objective of the methodology is to quantify the fuel design margins relative to the generic design criteria.

Framatome ANP would appreciate the NRC approval of this topical report by December 31, 2005.

Framatome ANP considers some of the material contained in the enclosed documents to be proprietary. As required by 10 CFR 2.390(b), an affidavit is enclosed to support the withholding of the information from public disclosure.

Very truly yours,

James F. Mallay, Director
Regulatory Affairs

Enclosures

cc: M. C. Honcharik
Project 728

AFFIDAVIT

STATE OF VIRGINIA)
) ss.
CITY OF LYNCHBURG)

1. My name is James F. Mallay. I am Director, Regulatory Affairs, for Framatome ANP ("FANP"), and as such I am authorized to execute this Affidavit.

2. I am familiar with the criteria applied by FANP to determine whether certain FANP information is proprietary. I am familiar with the policies established by FANP to ensure the proper application of these criteria.

3. I am familiar with the FANP information contained in topical report BAW-10247(P), "Realistic Thermal-Mechanical Fuel Rod Methodology for Boiling Water Reactors" which is referred to herein as "Document." Information contained in this Document has been classified by FANP as proprietary in accordance with the policies established by FANP for the control and protection of proprietary and confidential information.

4. This Document contains information of a proprietary and confidential nature and is of the type customarily held in confidence by FANP and not made available to the public. Based on my experience, I am aware that other companies regard information of the kind contained in this Document as proprietary and confidential.

5. This Document has been made available to the U.S. Nuclear Regulatory Commission in confidence with the request that the information contained in this Document be withheld from public disclosure.

6. The following criteria are customarily applied by FANP to determine whether information should be classified as proprietary:

- (a) The information reveals details of FANP's research and development plans and programs or their results.
- (b) Use of the information by a competitor would permit the competitor to significantly reduce its expenditures, in time or resources, to design, produce, or market a similar product or service.
- (c) The information includes test data or analytical techniques concerning a process, methodology, or component, the application of which results in a competitive advantage for FANP.
- (d) The information reveals certain distinguishing aspects of a process, methodology, or component, the exclusive use of which provides a competitive advantage for FANP in product optimization or marketability.
- (e) The information is vital to a competitive advantage held by FANP, would be helpful to competitors to FANP, and would likely cause substantial harm to the competitive position of FANP.

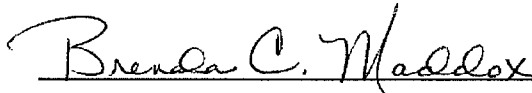
7. In accordance with FANP's policies governing the protection and control of information, proprietary information contained in this Document has been made available, on a limited basis, to others outside FANP only as required and under suitable agreement providing for nondisclosure and limited use of the information.

8. FANP policy requires that proprietary information be kept in a secured file or area and distributed on a need-to-know basis.

9. The foregoing statements are true and correct to the best of my knowledge, information, and belief.



SUBSCRIBED before me this 25th
day of August, 2004.



Brenda C. Maddox
NOTARY PUBLIC, STATE OF VIRGINIA
MY COMMISSION EXPIRES: 7/31/07



July 7, 2006
NRC:06:030

Document Control Desk
U.S. Nuclear Regulatory Commission
Washington, D.C. 20555-0001

Additional Information for the Review of BAW-10247P Revision 0, "Realistic Thermal-Mechanical Fuel Rod Methodology for Boiling Water Reactors."

Ref. 1: Letter, James F. Mallay (AREVA NP Inc.) to Document Control Desk (NRC), "Request for Review and Approval of BAW-10247(P) Revision 0, 'Realistic Thermal-Mechanical Fuel Rod Methodology for Boiling Water Reactors'," NRC:04:047, August 19, 2004.

AREVA NP requested the NRC's review and approval of the topical report BAW-10247(P) Revision 0, "Realistic Thermal-Mechanical Fuel Rod Methodology for Boiling Water Reactors" in Reference 1. A request for additional information was provided by the NRC in an email on November 25, 2005. The attachments to this letter (BAW-10247Q1(P) and BAW-10247Q1(NP)) provide responses to a portion of the questions. The responses to the remaining questions will be provided by October 20, 2006.

AREVA NP considers some of the material in the attachments to this letter to be proprietary. The affidavit provided with the original submittal of this topical report satisfies the requirements of 10 CFR 2.390(b) to support the withholding of the proprietary material from public disclosure.

Sincerely,

A handwritten signature in cursive script that reads "Ronnie L. Gardner".

Ronnie L. Gardner, Manager
Site Operations and Regulatory Affairs
AREVA NP

Enclosures

cc: G. S. Shukla
Project 728

AREVA NP INC.
An AREVA and Siemens company

3315 Old Forest Road, P.O. Box 10935 Lynchburg, VA 24506-0935
Tel.: 434 832 3000 - Fax: 434 832 3840 - www.aveva.com

**Response to Request for
Additional Information – BAW-10247(P)**

Comment

This submittal represents a significant departure from past thermal-mechanical analyses of fuel performance because simulated Monte Carlo type of random sampling is performed to determine a 99.9%/95% bounding analysis for normal operation and a 95%/95% bounding analysis for anticipated operational occurrences (AOO's). This new approach requires information about the sensitivity of this analysis approach to any biases (or assumed lack of) and uncertainties need to be explored in detail. Further information is also needed on whether the assumed uncertainties are consistent with the fuel performance data from out-of-reactor and in-reactor tests (from both test and commercial reactors).

The following includes two general comments on the identified submittals followed by specific requests for additional information (RAI's) that are separated into the following categories:

- I. General code modeling (RAI's #1-2)*
- II. Specific parameter modeling (RAI's #3-20)*
- III. Code applications for evaluating fuel design criteria per Section 4.2 of the USNRC Standard Review Plan (RAI's #21-32).*

The RAI's related to specific parameter modeling are further separated into understanding the model and verification of model to data.

General Comments

- A. The code does not appear to have separate calibration and verification databases as generally done for code verification (EMF-3014(P)). Also, calibration/verification data appears to be lacking for some licensing predictions. As a result several of the RAI's below will request code comparisons to additional data to verify that the code adequately predicts fuel performance.*
- B. There are three different documents in this submittal with some inconsistencies between the documents making it difficult to understand which document is correct. As a result several questions are related to understanding how the code and models work.*

I. General Code Modeling**Question 1:**

The time-stepping iteration scheme provided in Figures 4.4 and 4.5 is not clear (Section 4.4, EMF-2994(P)), in particular, how the mid-increment calculations are used with the final end-of step calculations. How is the average time-step temperature obtained and how is this temperature used?

Response 1:

[

]

The interactions between fuel rod components and evaluation of thermal conditions are represented by the intensive variables, such as fuel pellet and cladding stresses and temperatures. The extensive variables, such as fuel and cladding creep, fission gas release and gaseous swelling, etc., are those which characterize the fuel state and vary in time, being dependent on the intensive variables.

[

]

Question 2:

It appears that a convergence check is performed on contact pressure for the end-of-time step to determine if convergence is satisfied. Is this correct? Is there a convergence on fuel temperatures? Are there any other convergence criteria (Figures 4.6 and 4.7)?

Response to Request for
Additional Information – BAW-10247(P)

Response 2:

[

]

II. Specific Parameter Models in Code

Question 3:

BAW-10247(P) requests approval to a burnup of 62 GWd/MTU. To facilitate review of the code up to the requested burnup level, please provide a table that identifies the different models utilized in the code and the burnup range of the data used to verify these models. Only include those models that are burnup or time dependent. Please provide burnup levels as rod-average burnup.

Response 3:

[Empty response area with corner brackets]

Response to Request for
Additional Information – BAW-10247(P)



Question 4

The following are on the thermal calculations and the need for additional comparisons to integral thermal data (fuel centerline temperature measurements) to verify the integral thermal calculation. The thermal analysis methodology assumes that the fuel pellet is eccentric within the fuel cladding for commercial fuel rods while for calibration to experimental fuel rods with centerline thermocouples the code assumes that the fuel pellet is more concentric within the cladding (the fuel thermal conductivity appears to be increased early-in-life to compensate for the greater temperature drop across the fuel-cladding gap, see RAI #6). This assumption may be non-conservative for fuel temperatures in commercial fuel rods (results in biased lower predicted fuel temperatures than experimental rods) and will need further justification with additional thermal predictive comparisons to fuel rods with central thermocouples. Please provide the following comparisons to fuel centerline temperature measurements taken early-in-life (burnup < 10 GWd/MTU) from Halden rods with helium, xenon or argon fill gases. Comparisons are needed for the Rod 4 of IFA-432 (xenon fill gas), and Rods 1 (helium) and 2 (argon) of IFA-633 for Ramp 1 as identified in the Halden report HWR-764. The comparisons to Rod 4 of IFA-432 should include predicted minus measured versus burnup up to 10 GWd/MTU while the comparisons to IFA-633 Rods 1 and 2 (identical rods only fill gas is different) should be measured versus predicted for Ramp 1. A table of predicted and measured centerline temperatures along with predicted fuel surface temperatures and effective gap conductance values for these three rods needs to be provided. Please provide an estimate of the correction in fuel surface and centerline temperature between the eccentric and less concentric configurations for IFA-432 Rod 4, and IFA-633 Rods 1 and 2 as a function of linear heat generation rate (LHGR). Please provide this same information for the current Atrium 10 fuel design as a function of LHGR taking into account the effects of fission gas release (FGR) on gap conductance.

Response 4:

The response to this question will be provided at a later date.

Question 5

The following questions are related to the code comparisons to fuel centerline temperature data provided in EMF-3014(P).

Question 5a:

Several tables are provided that summarizes the statistical comparisons of the code predictions of centerline fuel temperatures to particular Halden experiments that measured fuel centerline temperatures. One measure of the comparisons is described as the mean quadratic deviation, (Section 5.5). Is this the same as the mean square residual error, $\Sigma(\hat{y}_{pred} - y_{meas})^2 / (n - \text{degrees of freedom})$ used in statistics?

Response 5a:

Yes, the formula indicated as mean square residual error was used, but was described in EMF-3014(P) as mean quadratic deviation. However, the terminology is equally correct, as “deviation” is the same as “residual error” and “quadratic” is similar to “square”.

Question 5b:

Examining all of the predictions of the upper thermocouple positions in the tables and also the predictions compared to measurements at high temperatures (Figure 5.35) it appears that the code may provide a biased under prediction of fuel temperatures when centerline temperatures are above 1400 °C. Please provide a plot of predicted minus measured temperatures versus measured temperature and similar plot versus burnup for measured temperatures only above 1350 °C. Also, provide a table of experimental rods with measured temperatures above 1350 °C providing the measured and predicted values along with the burnup level.

Response 5b:

The response to this question will be provided at a later date.

Question 5c:

It is stated that only the central four segments contain characterized fuel and barrier fuel for RISO FGP3 Framatome ANP rods (Section 5.5.9). Please offer further explanation on the differences in characterization of these rods.

Response 5c:

Four PWR segmented rods were irradiated in two assemblies in Biblis A. Each rod was made of six segments. Only the central four segments contain characterized fuel and barrier cladding (Ref. 5.1). The upper and lower segments were not used in the Risø FGP3 tests. No information is available on those segments. Only the characterized segments have been used in the Risø FGP3 tests.

Ref. 5.1: The Third Risø Fission Gas Project – ANF FUEL (ANF-Data), RISØ-FGP3-ANF, Pt.1, September 1990.

Question 5d:

Because there is only one rod with $UO_2-Gd_2O_3$ with fuel centerline temperature measurements this fuel type should have a larger uncertainty on fuel temperatures. This does not appear to be the case, please provide further justification on why the $UO_2-Gd_2O_3$ should not have a higher uncertainty on fuel temperatures than that used for UO_2 fuel (Section 5.5, EMF-3014(P)).

Response 5d:

[

]

Response to Request for
Additional Information – BAW-10247(P)

[

1

Response to Request for
Additional Information – BAW-10247(P)

Question 5e:

Please expand the scale of Figure 5.36, to a deviation of $\pm 25\%$ (Section 5.5, EMF-3014(P)).

Response 5e:

The figure below is a copy of Figure 5.36 (Section 5.5, EMF-3014(P)) with the scale expanded as requested:



Question 6:

The following RAI's are related to a possible bias in the fuel thermal conductivity models for UO_2 and $UO_2-Gd_2O_3$ and how the models are applied.

Question 6a:

No comparisons are provided to fuel thermal conductivity data. The thermal conductivity model appears to over predict fuel thermal conductivity at low fuel burnups and at high temperatures, please provide a comparison of the RODEX4 thermal conductivity model to the Ronchi et al thermal conductivity data (paper entitled thermal Conductivity of Uranium Dioxide up to 2900 K from Simultaneous Measurement of the Heat Capacity and Thermal Diffusivity Journal of

Response to Request for
Additional Information – BAW-10247(P)

Applied Physics, Vol. 85 no.2, pages 776 to 789.) This data appears to be the best up-to-date (using the most up-to-date experimental equipment) measurement of fuel thermal conductivity from unirradiated fuel.

Response 6a:

[

]

**Question 6b:**

The thermal conductivity degradation due to porosity development is accounted for in the fuel rim in (Section 5.12, EMF-2994(P)). There is an additional correction that increases the rim thermal conductivity discussed in Section 5.3.2 of EMF-3014(P). This increase is due to the fission gases precipitating out of the matrix as rim porosity and these gases no longer act as point defects that scatter the thermal phonon. Please provide a description of the integration of these two rim conductivity models with the fuel thermal conductivity model provided in Equation 7.18 of EMF-2994(P) and an example calculation of rim thermal conductivity as a function of burnup at the following isothermal temperatures of 500 °C, 600 °C and 700 °C.

Response to Request for
Additional Information – BAW-10247(P)

Response 6b:

[

]

Question 6c:

A thermal conductivity model is provided for UO_2 - Gd_2O_3 but the basis and data for this thermal conductivity model are not provided. This model over predicts the unirradiated UO_2 - Gd_2O_3 thermal conductivity model in FRAPCON-3 with the largest over prediction (6 to 13%) at the highest values of Gd_2O_3 . Please provide the data that this model is based on particularly at UO_2 - Gd_2O_3 contents of 8 weight percent and higher. This is of particular importance because very little in-reactor fuel centerline thermocouple data are provided for verifying the thermal behavior of UO_2 - Gd_2O_3 particularly for fuel at the higher UO_2 - Gd_2O_3 weight percent.

Response 6c:

[

]

Ref. 6c-1 G. Gradel, W. Dörr, and H. Gross, "Wärmeleitfähigkeit von UO_2/Gd_2O_3 Brennstoff aus Unterschiedlichen Fertigungsverfahren," Jahrestagung Kerntechnik '98, Munich, 26-28 May 1998.



Question 7:

The following questions are related to understanding the fission gas release model (EMF-2994(P)).

Question 7a:

For the gas release model, how are f_{sw} , f_{old} , and f_{new} combined to determine total release fractions (pp. 5-50 5-55) as a function of time or burnup? Please provide an example.

Response 7a:

At each time step, the following 3 quantities are calculated:

[

]

Question 7b:

What value is used for bu_{max} in the gas release model (p. 5-55)?

Response 7b:

The value of bu_{max} is 100 MWd/kgU

Question 7c:

Please provide plots of D_{eff} versus temperature at burnup levels of 10, 30 and 60 GWd/MTU.

Response 7c:

The plots of D_{eff} vs. temperature at various burnups are shown in the figure below.

Question 7d:

Equation 5.138 of EMF-2994(P) uses two variables hydrostatic stress in the matrix, σ , and p_{ext} that are not defined. How are they determined? Is p_{ext} the same as variable p_{ovp} defined on page 6-8 of EMF-3014(P)? Please explain further how these two variables are determined (p.5-56)?

Response 7d:

Yes, p_{ext} on p. 5-56 of EMF-2994(P) is the same as variable p_{ovp} defined on page 6-8 of EMF-3014(P). The approximate value of this over pressure in the grain boundary bubbles was taken from the literature and the final value was determined through fine tuning. The hydrostatic stress in the matrix is calculated by the code itself. [

] The calculation of the three principal stresses (radial, hoop and axial) is presented in Section 6.3, "Fuel Column Mechanics", of EMF-2994(P).

Question 7e:

Please provide FGR predictions as a function of burnup up to 75 GWd/MTU at isothermal temperatures of 800 to 1400 °C in 100 °C increments with no fuel-cladding contact pressure and with maximum contact pressure. Also provide FGR predictions for one axial node as a function of time (at 20 minutes, 1 hour, 24 hours and 48 hours) for 3 power ramps with an initial starting power at 20 kW/m ramped to terminal powers of 35, 40 and 45 kW/m for each of two burnup levels of 30 GWd/MTU and 60 GWd/MTU for a BWR design (base irradiation rod powers, prior to the ramp, to these burnups should be 20 kW/m to keep FGR low). The calculated fuel surface and centerline temperatures at terminal powers at 20 minutes and 24 hours need to be provided for each power ramp (Section 5.8).

Response 7e:

The response to this question will be provided at a later date.

Question 8:

The following are related to determining whether a bias exists and the uncertainties in the prediction of fission gas release (FGR) for fuel performance analyses particularly the rod pressure analyses.

Question 8a:

The FGR calculated for rod pressure analyses is usually at values between 10% to 30% release while the database in EMF-3014(P) and BAW-10247(P) includes a very large number of data with measured values below 5% release where the accuracy of the prediction is not of great importance for these analyses. There appears to be a biased under prediction on average at high release values for both the international and commercial database where the prediction is important for rod pressure analyses. Therefore, please provide statistics (bias and standard deviation) on data with measured FGR's above 5% and 10% release; and plot predicted minus measured versus measured release and versus rod-average burnup on linear scales (no log scales) for the international and commercial databases above 5% and 10% measured FGR.

Response 8a:

The data sub-sets with FGR greater than 5% and 10% from the international programs were processed using all the data and the results are shown in the table below in the columns labeled "FGR_all_5" and "FGR_all_10", respectively. Two additional groups of data, labeled "FGR_opt_5" and "FGR_opt_10", were obtained by eliminating 4 rods from the PK2 series of the Super Ramp and 5 rods from the HBRP programs because of their larger experimental uncertainty and inconsistency in results. The average (indicative of local bias) and the standard deviation were calculated for these sub-sets, both for (calculated/measured) and log (calculated/measured), as follows:



[

] The figures with the requested plots are presented below, where delta is (calculated-measured).



Response to Request for
Additional Information – BAW-10247(P)



Response to Request for
Additional Information – BAW-10247(P)



Response to Request for
Additional Information – BAW-10247(P)



Response to Request for
Additional Information – BAW-10247(P)



Response to Request for
Additional Information – BAW-10247(P)



Question 8b:

Also provide a histogram of FGR deviation on a linear scale for each of the international and commercial databases with measured FGR's above 5% and 10% release (Section 6.3, EMF-3014(P)).

Response 8b:

The response to this question will be provided at a later date.

Question 9:

The following are related to understanding the solid and gaseous swelling, densification and grain growth models (EMF-2994(P)).

Question 9a:

C_{sat} from Equation 5.142 is not defined, is this variable the same as C_{gb} defined on page 6-8 of EMF-3014(P) and how is r_{bmax} defined?

Response 9a:

C_{sat} is defined in the text before Equation 5.142, where C_{sat} is on the left-hand side of the equation and it is thus defined by that relationship. The variable C_{gb} is the assumed [] Therefore, the two variables are not the same, the second one is part of the definition of the first one.

C_{sat} is calculated by the code at each time step, since it depends on the current temperature, T , and the current matrix hydrostatic stress, through p_{gas} . The maximum bubble size, r_{bmax} , is dependent on the two model parameters N_{gb} and f_{cov} and it is defined by Equation 5.140.

Question 9b:

Please provide typical values used for P_u and P_s used in Equations 6.133 and 6.136, respectively. Please provide an example calculation of fuel swelling separating gaseous ($\Delta V/V_{gs}$) and macroscopic solid swelling ($\Delta V/V_{ss}$) using these values as a function of burnup at fixed isothermal temperatures of 800 °C, 1000 °C, 1200 °C and 1400 °C (for one radial node) (p. 5-57). The gaseous swelling model calculation should provide the values used for grain boundary bubble radius (r_b), surface density of grain boundary bubbles (N_{gb}), and grain diameter (d_{gr}), as a function of burnup and temperature.

Response 9b:

The response to this question will be provided at a later date.

Question 9c:

The coefficients for average energy per fission (κ) and fraction of energy released out of the fuel (η_{ex}) are not defined in Equation 5.175 nor could they be found elsewhere. These values are used in determining cesium release and solid swelling. Please define these values (p. 5-64).

Response 9c:

The energy per fission is calculated according to the following equation:

$$\kappa = \frac{\sum_i (\kappa_i N_i \sigma_{fi})}{\sum_i (N_i \sigma_{fi})} \quad i = \text{U235, U236, U238, Pu238, Pu239, Pu240, Pu241, Pu242}$$

with N_i : atomic density
 σ_{fi} : average one-group microscopic fission cross-section of nuclide i

Nuclide (i)	Energy per fission (κ_i) MeV	Fission cross section (σ_{fi}) barn
U235	203	46.71
U236	203	0.1975
U238	204	0.1004
Pu238	209	2.465
Pu239	209	106.2
Pu240	209	0.5840
Pu241	211	118.1
Pu242	211	0.4146

The references for the κ_i are: J. Nucl. Energy, Vol.23, pp. 517-536 and J. Nucl. Energy, Vol. 25, pp. 513-523. Note that the κ_i terms include an average energy per fission due to the neutron capture.

The fraction η_{ex} of the energy release out of the fuel is generally in the range 0.960 to 0.970 for BWR's and close to 0.974 for PWR's. The default value in the code is 0.970.

Question 10:

The following are related to validating the solid and gaseous swelling, grain growth models.

Question 10a:

The Halden data does not appear to have the solid swelling rate dependence on temperature as that calculated by the RODEX4 model. Please compare the solid swelling model to Halden experiments where solid swelling was measured both prior to a power ramp and following a power ramp such as for IFA-633 Rods 3 and 5 with UO₂ fuel.

Response 10a:

The response to this question will be provided at a later date.

Question 10b:

The gaseous swelling model is justified by comparison to four power ramped rods at relatively high burnups of 45 GWd/MTU and 62 GWd/MTU. EMF-3014(P) states that the large cladding deformation observed after the ramp testing cannot be explained by fuel thermal expansion only. The interpretation of the tests with RODEX4 showed that gaseous swelling contributed significantly to the deformation in the three Mark-BEB rods and one Super-Ramp rod. Please provide those analyses that demonstrate that gaseous swelling contributed to the measured strains in these rods, e.g., cladding strain predictions with and without gaseous swelling for these four rods.

Response 10b:

The figures below for the Mark-BEB rods illustrate the contribution of the gaseous swelling to the measured strains, by plotting the (calculated – measured) strains with and without gaseous swelling. It is apparent that good agreement is obtained only when gaseous swelling is taken into account. The plot for the Super-Ramp rod PK 2/3 will be provide later.



Question 10c:

Please provide fuel grain growth predictions of irradiated fuel data from the following references: J. A. Turnbull J., Nucl. Mater. 50, 1974 (60); C. Bagger et al., J. Nucl. Mater. 211, 1994 (11); Hargreaves and NewBigging data presented by J. B. Ainscough et al., J. Nucl. Mater. 49, 1973 (117).

Response 10c:

The response to this question will be provided at a later date.

Questions 11:

The following are related to understanding the cladding creep equations used for determining creep collapse and gap closure due to irradiation creep (EMF-2994(P)).

Question 11a:

How is the primary creep rate, $\dot{\epsilon}_{g_th_cr}$, determined from Equation 7.72 starting at time =0 because the denominator starts with a value of initial creep strain (p. 7-54)?

Response 11a:

[

]

[

]

Question 11b:

It is not clear which irradiation creep equation is used in RODEX4. Section 7.2.8 offers a generalized equation in Equation 7.78 (non-isotropic creep) while Appendix B provides Equation B.32 (assumes isotropic creep). These two equations provide different values for creep unless it is assumed that isotropic conditions are assumed, i.e., where A_0 and B_0 equal 1 in Equation 7.78. However, the coefficients A_0 and B_0 are defined in Equations 7.76 and 7.77 (coefficients to these equations are further defined in Table 7.3) such that the values for these coefficients are not defined to be isotropic. Framatome has verbally stated that Equation 7.78 is used in RODEX4 and was used to generate Figures 7.29 and 7.30. However, PNNL has not been able to reproduce these figures unless Equation B.32 is used or if isotropic conditions are assumed for Equation 7.78. What equation is used in RODEX4 and is cladding creep assumed to be anisotropic or isotropic (p. 7-78, 7-60, 7-61, and B-5)?

Response 11b:

RODEX4 uses the cladding irradiation creep equation 7.78 (Section 7.2.8, p.7-55), which is identical to Equation B.31 (Appendix B, p.B-5). Equation 7.78 was used to generate Figs.7.29 and 7.30 (p.7-60 and 7-61). Equation B.32 in Appendix B is valid only for pressurized thin tubes and is not used in RODEX4.

The difficulty in reproducing these two figures is due to a small difference in the anisotropy coefficients used to generate the figures from EMF-2994(P). [

value of P used in the figure was a prior value of the anisotropy coefficient from a previous report that remained unchanged by mistake. This figure will be corrected in the final update of the report.] The

Question 11c:

Please provide a description of how the COLAPX model is used to verify the calculation of creep collapse with RODEX4 (p. 6-27 EMF-2994(P)). Has the RODEX4 code been compared to any creep collapse data to verify that the code provides a conservative or best estimate prediction?

Response 11c:

COLAPX is not used in the verification of the creep collapse methodology. It was discussed on page 6-27 of EMF-3014(P) that COLAPX was used to benchmark/calibrate the ovality model in RODEX4. The verification of RODEX4 ovality model is presented in Section 7.4 of EMF-3014(P). RODEX4 has not been compared to creep collapse measurements.

Question 12:

The following questions are related to the cladding creep data used to verify the creep and ovality models in RODEX4 (EMF-3014(P)).

Question 12a:

Three different sets of coefficients (for CWSR Zr-4, CWSR Zr-2 and RX Zr-2 cladding types) are presented for the cladding creep model (Table 7.1). Which cladding creep model will be used in current and future US licensing applications?

Response 12a:

[]

Question 12b:

The irradiated creep data used to determine the coefficients for the irradiation creep model are provided but the data used to determine the coefficients to the thermal creep model are not provided. Please provide either a justification on why the thermal creep model is not a significant contributor to licensing analyses or provide this data and thermal creep model comparisons to this data (Section 7.1).

Response 12b:

The response to this question will be provided at a later date.

Question 12c:

The irradiation creep model does not include any temperature dependent term. Please provide data to justify a lack of temperature dependence for irradiation creep. Framatome has stated that this creep model (without temperature dependence) is the same as used in RODEX3. The irradiation creep model in RODEX3 was not reviewed in detail because this code was to be used for beginning of life analyses where cladding creep was not critical. Therefore, this creep model requires review.

Response 12c:

[

The cladding-to-coolant heat transfer in a BWR channel is predominantly by boiling heat transfer all along the fuel pin length and thus the cladding outer temperature varies very little

along the fuel pin longitudinal direction. Therefore, the temperature dependence of the irradiation creep model plays only a minor, second-order role in BWR applications.

Question 12d:

Examination of Figure 7.1 (9x9 fuel) suggests that cladding creepdown is not complete by a burnup of 35 GWd/MTU. Please provide further discussion on why creepdown is not complete because it is expected that cladding creepdown should be complete by this burnup level.

Response 12d:

The response to this question will be provided at a later date.

Question 12e:

Please identify those rods from which creep data were obtained when the fuel-cladding gap remained open and were used for creep model calibration. Were any rods used for creep model calibration when the cladding gap was closed?

Response 12e:

[

]

Question 12f:

Please compare RODEX4 creep predictions to the measured creep data from Halden experiment IFA-585. If this is not a valid comparison please provide justification.

Response 12f:

IFA-585 was a test with on-line monitoring of the cladding outer diameter, which was subject to variable inside pressure and constant outside pressure. Ovalization occurred throughout the test and it affected the measured diameter values. This adds to measurement uncertainty since it is not known what diameter of the ellipse is measured. It is especially a problem for IFA-585 because the strain gauge device was moved along the same cladding generatrix for all the scans performed during the test.

Other criticisms to the measurements of IFA-585 have been made in a Westinghouse paper by J. Foster at the LWR Topical Meeting, Park-City, Utah, 2000.

The simulation of the test with the RODEX4 creep model is presented in the Figures 12f-1 and 12f-2. The first cycle was ignored because the measuring device malfunctioned. [

]

Response to Request for
Additional Information – BAW-10247(P)

[

]

The discrepancy between calculations and measurements for the outward deformation cycles would imply that creep strain rate is higher in tension than in compression. This has been questioned in the Westinghouse paper mentioned before. [

]

It is concluded that the uncertainties associated with IFA-585 are too large, so that it should not be used for verification purposes.

┌

└

Question 12g:

RODEX4 uses a cladding ovality model for 5 different cladding types with different coefficients for each type based on a total of 13 data points with only one to four data points per cladding type. Based on the small amount of ovality data per cladding type it is impossible to estimate the uncertainties in this model suggesting a very large uncertainty in this code prediction for any of the five cladding types. Of the five cladding types presented which will be used for current and future BWR fuel designs in the U.S.? How does the very large uncertainty in predicted cladding ovality impact the different licensing analyses in which the code is used? Please provide an example with different assumed uncertainties for ovality (see RAI# 25).

Response 12g:

Two of the cladding types presented represent the AREVA NP manufacturing process and specifications. Two rods were evaluated for typical CWSR Zircaloy-4 cladding and one rod was evaluated for typical RX Zircaloy-2 cladding. These rods were used to establish the ovality equation fitting parameters, []. The preparation of the ovality cases was peripheral to other evaluations using these cases so that not all possible cases had been prepared. The additional cases available for these cladding types have now been evaluated.

[

]

Response to Request for
Additional Information – BAW-10247(P)

This can now be applied to the analysis of the relevant cases from the benchmarking as described in EMF-3014(P) and the additional cases.

An additional 5 ovality cases are available for CWSR cladding. The additional cases were combined with the 2 of the submittal to provide a total of 7 cases with representative CWSR Zircaloy-4 cladding. The cases were evaluated using the best estimate creep parameters for CWSR Zircaloy-4 cladding determined from the creepdown calibration. Table 12g-1 shows the results: initial ovality, final ovality, calculated ovality and the calculated/measured ratio.

The ovality equation factor of [] which was selected for the methodology is shown to have a conservative bias of about [] for the CWSR Zircaloy-4. The range of the results, [] is consistent with the variation that would be produced at this creep strain for the bounding parameters of the creep equation, because the measured uniform creepdown strains were between [] (for both stress-relieved and recrystallized claddings EMF-3014(P) Ref. 7.7). This was demonstrated by repeating the evaluation using a 30% higher thermal and irradiation creep coefficient. The results are shown in Table 12g-2.

The individual calculated/ measured results are all above [], and in fact are also equal to or above the average positive ovality bias of [] determined with nominal creep parameters. This shows that the creep uncertainty range encompasses the ovality modeling uncertainty.

Response to Request for
Additional Information – BAW-10247(P)

An additional 4 ovality cases are also available for annealed (RX) Zircaloy-2 cladding. The one initial annealed case in the submittal was combined with the 4 additional for a total of 5 rods. The results for these rods, initial ovality, final ovality, calculated ovality and the calculated/measured ratio, are shown in Table 12g-3.

In these cases the [] ovality equation F_o factor, selected based on one rod, also has a average conservative bias, approximately []. To verify the consistency of creep and ovality uncertainties, this calculation was also repeated with a multiplication of the creep parameter by [] as for the CWSR cases. This is consistent with Figure 12g-1 and the creepdown strains in the range []. The results are summarized in Table 12g-4.

In this case two of the calculated/measured ratios are still below 1.0. This is due to the low ovality for these cases. The lowest calculated ovalities are only 1 or 2 microns below the measured ovalities. The measurement uncertainty is thus a greater factor in these cases. In the methodology, []. This provides additional conservatism to the creep ovality analysis, and bounds the range determined for these low ovality uncertainty cases.

No ovality cases are available for CWSR Zircaloy-2, however the CWSR Zircaloy-2 creep parameters are very close to those for CWSR Zircaloy-4. Table 12g-5 shows the results for the CWSR Zircaloy-4 rods using the nominal CWSR Zircaloy-2 creep parameters.

Calculated creep results are slightly lower for this material based on its slightly lower creep rate. The CWSR Zircaloy-4 ovality fitting result, [] is considered to be applicable for CWSR Zircaloy-2 considering the close material similarity and the conservative fitting bias determined for CWSR Zircaloy-4. Margin is added to the creep ovality analysis by the axial interaction radial gap of 10 μm .

For the BWR clad applications, the ovality uncertainty produced by the creep parameter uncertainty is consistent with the measured results. The favorable bias of the ovality fitting parameter and the 10 micron contact gap provide margin to the creep collapse evaluation to accommodate the additional uncertainty in the low ovality RX clad results and for the slight material difference of CWSR Zircaloy-2.

Question 13:

The following are related to the assumption that the irradiation creep uncertainties are the same as the uncertainties in the thermal creep model. This assumption does not appear to be valid because the RODEX4 irradiation creep and thermal creep models are significantly different suggesting that the mechanisms for these two types of creep must be different. In addition, comparison of the irradiated creep model to irradiated creep data suggests that the uncertainty in irradiation creep is much greater than observed in thermal creep. This observation is based on the following model comparisons to irradiated creep data presented in EMF-3014(P) and BAW-10247(P).

Question 13a:

There does not appear to be a good correlation between predicted and measured creep in Figure 7.2 (9x9 fuel) and from Figure 7.3 the model under predicts creep in the 10x10 fuel designs at low fluences where creepdown is present. The small number of rods from which creep data were collected plus the large differences between predicted and measured creep (Figures 7.2 and 7.3) suggest that the model does not provide a valid mean of the data and, therefore, both the mean predictive uncertainty and overall uncertainty are very large (much larger, > factor of 3, than assumed for thermal creep).

Response 13a:

The response to this question will be provided at a later date.

Question 13b:

In addition, the intended application for RODEX4 is the Atrium 10 fuel design with very little data and the small amount of data provided is not predicted well by the code. It is implied that the large uncertainty in the irradiated data is due to uncertainties in fuel rod dimensions in fabrication, however, further examination does not appear to support this assumption. The example of the uncertainty contribution of cladding fabrication dimensions to cladding creepdown only demonstrates a plus or minus of 15 μm (at a 2σ level) in Figure 5.6 of BAW-10274(P) while the scatter in the data in Figure 7.1 of EMF-3014(P) is plus or minus 40 μm and the uncertainty in Figure 7.2 of EMF-3014(P) is approximately plus 50 μm and minus 70 μm from the model predicted values. This suggests that the fabrication uncertainties offer only a small fraction of the uncertainty in the cladding creep model and combined with the assumed uncertainty for the irradiation cladding creep (same as thermal creep) does not adequately address the uncertainty in the predicted versus measured irradiated creep data. Please provide further irradiation creep data, analyses and or creep model modifications to demonstrate that the uncertainty in the irradiation creep model equals that for the thermal creep model.

Response 13b:

The response to this question will be provided at a later date.

Question 14:

The following are related to understanding the cladding plastic deformation modeling during power increases due to normal operation, slow power transients and fast power transients (EMF-2994).

Question 14a:

It appears that the deformation model does not calculate plastic deformation due to stress exceeding the yield strength of the cladding and only calculates plastic deformation from creep. If this interpretation is correct, please explain in detail how plastic deformation is accounted for at high stresses and provide comparisons to axial tensile and biaxial test data at strain rates typical for application of the model (for normal operation, and slow and fast transients). If this is

not correct, please provide details and example about how high stress plastic deformation is calculated.

Response 14a:

The Engineering Cladding Creep Model is a unified constitutive deformation model, which models the visco-plastic deformation with the same formulation, since the basic microstructural processes are the same for creep and plasticity (except twinning which occurs mainly at very high stresses). The model has been applied with excellent results in the RODEX2, 3 and 4 suite of codes since 1980.

The Engineering Cladding Creep Model was first presented at the ANS/ENS International Topical Meeting on LWR Fuel Performance, Avignon, France, April 21-24, 1991. More recently, the theory of the model and results for both yield stress and creep comparisons were presented at the ANS 2000 International Topical Meeting on LWR Fuel Performance, Park City, Utah, April 10-13, 2000.

The strain rate equation representing the unified creep/plastic strain of the cladding can be used to solve for the yield stress at any temperature and for any given strain rate. This technique is used to interpret tensile and burst tests. It is also used to determine the parameters of the model. Figure 14a-1 below shows the results of a series of burst tests on irradiated cladding performed at different temperatures and different strain rates. The good agreement supports the validity of the unified constitutive model used in the code.

With respect to cladding creep modeling in the case of stress reversal, the creep rate is strongly underestimated at the beginning of the test. In other words, the strain hardening concept does not give proper results in the case of stress reversal.

During the period of irradiation when the pellet-cladding gap is open, the cladding is in compression. The dislocations in the cladding move in the direction imposed by the stress and pile up on point defects. When the stress is reversed, the dislocations are free to glide in the opposite direction. They recover part of their mobility. This corresponds to primary creep recovery in the physical model.

[

]





Question 14b:

Is clad yield stress modeled in RODEX4? If it is modeled please provide the model (along with comparisons to irradiated data) and how is it used.

Response 14b:

See the answer to the previous question: the plastic deformation is estimated together with creep deformation as part of the unified constitutive model. Thus the yield stress is implicitly modeled. The validation of the calculation of the yield stress by the engineering cladding creep model is illustrated in Figure 14a-1.

Question 15:

The following are related to the lack of data used to verify the cladding deformation models.

Question 15a:

The code has been compared to measured deformation from only four power ramped rods. The comparison to these four tests does not provide a valid estimate of any bias nor the uncertainty in the code calculations of fuel rod deformation. There are considerably more power ramped rods with measured cladding deformation than the four rods provided including rods ramped in R3/R2, DR-2, BR-2 HFR-Petten and Halden, (Section 7.3.2, EMF-3014(P)). Please provide a proposed list of ramped rods for RODEX4 code comparisons. Of particular interest are those experimental ramped rods that are closest to the licensing conditions experienced during normal operation and slow transient (control rod withdrawal error) analysis of cladding strain, e.g., maximum strain is calculated when the fuel cladding gap is closed and the power range for this transient. Once an agreement is reached (between Framatome ANP, NRC and PNNL) on which rods should be used please provide these code to data comparisons. If power ramp data exist that are applicable to the strain analyses for fast transients (feedwater controller failure) these data comparisons should also be provided.

Response 15a:

A review of the profilometry recordings of ramp tested rods available in the AREVA NP calibration database has been made. This includes the following projects:

- Inter-Ramp
- Over-Ramp
- Super-Ramp
- Super-Ramp Extension
- Super-Ramp II
- Risø TFGP
- Risø FGP3
- BAW Mark-BEB

Only four rods show a cladding deformation of 1% or more during the ramp test: the Super-Ramp rod PK2/3 and the three BAW Mark-BEB rods. The RODEX4 results for these four rods were presented in report EMF-3014(P). These rods are also the only rods where gaseous swelling plays a significant role.

Most BWR rods show only small cladding deformations after ramp (no more than a few micrometers). Sometimes the rod diameter after irradiation is larger than the reported as-fabricated diameter (Super-Ramp BG8, BG9 and BK7 series). For others, such as the Risø FGP3 GE or Super-Ramp II rods, the reported LHGRs are questionable (In the Risø FGP3 the reported LHGRs are non-consistent with the temperature measurements; in Super-Ramp II repeated mass flow rate calibrations gave very different LHGR estimates).

The HFR-Petten LHGR data are in general less reliable than the Risø or Studsvik data (see discussion in DOE/ET/34030-4 CEND-402 Report, Appendix).

The more reliable data seem to be the PWR data from the Over-Ramp and Super-Ramp Programs, as well as data from the Risø FGP3 ANF rods. The next table suggests a series of

additional rods which could be used to estimate the uncertainties on the cladding deformation predictions.

Program	Rod	Ramp Terminal Level (kW/m)	Failed/non-failed	Reference
Over-Ramp	G20/1	42.0	NF	STOR-28, Fig.7
	G20/2	44.5	NF	STOR-28, Fig.8
	G20/3	48.2	F	STOR-28, Fig.9
	W5/1	44.5	F	STOR-23R, Figs. 2 to 4
	W5/2	37.0	NF	STOR-23R, Figs. 5 to 7
Super-Ramp	PK1/1	41.5	NF	SR-81/27, Fig.1
	PK4/1*	39.0	NF	STSR-2, Fig.1 a and b
	PK4/2*	44.5	NF	STSR-2, Fig.2 a and b
	PK6/2	40.0	NF	STSR-2, Fig.5 a and b
	PW3/2	35.3	NF	STSR-14, App. 7 to 10
Risø FGP3	PW3/4	37.2	F	STSR-14, App. 11 to 14
	AN2	44.4	NF	RISØ-FGP3-AN2, Fig.6-3
	AN8	47.2	NF	RISØ-FGP3-AN8, Fig.6-3

* gadolinia fuel

Question 15b:

Please provide code comparisons to the Halden power ramp data including axial and diametral deformation from IFA-520, IFA-525 (HWR-122) and IFA-509 Rod 3 (HWR-162).

Response 15b:

The response to this question will be provided at a later date.

Question 15c:

The MATPRO correlation for the effects of cold work and fast neutron fluence on Young modulus and shear modulus are not used. These correlations can affect the moduli by up to 15% (p. 7-47, EMF-2994(P)). Please justify why these effects are ignored.

Response 15c:

[

]

The effect of cold work suggested in MATPRO is based on a report by Bunnell et al. In the same MATPRO document (MATPRO-1993, p. 4-46) it is stated that *“Unfortunately, the effect of cold work suggested by Bunnell’s dynamic measurements of Young’s modulus is opposite to the trend reported by Shober et al. from static measurements. The dynamic measurements show a slight decrease in Young’s modulus with cold work, and the static measurements show a slight increase in Young’s modulus with cold work. Since neither source provides usable texture information, it is impossible to tell whether the change with cold work is due to associated changes in texture, to a separate effect associated with the cold work, or to a fundamental difference in the quantity that is being measured with the different techniques. The small decrease implied by Bunnell’s data was tentatively included in the (MATPRO) models for elastic moduli because of the greater precision of the dynamic data.”*

Other investigators, such as Busby (who reports axial Young’s modulus measurement for Zircaloy-4 for five combinations of cold work and heat treatment), do not report any significant effect of cold work. The cold work effect seems therefore to be too speculative to be taken into account the way it is in MATPRO.

Also, the fluence dependence in the MAPTRO model is largely assumed because not enough data are available. The uncertainty associated with this is very large. The MATPRO model shows very quick saturation and thus the higher burnup region of interest is not affected by the lack of a fluence dependence.

Question 16:

The following are related to understanding the fuel pellet deformation modeling.

- a. *In the last paragraph in Section 6.2.5.2, in what way were the results from the 1-D model for deformation at pellet ends incompatible with observation (page 6-26, EMF-2994(P))?*
- b. *Please provide an illustrated example of how dish filling is calculated (p 6-5). In Equation 6-34, please provide a value for α_{dish} and a comparison of predicted and measured values of dish filling along with a tabulation of this data (p. 6-34).*
- c. *It is stated that “an additional hoop strain component, $\epsilon_{\theta\text{crack}}$, has been introduced into the circumferential compatibility equation to simulate the tangential displacement associated with pellet cracking.” Please provide a prediction of the hoop strain displacement in μm due to cracking as a function of LHGR and any other important parameters for fuel displacement due to cracking (page 6-4). This calculation is wanted to determine the extent of gap closure for the experimental data base and the licensing analyses of commercial fuel rods.*

Response 16:

The Response these questions will be provided at a later date.

Question 17:

The following are related to validating the cladding crud, oxidation and hydriding models for their intended application.

Question 17a:

What value is used for crud conductivity?

Response 17a:

[] The oxide thickness calibration includes some residual crud which was not removed by water jet cleaning or brushing and was assumed in the calibration to be oxide.

The crud layer thickness and composition can present a large variation between different plants. The crud is considered to be a plant specific issue and was not applied in the realistic fuel rod methodology. Typical crud conductivity values may be found in references 17.1, 17.2, and 17.3.

- 17.1 Solomon, Y., "An Overview of Water Chemistry for PWRs," BNES, London, 1978.
- 17.2 Macbeth, R.V., "Fouling in Boiling Water Systems, Two-Phase Flow and Heat Transfer," Harwell Series, Oxford Press, 1978.
- 17.3 Cohen, P., "Heat and Mass Transfer for Boiling in Porous Deposits with Chimneys" AIChE. Symposium, Volume 70, Issue 138, 1974.

Question 17b:

The value for oxide conductivity appears to be low. This may be conservative for some applications but not for MCPR analyses (p. 7-65, EMF-2994(P)). Are their other applications where a low oxide thermal conductivity would be non-conservative?

Response 17b:

The RODEX4 code is not directly applied in the MCPR analysis, and in fact the existing MCPR methodology does not assume any oxide layer on the outside surface of the cladding. The conservative feature mentioned in EMF-2994(P) was only considered with respect to the RODEX4 methodology described in BAW-10247(P). A low conductivity would be conservative or neutral for the applications of this methodology.

The oxide thermal conductivity has been conservatively set [] As mentioned on p. 7-65 of EMF-2994(P), this range was the result of measurements performed on cladding with the oxide formed during irradiation and reported in Ref. 7-10 of EMF-2994(P).

The paper of Stehle and Garzarolli shows the oxide layer thermal conductivity for 30 PWR-irradiated specimens with oxide thicknesses ranging from 15 to 50 μm . The results are as follows:

Oxide thickness	Number of specimens	Thermal conductivity range
15 μm	10	1.5 – 1.9 W/m-K
29 μm	11	1.5 – 2.0 W/m-K
50 μm	9	1.5 – 1.6 W/m-K

The thicker oxide specimens have the lower conductivity, because of their lower density. The scatter band is also smaller than for thinner oxide layer. [

]

This value is smaller than the values obtained at Halden in the frame of the NFIR project ("In-Pile Determination of the Thermal Conductivity of Oxide Layer on LWR Cladding," EPRI TR-107718-P2, October 1998). The measured values of oxide thermal conductivity ranged from 1.8 to 3.1 W/m-K. No oxide thickness dependence was observed. The small number of specimens (eleven), the larger scatter band, and the fact that some of the test results may have been affected by crud, lead to the conclusion that these results are not as reliable as the Garzarolli results.

Question 17c:

There is a significant under prediction of the cladding oxidation data in Figure 9.2, EMF-3014(P). How many individual fuel rods are the BWR 10x10 oxidation data taken from? It appears that the uncertainty may be large for this fuel design. What is the standard deviation for oxidation (and standard deviation on the mean) and show this on a plot of measured versus predicted that discriminates between the different BWR fuel designs? Also, please provide the power histories of the BWR 10x10 rods with the highest burnup used to verify the corrosion model for this design. This data is needed to confirm that the power histories are representative of those experienced in commercial fuel operation.

Response 17c:

The apparent under prediction is due to the unsymmetrical appearance of the data. This is seen in Figure 4.29 of BAW-10247(P)/ 9.1 of EMF-3014(P) and also in 4.30 of BAW-10247(P)/ 9.2 of EMF-3014(P). This is due to two factors. First, some crud affected data have been included where the first cycle measurements were higher than the second cycle measurement of the same rods. This introduced more scatter on the high side for one fuel exam. This is the reason for the atypically high oxide thicknesses for low and medium burnups in Figure 4.29 of BAW-10247(P)/ 9.1 of EMF-3014(P), which also creates the larger under prediction sub-set at the bottom of Figure 4.30 of BAW-10247(P)/ 9.2 of EMF-3014(P). Secondly, some low burnup high reactor residence measurements are included, toward the rod ends, which appear to have high oxidation for their burnup (see question 31 for the data description). This affects the appearance of Figure 4.29 which is plotted versus burnup.

The data have been revised with the removal of data for the lower third of ten rods for the first exam for reactor E03. These rods had not been washed prior to thickness measurement. The

second cycle exam showed lower oxide thickness results in this region. Additional data were also obtained for subsequent exams at reactors E03 and A11 which were added. Figure 17c-1 shows this data with the new presentation of oxide thickness versus irradiation time.

In the RODEX4 corrosion calculations the uncertainty is applied to the corrosion equation and not to the final oxide thickness. The corrosion equation best fit parameter, the +/- one standard deviation parameters, and the upper and lower limit corrosion equation parameters are shown in Table 17c-1. The best fit and uncertainty determination has not been revised from the original data fit of the submittal.

Calculated versus measured plots were made for all the benchmark cases with each of the best fit, +/- one sigma, and +/- maximum corrosion equation uncertainty parameters. The best fit calculated/measured results are shown in Figure 17c-2. The + and - one standard deviation calculated/measured results are shown in Figures 17c-3 and 17c-4. The maximum and minimum 95/95 uncertainty calculated/measured results are shown in Figures 17c-5 and 17c-6.

[

]



All the reported oxide data are for the same ATRIUM 10 type fuel. For reactor A11, 32 different rods were measured. For reactor E03, 32 rods were also measured. Ten of the same rods were measured in a second exam. For reactor C04, the 4 high burnup rods were measured. Rod numbers are summarized in Table 17c-2.



The power histories for the high burnup C04 rods' measured nodes are shown in Figures 17c-7, 17c-8 and 17c-9.



Response to Request for
Additional Information – BAW-10247(P)



Response to Request for
Additional Information – BAW-10247(P)



Response to Request for
Additional Information – BAW-10247(P)



Response to Request for
Additional Information – BAW-10247(P)



Response to Request for
Additional Information – BAW-10247(P)



Response to Request for
Additional Information – BAW-10247(P)







Question 17d:

RODEX4 uses a hydrogen pickup value of 0.12 for PWR and BWR (p. 5-48, EMF-2994(P)). FRAPCON uses a value of 0.15 for PWR's and 0.29 for BWR's (see NUREG/CR-6534, Volume 4, Section 5.4). Please provide data to justify the use of 0.12 for BWR conditions.

Response 17d:

A pickup fraction value of 0.29 is presented in Section 4.16 of the MATPRO document (NUREG/CR-6150, Vol.4, November 1993). In the same document it is actually recommended to use a pick up fraction of 0.29 prior to the transition and 1.0 after transition for Zircaloy-2 in BWR's.

[

]

**Question 18:**

For the grain growth model, it is not obvious how g_s (gaseous swelling and no units are given for g_s) on p. 5-44 is calculated from the equations for gaseous swelling described in Section 5.9. Please define and provide an example of how g_s is determined from the equations provided.

Response 18:

The “ g_s ” variable has no units because it is dimensionless. It is the local value of the gaseous swelling which is calculated as described in Section 5.9 as $\Delta V/V$, where “ g_s ” is the same as V_{gs} in Equation (5.139).

Question 19:

For fuel enthalpy, the UO_2 and PuO_2 correlations come from MATPRO. Where does the Gd_2O_3 correlation come from? (p.7-15)

Response 19:

The gadolinia correlation comes from a library of material properties developed by AREVA in 1984.

The model predictions are compared with measurement data obtained by Takahashi et al. at the University of Tokyo (Reference 19.1). Takahashi used two independent methods to determine the enthalpy of gadolinia fuel: the drop calorimetry method carried out up to 1000 K and the differential scanning calorimetry (DSC) up to 1500 K. Only the drop calorimetry results are given in numerical form. The DSC results are presented in graphic form. Takahashi noticed that the heat capacity of 10 weight % gadolinia fuel obtained by DSC method is 2 to 3% below the drop calorimetry data between 350 and 1000 K.

In Figure 19.1 the Rodex4 model predictions are compared with the drop measurement results for 10 weight % Gd fuel. [

]

Ref. 19.1 Y. Takahashi and M. Asou, "High-temperature heat-capacity measurements on (U,Gd)O₂ by drop calorimetry and DSC," J.Nucl.Mat. 201 (1993) 108-114.

Response to Request for
Additional Information – BAW-10247(P)



Question 20:

For cladding axial growth. (p. 7-62)

Question 20a:

RXA ZRY-2 model predicts very low growth using model parameters from EMF-3014(P), p. 7-39, however, the measured growth values provided in Figure 7.25 of EMF-3014(P) are much greater than those expected from the model parameters in EMF-3014(P). Please explain this inconsistency.

Response 20a:

All the previous experimental studies have shown that the growth of RXA Zry-2 is less than that of CWSR Zry-2 or Zry-4. This is because of the specific RX texture which reduces axial irradiation growth. Therefore, lower values for the two irradiation growth model parameters are to be expected.

The available axial elongation database for RXA Zry-2 is quite small and comprises data from just one reactor. The calibration has been redone and more physically reasonable values have been obtained;

[

]

Therefore, there is no inconsistency between the measured values in Fig. 7.25 and the free irradiation growth predictions, because the measured values are total elongation values, which also account for the creep deformations. In any case, the initial calibration of the irradiation growth based on the reduced database was overdone and provided relatively nonphysical values. The new set of parameter values, mentioned above, provides as good a fit and will be used instead of the old values.

Question 20b:

Why is there such a large difference between the growth of 9x9 and 10x10 fuel designs given in Figure 7.31 of EMF-2994(P)?

Response 20b:

Figure 7.31 shows only the growth component of the axial elongation due to both creep and growth. For the measured 10x10 rods at an average fast fluence of about $7 \times 10^{21} \text{ n/cm}^2$, the axial creep is about [] of the elongation and the growth is about [] The 10x10 growth equation component, about [] lower than the 9x9 equation, thus represents an elongation difference of about []

Figure 20b-1 below shows the calculated/measured 9x9 and 10x10 elongation data on the same plot using the 9x9 derived growth correlation. This figure was generated using the latest version of RODEX4 and includes additional data which was not available at the time EMF-3014 was prepared. In this presentation the results for the 10x10 data set fall within the range of the 9x9 calculated/measured results, but with higher calculated than measured results. A slightly lower 10x10 growth is also seen in the overall AREVA NP elongation data set for all reactors shown in Figure 3-1 of Response 3.

The difference between the growth data of 9x9 and 10x10 fuel designs may partly be explained by normal statistical fluctuations. Some of the difference might be explained by a slightly different texture in the 9x9 and 10x10 cladding due to different diameter reductions during the fabrication process.

As discussed in Response 23, the creep component uncertainty is used in the methodology but not the growth uncertainty which is of lesser overall importance. Using a 9x9 growth correlation, although not a strong factor, might produce a conservative bias in the 10X10 gas pressure analysis.

III. Code Application

The following are from the review of BAW-10247(P) unless otherwise stated.

Question 21:

What is the minimum number of axial and radial regions (nodes) used for licensing calculations (Section 4.1 of EMF-2994(P)) and how are the former related to control rod withdrawal?

Response 21:

[

]

Question 22:

The application of the code does not mention use for initializing stored energy for LOCA. Please confirm that the code will not be used for stored energy and discuss the code that will be used to determine fuel stored energy for initializing LOCA analyses.

Response 22:

The code RODEX4 will not be used for LOCA analyses at this time. It may be used in the future but a separate submittal will be made for that use.

The current NRC approved BWR LOCA methodology (EMF-2361PA) uses the code RODEX2 for LOCA analyses.

Question 23:

The model parameter uncertainties are provided for only three parameters, however, there are several other model parameters that are known to impact fuel performance calculations for normal operation such as fuel thermal expansion, densification and swelling to name a few. These three parameters are important for both rod pressure and cladding deformation analyses. Another parameter important for cladding collapse analyses is cladding ovality. Please provide a justification of why the uncertainties in these model parameters are not included (Section 2.3.4). Please perform a sensitivity analysis to show the effect of these parameters on rod pressure (include axial rod growth in the rod pressure sensitivity analysis) and cladding deformation, e.g., strain increment and axial gap formation, analyses at various burnup levels.

Response 23:

The response to this question will be provided at a later date.

Question 24:

Many of the models in the code and the code predictions will have different error distributions (and perhaps biases) at different burnup and power levels (see RAI #8 for a possible bias in FGR), however, the statistical analysis presented appears to ignore this variation in error and bias. Please provide justification on why it is acceptable to ignore these variations.

Response 24:

The code was calibrated as best-estimate, i.e. with no overall bias and as little bias as possible for any sub-interval of the application domain. Nevertheless, it is impossible to avoid small local biases. However, these negligible local biases are included in the overall uncertainty. A slight local bias is typically coupled with a smaller scatter, so that the overall uncertainty covers this adequately within the framework of the random sampling (see answer 8a). FGR is a function of the power history and a large number of additional parameters. The main modeling parameter was selected as the [] This model parameter uncertainty represents the collective action of all the other contributing parameters.

The uncertainty of this model parameter was determined from the set of differences between predictions and measurements []
The differences between predictions and measurements were characterized in a normalized manner, i.e. the ratio of predicted over measured. In order to assure symmetry around the best agreement line, the log of the ratio was used as the normalized agreement factor. As seen in Figure 6.1 of EMF-3014(P), the scatter of this normalized agreement factor is larger at low FGR than at high FGR. Of course a higher uncertainty is tolerable at low FGR. Nevertheless, the use of the whole set [] for the determination of the FGR model parameter uncertainty assures that a conservative value is evaluated for the high FGR domain. Therefore, the local small under predictive bias at high FGR is covered by the globally estimated variance which is larger than the local variance.

Question 25:

Random errors due to uncertainties can sometimes be of lesser importance in Monte Carlo (random error) analyses than biases in the data, particularly when you are interested in the extremes of the data. Have sensitivity analyses been performed to determine the impact for a given bias (e.g., see RAI's #4, 5, 6, 8, 12, 13, 15, 17 and 24) on the predicted outcome of analyses in Section 6 of BAW-10247? In like manner have sensitivity analyses been performed to examine the impact of an increase in uncertainties on the predicted outcome? If not please provide these sensitivity analyses for how biases and increases in parameter uncertainties in the diffusion coefficient, irradiation creep model and cladding oxidation impact licensing analyses.

a For example, please assume that the gas atom diffusion coefficient provided in EMF-2994 and EMF-3014 is currently biased low and needs to be increased by a factor of 1.5 (uncertainty remains unchanged) and determine how this impacts the rod pressure analyses for BWR-6 and BWR-4 plants presented in Section 6 of BAW-10247. Please assume that the uncertainty on the diffusion coefficient is 20% higher than assumed in the rod pressure analyses in Section 6 (no bias).

b Please assume that the irradiation creep model is biased 33% (1.33) higher and 33% (0.67) lower than currently assumed and show how this impacts column gap formation and creep collapse analysis. Please assume the uncertainty in the irradiation creep model is a factor of 2 higher than assumed and show how this impacts column gap formation and creep collapse.

c Please assume that the cladding ovality model is biased (also assume an uncertainty exists in this model) and show how this impacts column gap formation and creep collapse analysis.

d Please perform similar sensitivity analyses for cladding steady strain and strain increments as a function of burnup. For these sensitivity analyses assume that the following on an individual basis, the fuel thermal expansion is 15% higher than assumed and solid fuel swelling is 50% higher than assumed. Also perform analyses assuming the thermal creep is 20% higher than assumed.

e Please perform similar analyses for fuel melting assuming that fuel thermal conductivity is biased 20% lower than assumed and the uncertainty in fuel thermal conductivity is 50% higher than assumed (bias and uncertainty effects should be separate).

Response 25:

The Response these questions will be provided at a later date.

Question 26:

The non-parametric terminology applies to using the most extreme result of 2995 realizations. However, when input distributions are assumed to be normal or uniform, the approach has become parametric since such parametric distributions are being fit to empirical/historical data. A truly non-parametric approach might simply select repeatedly sample/historical values from the data itself. Then the parametric distributions of the input quantities do not need to be determined. If sufficient data are not available over the range of interest, then fitting a distribution can offer an uncertain outcome. And if a vector of input values is available, such as a whole set of manufacturing information for a rod, then randomly selecting such a vector of values takes care of the correlation aspect. This assumes independence of the vector components, and if they are not independent this may not result in a valid outcome. Please discuss (with examples) correlations that may exist between the input data, power and model uncertainties and how these may impact the probability distributions that are calculated.

Response 26:Statistical methodology

The "non-parametric" terminology refers to the statistical method used to evaluate the extreme values of the distribution of the code outputs of interest. The non-parametric order statistic technique was developed in order to determine a certain quantile of a population from a sample without the need to know or assume a particular distribution for the population.

The population in our case is, for example, the set of life-maximum fuel rod internal gas pressure code calculations for all possible fuel rods from all possible cores. Each fuel rod/power history has a distribution of its internal gas pressures and all individual distributions

are lumped into the overall distribution that is analyzed in the methodology in terms of the global 99.9% statement.

The distribution of the individual calculation values for the various criteria is the result of the uncertainty in input parameters which were classified as manufacturing, power history and model parameters. In order to have a representative sampling of these parameters a random sampling of the individual populations was performed.

The characteristics of the population in this case are defined by the manufacturing records. Samples from each lot of fuel pellets or cladding are statistically characterized and these data have been processed to estimate with high confidence levels the population in terms of distribution: average and standard deviation. The only possible approach to sample the overall population is to randomly sample the determined distribution of the respective parameter. Again, this overall population is only known in a statistical sense, as only a limited number of samples are measured and/or recorded from each lot or batch.

[

]

[

[

]









Question 27:

Please provide a detailed description of the methodology used to subtract the rod power uncertainty from the model parameter uncertainties. Please provide an example. Also, there is a difference in dimensional and power uncertainties between experimental and commercial rod data. Are these differences applied in the calibration of the models and the statistical analyses of uncertainties and if so how is this done? Also some experimental rods will have lower uncertainties than others, are these differences considered in the calibration of the models and statistical analyses of uncertainties?

Response 27:

The code response function for a particular output of interest, Y, can be characterized through benchmarking by the following function describing the comparison between calculations and measurements:

$$Y = \text{Log}[C/M] \quad (27.1)$$

In the above formula, C, is a calculated value corresponding to the measured value, M. The dependent variable Y and the independent variables C and M can be any of the fuel code's

critical outputs of interest, and in the following it was applied to the fission gas release. The mathematical form chosen has the advantage of providing a symmetrical distribution of the comparison values around the perfect agreement value of zero; an over prediction by a factor of x , and an under prediction by a factor of $1/x$, will be represented as the symmetrical values $+\log(x)$ and $-\log(x)$, respectively.

The parameters affecting the outcome of the code calculation can be classified as either environmental, fabrication, or modeling parameters. The first group, namely environmental, consists of factors associated with irradiation and cooling conditions and the second with fuel rod characterization. The modeling parameters group includes the critical parameters in key models which affect the most the particular output.

All of these parameters are considered in a normalized manner, i.e. the ratio of the current value to the nominal value. This relative variation is suitable to uncertainty analyses and studies and the modeling parameter nominal values are those arrived at through the calibration process.

The most important environmental parameter is the linear heat generation rate, P , while the most important modeling parameter affecting fission gas release is, D , the effective diffusion coefficient for noble gas atom intragranular diffusion. All the other uncertainties will be incorporated in the uncertainty derived for the effective diffusion coefficient, because not enough information is available in order to quantify these other uncertainties.

With the above simplifications, a first order uncertainty analysis can be carried out in order to unfold the model parameter uncertainty, as follows. Using the notations described above the output variable Y can be written, in general, as function of P and D :

$$Y = f(P, D) \quad (27.2)$$

By expanding f in a Taylor series, truncated after the first order terms, Y can be approximated by a linear form as:

$$Y - Y_0 = S_P \cdot (P - P_0) + S_D \cdot (D - D_0) \quad (27.3)$$

where, S_P and S_D are the partial derivatives of Y with respect to P and D , known also as sensitivity coefficients.

The variance and standard deviation can be easily calculated from Equation (27.3) and, standard statistics textbook results are:

$$ST^2(Y) = S_P^2 ST^2(P) + S_D^2 ST^2(D) \quad (27.4)$$

The standard deviation of the output of interest Y , $ST(Y)$, can easily be estimated from the calibration results and the linear heat generation rate standard deviation, $ST(P)$, is available from uncertainty studies for neutronics codes and measurements. The partial derivative coefficients can be estimated numerically by repeating the benchmarking calculations with slightly modified values of P and D . Then, the desired model parameter uncertainty, $ST(D)$ can be deduced from Equation (27.4), as:

$$ST(D) = [ST^2(Y) - S_P^2 ST^2(P)]^{0.5} / S_D \quad (27.5)$$

This is applied as a multiplication adjustment factor to the best-estimate value of the diffusion coefficient.

In most cases all applicable data were used to determine uncertainties. When sufficient data was available from the International data set alone to determine uncertainties, this was done so that a more precise uncertainty range could be established. In cases such as creep or corrosion of AREVA NP rods the commercial data set was used. In all cases no special treatment was applied for the cases with known lower experimental uncertainty. The upper bound of the typical experimental uncertainty was conservatively applied to all cases.

The use of the data for each parameter is described in Section 4.2 of BAW-10247(P) and is summarized below:

Centerline temperature

All data are from experimental rods. Measured dimensions, creep, corrosion and powers were used. Any measurement uncertainties of these parameters were reflected in the measured/calculated results.

Fission gas release

The experimental (International database) rods with greater than [] release as described in 5.4.1 were used to develop the fission product release uncertainty. They were evaluated with measured dimensions. Dimensional measurement uncertainty is thus reflected in the measured/calculated results. A power uncertainty was introduced based on the experimental reports of power uncertainty. It was used so as to separate out the effects of power and fission product model uncertainties on the fission gas release results. Measured or specified dimensions and powers of the commercial rods were used also with the same power uncertainty to confirm the best estimate fit of the commercial rod database results.

Clad creep

Commercial rod creepdown measurements were used. Initial dimensional uncertainties and operational power uncertainties are reflected in the measured /calculated results. Because of the large dimensional uncertainty (see 5.4.2), the thermal creep data were used to develop the thermal and irradiation creep uncertainty.

Creep ovality

Measured ovalities of commercial rods are used. The measured/calculated response may reflect additional dimensional or power measurement uncertainty.

Ramp strain

The best characterized rods with the highest strain and burnup were used to verify best estimate behavior. Any dimensional and power uncertainty is reflected in the measured/calculated results.

Axial elongation

The commercial rod results were used to verify best estimate response. Dimensional and power uncertainties are reflected in the results. No uncertainty was derived as the creep uncertainty already affects the elongation. These elongation results are not used in the fuel bundle methodology.

Rod free volume

International and commercial cases are used. Dimensional and power uncertainties are reflected in the measured/calculated results. No uncertainty is developed.

Clad oxidation

Commercial results are used. Power uncertainties are reflected in the results. Both power and crud deposition uncertainties are reflected in the oxidation uncertainty.

Question 28:

The following address the application and accuracy of transient analyses.

Question 28a:

How does the code determine whether to use the steady-state or transient temperature solution?

Response 28a:

[

]

Question 28b:

Please provide a plot of the difference between the transient analytical and code predicted centerline temperatures in terms of the percent difference as a function of time to illustrate the accuracy of the transient solution (Figure 3.1, (Section 3.2, EMF-3014(P)). Provide this same plot for the mid-radius temperatures. Please provide an example of how calculation of the analytical solution is performed such that it can be duplicated by an independent party.

Response 28b:

The requested information is shown in the two figures below. An example is presented in EMF-3014 which was calculated in Excel (which has Bessel function capability) and by truncating the series to the first six terms.





Question 29:

The following address the application of power transients on fuel rod internal pressure analyses.

Question 29a:

Are normal operational transients included in the rod pressure analysis? If so, please provide an example (see RAI# 32). If not please explain why these transients are not considered and an example of the impact of an operational transient at moderate burnup (30 GWd/MTU) and high burnup (55GWd/MTU) on rod internal pressure.

Response 29a:

The realistic power histories as calculated with the reactor simulator code include the normal operational maneuvers as defined by the control rod sequence exchanges. The exchanges depend on the reactor history, but are usually at intervals of 1300 to 3300 MWD/MTU of cycle burnup. Assemblies are typically in controlled cells and significantly affected by the control blade moves for about half their life. [

]

[

]

Additional maneuvers can occur during normal operation which would generally be a reduction in power or shutdown for some reason and a return to approximately the same power. Other events could be infrequent transients controlled within the LHGR limit. These events are not included in the evaluated histories.

This is because the uncertainties applied at the times of the projected blade moves are expected 1) to cause equal or greater power changes than events with a recovery from a power reduction or shutdown to the same power distribution, 2) because the uncertainty of the projected moves includes a range extending to the LHGR limit which would encompass infrequent transients, 3) because the power uncertainties are applied over the full length of each exchange interval resulting in a stronger effect on gas release than a typical transient, and 4) because the number of sequence exchange uncertainties applied, [

] approximately represent the typical reactor

power reduction cycles.

The sensitivity studies, Table 6.4 of BAW-10247(P), show a nominal evaluation of a BWR-6 and the same evaluation with the introduction of the sequence exchange power uncertainties. The maximum gas pressure result is [] for the nominal case and [] with the application of the power uncertainties.

The design transients (AOOs), which go above the LHGR limit, are not included in the operational histories. These events, requiring an additional reactor system failure to occur, are rarely observed and are not put in the power histories (see also response 29b).

[

] we believe

the effect of additional reactor maneuvers and transients on the gas pressure analysis is encompassed by the power uncertainty application in the methodology.

Question 29b:

It appears that slow power transients (due to CRWE) are not included in the rod internal pressure analyses presented in Section 6. Please provide justification on why these transients are not included. Please provide rod internal pressure analyses that include slow power AOO events at 25, 35, 45 and 55 GWd/MTU.

Response 29b:

The rationale for the AOO category licensing requirements is the very small probability of occurrence of these AOO events, such as the CRWE transients. As defined in NRC Regulatory Guide 1.70, Chapter 15, 15.X.X Event Evaluation, these are incidents of moderate frequency, which may occur during a calendar year for a particular plant. The actual frequency is much less than 1 per year, which is the upper bound for that category. In reality, the vast majority of BWR power reactors have annunciators that promptly set off an alarm to notify the operators of any possible CRWE. We are not aware of any CRWE reported by utilities in the recent past experience.

The effect of CRWE on maximum internal rod gas pressure was determined by the studies described in Section 6.2.2 of BAW-10247(P), although the pressures were not reported. For the transition batch reported in Table 6.7 of BAW-10247(P) there is an increase in the maximum internal rod gas pressure as determined by the methodology of about []. For the equilibrium batch the UO₂ rods with CRWE in the first cycle show an increase of [] while all the other 3 remaining cases show a decrease of up to []. These pressure differences are applied to nominal pressures in the range of [] as shown in Table 6.6.

Therefore, we consider the CRWE impact on internal gas pressure a second-order effect.

Question 29c:

Section 5.4.5 mentions that an additional manufactured pellet grain size characterization uncertainty is used. This has not been mentioned in any of the other discussions on model uncertainties and appears to apply to the fission gas release model and the rod internal pressure analyses. Please discuss this uncertainty on the analysis of rod pressure and any other analyses that it might apply to.

Response 29c:

The grain size is a manufacturing parameter and it was mentioned in Section 5.3.4, as part of the list of manufacturing parameters whose uncertainties are considered in the methodology analyses.

The uncertainty of the fission gas release model parameter was derived from the international programs database, which had the grain size information well defined.

Therefore, the contribution of the grain size uncertainty is taken into account in the methodology analyses.

Question 30:

The following questions are related to the uncertainties applied to planned rod power operation for a specific plant and fuel batch.

Question 30a:

A statistical variation (uncertainty) is applied to possible deviations in rod powers from planned fuel management. It appears that this approach may not be appropriate if actual plant operation goes outside of its planned operation such that the peak rods are pushed closer to their fuel design limit. This implies that the mean of the distribution has been shifted for this fuel batch and would make the statistical assumptions in the earlier analysis no longer valid and non-conservative for this fuel batch. Please provide further justification including an example demonstrating that the use of an uncertainty on planned fuel management is acceptable.

Response 30a:

BWR fuel operation management, as practiced by the majority of the utilities, follows as closely as possible the projected control rod patterns. The reason for this is to have the licensing basis for the cycle remain valid during plant operation. Small departures from the design operation are allowed on a short term, local basis. These will not impact the overall power distribution histories.

The flow is generally maintained very closely to that assumed on the design. Typically, the flow is lower at the beginning of the cycle and the axial power profile is bottom peaked. Towards the end of the cycle when fuel burnup moves the axial power profile peaking toward the top, the flow is increased to compensate for the reduced fuel reactivity. In a BWR increased flow increases neutron moderation and causes a global power increase.

Even if the utility operators have another loading scheme, so that the location of the peak fuel rod is different, it will be equivalent from the statistical point of view.

The application examples are characterized by a table (see Table 6.1 in BAW-10247(P)) describing the basic reactor parameters: reactor power, core size, maximum flow rate, and fuel type, and batch parameters: cycle lengths, batch sizes, batch burnups and maximum assembly burnup. Given these basic parameters, or a small range on these parameters, the analysis will be applicable to a number of batches for the given reactor.

In the batch related parameters (see Table 6.1 and 6.4 in BAW-10247(P) of the application examples) the important parameters characterizing the batches analyzed are the cycle lengths and batch burnups. These parameters define the batch average power and do not vary from design so the licensing basis analyses for the cycle remain valid.

Within these basic batch parameters the possible deviations in fuel management can be encompassed with the described axial and radial power variations for each selected rod.

Question 30b:

It is stated at the bottom of page 6-3 that "the sampling of the different power histories in the core". This implies the sampling is from the entire fuel population in the core, however, aren't the licensing analyses performed on a fuel batch basis rather than an entire core because different fuel designs can be present (likely event for Framatome BWR fuel) within any given reactor. If the analyses are on a batch basis, shouldn't the power sampling be taken from the fuel batch in question and not from all the fuel in the core?

Response 30b:

Indeed the sampling is only from the set of power histories associated with the fuel batch which is being analyzed. The wrong impression was created by the statement at the bottom of page 6-3, which will be corrected. Nevertheless, everywhere else it is made very clear that the analysis is applied to the considered reload fuel batch.

Question 30c:

Please provide a power distribution for each of the BWR-6 and BWR-4 (transition batch) analyses provided in Section 6 at burnup levels of 0, 10, 20, 30, 40, 50 and 60 GWd/MTU.

Response 30c:

The response to this question will be provided at a later date.

Question 31:

The proposed maximum clad oxidation limit is greater than the NRC guideline of 100 microns (Page 3-1). The value used for the oxidation limit needs to be consistent with the model and data used to calibrate and verify this model (see RAI# 17). Please provide an explanation of how the oxidation data is obtained that is used for the oxidation model development. For example, oxidation measurements from eddy current consist of up to more than a thousand measurements per rod; are the data used for model development a running average over a particular length and circumference or are they individual measurements or are there different measurement approaches used for different fuel examinations? If they are an average for a given axial location please discuss what length and/or circumference are they averaged over? Are the oxidation data used for model development from the entire fuel rod length (or portions of the rod) or are they the maximum values at one location for each rod? Are all the data used for the oxidation model development measured in a consistent manner?

Response 31:

The NRC recommended limit of 100 microns in other vendor approvals is applied to design fuel rods with a nominal oxidation projection. The AREVA NP [

]

The oxidation data used for the submittal are span maximum values. Up to 8 values are reported for a fuel rod. Each span value is selected at the maximum oxide location in that span.

The span maximum values are typically 0 to 20 % greater than span average values in the 10x10 BWR data. Systematic axial profiles (as in a PWR which has a consistently increasing oxide thickness with clad temperature over the rod length) are not apparent. The oxidation equation and uncertainty developed from the span maximum values are appropriate for the maximum corrosion calculation. They are projected to be conservatively biased slightly high for temperature and gas release calculations.

Oxide measurement and data reduction approaches have evolved but the goal of the selection of a maximum over a short measurement distance has remained the same. The AREVA NP values up to 9x9 type fuel, have been derived from measurements via a running average over 40 mm of a helical scan in European reactors and for US and Asian reactors primarily by a

graphical reduction of the span maximum of a linear scan. Data reduced on the maximum running average basis were determined to be consistent with data reduced with a graphical selection of the local maximum for the same 9x9 fuel in the same exam. Linear scans of the same rod on different axis are sometimes performed and have been used as separate data for each scan. For 10x10 fuel the measurement techniques have been primarily a newer maximum running average over 50 mm for a linear scan in Europe, and the same graphical reduction of the linear scan in the US and Asia. The 10x10 data shown are a combination of these two methods.

The oxidation data are derived in a consistent manner. [

]

Question 32:

Details of the input used in each example analyses in Section 6 will need to be provided such as the best estimate values as well as uncertainties for the parameters included in the Monte Carlo analysis. For example, the following input and output is needed for analyses of the BWR-6 and BWR-4 Atrium-10 applications with standard cladding.

- a. *Please provide the input and output details (also see RAI# 29) of the mean prediction of rod pressure and the 99.9%/95% prediction. The input should include all of the necessary input including dimensional, rod power histories, axial power shapes and multiplier on the diffusion coefficient to perform an individual RODEX4 calculation for the mean and 99.9%/95% prediction. The output should include fuel centerline temperatures, gap conductance, effective diametral gap size, and fission gas release as a function of burnup.*
- b. *Please provide the same input and output for strain increment calculations for normal operation (mean and 99.9%/95%) and AOO's (mean and 95%/95%) for slow and fast transients at burnups of 10, 20, 30 and 40 GWd/MTU. For the strain calculations please provide additional output of densification, solid swelling, and gaseous swelling at these burnup levels. Is gaseous swelling calculated for these analyses or any other licensing analyses?*
- c. *Please provide the input and output details of the mean prediction and the 99.9%/95% prediction for the calculation of axial column gap due to cladding ovality. The output should include the fuel densification, solid swelling, effective diametral gap size, cladding creep and ovality, and burnup level at which axial gap and maximum ovality (cladding-fuel contact at two locations circumferentially) is calculated.*
- d. *Please provide the input and output details of the mean prediction and the 99.9%/95% prediction for the calculation of maximum cladding oxidation. The output should include the cladding oxidation, fuel centerline temperatures, gap conductance, and effective diametral gap size as a function of burnup.*
- e. *Please provide the input and output details of the mean and the 95%/95% prediction for the calculation of fuel melting for slow and fast transients (AOO's) at burnup levels of 0, 10, 20, 30 and 40 GWd/MTU.*

Response 32:

The input and output from the requested cases has been provided on the attached CD-ROM.

The response consists of sets of five files contained in 18 directories and 6 spreadsheets containing supplemental data and plots. The set of five files in each directory consist of a .txt file containing information to allow the auditors to create input decks for the audit code and four RODEX4 output files, ftn08, ftn24, ftn25, and ftn26. The directories are listed in the following table.

Directory Name	.txt File Name	Sub-Question
bwr4_uo2_110_max_oxide	bwr4_uo2_110_nom_max_oxide.txt	32d
bwr4_uo2_110_max_pressure	bwr4_uo2_100_nom_maxp.txt	32a
bwr4_uo2_110_max_strain_incr	bwr4_uo2_110_nom_max_dstrain.txt	32b
bwr4_uo2_crwe_max_strain_incr	bwr4_uo2_crwe_nom_max_dstrain.txt	32b
bwr4_uo2_crwe_max_temperature	bwr4_uo2_crwe_nom_max_temp.txt	32e
bwr4_uo2_max_oxide	bwr4_uo2_nom_max_oxide.txt	32d
bwr4_uo2_max_pressure	bwr4_uo2_nom_maxp.txt	32a
bwr4_uo2_max_strain_incr	bwr4_uo2_nom_max_dstrain.txt	32b
bwr4_uo2_rxa_max_oxide	bwr4_uo2_rxa_nom_max_oxide.txt	32d
bwr4_uo2_rxa_max_pressure	bwr4_uo2_rxa_nom_maxp.txt	32a
bwr4_uo2_rxa_max_strain_incr	bwr4_uo2_rxa_nom_max_dstrain.txt	32b
bwr6_gad_max_pressure_and_oxide	bwr6_gad_nom_maxp.txt	32a, 32d
bwr6_gad_max_strain_incr	bwr6_gad_nom_max_dstrain.txt	32b
bwr6_uo2_max_pressure_and_oxide	bwr6_uo2_nom_max_press_and_oxide.txt	32a, 32d
bwr6_uo2_max_strain_incr	bwr6_uo2_nom_max_dstrain.txt	32b
bwr6_uo2_rxa_max_oxide	bwr6_uo2_rxa_nom_max_oxide.txt	32d
bwr6_uo2_rxa_max_pressure	bwr6_uo2_rxa_nom_maxp.txt	32a
bwr6_uo2_rxa_max_strain_incr	bwr6_uo2_rxa_nom_max_dstrain.txt	32b

Six spreadsheets were produced to generate plots of clad creep strain and oxidation. The spreadsheets and the corresponding sub-questions are listed below.

Spreadsheet	Plot	Sub-Question
BWR4_UO2_CRWE_Clad_Hoop_Strain.xls	Clad Hoop Strain	32b
BWR4_UO2_Clad_Hoop_Strain.xls	Clad Hoop Strain	32b
BWR4_UO2_Max_Oxide.xls	Clad Oxide	32d
BWR4_UO2_OverPow_Clad_Hoop_Strain.xls	Clad Hoop Strain	32b
BWR4_UO2_OverPow_Oxide.xls	Clad Oxide	32d
BWR4_UO2_RXA_Clad_Hoop_Strain.xls	Clad Hoop Strain	32b



November 7, 2006
NRC:06:048

Document Control Desk
U.S. Nuclear Regulatory Commission
Washington, D.C. 20555-0001

Response to a Request for Additional Information Regarding BAW-10247(P), "Realistic Thermal-Mechanical Fuel Rod Methodology for Boiling Water Reactors"

Ref.: 1. Letter, James F. Mallay (AREVA NP) to Document Control Desk (NRC), "Request for Review and Approval BAW-10247(P), 'Realistic Thermal-Mechanical Fuel Rod Methodology for Boiling Water Reactors'," NRC:04:047, August 19, 2004.

Ref.: 2. Letter, Ronnie L. Gardner (AREVA NP) to Document Control Desk (NRC), "Additional Information for the Review of BAW-10247P Revision 0, 'Realistic Thermal-Mechanical Fuel Rod Methodology for Boiling Water Reactors'," NRC:06:030, July 7, 2006.

AREVA NP Inc. requested the NRC's review and approval of the topical report BAW-10247P Revision 0, "Realistic Thermal-Mechanical Fuel Rod Methodology for Boiling Water Reactors," in Reference 1. A partial response to a request for additional (RAI) on the topical report was provided in Reference 2. This letter provides the remaining portion of the response to the RAI.

AREVA NP considers some of the information in the attachments to this letter to be proprietary. The affidavit provided with the original submittal of this topical report satisfies the requirements of 10 CFR 2.390(b) to support the withholding of the proprietary information from public disclosure.

Sincerely,

A handwritten signature in cursive script that reads "Ronnie L. Gardner".

Ronnie L. Gardner, Manager
Site Operations and Regulatory Affairs
AREVA NP Inc.

cc: H. D. Cruz
J. H. Thompson
Project 728

AREVA NP INC.
An AREVA and Siemens company

3315 Old Forest Road, P.O. Box 10935 Lynchburg, VA 24506-0935
Tel: 434 832 3000 - Fax: 434 832 3840 - www.aveva.com

**Response to Request for
Additional Information – BAW-10247(P)**

(Second Part of Responses to First RAI)

I. General Code Modeling

Question 1:

For question and response see BAW-10247Q1(P) Revision 000.

Question 2:

For question and response see BAW-10247Q1(P) Revision 000.

II. Specific Parameter Models in Code

Question 3:

For question and response see BAW-10247Q1(P) Revision 000.

Question 4

The following are on the thermal calculations and the need for additional comparisons to integral thermal data (fuel centerline temperature measurements) to verify the integral thermal calculation. The thermal analysis methodology assumes that the fuel pellet is eccentric within the fuel cladding for commercial fuel rods while for calibration to experimental fuel rods with centerline thermocouples the code assumes that the fuel pellet is more concentric within the cladding (the fuel thermal conductivity appears to be increased early-in-life to compensate for the greater temperature drop across the fuel-cladding gap, see RAI #6). This assumption may be non-conservative for fuel temperatures in commercial fuel rods (results in biased lower predicted fuel temperatures than experimental rods) and will need further justification with additional thermal predictive comparisons to fuel rods with central thermocouples. Please provide the following comparisons to fuel centerline temperature measurements taken early-in-life (burnup < 10 GWd/MTU) from Halden rods with helium, xenon or argon fill gases. Comparisons are needed for the Rod 4 of IFA-432 (xenon fill gas), and Rods 1 (helium) and 2 (argon) of IFA-633 for Ramp 1 as identified in the Halden report HWR-764. The comparisons to Rod 4 of IFA-432 should include predicted minus measured versus burnup up to 10 GWd/MTU while the comparisons to IFA-633 Rods 1 and 2 (identical rods only fill gas is different) should be measured versus predicted for Ramp 1. A table of predicted and measured centerline temperatures along with predicted fuel surface temperatures and effective gap conductance values for these three rods needs to be provided. Please provide an estimate of the correction in fuel surface and centerline temperature between the eccentric and less concentric configurations for IFA-432 Rod 4, and IFA-633 Rods 1 and 2 as a function of linear heat generation rate (LHGR). Please provide this same information for the current Atrium 10 fuel design as a function of LHGR taking into account the effects of fission gas release (FGR) on gap conductance.

Response 4:

The thermal analysis methodology assumes that the fuel pellet column is eccentric in the rod based on manufacturing considerations. [

Response to Request for
Additional Information – BAW-10247(P)

[

]

Table 4-1 Fractional Fission Gas Release



Figure 4-1 [

]

**Figure 4-2 ATRIUM 10 Fuel at the Constant LHGR of 20 kW/m
Effect of Pellet Eccentricity on Fuel Centerline and Surface Temperatures**

**Figure 4-3 ATRIUM 10 Fuel at the Constant LHGR of 25 kW/m
Effect of Pellet Eccentricity on Fuel Centerline and Surface Temperatures**



**Figure 4-4 ATRIUM 10 Fuel at the Constant LHGR of 30 kW/m
Effect of Pellet Eccentricity on Fuel Centerline and Surface Temperatures**



**Figure 4-5 ATRIUM 10 Fuel at the Constant LHGR of 35 kW/m
Effect of Pellet Eccentricity on Fuel Centerline and Surface Temperatures**



**Figure 4-6 ATRIUM 10 Fuel at the Constant LHGR of 40 kW/m
Effect of Pellet Eccentricity on Fuel Centerline and Surface Temperatures**



**Figure 4-7 ATRIUM 10 Fuel at the Constant LHGR of 44 kW/m
Effect of Pellet Eccentricity on Fuel Centerline and Surface Temperatures**

Question 5

The following questions are related to the code comparisons to fuel centerline temperature data provided in EMF-3014(P).

Questions 5a, 5c, 5d, 5e:

For questions and responses see BAW-10247Q1(P) Revision 000.

Question 5b:

Examining all of the predictions of the upper thermocouple positions in the tables and also the predictions compared to measurements at high temperatures (Figure 5.35) it appears that the code may provide a biased under prediction of fuel temperatures when centerline temperatures are above 1400 °C. Please provide a plot of predicted minus measured temperatures versus measured temperature and similar plot versus burnup for measured temperatures only above 1350 °C. Also, provide a table of experimental rods with measured temperatures above 1350 °C providing the measured and predicted values along with the burnup level.

Response 5b:

The requested plots are provided in the two figures below. As can be seen from the Figure 5b-1 a slight under prediction is noticeable. [

]

Table 5b-1 Exposure Dependent Statistics

Figure 5b-1 Data Set with T > 1350 °C

Figure 5b-2 Data set with T > 1350 C

Questions 6a, 6b, and 6c:

For questions and responses see BAW-10247Q1(P) Revision 000.

Question 7:

The following questions are related to understanding the fission gas release model (EMF-2994(P)).

Questions 7a, 7b, 7c, and 7d:

For questions and responses see BAW-10247Q1(P) Revision 000.

Question 7e:

Please provide FGR predictions as a function of burnup up to 75 GWd/MTU at isothermal temperatures of 800 to 1400 °C in 100 °C increments with no fuel-cladding contact pressure and with maximum contact pressure. Also provide FGR predictions for one axial node as a function of time (at 20 minutes, 1 hour, 24 hours and 48 hours) for 3 power ramps with an initial starting power at 20 kW/m ramped to terminal powers of 35, 40 and 45 kW/m for each of two burnup levels of 30 GWd/MTU and 60 GWd/MTU for a BWR design (base irradiation rod

powers, prior to the ramp, to these burnups should be 20 kW/m to keep FGR low). The calculated fuel surface and centerline temperatures at terminal powers at 20 minutes and 24 hours need to be provided for each power ramp (Section 5.8).

Response 7e:

[

]

Figure 7e-1 Fission Gas Release For Zero Hydrostatic Pressure and 7 μm mli grain size



Figure 7e-2 Fission Gas Release for 40 MPa Hydrostatic Pressure and 7 μm mli grain size



Figure 7e-3 Fission Gas Release For Zero Hydrostatic Pressure and 15 μm mli grain size

**Figure 7e-4 Fission Gas Release for 40 MPa Hydrostatic Pressure and
15 μm mli grain size**

Figure 7e-5 Fission Gas Release for Power Ramps at a Burnup of 30 MWd/kgU



Figure 7e-6 Surface and Center Temperatures for Ramps at a Burnup of 30 MWd/kgU



Figure 7e-7 Fission Gas Release for Power Ramps at a Burnup of 60 MWd/kgU



Figure 7e-8 Surface and center temperatures for ramps at a burnup of 60 MWd/kgU

Question 8:

The following are related to determining whether a bias exists and the uncertainties in the prediction of fission gas release (FGR) for fuel performance analyses particularly the rod pressure analyses.

Question 8a:

For question and response see BAW-10247Q1(P) Revision 000.

Question 8b:

Also provide a histogram of FGR deviation on a linear scale for each of the international and commercial databases with measured FGR's above 5% and 10% release (Section 6.3, EMF-3014(P)).

Response 8b:

To supplement the plots provided in the BAW-10247Q1(P) Revision 000 response 8a histograms were prepared. The histograms for measured FGR's above 5% and 10% release are provided in Figure 8b-1 through 8b-4 for the full and optimized international database. These support the conclusions stated in the response to Question 8a.

Figure 8b-1 Histogram for FGR > 5%, International Programs

Figure 8b-2 Histogram for FGR > 10%, International Programs

Figure 8b-3 Histogram for FGR > 5%, International Programs – Optimized



Figure 8b-4 Histogram for FGR > 10%, International Programs - Optimized

Question 9:

The following are related to understanding the solid and gaseous swelling, densification and grain growth models (EMF-2994(P)).

Questions 9a and 9c:

For questions and responses see BAW-10247Q1(P) Revision 000.

Question 9b:

Please provide typical values used for P_u and P_s used in Equations 6.133 and 6.136, respectively. Please provide an example calculation of fuel swelling separating gaseous ($\Delta V/V_{gs}$) and macroscopic solid swelling ($\Delta V/V_{ss}$) using these values as a function of burnup at fixed isothermal temperatures of 800 °C, 1000 °C, 1200 °C and 1400 °C (for one radial node) (p. 5-57). The gaseous swelling model calculation should provide the values used for grain boundary bubble radius (r_b), surface density of grain boundary bubbles (N_{gb}), and grain diameter (d_{gr}), as a function of burnup and temperature.

Response 9b:

P_u is identified as the manufacturing variable B9 on p. 5-13 of BAW-10247 and its distribution is presented in Figure 5.2 of BAW-10247. [

]

Figure 9b-1 Gaseous Swelling for Zero Hydrostatic Pressure and 7 μm mli grain size

Figure 9b-2 Gaseous Swelling for 40 MPa Hydrostatic Pressure and 7 μm mli grain size



Figure 9b-3 Gaseous Swelling for Zero Hydrostatic Pressure and 15 μm mli grain size



Figure 9b-4 Gaseous Swelling for 40 MPa Hydrostatic Pressure and 15 μm mli grain size



Figure 9b-5 Solid Swelling for Zero MPa Hydrostatic Pressure and 7 μm mli grain size

Figure 9b-6 Solid Swelling for 40 MPa Hydrostatic Pressure and 7 μm mli grain size

Figure 9b-7 Solid Swelling for zero MPa Hydrostatic Pressure and 15 μm mli grain size

Figure 9b-8 Solid Swelling for 40 MPa Hydrostatic Pressure and 15 μm mli grain size

Question 10:

The following are related to validating the solid and gaseous swelling, grain growth models.

Question 10a:

The Halden data does not appear to have the solid swelling rate dependence on temperature as that calculated by the RODEX4 model. Please compare the solid swelling model to Halden experiments where solid swelling was measured both prior to a power ramp and following a power ramp such as for IFA-633 Rods 3 and 5 with UO₂ fuel.

Response 10a:

The IFA-633 Rods 3 and 5 are similar both as design/fabrication as well as power history. Also, the fuel pellet stack elongation measurements of the two fuel rods are similar. Therefore, only one RODEX4 run was performed. The Halden reports HWR-764 and HPR-832 as well as information received from PNNL were used to develop the input file and the power history.

There is no information on solid swelling prior to and after a power ramp. It is not possible to separately measure the solid swelling before and after a ramp, because what is measured (which applies to IFA-633) is the total fuel stack elongation or the cladding outer diameter. In either case, the measured fuel deformation is the combined effect of several processes of which solid swelling is just one.

[

]

Response to Request for
Additional Information – BAW-10247(P)

[

]

Figure 10a-1 [

]

Question 10b:

The gaseous swelling model is justified by comparison to four power ramped rods at relatively high burnups of 45 GWd/MTU and 62 GWd/MTU. EMF-3014(P) states that the large cladding deformation observed after the ramp testing cannot be explained by fuel thermal expansion only. The interpretation of the tests with RODEX4 showed that gaseous swelling contributed significantly to the deformation in the three Mark-BEB rods and one Super-Ramp rod. Please provide those analyses that demonstrate that gaseous swelling contributed to the measured strains in these rods, e.g., cladding strain predictions with and without gaseous swelling for these four rods.

Response 10b:

The figures for the Mark-BEB rods, showing ramp strain with and without the contribution of gaseous swelling, were provided in BAW-10247Q1(P) Revision 000. Additional rods were proposed for ramp strain analysis in BAW-10247Q1(P) Revision 000, Response 15a. In these rods as well, gaseous swelling contributes to the measured strains. The results for these rods and the original 4 cases reported in EMF-3014(P) are provided and discussed in the current revised response to Question 15a. This response includes calculated/measured ramp strain comparisons for the initial 4 cases and the 13 additional ramp test cases.

Question 10c:

Please provide fuel grain growth predictions of irradiated fuel data from the following references: J. A. Turnbull J., Nucl. Mater. 50, 1974 (62-68); C. Bagger et al., J. Nucl. Mater. 211, 1994 (11); Hargreaves and NewBigging data presented by J. B. Ainscough et al., J. Nucl. Mater. 49, 1973 (117).

Response 10c:**Turnbull reference (CEGB Grain Growth Experiment):**

The capsule irradiation of the CEGB grain growth samples was modeled using RODEX4 with the appropriate fuel parameters, power and time conditions. Since the capsule was electrically heated, the temperatures were established with a special RODEX4 input allowing imposition of the temperatures in each ring of the pellet region. The resultant pellet grain size, swelling, and gas release were calculated.

The power for the 3 mm diameter pellet was established at 1.9 kw/m so as to produce the reported burnup of 0.4% FIMA in 143.3 days. This is consistent with the time on the plot. [

]

Response to Request for
Additional Information – BAW-10247(P)

[

]

Table 10c-1 Comparative Results 7 micron Samples

Table 10c-2 Comparative Results for 40 micron Samples**Bagger et al. reference (Measured Grain Size after Riso AN2 Bump Test):**

The C. Bagger et al. reference refers to the PIE grain size measurements of the AN2 Bump Test of the Third Riso Fission Gas Project. This is at a burnup of 41.54 MWd/kgU and after a ramp to 39 kw/m. RODEX4 was run for the test rod AN2, referred to as CB6 in the project report, with the rod divided into 10 equal axial sections and 10 radial pellet sections. The RODEX4 results after the ramp are interpolated axially to the center of the CB6-9, CB6-19 and CB6-29 measurement sections. The RODEX4 results are plotted radially at the average radius of each of the 10 pellet radial zones. The RODEX4 results show overall good agreement when compared to the exam measurements in Figures 10c-1, 10c-2 and 10c-3.



Figure 10c-1 Comparison of AN2 Measured Grain Size Distribution after Ramping with RODEX4 Calculation (Section CB6-9)



Figure 10c–2 Comparison of AN2 Measured Grain Size Distribution after Ramping with RODEX4 Calculation (Section CB6-29)



Figure 10c-3 Comparison of AN2 Measured Grain Size Distribution after Ramping with RODEX4 Calculation (Section CB6-19)

Ainscough et al. Reference (Limiting Grain Size Projections) :

The J. B. Ainscough et al. reference develops equations for projecting grain size versus temperature and burnup. [

]

The calculation used to model the CEGB experiment (Turnbull reference above) was used to set up a matrix of RODEX4 calculations for the various temperatures and powers, and for the starting grain size of 5 microns (mean linear intercept), to produce a matrix of limiting grain size results comparable to Table 14 of the Ainscough reference.

[

]

Table 10c-3 Effect of rating on limiting grain size

Summary 10c:

[

]

Questions 11:

The following are related to understanding the cladding creep equations used for determining creep collapse and gap closure due to irradiation creep (EMF-2994(P)).

Questions 11a, 11b, and 11c:

For questions and responses see BAW-10247Q1(P) Revision 000.

Question 12:

The following questions are related to the cladding creep data used to verify the creep and ovality models in RODEX4 (EMF-3014(P)).

Questions 12a, 12c, 12e, 12f, and 12g:

For questions and responses see BAW-10247Q1(P) Revision 000.

Question 12b:

The irradiated creep data used to determine the coefficients for the irradiation creep model are provided but the data used to determine the coefficients to the thermal creep model are not provided. Please provide either a justification on why the thermal creep model is not a significant contributor to licensing analyses or provide this data and thermal creep model comparisons to this data (Section 7.1).

Response 12b:

Cladding total creep is the sum of two components: thermal creep and irradiation induced creep. Irradiation induced creep is the dominant component at low stress. This happens during steady state operation when the stress in the cladding results from the pressure differential between the inside and the outside of the cladding. In ATRIUM 10 fuel the absolute value of the hoop stress is then of the order of 50 to 60 MPa. By contrast, thermal creep is dominant during severe pellet-cladding mechanical interaction (PCI) when the hoop stress reaches values above 200 MPa.

During steady-state operation thermal creep is generally limited (less than 0.2%). Thermal creep is essentially primary creep. Its contribution is significant only at very low burnup when zircaloy strain hardening and irradiation hardening are not yet effective. After a few months secondary irradiation creep controls cladding creep down before gap closure and slow creep out after gap closure.

During a fast power ramp in strong PCI conditions the time is too short for irradiation creep to be effective. The cladding deformation is then controlled by thermal creep only.

The thermal creep parameters of AREVA NP (SPC) CWSR (SRA) zircaloy cladding were derived from 48 mechanical tests, 22 carried out on non-irradiated material and 26 on irradiated material in the frame of the ZODIAC program.

ZODIAC (Zircaloy High Dose Irradiation and Creep) is an international program managed by BELGONUCLEAIRE to study the zircaloy cladding mechanical properties. Only partial results of the ZODIAC program have been published so far (M. R. Billaux, V. I. Arimescu, F. Sontheimer & H. Landskron, "Fuel and Cladding Properties at High Burnup," International Topical Meeting on Light Water Reactor Fuel Performance, Park City, Utah, April 10-13, 2000.)

The following pages provide a summary of an evaluation of this data. The summary includes:

- A description of the tested material,
- A brief description of the mechanical tests,
- The essential test results,
- The methodology used to derive the creep parameters from the test results,
- The values of the creep parameters, and
- The verification and validation of the creep parameters.

This verification and validation work shows that the RODEX4 thermal creep model is valid at both low and high stress. It is able to reproduce all the results of the out-of-reactor mechanical tests on non-irradiated and irradiated AREVA NP zircaloy cladding with a reasonable accuracy. This includes:

- Uniaxial (z) tensile tests,
- Biaxial (θ, z) tensile tests,
- Uniaxial (z) creep tests,
- Biaxial (θ, z) creep tests, and
- Uniaxial (z) relaxation tests.

1.0 Analysis of Mechanical Tests on AREVA NP Material

1.1 AREVA NP Material

[

]

[

]

1.2 ***Rod Characterization and Irradiation History***

[

]

Table 12b-1 Characterization of the AREVA NP Fuel Rod



Table 12b-2 Post-Irradiation Data of AREVA NP Fuel





Figure 12b-1 Power History of AREVA NP Rods in Blayais 1



Figure 12b-2 Fast Fluence Axial Distribution in AREVA NP Rods

1.3 *PIE Creepdown Results*

[

]

1.4 *Mechanical Tests*

[

]

Table 12b-3 General Test Matrix on AREVA NP Cladding

1.4.1 Tensile Tests

[

]

Table 12b-4 Tensile Tests on AREVA NP Cladding

1.4.1.1 Uniaxial Tensile Tests

[

]

[

]

**Table 12b-5 Summary of the Uniaxial Tensile Test Results on AREVA NP
Material**



[

]

1.4.1.2 Biaxial Tensile Tests on Non-Irradiated Material

[

]

**Table 12b-6 Summary of the Biaxial Tensile Tests Results on
AREVA NP Non-Irradiated Material**

1.4.1.3 Biaxial Tensile Tests on Irradiated Material

**Table 12b-7 Biaxial Tensile Test Matrix for AREVA NP Irradiated
Material for Different Strain Rates**

Response to Request for
Additional Information – BAW-10247(P)

[

**Table 12b-8 Summary of the Biaxial Tensile Test Results on
AREVA NP Irradiated Material**



**Table 12b-9 Hoop Yield Stress from Biaxial Tensile Tests on
AREVA NP Irradiated Material (in MPa) for Different Strain Rates**





**Figure 12b-3 Synthesis of the Biaxial Tensile Test Results on
AREVA NP Cladding**

1.4.1.4 Summary

[

]

**Table 12b-10 Summary of the Yield Stress Results on
AREVA NP Material**

**Table 12b-12 Summary of the Uniaxial Creep Tests on
AREVA NP Material**

[

]

1.4.2.2 Biaxial Creep Tests on Non-Irradiated Material

[

]

**Table 12b-13 Summary of the Biaxial Creep Tests Results on
AREVA NP Non-Irradiated Material**

1.4.2.3 Biaxial Creep Tests on Irradiated Material

[

]

**Table 12b-14 Biaxial Creep Test Matrix for AREVA NP Irradiated
Material for Different Hoop Stresses**

[

]

1.4.3 Relaxation Tests

[

]

**Table 12b-15 Summary of the Biaxial Creep Test Results on
AREVA NP Irradiated Material**



**Table 12b-16 Time to Get 0.2% Hoop Permanent Strain of
AREVA NP Irradiated Material (in ks) for Different Hoop Stresses**



Table 12b-17 Relaxation Tests on AREVA NP Cladding





**Figure 12b-4 Primary Creep in Biaxial Creep Tests on
AREVA NP Irradiated Material**



**Figure 12b-5 Synthesis of the Biaxial Creep Test Results on
AREVA NP Irradiated Cladding**

2.0 Determination of the Model Parameters

2.1 *Computer Simulation of the Mechanical Tests*

[

]

2.2 Contractile Strain Ratios

[

]

**Table 12b-18 Contractile Strain Ratio Calculated
from Strain Measurements in Uniaxial Longitudinal
Tests on AREVA NP Irradiated Material**

┌

┐

Response to Request for
Additional Information – BAW-10247(P)

[

]

⌋

⌋

**Figure 12b-6 Hoop and Axial Strains in Uniaxial Longitudinal
Creep Tests on AREVA NP Irradiated Material**

[

]

[

]

Table 12b-19 Kearns and Anisotropy Factors of AREVA NP Materials

⌈

⌋

2.3 Determination of the Creep Model Parameters

[

]

[

]

Table 12b-20 Creep Parameters for AREVA NP Materials

[

]

Response to Request for
Additional Information – BAW-10247(P)

3.0 Verification and Validation

3.1 *Non-Irradiated Cladding*

3.1.1 Tensile tests

[

]

**Table 12b-21 Measured and Predicted Yield Stress of
AREVA NP Non-Irradiated Cladding**

[

]

Response to Request for
Additional Information – BAW-10247(P)

[]

3.1.2 Creep Tests

[]

**Table 12b-22 Measured and Predicted Creep Strain of
AREVA NP Non-Irradiated Cladding**

[]

3.2 Irradiated Cladding

3.2.1 Biaxial Tensile Tests

[]

[

]

**Table 12b-23 Measured and Predicted Yield Stress of AREVA NP
Irradiated Cladding**

3.2.2 Uniaxial Tensile Test

[

]

3.2.3 Biaxial Creep Tests

[

]

[

]

**Table 12b-24 Measured and Predicted Permanent Hoop Strain in
Biaxial Creep Tests on AREVA NP Irradiated Cladding**

3.2.4 Uniaxial Creep Tests

[

]

**Table 12b-25 Measured and Predicted Creep Strains in Uniaxial
Longitudinal Creep Tests on AREVA NP Irradiated Cladding**

3.2.5 Relaxation Tests

[

]

**Table 12b-26 Extent of Relaxation in the Relaxation Tests on
AREVA NP Cladding**

3.3 Rod Profilometry

[

]



**Figure 12b-7 Predicted and Measured Yield Stresses in
Biaxial Tensile Tests on AREVA NP Irradiated Cladding**



**Figure 12b-8 Predicted and Measured Time to Get 0.2% Permanent
Hoop Strain in Biaxial Creep Tests on AREVA NP Irradiated Cladding**

**Figure 12b-9 Calculated Stress Relaxation
of Non-Irradiated AREVA NP Sample ZS-2**

**Figure 12b-10 Calculated Stress Relaxation
of Irradiated AREVA NP Sample RXI**

**Figure 12b-11 Calculated Stress Relaxation
of Irradiated AREVA NP Sample RXN**

**Figure 12b-12 Calculated Stress Relaxation
of Irradiated AREVA NP Sample RXO**



**Figure 12b-13 Calculated and Measured Creepdown of
AREVA NP Rod A02**



**Figure 12b-14 Calculated and Measured Creepdown of
AREVA NP Rod T01**



**Figure 12b-15 Calculated and Measured Creepdown of
AREVA NP Rod U10**

Question 12d:

Examination of Figure 7.1 (9x9 fuel) suggests that cladding creepdown is not complete by a burnup of 35 GWd/MTU. Please provide further discussion on why creepdown is not complete because it is expected that cladding creepdown should be complete by this burnup level.

Response 12d:

The cladding creepdown, depending on the pellet properties, may continue until 45 MWd/kgU, after which an upturn in cladding deformation is observed. The UO₂ ADU/DC pellets for BWRs have densification/swelling properties that lead to an upturn in fuel deformation around 45 MWd/kgU. This is illustrated in Figure 12d-1 which presents the data from Figure 7.1 plotted vs. burnup.



Figure 12d-1 Diametral creepdown vs Burnup

The cladding creepdown evolution may be better illustrated if the fuel rod burnup is replaced by the local fast fluence as in the figure below, where the upturn in cladding deformation for both measurements and calculations is more apparent:

**Figure 12d-2 Diametral Creepdown vs Fluence****Question 13:**

The following are related to the assumption that the irradiation creep uncertainties are the same as the uncertainties in the thermal creep model. This assumption does not appear to be valid because the RODEX4 irradiation creep and thermal creep models are significantly different suggesting that the mechanisms for these two types of creep must be different. In addition, comparison of the irradiated creep model to irradiated creep data suggests that the uncertainty in irradiation creep is much greater than observed in thermal creep. This observation is based on the following model comparisons to irradiated creep data presented in EMF-3014(P) and BAW-10247(P).

Question 13a:

There does not appear to be a good correlation between predicted and measured creep in Figure 7.2 (9x9 fuel) and from Figure 7.3 the model under predicts creep in the 10x10 fuel designs at low fluences where creepdown is present. The small number of rods from which creep data were collected plus the large differences between predicted and measured creep (Figures 7.2 and 7.3) suggest that the model does not provide a valid mean of the data and, therefore, both the mean predictive uncertainty and overall uncertainty are very large (much larger, > factor of 3, than assumed for thermal creep).

Response 13a:

The large uncertainties in measured diameter are reflected in Figures 7.1 and 7.2 of EMF-3014(P) which influence the measured-predicted comparison. These uncertainties are in both the initial dimensions of the measured cladding and in the post-irradiation measurement of the outer cladding diameter. This accounts for the large horizontal scatter bands in the plots. This is also why the irradiation creep measurements were not used to establish the cladding creep uncertainty (see Section 5.4.2 of BAW-10247).

The larger 9x9 data set was used to establish the cladding creep rate and only confirmed with the 10x10 data shown in Figure 7.3. The free cladding creepdown data are well predicted. This is illustrated in Figures 12d-1 and 12d-2 of the Response 12 above. To further illustrate that the creepdown prediction is best-estimate Figure 13a-1 was prepared. It shows that the scatter of predicted/measured is the same over the fast fluence range.

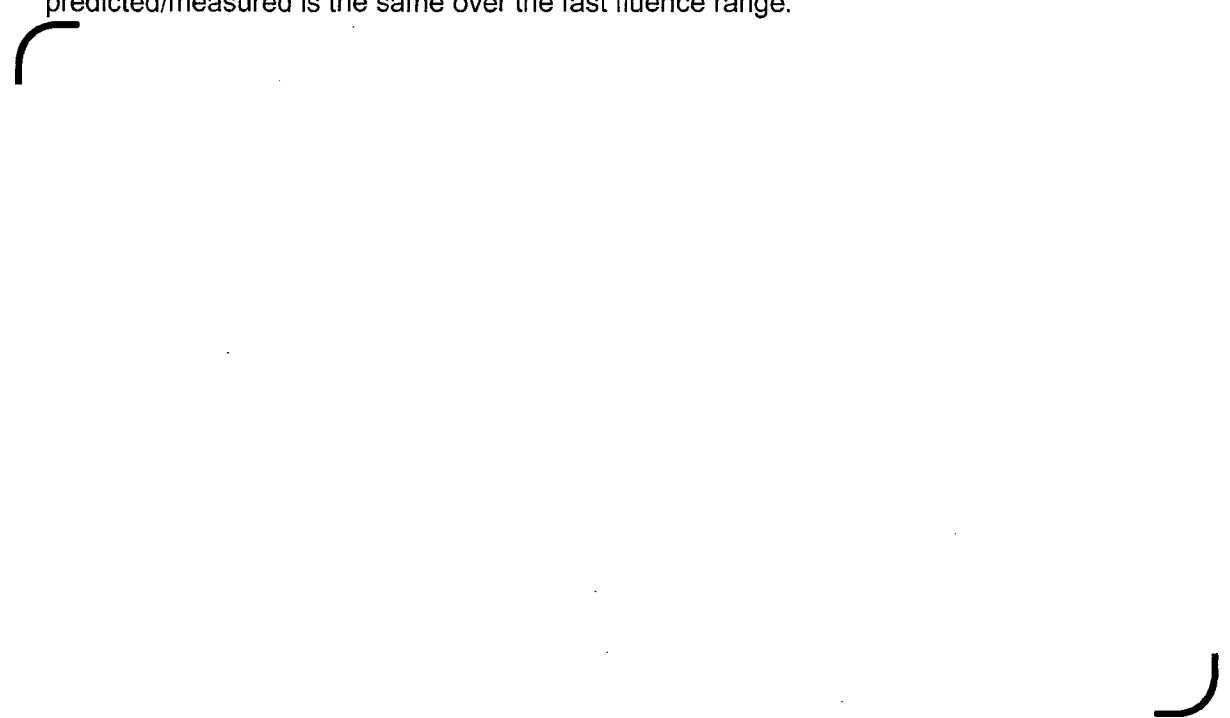
The figure area is mostly blank, with a large curved mark on the left side and a smaller curved mark on the right side.

Figure 13a-1 P/M Creepdown vs Fast Fluence

An additional figure, Figure 13a-2, is provided which, in addition to the data presented in EMF-3014(P), has new 10x10 data which have been acquired after the submittal. The new data spans the range from free creepdown to PCI. This figure illustrates that the 10x10 behavior is well predicted with the parameters derived for the larger 9x9 data set.

The improved prediction at high burnup (high fast fluence) as illustrated in Figure 13a-2 is due to improving the fuel pellet deformation evaluation by using a SWMDEN value (see response to Question 9b) of 0.975. This value better characterizes the 10x10 fuel pellets which are of more recent production.



Figure 13a-2 Creepdown including expanded data base

Question 13b:

In addition, the intended application for RODEX4 is the Atrium 10 fuel design with very little data and the small amount of data provided is not predicted well by the code. It is implied that the large uncertainty in the irradiated data is due to uncertainties in fuel rod dimensions in fabrication, however, further examination does not appear to support this assumption. The example of the uncertainty contribution of cladding fabrication dimensions to cladding creepdown only demonstrates a plus or minus of 15 μm (at a 2σ level) in Figure 5.6 of BAW-10274(P) while the scatter in the data in Figure 7.1 of EMF-3014(P) is plus or minus 40 μm and the uncertainty in Figure 7.2 of EMF-3014(P) is approximately plus 50 μm and minus 70 μm from the model predicted values. This suggests that the fabrication uncertainties offer only a small fraction of the uncertainty in the cladding creep model and combined with the assumed uncertainty for the irradiation cladding creep (same as thermal creep) does not adequately address the uncertainty in the predicted versus measured irradiated creep data. Please provide further irradiation creep data, analyses and or creep model modifications to demonstrate that the uncertainty in the irradiation creep model equals that for the thermal creep model.

Response 13b:

[This data as presented in Figure 5.6 of BAW-10274P are also illustrated by the group around a fast fluence of $4 \cdot 10^{21}$ n/cm² in Figure 7.3 of EMF-3014(P). These data are representative of diameter measurements and calculations during the free creepdown domain and therefore relevant for the derivation of creep uncertainty.

The larger scatters in Figures 7.1 and 7.2 of EMF-3014(P) are due to higher burnup data which are affected by larger uncertainties because of the compounded effect of fuel properties' variation. This is illustrated in the Figure 13b-1 below, where the data in Figures 7.1 and 7.2 of EMF-3014(P) are plotted as (calculated – measured) versus burnup. It is apparent that the maximum scatter is present when the pellet-to-cladding contact is established and remains for the "soft contact" period when strain reversal occurs.

Figure 13b-1 Predicted – Measured, diametral creep

Response to Request for
Additional Information – BAW-10247(P)

[

[

]

Table 13b-1 Thermal Creep Data



Table 13b-2 Creepdown Measurements



Questions 14a and 14 b:

For questions and responses see BAW-10247Q1(P) Revision 000.

Question 15:

The following are related to the lack of data used to verify the cladding deformation models.

Question 15a:

The code has been compared to measured deformation from only four power ramped rods. The comparison to these four tests does not provide a valid estimate of any bias nor the uncertainty in the code calculations of fuel rod deformation. There are considerably more power ramped rods with measured cladding deformation than the four rods provided including rods ramped in R3/R2, DR-2, BR-2 HFR-Petten and Halden, (Section 7.3.2, EMF-3014(P)). Please provide a proposed list of ramped rods for RODEX4 code comparisons. Of particular interest are those experimental ramped rods that are closest to the licensing conditions experienced during normal operation and slow transient (control rod withdrawal error) analysis of cladding strain, e.g., maximum strain is calculated when the fuel cladding gap is closed and the power range for this transient. Once an agreement is reached (between Framatome ANP, NRC and PNNL) on which rods should be used please provide these code to data comparisons. If power ramp data exist that are applicable to the strain analyses for fast transients (feedwater controller failure) these data comparisons should also be provided.

Response 15a:

A review of the profilometry recordings of ramp tested rods available in the AREVA NP calibration database was made as discussed under this question in BAW-10247Q1(P) Revision 000. This included the following projects:

- Inter-Ramp
- Over-Ramp
- Super-Ramp
- Super-Ramp Extension
- Super-Ramp II
- Risø TFGP
- Risø FGP3
- BAW Mark-BEB

The four rods presented in report EMF-3014(P) showed a cladding deformation of 1% or more during the ramp test: the Super-Ramp rod PK2/3 and the three BAW Mark-BEB rods. In these rods gaseous swelling plays a significant role.

Most BWR rods show only small cladding deformations after ramp (no more than a few micrometers). Sometimes the rod diameter after irradiation is larger than the reported as-fabricated diameter (Super-Ramp BG8, BG9 and BK7 series). For others, such as the Risø FGP3 GE or Super-Ramp II rods, the reported LHGRs are questionable (In the Risø FGP3 the

reported LHGRs are non-consistent with the temperature measurements; in Super-Ramp II repeated mass flow rate calibrations gave very different LHGR estimates).

The HFR-Petten LHGR data are in general less reliable than the Risø or Studsvik data (see discussion in DOE/ET/34030-4 CEND-402 Report, Appendix).

The more reliable data seem to be the PWR data from the Over-Ramp and Super-Ramp Programs, as well as data from the Risø FGP3 ANF rods.

In BAW-10247Q1(P) Revision 000 a list of additional ramp test rods which could be used to estimate the uncertainties in the cladding deformation predictions was provided. The RODEX4 calculations were performed for these rods. The rods are listed in Table 15a-1 with the 4 rods already described in EMF-3014(P). The calculation results are provided for all the rods.

Table 15a-1 – Ramp Test Rods for Evaluating Cladding Deformation Predictions

Program	Rod	Ramp Terminal Level (kW/m)	Hold Time
Over-Ramp	G20/1	42.0	24 h
	G20/2	44.5	24 h
	G20/3	48.2	10 min
	W5/1	44.5	16 min
	W5/2	37.0	24 h
Super-Ramp	PK1/1	41.5	12 h
	PK2/3	43.8	12 h
	PK4/1*	39.0	12 h
	PK4/2*	44.5	12 h
	PK6/2	40.0	12 h
	PW3/2	35.3	12 h
	PW3/4	37.2	12 min
Risø FGP3	AN2	44.4	61.7 h
	AN8	47.2	4.1 h
Mark-BEB	65-2	62.3	12 h
	65-4	62.4	12 h
	66-2	62.3	12 h

* gadolinia fuel

Calculations were performed with RODEX4 for the steady state and ramp test irradiations of these rods. Rod characteristics, irradiation parameters and measured results were taken from the program reports. Pellet and clad parameters derived from the reports were checked by comparison of the steady state calculation with the measurement results. Since the ramp programs include a variety of fuel types, the parameters were in some cases optimized consistent with the measured steady state creepdown.

The RODEX4 strain increment results provided at the end of the ramp tests show the difference between the pre-ramp and post-ramp axial strain profiles at pool side or hot cell measurement conditions. The calculated cladding diameters are corrected for cladding outer corrosion. Figures 15a-1 through 15a-17 show the results for the rods in the order listed in Table 15a-1.

Each plot shows four axial profiles: the measured and the RODEX4 calculated diameter change for the mid-pellet region and for the pellet end (ridge). The diameter changes are relative to clad diameters of about 10 mm, so a diameter increase of 100 μm approximates a clad strain value of 1%. The comparison of both mid pellet diameter change and pellet end ridge changes with the measurement results provides confirmation of the validity of the RODEX4 models.

The rods are divided into 10 or 12 axial nodes in the ramp regions. The nodal results give a smoothed curve in the Excel plots. The measured profiles were similarly divided into axial zones with the average of the mid-pellet measurements and the average of the pellet ridges determined for each zone. A smoothed "measurement" curve for the 10 or 12 zones is similarly plotted in Excel. [

]

Response to Request for
Additional Information – BAW-10247(P)

[

]



**Figure 15a-1 Over-Ramp Rod G20/1
Cladding Diameter Increase during the Ramp Test**



**Figure 15a-2 Over-Ramp Rod G20/2
Cladding Diameter Increase during the Ramp Test**



**Figure 15a-3 Over-Ramp Rod G20/3
Cladding Diameter Increase during the Ramp Test**



**Figure 15a-4 Over-Ramp Rod W5/1
Cladding Diameter Increase during the Ramp Test**



**Figure 15a-5 Over-Ramp Rod W5/2
Cladding Diameter Increase during the Ramp Test**



**Figure 15a-6 Super-Ramp Rod PK1/1
Cladding Diameter Increase during the Ramp Test**



**Figure 15a-7 Super-Ramp Rod PK2/3
Cladding Diameter Increase during the Ramp Test**



**Figure 15a-8 Super-Ramp Rod PK4/1
Cladding Diameter Increase during the Ramp Test**



**Figure 15a-9 Super-Ramp Rod PK4/2
Cladding Diameter Increase during the Ramp Test**



**Figure 15a-10 Super-Ramp Rod PK6/2
Cladding Diameter Increase during the Ramp Test**



**Figure 15a-11 Super-Ramp Rod PW3/2
Cladding Diameter Increase during the Ramp Test**



**Figure 15a-12 Super-Ramp Rod PW3/4
Cladding Diameter Increase during the Ramp Test**

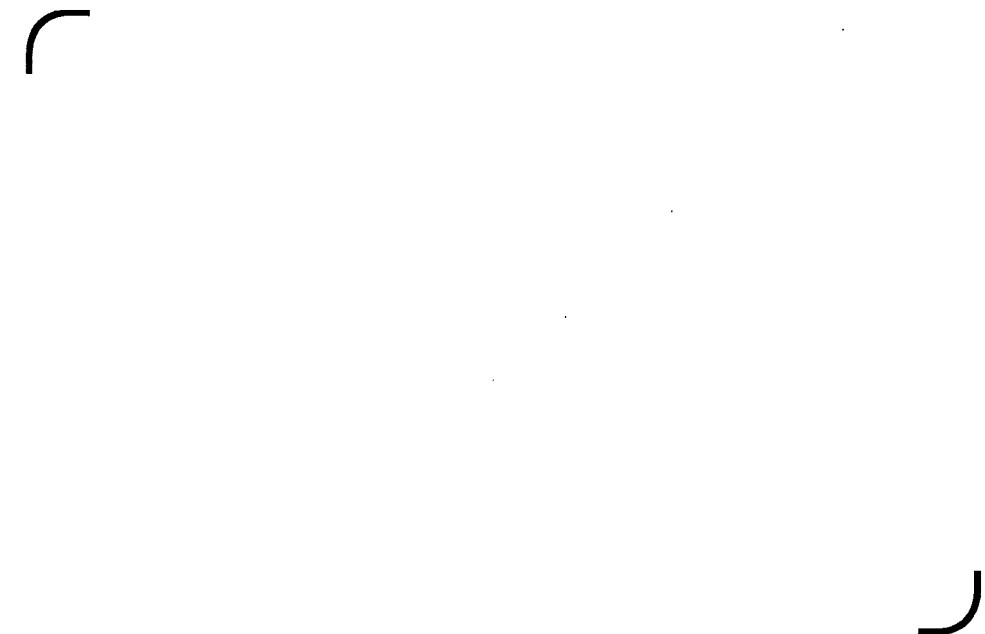


**Figure 15a-13 Risø FGP3 Rod AN2
Cladding Diameter Increase during the Ramp Test**



**Figure 15a-14 Risø FGP3 Rod AN8
Cladding Diameter Increase during the Ramp Test**



**Figure 15a-15 Mark-BEB Rod 65-2
Cladding Diameter Increase during the Ramp Test**



**Figure 15a-16 Mark-BEB Rod 65-4
Cladding Diameter Increase during the Ramp Test**



**Figure 15a-17 Mark-BEB Rod 66-2
Cladding Diameter Increase during the Ramp Test**



**Figure 15a-18 Cladding Strain during Ramp Tests at Mid-Pellet
Whole Database (17 Ramp Tests)**



**Figure 15a-19 Cladding Strain during Ramp Tests at Pellet End
Whole Database (17 Ramp Tests)**



**Figure 15a-20 Cladding Strain during Ramp Tests at Mid-Pellet Ramp Tests
with Rods Representative of Current AREVA Fuel (9 Ramp Tests)**



**Figure 15a-21 Cladding Strain during Ramp Tests at Pellet End Ramp Tests
with Rods Representative of Current AREVA Fuel (9 Ramp Tests)**

Question 15b:

Please provide code comparisons to the Halden power ramp data including axial and diametral deformation from IFA-520, IFA-525 (HWR-122) and IFA-509 Rod 3 (HWR-162).

Response 15b:

The IFA-520 and IFA-525 power ramp tests on instrumented experimental fuel rods, reported in HWR-122, are difficult to interpret and consequently difficult to simulate with a fuel code; these difficulties are explained below.

[

]

[

]

Question 15c:

For question and response see BAW-10247Q1(P) Revision 000.

Question 16:

The following are related to understanding the fuel pellet deformation modeling.

- a. *In the last paragraph in Section 6.2.5.2, in what way were the results from the 1-D model for deformation at pellet ends incompatible with observation (page 6-26, EMF-2994(P))?*
- b. *Please provide an illustrated example of how dish filling is calculated (p 6-5). In Equation 6-34, please provide a value for α_{dish} and a comparison of predicted and measured values of dish filling along with a tabulation of this data (p. 6-34).*

- c. *It is stated that "an additional hoop strain component, ϵ_{0crack} , has been introduced into the circumferential compatibility equation to simulate the tangential displacement associated with pellet cracking." Please provide a prediction of the hoop strain displacement in μm due to cracking as a function of LHGR and any other important parameters for fuel displacement due to cracking (page 6-4). This calculation is wanted to determine the extent of gap closure for the experimental data base and the licensing analyses of commercial fuel rods.*

Response 16a:

The pellet end geometry is complex. Moreover it is manufacturer dependent. Pellets may have dishes or not. They may have chamfers or larger land tapers.

[

]

Response 16b:

[

]

Calculations were performed with RODEX4 for the steady state and ramp test irradiations of these rods. Rod characteristics, irradiation data and measured results were taken from program reports. No adjustment of the pellet densification and cladding creep parameters has been made.

Table 16b-1 Ramp Test Rod for Evaluating Dish Filling Predictions

RODEX4 calculates the dish profile at any axial level and any time using the method described above. The results, presented in Figures 16b-1 through 16b-7 show for each rod the dish profile at the level of the peak power node at the end of the ramp test just before reactor shut down. The results are presented in a way that makes easy the comparison with the experimental results. The ceramography cross-sections are also located close to the peak power location during the ramp tests.

The comparison shows a good agreement between predictions and experimental results for different pellet designs, different ramp terminal levels and different hold times.

**Figure 16b-1 Over-Ramp Rod A20/1
Dish Filling after Ramp Testing at 44 kW/m for 24 h
RODEX4 Predictions and Experimental Results**

**Figure 16b-2 Over-Ramp Rod F20/3
Dish Filling after Ramp Testing at 43.2 kW/m for 22 min
RODEX4 Predictions and Experimental Results**

**Figure 16b-3 Over-Ramp Rod F30/4
Dish Filling after Ramp Testing at 44.5 kW/m for 19.6 h
RODEX4 Predictions and Experimental Results**

**Figure 16b-4. Over-Ramp Rod G20/2
Dish Filling after Ramp Testing at 44.5 kW/m for 24 h
RODEX4 Predictions and Experimental Results**

**Figure 16b-5 Super-Ramp Rod PK1/2
Dish Filling after Ramp Testing at 44 kW/m for 12 h
RODEX4 Predictions and Experimental Results**

**Figure 16b-6 Super-Ramp Rod PK2/2
Dish Filling after Ramp Testing at 46.0 kW/m for 12 h
RODEX4 Predictions and Experimental Results**

**Figure 16b-7 Super-Ramp Rod BK7/3
Dish Filling after Ramp Testing at 32.5 kW/m for 12 h
RODEX4 Predictions and Experimental Results**

Response 16c:

Three ATRIUM 10 rods were calculated with RODEX4 up to 40 MWd/kgU. In each calculation the rod average LHGR was maintained constant during irradiation. To make the interpretation easy, the axial power distribution was modeled as uniform. The power levels in the three rods were respectively 20, 30, and 40 kW/m, respectively. These calculations are identical to those presented in the response to question 4.

[

]



**Figure 16c-1 ATRIUM 10 Fuel at the Constant LHGR of 20 kW/m
Width of the Pellet Radial Cracks at Several Pellet Exposures**

**Figure 16c-2 ATRIUM 10 Fuel at the Constant LHGR of 30 kW/m
Width of the Pellet Radial Cracks at Several Pellet Exposures**

**Figure 16c-3 ATRIUM 10 Fuel at the Constant LHGR of 40 kW/m
Width of the Pellet Radial Cracks at Several Pellet Exposures**

**Figure 16c-4 ATRIUM 10 Fuel
Fuel Radial Relocation due to Pellet Cracking**

Questions 17a, 17b, 17c, and 17d:

For questions and responses see BAW-10247Q1(P) Revision 000.

Question 18:

For question and response see BAW-10247Q1(P) Revision 000.

Question 19:

For question and response see BAW-10247Q1(P) Revision 000.

Questions 20a and 20b:

For questions and responses see BAW-10247Q1(P) Revision 000.

III. Code Application

The following are from the review of BAW-10247(P) unless otherwise stated.

Question 21:

For question and response see BAW-10247Q1(P) Revision 000.

Question 22:

For question and response see BAW-10247Q1(P) Revision 000.

Question 23:

The model parameter uncertainties are provided for only three parameters, however, there are several other model parameters that are known to impact fuel performance calculations for normal operation such as fuel thermal expansion, densification and swelling to name a few. These three parameters are important for both rod pressure and cladding deformation analyses. Another parameter important for cladding collapse analyses is cladding ovality. Please provide a justification of why the uncertainties in these model parameters are not included (Section 2.3.4). Please perform a sensitivity analysis to show the effect of these parameters on rod pressure (include axial rod growth in the rod pressure sensitivity analysis) and cladding deformation, e.g., strain increment and axial gap formation, analyses at various burnup levels.

Response 23:

[

]

Response to Request for
Additional Information – BAW-10247(P)

[

]

[

]

Question 24:

For question and response see BAW-10247Q1(P) Revision 000.

Question 25:

Random errors due to uncertainties can sometimes be of lesser importance in Monte Carlo (random error) analyses than biases in the data, particularly when you are interested in the extremes of the data. Have sensitivity analyses been performed to determine the impact for a given bias (e.g., see RAI's #4, 5, 6, 8, 12, 13, 15, 17 and 24) on the predicted outcome of analyses in Section 6 of BAW-10247? In like manner have sensitivity analyses been performed to examine the impact of an increase in uncertainties on the predicted outcome? If not please provide these sensitivity analyses for how biases and increases in parameter uncertainties in the diffusion coefficient, irradiation creep model and cladding oxidation impact licensing analyses.

a For example, please assume that the gas atom diffusion coefficient provided in EMF-2994 and EMF-3014(P) is currently biased low and needs to be increased by a factor of 1.5 (uncertainty remains unchanged) and determine how this impacts the rod pressure analyses for BWR-6 and BWR-4 plants presented in Section 6 of BAW-10247. Please assume that the uncertainty on the diffusion coefficient is 20% higher than assumed in the rod pressure analyses in Section 6 (no bias).

b Please assume that the irradiation creep model is biased 33% (1.33) higher and 33% (0.67) lower than currently assumed and show how this impacts column gap formation and creep collapse analysis. Please assume the uncertainty in the irradiation creep model is a factor of 2 higher than assumed and show how this impacts column gap formation and creep collapse.

c Please assume that the cladding ovality model is biased (also assume an uncertainty exists in this model) and show how this impacts column gap formation and creep collapse analysis.

d Please perform similar sensitivity analyses for cladding steady strain and strain increments as a function of burnup. For these sensitivity analyses assume that the following on an individual basis, the fuel thermal expansion is 15% higher than

*assumed and solid fuel swelling is 50% higher than assumed. Also perform analyses assuming the thermal creep is 20% higher than assumed.
e Please perform similar analyses for fuel melting assuming that fuel thermal conductivity is biased 20% lower than assumed and the uncertainty in fuel thermal conductivity is 50% higher than assumed (bias and uncertainty effects should be separate).*

Response 25:

[

]

[

]

[

]

Response to Request for
Additional Information – BAW-10247(P)

[

]

Table 25-1 Sensitivity Study Results BWR-6 UO₂ Rods

Figure 25-1 Comparison Of The Effects Of Shifting The Mean To An Increase Of The Standard Deviation.

Question 26:

For question and response see BAW-10247Q1(P) Revision 000.

Question 27:

For question and response see BAW-10247Q1(P) Revision 000.

Questions 28a and 28b:

For questions and responses see BAW-10247Q1(P) Revision 000.

Response to Request for
Additional Information – BAW-10247(P)

Questions 29a, 29b, and 29c:

For questions and responses see BAW-10247Q1(P) Revision 000.

Question 30:

The following questions are related to the uncertainties applied to planned rod power operation for a specific plant and fuel batch.

Questions 30a and 30b:

For questions and responses see BAW-10247Q1(P) Revision 000.

Question 30c:

Please provide a power distribution for each of the BWR-6 and BWR-4 (transition batch) analyses provided in Section 6 at burnup levels of 0, 10, 20, 30, 40, 50 and 60 GWd/MTU.

Response 30c:

[

]

Response to Request for
Additional Information – BAW-10247(P)

[

]

┌

┐

Figure 30c-1 BWR 6 Transition Batch [

]



Figure 30c-2 BWR 6 Transition Batch [

]



Figure 30c-3 BWR 6 Transition Batch [

]



Figure 30c-4 BWR 6 Transition Batch [

]

Figure 30c-5 BWR 6 Transition Batch [

]

Figure 30c-6 BWR 6 Transition Batch [

Figure 30c-7 BWR 6 Transition Batch [

Response to Request for
Additional Information – BAW-10247(P)

Figure 30c-8 BWR 6 Transition Batch – [

]

Figure 30c-9 BWR 6 Transition Batch – [

]

Response to Request for
Additional Information – BAW-10247(P)

Figure 30c-10 BWR 4 TransitionBatch – [

]

Figure 30c-11 BWR 4 Transition Batch – [

]

Figure 30c-12 BWR 4 Transition Batch – [

]

Figure 30c-13 BWR 4 Transition Batch – [

]

Response to Request for
Additional Information – BAW-10247(P)

Figure 30c-14 BWR 4 Transition batch – [

]

Figure 30c-15 BWR 4 Transition Batch – [

U]

Figure 30c-16 BWR 4 Transition Batch – [

]

Figure 30c-17 BWR 4 Transition Batch – [

]

Response to Request for
Additional Information – BAW-10247(P)

Question 31:

For question and response see BAW-10247Q1(P) Revision 000.

Question 32:

For question and response see BAW-10247Q1(P) Revision 000.



December 11, 2006
NRC:06:057

Document Control Desk
U.S. Nuclear Regulatory Commission
Washington, D.C. 20555-0001

Additional Information for the Review of BAW-10247(P), "Realistic Thermal-Mechanical Fuel Rod Methodology for Boiling Water Reactors"

- Ref.: 1. Letter, James F. Mallay (AREVA NP) to Document Control Desk (NRC), "Request for Review and Approval of BAW-10247(P), 'Realistic Thermal-Mechanical Fuel Rod Methodology for Boiling Water Reactors'," NRC:04:047, August 19, 2004.
- Ref.: 2. Letter, Ronnie L. Gardner (AREVA NP) to Document Control Desk (NRC), "Additional Information for the Review of BAW-10247P Revision 0, 'Realistic Thermal-Mechanical Fuel Rod Methodology for Boiling Water Reactors'," NRC:06:030, July 7, 2006.
- Ref.: 3 Letter, Ronnie L. Gardner (AREVA NP) to Document Control Desk (NRC), "Response to a Request for Additional Information Regarding BAW-10247(P) Revision 0, 'Realistic Thermal-Mechanical Fuel Rod Methodology for Boiling Water Reactors'," NRC:06:048, November 7, 2006.

AREVA NP Inc. requested the NRC's review and approval of the topical report BAW-10247P Revision 0, "Realistic Thermal-Mechanical Fuel Rod Methodology for Boiling Water Reactors," in Reference 1. Responses to a request for additional (RAI) on the topical report were provided in References 2 and 3.

This letter provides supplementary information to the topical report to address the impact of channel bow on the parameters calculated with the realistic thermal-mechanical methodology. The information provided on the enclosed CDs to this letter will be included as Appendix B in the approved version of the topical report issued following receipt of the NRC Safety Evaluation Report (SER) for this topical report.

AREVA NP considers some of the information on the CDs to be proprietary. The affidavit provided with the original submittal of this topical report satisfies the requirements of 10 CFR 2.390(b) to support the withholding of the proprietary information from public disclosure.

Sincerely,

A handwritten signature in black ink, appearing to read 'Ronnie L. Gardner', is written over a horizontal line.

Ronnie L. Gardner, Manager
Site Operations and Regulatory Affairs
AREVA NP Inc.

Enclosures

AREVA NP INC.
An AREVA and Siemens company

cc: H. D. Cruz
J. H. Thompson
Project 728

Appendix B Channel Bow

B.1 Introduction

The purpose of this appendix is to describe the approach to account for channel bow in the RODEX4 statistical methodology. It is important to account for the impact of channel bow on the mechanical criteria evaluated with the RODEX4 statistical methodology because the impact of channel bow on the fuel rod power can be quite large, up to 10% on a nodal rod power basis.

The size of the water gaps between adjacent fuel channels is altered by the fuel channel bow. When the channel bow results in an enlargement of the local water gap, the neutron thermal flux is increased locally. The power in the neighboring fuel rods will therefore be higher than in the non-bowed condition. The reverse is true when the local water gaps are reduced.

A channel bow correlation was developed and implemented into the MICROBURN-B2 core simulator for the purpose of accounting for channel bow effects on the realistic power histories used in the RODEX4 statistical methodology. [

]

The channel bow model uncertainty is determined [

]

B.2 Methodology Modification for the Channel Bow

The process for accounting for the impact of channel bow on the criteria evaluated with the RODEX4 statistical methodology is described below. The process is described first and then the development of the individual components are described in later sections of this appendix.

[

]

[

]

[

.]

B.3 Channel Bow Model Uncertainty Implementation in FROSTY

The channel bow related power uncertainty is added to the other power uncertainties as described in step "d" above. The process is as follows.

[

]

[

]

B.4 Channel Bow Model

The main cause of the bow in the fuel channel is the differential irradiation growth between the two opposing sides. The fuel channel accommodates this differential axial growth by bending such that the convex side is the longer side. Neglecting the elastic stresses and strains, the bending is assumed to be a fully permanent deformation; a model for this bending is described below.

[

]

[]

B.5 Channel Irradiation Growth Correlation

[]

B.6 Implementation into MICROBURN-B2

The MICROBURN-B2 core simulator computes the maximum channel bow magnitude for each assembly consistent with Equations B.6 and B.7. The assembly maximum bow is then used to determine the axial bow profile as a quadratic function with its peak at the axial mid-plane and with the zero function values at the top and the bottom of the channel.

[]

[

]

B.7 Uncertainty of the channel bow model

[

]

B.8 AOO Fast Transient Methodology

[

]

[

]

B.9 Sample Problems, Steady State

In Section 6.0, sample applications were presented for a C-lattice BWR-6 plant and for a D-lattice BWR-4 plant. The equilibrium cycles evaluated in these two applications have been repeated with the channel bow methodology presented above in order to illustrate the impact of channel bow effect on the results with respect to the criteria.

The results for the BWR-6 application example are presented in Tables B.3 and B.4, for the nominal power case and the 10% power uprate case, respectively. Due to the changes in RODEX4 and FROSTY since the submittal in 2004, the original, non-bowed case has been re-calculated. The results are consistent but not identical with those previously presented in Section 6.

The first column of Table B.3 shows the results for the reference case without the effects of channel bow (a repeat of the original calculation) while the second column shows the results including the effects of the channel bow methodology presented in this appendix. [

]

[

]

B.10 Sample Problem, AOO Fast Transient

[

]

[

]

Table B.1 - Input Parameters for Bow Calculation

	A32	A30
Active channel length (inch)	149.45	144.24
BOL nominal channel length (inch)	166.906	162.156
BOL nominal channel width (inch)	5.438	5.478

Table B.2 - Channel Bow Bias and Standard Deviation



Table B.3 - BWR 6 Equilibrium Cycle Results Comparison



Table B.4 - BWR 6 Equilibrium Cycle, 110% Power, Results Comparison



Table B.5 - BWR 4 Equilibrium Cycle Results Comparison



**Table B.6 - Summary of the BWR-4 Sample Feedwater
Controller Failure Analysis with
and without Channel Bow**





Figure B.1 - Illustration of Simplified Channel Bow Geometry



Figure B.2 - Calculated and Measured Channel Bows





Figure B.3 - Channel Bow with Enhanced Uncertainty Bands



**Figure B.4 - BWR-6 Equilibrium Batch – maximum
Rod Internal Pressure with and without Channel Bow**





**Figure B.5 - BWR-4 Equilibrium Batch – maximum
Rod Internal Pressure with and without Channel Bow**



**Figure B.6 - Statistical Measure Of The Global
Relative Nodal Power Variation Due To Channel Bow**





Figure B.7 - Maximum Nodal Power Variation Due to Channel Bow

References

1. M. Griffiths, et. al., "Accelerated Irradiation Growth of Zirconium Alloys," "Zirconium in the Nuclear Industry," Eighth International Symposium, ASTM STP1023, p.658, 1989
2. V. Garat, V. Chabretou, V. I. Arimescu, P. Blanpain, "Modelisation for IFA 653 experiment according to AREVA NP design laws," NFIR-IV, 49th NFIR Steering Committee Meeting, Wilmington, NC, May 2006
3. F. Garzarolli, P. Dewes, G. Maussner and H-H Basso, "Effects of High Neutron Fluences on Microstructure and Growth of Zircaloy-4," "Zirconium in the Nuclear Industry," Eighth International Symposium, ASTM-STP 1023, 1988.
4. Letter, Ronnie L. Gardner (AREVA NP) to Document Control Desk (NRC), "Additional Information for the Review of BAW-10247(P), Realistic Thermal-Mechanical Fuel Rod Methodology for Boiling Water Reactor," NRC:05:041, July 14,2005.



August 31, 2007
NRC:07:042

Document Control Desk
U.S. Nuclear Regulatory Commission
Washington, D.C. 20555-0001

**Response to a Second Request for Additional Information for the Review of
BAW-10247(P), "Realistic Thermal-Mechanical Fuel Rod Methodology for Boiling
Water Reactors"**

- Ref.: 1. Letter, James F. Mallay (Framatome ANP) to Document Control Desk (NRC), "Request for Review and Approval BAW-10247(P), 'Realistic Thermal-Mechanical Fuel Rod Methodology for Boiling Water Reactors'," NRC:04:047, August 19, 2004.
- Ref.: 2. Letter, Ronnie L. Gardner (AREVA NP) to Document Control Desk (NRC), "Additional Information for the Review of BAW-10247P Revision 0, 'Realistic Thermal-Mechanical Fuel Rod Methodology for Boiling Water Reactors'," NRC:06:030, July 7, 2006.
- Ref.: 3. Letter, Ronnie L. Gardner (AREVA NP) to Document Control Desk (NRC), "Response to a Request for Additional Information Regarding BAW-10247(P) Revision 0, 'Realistic Thermal-Mechanical Fuel Rod Methodology for Boiling Water Reactors'," NRC:06:048, November 7, 2006.
- Ref.: 4. Letter, Ronnie L. Gardner (AREVA NP) to Document Control Desk (NRC), "Additional Information for the Review of BAW-10247(P) Revision 0, 'Realistic Thermal-Mechanical Fuel Rod Methodology for Boiling Water Reactors'," NRC:06:057, December 11, 2006.

AREVA NP Inc. (AREVA NP) requested the NRC's review and approval of the topical report BAW-10247(P) Revision 0, "Realistic Thermal-Mechanical Fuel Rod Methodology for Boiling Water Reactors," in Reference 1. Responses to a request for additional (RAI) on the topical report were provided in References 2 and 3. Supplementary information to address the impact of channel bow on the parameters calculated with the realistic thermal-mechanical methodology was provided in Reference 4.

This letter provides a response to a second RAI received from the NRC in an email dated January 3, 2007. The response is contained in the report BAW-10247Q4P, "Response to Request for Additional Information – BAW-10247(P)." A proprietary and a non-proprietary version of the responses are provided on the enclosed CDs.

AREVA NP INC.
An AREVA and Siemens company

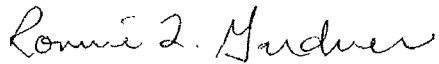
3315 Old Forest Road, P.O. Box 10935 Lynchburg, VA 24506-0935
Tel.: 434 832 3000 - Fax: 434 832 3840 - www.aveva.com

Document Control Desk
August 31, 2007

NRC:07:042
Page 2

AREVA NP considers some of the information in the enclosures to this letter to be proprietary. The affidavit provided with this letter satisfies the requirements of 10 CFR 2.390(b) to support the withholding of the proprietary information from public disclosure.

Sincerely,



Ronnie L. Gardner, Manager
Site Operations and Corporate Regulatory Affairs
AREVA NP Inc.

Enclosures

cc: H. D. Cruz
J. H. Thompson
Project 728

requested qualifies under 10 CFR 2.390(a)(4) "Trade secrets and commercial or financial information".

6. The following criteria are customarily applied by AREVA NP to determine whether information should be classified as proprietary:

- (a) The information reveals details of AREVA NP's research and development plans and programs or their results.
- (b) Use of the information by a competitor would permit the competitor to significantly reduce its expenditures, in time or resources, to design, produce, or market a similar product or service.
- (c) The information includes test data or analytical techniques concerning a process, methodology, or component, the application of which results in a competitive advantage for AREVA NP.
- (d) The information reveals certain distinguishing aspects of a process, methodology, or component, the exclusive use of which provides a competitive advantage for AREVA NP in product optimization or marketability.
- (e) The information is vital to a competitive advantage held by AREVA NP, would be helpful to competitors to AREVA NP, and would likely cause substantial harm to the competitive position of AREVA NP.

The information in the Document is considered proprietary for the reasons set forth in paragraphs 6(b) and 6(c) above.

7. In accordance with AREVA NP's policies governing the protection and control of information, proprietary information contained in this Document have been made available; on a limited basis, to others outside AREVA NP only as required and under suitable agreement providing for nondisclosure and limited use of the information.

8. AREVA NP policy requires that proprietary information be kept in a secured file or area and distributed on a need-to-know basis.

9. The foregoing statements are true and correct to the best of my knowledge, information, and belief.

Jerald Holm

SUBSCRIBED before me this 31
day of August, 2007.

Susan K. McCoy

Susan K. McCoy
NOTARY PUBLIC, STATE OF WASHINGTON
MY COMMISSION EXPIRES: 1/10/2008



AREVA NP Inc.

BAW-10247Q4NP
Revision 0

**Response to Request for
Additional Information – BAW-10247(P)**

Copyright © 2007

AREVA NP Inc.
All Rights Reserved

Table of Contents

<u>Question</u>	<u>Page</u>
Question 1.....	12
Question 2.....	13
Question 3.....	35
Question 4.....	37
Question 5.....	50
Question 6.....	57
Question 7.....	62
Question 8.....	64
Question 9.....	64
Question 10.....	66
Question 11.....	67
Question 12.....	69
Question 13.....	74
Question 14.....	74
Question 15.....	77
Question 16.....	78
Question 17.....	78
Question 18.....	84
Question 19.....	86

This document contains a total of 94 pages.

**Second Round of RAIs on RODEX4 Documents
(BAW-10247, EMF-2994, and EMF-3014)**

To assist in the review process, two sets of tables have been provided below independent of any specific RAI question. The first set of tables provide a summary of the changes that have been made to the RODEX4 code and proposed changes to the methodology since the original submittal of BAW-10247(P) back in August of 2004. The second set of tables provides a complete listing of all the various parameters that are considered in the statistical methodology and the uncertainties that are applied to them.

RODEX4 Methodology Changes

The following table lists the changes to the RODEX4 statistical methodology that have been proposed since the original submittal of BAW-10247(P) in August of 2004.

Table A – RODEX4 Methodology Changes since Original Submittal

RODEX4 Code Changes

Since the original submittal of BAW-10247 for review in August of 2004, the RODEX4 code has been changed to address issues identified during the review process. Four new code versions have been made, versions UAPR05, UOCT06, UNOV06, and UJUN07, each of which contained multiple changes. Some of these changes were implemented to fix errors and others were made to add calculational flexibility needed to respond to RAIs. The following table lists the pertinent changes and provides a brief discussion of their impact.

Table B – RODEX4 Code Modifications since Original Submittal



Table C – Steady State Uncertainty Summary



Slow Transient Uncertainty Parameters

Table D – Slow Transient Uncertainty Summary



Fast Transient Uncertainty Parameters

Table E – Fast Transient Uncertainty Summary

Summary Comparison of the Realistic and Old Methodologies

The margin gains and losses to the transition to the new methodology should be generally applicable. The steady state results provided below were taken from the BWR-6 sample case and from the BWR-4 EPU cases for the steady state and transient results. In some cases, improved LHGR limits may be achieved.

Table F – Summary Comparison of Realistic and Old Methodology (from response 3)



General Comment:

In general, there has been little justification for the uncertainty values that have been selected. In particular, for model parameters, there should be plots showing that the model at its upper and lower limits, bound a large portion (95/95) of the data. Please keep this in mind when responding to the following RAIs and, whenever possible, demonstrate quantitatively that the selected uncertainty values sufficiently bound the measured data.

Question 1:

The responses provided in the November, 2006 letter did not provide the results from the sensitivity analyses requested in RAI# 23 from the first round of RAIs. The first round RAI #23 requested that sensitivity analyses be provided on those RODEX4 model uncertainties not considered in the methodology but this request did not provide many specifics. The current request is intended to supplement the first round RAI# 23 and provide specifics on the sensitivity analyses that should be provided. Please perform the following sensitivity analyses for rod pressure and strain increments as a function of burnup for the BWR-4 equilibrium core and document the results in a table similar to Table 1.1;

- a) Assume the mean fuel thermal expansion is biased 4% higher than RODEX4 assumed^b
- b) Assume there is a 30% (95/95) uncertainty in solid swelling and how these impact rod pressure, cladding strain and strain increment calculations.
- c) Please determine the uncertainty in rod growth based on the limited axial irradiation growth data and perform a sensitivity analysis to determine the effect of irradiation growth on rod pressure calculations.
- d) The slow transient analyses also have no [] model even though it may impact the slow transient strain analysis. In addition, there is considerable uncertainty in this model due to the small amount of data used to verify this model and the large variability in the data used to develop this model. Please perform slow transient analyses assuming the uncertainty in this model is 40% (95/95).
- e) The slow transient analysis also does not consider the [] . Please perform this analysis using the same uncertainties for these parameters as used for the fast transient conditions.

Perform each of the listed analyses individually and provide the information indicated in Table 1.1. For all the sensitivity analyses that require a strain value, please list both the total strain (elastic + permanent) and the permanent strain.

Based on the requested sensitivity analyses, please provide a justification of why the uncertainties in these model parameters are not included (Section 2.3.4).

^b The FRAPCON-3 thermal expansion differs from the RODEX4 expansion by 4% within given temperature ranges. In addition, the standard deviation on the thermal expansion data available to PNNL demonstrates a significantly larger value than that assumed for RODEX4.

Table 1.1. Sensitivity analysis for thermal expansion, solid swelling, and gaseous swelling for a BWR-4 and equilibrium batches²

Response 1:

Because of the similar nature of the sensitivity studies requested in questions 1 and 2, the results of these studies are presented in a combined three part response at the end of question 2. Specifically, items 1a, 1b, 1c, and 1d are addressed in the first part of response 2, item 1b is further addressed in the second part and item 1e is addressed in the third part. Please refer to the response to question 2.

Question 2:

The responses provided in the November, 2006 letter did not provide the sensitivity analyses requested in RAI# 25 from the first round of RAIs. The first round RAI# 25 requested sensitivity analyses on the impact of RODEX4 model biases and variations in uncertainty on those models considered to have uncertainties in the RODEX4 statistical methodology. The first round questions suggested in RAIs #4, 5, 6, 8, 12, 13, 15, 17 and 24 that there may be biases and greater uncertainties than those considered by RODEX4. This request is intended to supplement the RAI# 25 and provide specifics on the sensitivity analyses that should be

provided for the irradiation creep model and cladding oxidation impact licensing analyses for steady-state and slow transients. Please perform the following sensitivity studies and document the results in tables similar to Tables 2.1 – 2.4.

- a. Please assume that the irradiation creep model is biased 30% ($1.30 \times \text{nominal}$) higher than currently assumed and show how this impacts column gap formation and rod pressure analysis. In addition, please assume the uncertainty in the irradiation creep model is 50% (95/95) rather than the current value of 30% and show how this impacts column gap formation, the rod pressure limit and rod pressure analyses, see Table 2.1.

Table 2.1. Sensitivity analysis for irradiation creep model for a BWR-4 and equilibrium batches²

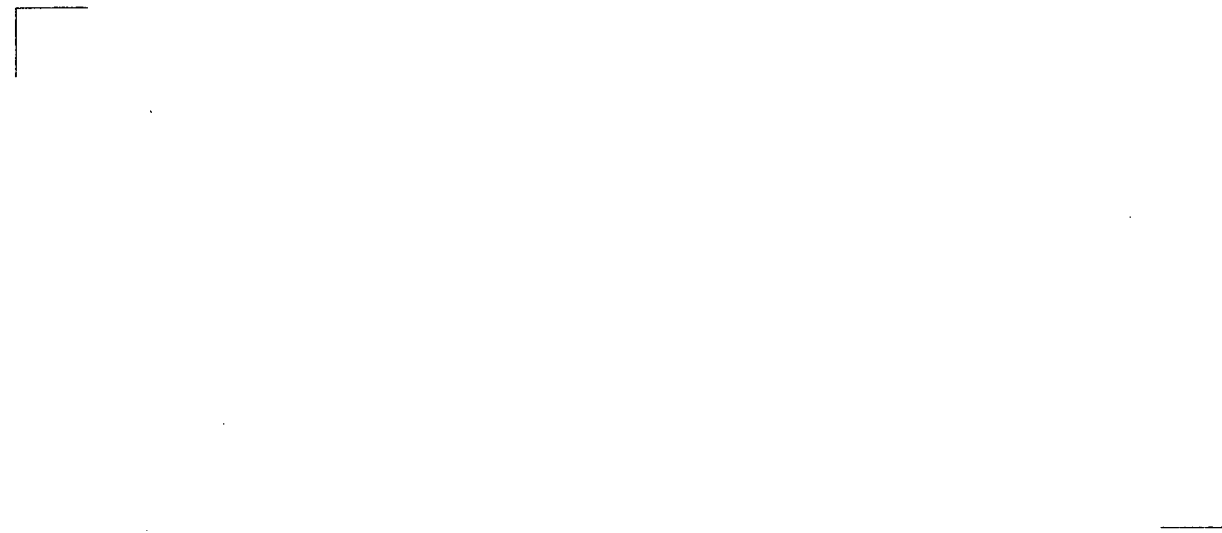
- b. Please perform rod pressure (pressure limit and rod pressure analyses) and cladding strain (slow transient and fast transient) analyses assuming the thermal creep is 20% higher than assumed ($1.2 \times \text{nominal}$), see Table 2.2.

Table 2.2. Sensitivity analysis for thermal creep model for a BWR-4 and equilibrium batches²

A large rectangular area that has been redacted, leaving only a white space. It is bounded by a thin black line on the top, left, and right sides, with a corner bracket on the top-left and bottom-right.

- c. Please perform a sensitivity analysis for cladding strain assuming the uncertainty in cladding oxidation is 25% higher than assumed ($1.25 \times \text{nominal}$), see Table 2.3.

Table 2.3. Sensitivity analysis for cladding oxidation model for a BWR-4 and equilibrium batches²

A large rectangular area that has been redacted, leaving only a white space. It is bounded by a thin black line on the top, left, and right sides, with a corner bracket on the top-left and bottom-right.

Response 2:

Summary

The response to questions 1 and 2 is divided into three parts.

Part 1 consists of individual fuel rod studies performed by varying a single parameter. It addresses questions 1a, 1b, 1c, 1d, 2a, 2b, and 2c. [

]

Part 2 consists of a verification of the ATRIUM 10 steady strain calculated-minus-measured results on a 95/95 basis. It addresses questions 1b, 2a, and 2c. [

]

Part 1 – Individual Rod Sensitivity Studies (1a, 1b, 1c, 1d, 2a, 2b and 2c)

Questions 1 and 2 requested various studies to assess the impact of assumed biases or increased uncertainty ranges for the model parameters shown in Tables 1.1 and 2.1 through 2.3. The parameters from the various tables in these questions are:

[

]

[

]

References

- 2.1 D. G. Martin, "The Thermal Expansion of Solid UO_2 and (U, Pu) Mixed Oxides - A Review and Recommendations," J. Nucl. Mat., No.152, 1988, pp. 94-101

- 2.2 J. K. Fink, "Thermal Expansion of Solid Uranium Dioxide", International Nuclear Safety Center, ANL web site <http://www.insc.anl.gov/matprop/uo2>

Table 2.4 Maximum Rod Pressure Sensitivity Results



Table 2.5 Maximum Steady Clad Strain Sensitivity Results



Table 2.6 Maximum CRWE Transient Strain Sensitivity Results



Table 2.7 Maximum Axial Gap Sensitivity Results





Figure 2.1 Thermal Expansion versus Temperature for RODEX4 and FRAPCON



Figure 2.2 Thermal Expansion Ratio, RODEX4 / FRAPCON

Revised Model Uncertainties:

[

]

Table 2.9 Clad Deformation Model Uncertainties

Measurement Uncertainties:

[

]

Table 2.10 Clad Deformation Database Measurement Uncertainties

[

]

[

]

Table 2.11 Statistical Verification for Rod Creepdown Data

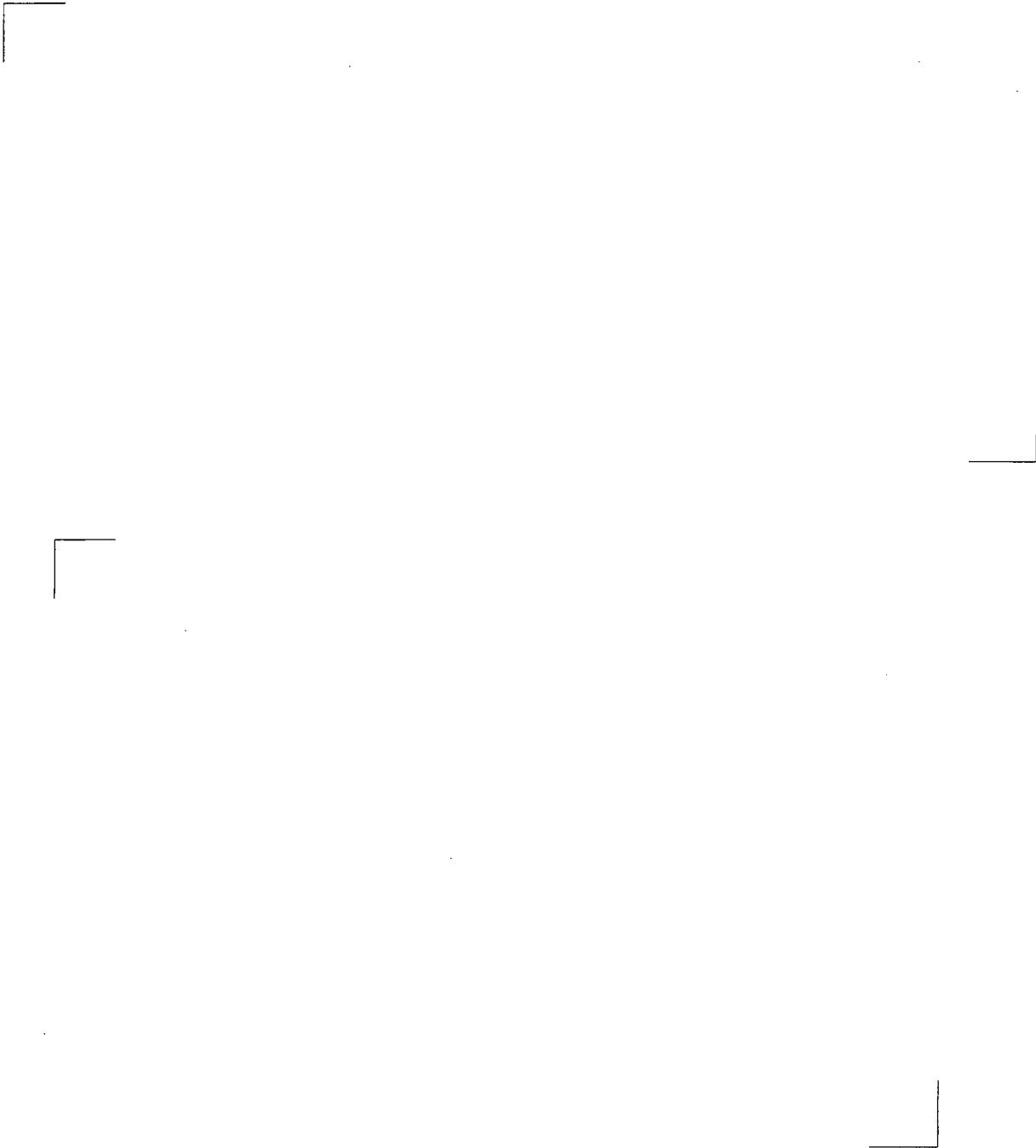


Figure 2.3 Measured Creepdown Data



Figure 2.4 Calculated and Measured Creepdown Data



Figure 2.5 Calculated minus Measured Creepdown



Figure 2.6 Data Evaluation Set 1



Figure 2.7 Data Evaluation Set 2

Part 3 – Evaluation of Slow Transients with Additional Uncertainties (1e)

Quantification of Transient Uncertainties:

The temperature and ramp strain results were previously calibrated as described in EMF-3014 and BAW-10247Q2(P) Responses 5 and 15. [

]

Slow Transient Methodology:

[

]

[

]



Figure 2.8 Predicted vs. Measured Centerline Temperatures – Best Estimate



Figure 2.9 Predicted Measured Fuel Centerline Temperature Deviation – Best Estimate



Figure 2.10 Predicted vs. Measured Centerline Temperatures - Conservative



**Figure 2.11 Predicted – Measured Fuel Centerline Temperature
Deviation versus Local Exposure - Conservative**



Figure 2.12 Cladding Strain Increment at Mid-Pellet from Ramp Test



Figure 2.13 Cladding Strain Increment at Pellet-End from Ramp Test



**Figure 2.14 Strain Calibration Considering Thermal Expansion and
Conductivity and Power Uncertainties**

**Table 2.12 Uncertainty Parameters for Quantification of
Thermal and Ramp Test Calibrations**



**Table 2.13 Slow Transient CRWE Results Summary
BWR-4 Transition, UO₂-Gd₂O₃ Rods , 2nd cycle**



Question 3:

Please provide the margins to the column gap formation, rod pressure, and fast and slow transient strain and fuel melt limits using the old methodology for a given design using the same fuel batch and core as performed using the new methodology. Table 6.9 of BAW-10247 provides some of these margins except for the fast and slow transients. Please compare these margins to those utilizing the new methodology and confirm that all analyses are for the same fuel batch and core. Please discuss what changes in methodology accounts for the margin difference between the old and new methodology.

Response 3:

The BWR-4 transition cycle analysis results for the RODEX2A and RODEX4 methodologies are compared for the same fuel batch and core. The BWR-4 analysis is for a 110% EPU cycle. The RODEX4 methodology results were updated for this response. The updates include RODEX4 corrections, an improvement of the RODEX4 cladding creep and pellet accommodation benchmarking and the additional uncertainties (see (BAW-10247Q4(P)) response 2). The channel bow uncertainty was not included. The comparative RODEX4 and RODEX2A/COLAPX results are summarized in Table 3.1.

[

]

[

]

Table 3.1 BWR-4 (EPU) Comparative Methodology Results

° At burnup of minimum margin in RODEX2.

Table 3.2 Summary of Typical Margin Impact of Changing to RODEX4

Question 4:

The November 2006 response did not perform the rod pressure analyses that were requested in the first round RAI # 29a and 29b to demonstrate the impact of a slow power transient (due to an AOO such as a CWRE). The GDC 10 requires that fuel failure not be allowed for normal operation and AOOs. Therefore, slow power transients due to AOOs have been required for rod pressure analyses for all PWR and BWR fuel vendors in the past that perform best estimate analyses of rod pressure with a statistically derived bound. In addition, PNNL has examined the RODEX4 FGR predictions of experimental rods that have been power ramped. These comparisons to FGR data shows that RODEX4 underpredicts FGR from the power ramped rods. A comparison is also made to the RODEX4 transient release predictions presented in the response to RAI# 7e from the first round of RAIs (Figures 4.1 and 4.2) with those predicted with the FRAPCON-3.3 gas release model for the same Atrium10 design. These comparisons demonstrate that RODEX4 predicts significantly lower FGR than FRAPCON-3.3 by a factor of 1.5 or greater depending on the rod power and burnup level (see Figures 4.1 and 4.2 for burnups of 30 and 60 GWd/MTU, respectively). The RODEX4 FGR predictions provided in

response to the first round RAI#7 also demonstrates that RODEX4 has a significant dependence on grain size such that has not been demonstrated by comparisons to FGR data with differing grain size. In addition, the grain size used for the Atrium 10 design is significantly larger than 90% of the FGR data. Please provide a plot of predicted minus measured fission gas release as a function of grain size for the rods in the fission gas release assessment database. Also please provide a plot of predicted divided by measured fission gas release as a function of grain size for these same rods.

Therefore, the RODEX4 predictions of FGR need to be increased (can be accomplished by various means such as increasing the diffusion coefficient and/or fixing the grain size to a small value). Please perform a rod pressure analysis assuming a slow power AOO transient has occurred that results in the highest FGR. Please provide the input and output details of this calculation such that an audit calculation can be performed with FRAPCON similar to the information provided in Round 1 RAI #32. Please show either; a) how existing conservatism in the rod pressure analysis bound the possible rod pressure increase due to AOOs, or b) propose how AOO transients will be included in the rod pressure analysis.



Figure 4.1 Reproduction of Figure 7e-5 from first round of responses with FRAPCON-3.3 predictions added at equivalent power and burnup.



Figure 4.2 Reproduction of Figure 7e-7 from first round of responses with FRAPCON-3.3 predictions added at equivalent power and burnup.

Response 4:

Introduction

The response to this question is broken up into several parts. In the first part it is shown that RODEX4 provides good predictions of fission gas release (FGR) in the range of interest and beyond. In the second part the FGR model with respect to grain size is addressed. In the third section, the evaluation of the rod pressure using the AOO slow transients is discussed.

Part 1 The RODEX4 FGR Predictions

The sub-set of the FGR database that consists of power ramps was thoroughly analyzed with respect to power and manufacturing uncertainties. An optimized sub-set was then defined, consisting of the most reliable transient data cases. The initial appearance of an under prediction of fission gas release is shown to be due to poor measurement data.

One of the main considerations in the selection process was the accuracy of both the rod average power value and the axial power profile. In some cases, the axial power profile was provided with only a few points and in other cases, there was a large uncertainty with respect to its shape and the peak power location. These factors contributed to a power uncertainty greater than the typical 5% standard deviation.

[

]

[

]

The results of the RODEX4 benchmarking on this optimized transient FGR data set for FGR greater than 5% are shown in Figure 4.3 on a logarithmic scale and in Figure 4.4 on a linear scale. The statistics of the two benchmarking measures, namely, the (predicted/measured) ratio and the logarithm of (predicted/measured), are presented in Table 4.1.

[

]

[

]

In addition, Figure 4.8 in the original submittal, BAW-10247(P), shows the RODEX4 FGR calculated to measured comparisons for our commercial database. This plot shows excellent, best estimate, agreement with the measured data and provides further evidence that the RODEX4 FGR model provides good FGR predictions over a wide range of conditions.

While investigating the differences in FGR predicted by RODEX4 and FRAPCON-3 for the hypothetical audit power ramps of Q7e, it was discovered that the FRAPCON-3 runs performed by PNNL used a higher fuel enrichment. This caused a different radial power profile and finally led to higher fuel temperatures in the FRAPCON-3 runs. [

]

Re-runs of the audit power ramps were performed with a reduced grain size of []. In addition the oxidation rate was increased in the RODEX4 runs to make the temperatures closer to the temperatures in FRAPCON-3, as illustrated in Figure 4.13. This makes possible a direct comparison of the FGR predictions of the two codes with a similar temperature distribution. The results are presented in Figure 4.14 and show very good agreement.

Part 2 Grain size Dependence of FGR in RODEX4

The dependence of the FGR on the grain size in RODEX4 is consistent with the experimental data base. The diffusion of gas atoms takes place inside the grain to the grain boundary. A similar modeling was adopted in FRAPCON-3, but in it the grain size is kept constant.

[

]

[

]

As shown in the part 1 response, the excellent agreement between the predicted fuel rod FGR and the measured FGR, over the production range seen for the ATRIUM-9 and ATRIUM-10 fuel, serves as verification that the grain size dependence is being adequately modeled.

Part 3 Rod Pressure Analysis With AOO Slow Transients

[

]

The duration of the high power dwell time of the CRWE scenario is 4 hours. There are two well characterized power ramps in the RODEX4 database with a short hold time that makes them relevant for the validation of the fission gas release calculation during CRWE events. One is the GE-7 case from Super-Ramp 2 international program, with a 4 hour hold time and the other is the REGATE L-3 test with a hold time of 1.5 hours. Table 4.2 shows excellent agreement between RODEX4 predictions and measured values (the two measured values for the REGATE case represent the Kr-85 gamma scan and the puncturing values, respectively) for these two tests. This validates the application of RODEX4 to the CRWE analysis with respect to the transient fission gas release during large and short power ramps.

Another way of validating the FGR prediction by RODEX4 during short hold time power transients, was to compare with FRAPCON-3 for a grain size of 10.7 MLI, which is closer to the fixed grain size in FRAPCON-3. The hypothetical audit power ramps of Q7e were limited to a 4 hours hold time and the results obtained with RODEX4 and FRAPCON-3 are presented in Table 4.3. It can be concluded that very good agreement exists between the two codes with respect to the transient FGR during short hold time transients.

Table 4.1 Optimized Transient FGR dataset Statistics



Table 4.2 Simulation of short hold time transient FGR



Table 4.3 RODEX4 comparison to FRAPCON-3 for short hold time transients

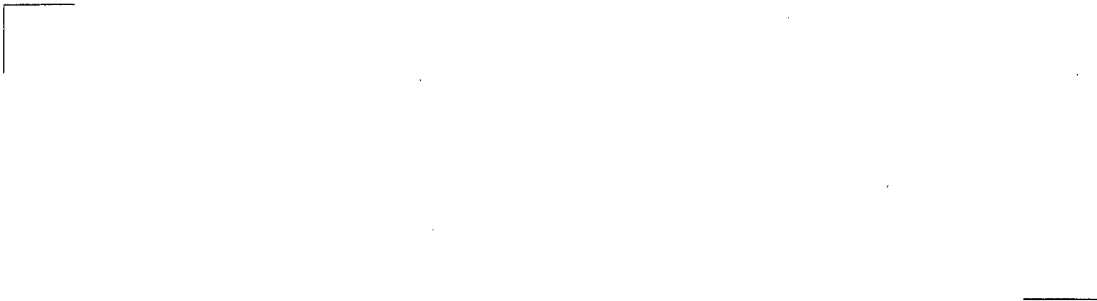




Figure 4.3 Transient FGR Results, Logarithmic Scale



Figure 4.4 Transient FGR Results, Linear Scale



Figure 4.5 Transient FGR Results, Linear Scale, with LHGR and Diffusion Coefficient Biased to the 95%/95% upper bounds.



Figure 4.6 3D grain sizes for the fuels in the FGR database



Figure 4.7 Mean linear intercept grain sizes for the fuels in the FGR database



Figure 4.8 Predicted – Measured Comparison of FGR vs. Grain Size



Figure 4.9 Predicted / Measured Comparison of FGR vs. Grain Size



Figure 4.10 Nodal LHGR's during the Mark-BEB 66-2 power ramp



Figure 4.11 Nodal temperatures during the Mark-BEB 66-2 power ramp



Figure 4.12 Nodal FGR's during the Mark-BEB 66-2 power ramp



Figure 4.13 Fuel centerline temperature during audit hypothetical power ramps with increased oxidation rate in RODX4 in order to achieve equal temperatures to FRAPCON-3



Figure 4.14 RODEX4 to FRAPCON-3 comparison for audit hypothetical power ramps with a grain size of 10.7 microns, MLI and increased oxidation rate in RODX4 in order to achieve equal temperatures to FRAPCON-3

Question 5:

Section 5.2.2 of BAW-10247 provides a range of uncertainty between planned fuel management and actual operation. The uncertainty used for RODEX4 is based on the lower value for this range in Section 5.2.2. Why should this lower value be used rather than the upper-bound value? The explanation provided in how the “Operational Flexibility Uncertainty” is applied in relation to the FDL is not clear in Appendix A of BAW-10247, an example and further explanation is needed (also see RAI #15 in relation to the FDL).

Response 5:

The operational flexibility uncertainty (OFU) accounts for differences between the planned operation and the actual operation. [

[

]

[]



Figure 5.1 BWR-4 Equilibrium Cycle, Maximum LHGRs



Figure 5.2 BWR-4 Equilibrium Cycle, Power Uncertainty as Fraction of FDL



Figure 5.3 BWR-4 Transition Cycle, Maximum LHGRs



Figure 5.4 BWR-4 Transition, Power Uncertainty as Fraction of FDL

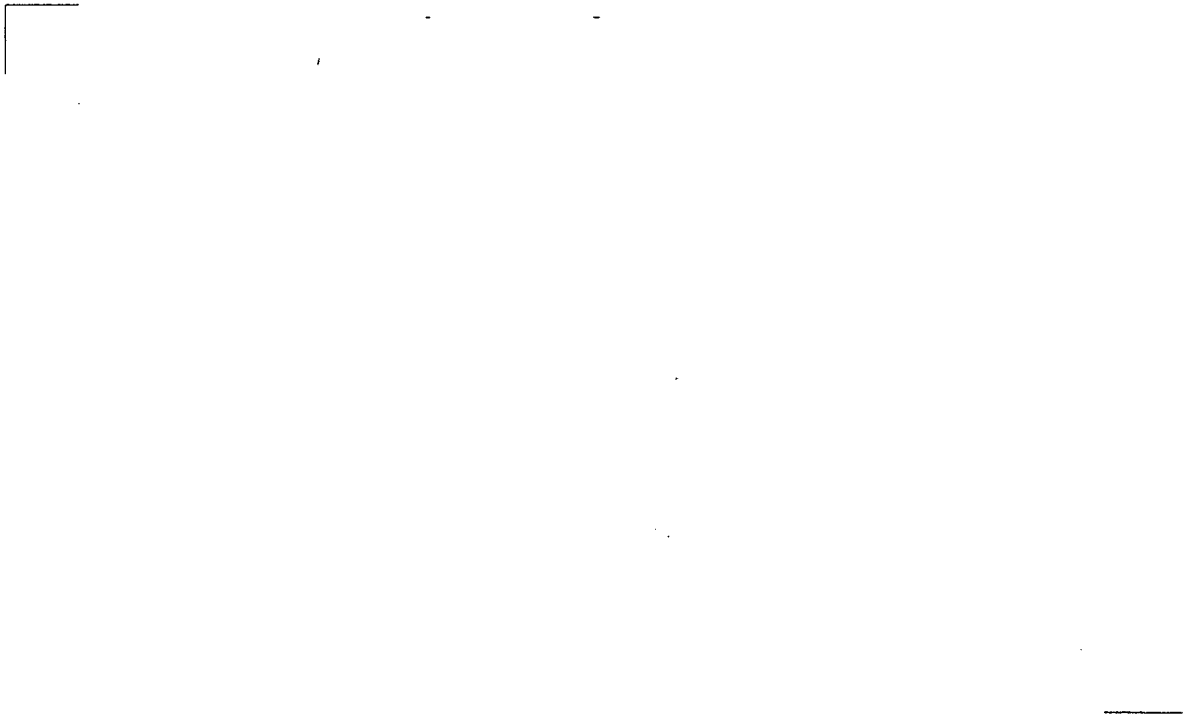


Figure 5.5 BWR-6 Equilibrium Cycle, Maximum LHGRs



Figure 5.6 BWR-6 Equilibrium Cycle, Power Uncertainty as Fraction of FDL



Figure 5.7 BWR-6 Transition Cycle, Max LHGRs



Figure 5.8 BWR-6 Transition, Power Uncertainty as Fraction of FDL



Figure 5.9 BWR-6 Equilibrium Cycle, Top 10 Adjusted Power Histories, Normalized



Figure 5.10 BWR-6 Equilibrium Cycle, Top 10 Adjusted Power Histories

Question 6:

The mean input and standard deviation for the fabrication parameters appears to be based on recent historical data for the past one to two years. It is known that the mean of fabrication data can shift with time depending on several factors including machine wear, drift in calibration and other factors such that the mean can vary significantly within the specification range. This may be true even though the standard deviation does not significantly change. This can result in a significant bias in the parameter that could impact the analysis. Therefore, the statistics of the mean fabrication parameter of each batch need to be continually verified to ensure that they do not significantly vary from that assumed in the RODEX4 analyses. In addition, the standard deviation can change with time also due to machine wear or a change in machinery or other factors. This is of concern because the RODEX4 standard deviation is not based on the fabrication specification range but rather on recent experience. Therefore, the standard deviation needs to be continually verified to demonstrate that it does not significantly vary from that assumed in the RODEX4 analyses. Please define the allowable limits of mean and standard deviation variation based on sensitivity analyses or other proposed methods and propose a methodology for how these new values of mean and standard deviation will be determined and implemented if a change is necessary.

Response 6:

The BAW-10247(P) submittal contained manufacturing data from the 2001 time frame. In the response to Question 26 of the first RAI, (BAW-10247Q1(P)), additional manufacturing data were presented for the purpose of evaluating possible correlations between different manufacturing parameters. The additional data included some of the pellet and cladding manufacturing parameters for the 2005/2006 time frame.

[

]

[

]

[

]

Table 6.1 Summary of Manufacturing Parameters

Table 6.2 BWR-6 Equilibrium Core Calculations Varying Manufacturing Uncertainties



Table 6.3 Batch Variation Summary of Manufacturing Parameters



Question 7:

Based on the FRAPCON-3 audit calculations of the power ramps performed in response to Round 1 RAI #7e, it appears that RODEX4 significantly underpredicts the centerline temperature relative to FRAPCON-3 (115°C-170°C) with the differences being greater at the higher ramped powers for the cases at 30 GWd/MTU. However, the two codes predict very similar results at 60 GWd/MTU. It has been noted that the thermal conductivity in RODEX4 is about 15-7% greater than in FRAPCON-3 at 20-40 GWd/MTU. The maximum temperature case provided in response to Round 1 RAI #32 did not contain any power ramps close to or above the LHGR limit. Please provide input and output similar to the information provided in Round 1 RAI #32 for fuel melt and strain increment (output for strain increment should include elastic + permanent and the permanent only) audit calculations of feedwater controller failure, Table 6.8 of BAW-10247(P). This will allow PNNL to determine if RODEX4 provides adequate predictions of temperature at high LHGR and strain increment levels, and determine if RODEX4 will provide conservative predictions of fuel melting and strain margins. Please provide these calculations at 20, 40 and 60 GWd/MTU for a FDL Set back of 70% or less.

Response 7:

The temperature calculations reported in the response to Q4, showed that FRAPCON-3 calculates higher temperatures than RODEX4 by up to 100 °C at 30 MWd/kgU. However, at 60 MWd/kgU, RODEX4 calculates higher temperatures than FRAPCON-3 by up to 60 °C.

The RODEX4 benchmarking of the Halden temperature database is illustrated in Figure 5.36 of BAW-10247(P) as (prediction/measurement) vs. burnup. There is no bias for the whole burnup range which includes the two burnup values selected for the case studies requested in Round 1 RAI Q7, which are referred to in this question. Comparisons to measured data are more appropriate than code-to-code comparisons. Thus, it is concluded that RODEX4 properly evaluates the temperature distribution over the whole burnup range.

The cases corresponding to an FDL set back of 70% or less, from Table 6.8 of BAW-10247(P) are: 1 to 4 and 7. These cases are presented below as the results of the worst-case combination of the parameters which are subject to uncertainty for AOO fast transients.

As described in Section 3.4.5, RODEX4 is run using a steady-state power history with one axial node running along the FDL line, or a fraction of it according to the FDL set back. The input data for this run are presented in the "input_fdl_uo2" and "input_fdl_gad" files, for the UO₂ and UO₂-Gd₂O₃ fuels, respectively. The power history is listed in the "ftn24" files for each of the cases requested.

A special RODEX4 module is activated after each 1 MWd/kgU burnup increment along the FDL power history (or scaled down power history based on the FDL setback). This special module performs a side (i.e. not feeding back into the main RODEX4 calculation) transient thermal conduction calculation coupled with a thermal-elastic analysis for a given power transient. The transient relative power history is given in the files called "xtrans" for each of the requested cases. The structure of the "xtrans" file is:

- 1st line: the total number of power entries
- 2nd line: final time[s]
- 3rd line: time step[s] – RODEX4 parameter
- Next lines: time[s] and relative power

The parameters which are treated with uncertainties are those listed on p. 6-19 of BAW-10247(P). The uncertainties used for these parameters are listed in the files "xtrinp1s" and "xtrinp1m" for the maximum strain and maximum central temperature, respectively. The only difference is that the last two power parameters have been combined into a single power parameter (using the square root of sum of squares rule). The first four and the last parameters are relative values which need to be multiplied by the standard deviation (see Table 5.5 of BAW-10247(P)).

The results are presented in the files "aoodet1" and "aoodet2" for the maximum strain and the maximum temperature, respectively, for all the requested cases. The second column lists the burnup, the third column lists the elastic + plastic hoop strain (%) and the fourth column is the centerline temperature [°C]. The aoomax1 and aoomax2 contain on the second and third columns the overall maximum strain and temperature values.

Question 8:

The coefficients for the UO_2 fission gas release model are given in EMF-3014(P) but no mention is made of coefficients for $\text{UO}_2\text{-Gd}_2\text{O}_3$. Are the coefficients for the FGR model in RODEX4 the same for these two fuel types?

Response 8:

Yes, the coefficients are assumed to be the same.

Question 9:

Section 7.3 of EMF-3014 provides a discussion of the ROPE-II tests with 3 widely different values of overpressure provided for Rod K1 with values of > 10 MPa (Table 7.6), 13.8 MPa (Section 7.3.1) and RODEX4 calculated value of 19 MPa (Section 7.3.2) suggesting significant uncertainty in the exact value of overpressure for this rod. This rod is of particular interest because significant cladding creepout was measured in this rod. Please provide a discussion about the variability in the overpressure for this rod.

Response 9:

After base irradiation in the Obrigheim reactor, Rod K1 was refabricated with an extended gas plenum of 11.4 cm^3 for an active length of 310 mm. In cold conditions the plenum volume is equal to 94% of the free volume. The plenum is completely separated from the pellet stack so that its temperature could be more easily controlled during the test (336°C). Since fission gas release was negligible during the test, the rod inner pressure was almost constant.

In the refabrication process, Rod K1 was pre-pressurized at 13.4 MPa (best estimate value calculated from the rod puncturing data). Studsvik Nuclear made an estimate of the internal pressure during the test using the perfect gas law and found 28 MPa (Reference 9.1). This corresponds to a rod overpressure of 13.8 MPa. This value is significantly higher than the value of > 10 MPa shown in the initial test specifications.

In the present version of RODEX4 it is not possible to change the plenum volume during irradiation. The RODEX4 calculation was initially performed with the initial small plenum as it existed before rod refabrication. The code predicted a rod overpressure of 19 MPa during the test. The results of that calculation are presented in EMF-3014 (Figure 7.18). The overestimate of the cladding deformation is due to the overprediction of the calculated rod inner pressure.

The ROPE-II calculations have been revisited and the error in the plenum volume identified. A second calculation was performed with the extended plenum. RODEX4 now predicts a rod overpressure of 14.7 MPa, which is in fairly good agreement with the Studsvik estimate. Since the RODEX4 calculation takes into account the gas present in the fuel rod, it is much more accurate than the Studsvik estimate. The calculated rod overpressure varied during irradiation in the range between 14.65 and 14.84 MPa (14.7 ± 0.2 MPa).

The cladding diameter results of the second calculation are shown in Figure 9.1. The figure shows that no adjustment of the cladding creep model is necessary to get a good prediction of cladding lift-off. Note that the reference point is different in Figure 7-18 of EMF-3014 and in

Figure 9.1. The irradiation was subdivided into a 70-hour first noise cycle, six 440-hour long irradiation cycles and a 20 hour final noise cycle. The cladding deformation jump during the first noise cycle has never been explained. Changing the reference point shows the cladding deformation during the long term irradiation cycles only.



**Figure 9.1 ROPE-II Rod K1
Cladding Lift-off under the Effect of a Constant Rod Overpressure of 14.7 MPa**

Rod K2 was also calculated with RODEX4. The RODEX4 predictions are shown in Figure 9.2 together with the measurement data. The rod overpressure during the test is 7.6 MPa.



**Figure 9.2 ROPE-II Rod K2
Cladding Lift-off under the Effect of a Constant Rod Overpressure of 7.6 MPa**

Reference 9.1: "ROPE II – Final Report of the ROPE II Project, Studsvik-ROPE II-20, September 1995.

Question 10:

The November 2006 response modified the coefficients to the RX Zr-2 axial growth model from those provided in EMF-3014. The original model was compared to axial elongation data in Figure 7.25 of EMF-3014. Please compare the model with the modified coefficients to these same data for RX Zr-2.

Response 10:

The new comparison is shown in Figure 10.1. The calculated rod elongation can only be larger than in Figure 7.25 of EMF-3014, since the latter shows the elongation with essentially no axial growth. The model parameters were optimized using the Risø data only.



Figure 10.1 Validation of Axial Elongation of Rods with RX Zircaloy-2 Cladding

Question 11:

The RODEX4 prediction of free void volume to commercial fuel rod data shows considerable scatter and overprediction in some of these data (Figure 8.2 and Table 6.3 of EMF-3014). An over-prediction is non-conservative for the rod pressure analysis. This suggests that the RODEX4 rod pressure analysis should account for an over-predictive bias in void volume or an uncertainty in this parameter. Do the uncertainty in the creep and irradiation growth model account for the uncertainty observed in the free void volume data? Also, see RAI #1 above. Please provide a figure of RODEX4 predicted-minus-measured void volume versus burnup of the commercial rod void volume data. Please discuss the overprediction and uncertainty further including possible methods for accounting for this bias and uncertainty in the rod pressure analyses.

Response 11:

The RODEX4 predicted-minus-measured void volume versus burnup is presented in Figure 11.1 for the commercial database. The results show an almost best estimate response of the code except for the D24 rods at high burnup. For the D24 rods the code overestimates the free volume. The D24 fuel rods have a non-standard design with a large lower plenum in addition to the upper plenum. [

]

[

]



Figure 11.1 Validation of the Rod Free Volume

It is concluded that RODEX4 appropriately models the free void volume for traditional fuel designs for rod pressure analyses. In addition, the uncertainties on the rod free volume are adequately covered by the dimensional and creep uncertainties as shown in Figure 11.2. Figure 11.2 shows the result of conservative calculations. The conservatism has been obtained by modifying the upper plenum length, the dish volume, the cladding inner and outer diameters, pellet low burnup densification and cladding creep within the uncertainty ranges.



Figure 11.2 Conservative Rod Free Volume Predictions with Dimensional and Creep Uncertainties

Figure 11.2 shows that the results are conservative for all the rods of the database. Uncertainty analysis were not performed for several European reactors / rods for which manufacturing uncertainties were not available.

Question 12:

This is a follow up to RAI #12f from the first round RAIs. Please provide creep predictions in the hoop direction for a typical 10x10 cladding for CWSR Zr-2 and RX Zr-2 at an internal pressure of 100 psi and external pressure of 1050 psi constant out to 1200 days with a typical BWR cladding (assume no PCMI) fast flux and temperature. Also perform the same predictions with an internal pressure of 2200 psi and external pressure of 1050 psi. Identify primary creep, steady-state irradiation creep and if present thermal creep. Also, please provide the calculated generalized stress and strain and the stress components for each direction.

Response 12:

RODEX4 calculations were performed for a typical ATRIUM-10 cladding subjected to the internal and external pressures specified in the question. The internal pressure of 2200 psi was increased slightly (by ~4%) to 2287 psi in order to get identical hoop stress magnitude under compressive and tensile loads, which appears to be the intent of the question. The same calculation was performed for Zr-2 CWSR and RX cladding. The RODEX4 code was modified for this special purpose by substituting the internal gas pressure calculation with an input value. A user input pellet-to-cladding gap was specified sufficiently large to remain open and avoid

PCMI throughout the calculation. Figure 12.1 shows the absolute value of the permanent diameter change under both compression and tension for the CWSR cladding and demonstrates that the tensile load results in larger strain than associated with compression with the same hoop stress magnitude. Figure 12.2 demonstrates the same for RX cladding.

Figure 12.3 provides the creep components in the case of CWSR cladding under tensile hoop stress. These are the irradiation- and thermal-induced creep components. Primary creep is evident in the early thermal creep response. [

]

Table 12.1: Stress components for the creep exercise with high and low internal pressure with CWSR and RX cladding.



Figure 12.1 Diameter change due to creep for a typical ATRIUM-10 CWSR cladding with internal pressure of 2287 psi (tension) and 100 psi (compression).



Figure 12.2 Diameter change due to creep for a typical ATRIUM-10 RX cladding with internal pressure of 2287 psi (tension) and 100 psi (compression).



Figure 12.3 Diameter change due to creep for a typical ATRIUM-10 CWSR cladding with internal pressure of 2287 psi (tension). Irradiation- and thermal-induced creep components are shown.



Figure 12-4: Diameter change due to creep for a typical ATRIUM-10 CWSR cladding with internal pressure of 100 psi (compression). Irradiation- and thermal-induced creep components are shown.



Figure 12.5 Diameter change due to creep for a typical ATRIUM-10 RX cladding with internal pressure of 2287 psi (tension). Irradiation- and thermal-induced creep components are shown.



Figure 12.6 Diameter change due to creep for a typical ATRIUM-10 RX cladding with internal pressure of 100 psi (compression). Irradiation- and thermal-induced creep components are shown

Question 13:

Does RODEX4 have a failure limit or threshold for PCI or PCMI and if so describe the model and how is it implemented?

Response 13:

No, RODEX4 does not have a PCI or PCMI failure model.

Question 14:

[

]

Response 14:

[

] This is explicitly stated with respect to the SAFDL related to overheating of the cladding in Section 4.4 Thermal and Hydraulic Design of the Standard Review Plan (1987). This section states:

"The CPB acceptance criteria are based on meeting the relevant requirements of General Design Criterion 10 (Ref. 1.), as it relates to the reactor core being designed, with appropriate margin to assure that specified acceptable fuel design limits are not exceeded during normal operation or anticipated operational occurrences (AOO).

Specific criteria necessary to meet the requirements of GDC 10 are as follows:

1. SRP Section 4.2 specifies the acceptance criteria for evaluation of fuel design limits. One of the criteria provides assurance that there be at least a 95% probability at a 95% confidence level that the hot fuel rod in the core does not experience a departure from nucleate boiling (DNB) or transition condition during normal operation or anticipated operational occurrence.

Uncertainties in the values of process parameters, core design parameters, and calculation methods used in the assessment of thermal margin should be treated with at least a 95% probability at a 95% confidence level.

Two examples of acceptable approaches to meet this criterion are:

- a) For departure from nucleate boiling ratio (DNBR), critical heat flux ratio (CHFR) or critical power ratio (CPR) correlations there should be a 95% probability at the 95% confidence level, that the hot rod in the core does not experience a departure from nucleate boiling transition condition during normal operation or anticipated operational occurrences; or
- b) For DNBR, CHFR or CPR correlations, the limiting (minimum) value of DNBR, CHFR, of CPR is to be established such that at least 99.9% of the fuel rods would not be expected to experience departure from nucleate boiling or boiling transition during normal operation or anticipated operational occurrences."

[

]

[

]



Figure 14.1 BWR-6 Equilibrium Cycle Gas pressure Distribution



Figure 14.2 BWR-6 110% Power Uprate Gas Pressure Distribution

Question 15:

[

]

Response 15:

The crud layer thickness and composition can present large variations between different plants. They are strongly dependent on water chemistry. The prediction of the level of crud in a plant is outside the scope and capabilities of a fuel rod performance code.

Since water chemistry is not modeled in RODEX4 and the water chemistry of a specific reactor can be modified without notice by the utility even after the reload analysis is completed, crud deposition is not applied in the realistic fuel rod methodology.

In RODEX4 the crud layer can be modeled as an additional resistance between the coolant film and the corrosion layer. A crud heat transfer can be input and changed with burnup. Special crud studies can therefore be performed with RODEX4 on a plant specific basis if a customer believes that their plant has sufficient crud to require accounting for in the fuel rod analysis.

Question 16:

This is a follow-up to the AREVA response to RAI# 17 d. The hydrogen pickup fraction used in RODEX4 is more than a factor of 2 lower than the value used by FRAPCON-3.3 and as recently presented in the open literature. The response has provided a small amount of hydrogen pickup fraction with a large scatter and a value as high as 0.29. A recent search of the open literature by PNNL has demonstrated a very large range of pickup fractions in BWR Zr-2 cladding that appear to be a function of burnup with the highest pickup fractions above those used by FRAPCON-3 at burnups of 75 GWd/MTU (see References 1 and 2). It is apparent that the BWR operating parameters that impact the pickup of hydrogen in BWR cladding is poorly understood. A conservative pickup fraction is recommended for licensing analyses until hydrogen pickup in BWR Zr-2 cladding is better understood. Please provide hydrogen pickup data along with a proposed pickup fraction that bounds these data.

Response 16:

Recent publications such as Reference 16.1 indicate that

- At low burnup the hydrogen pickup fraction in BWR Zircaloy-2 is relatively high (up to 30%), but the hydrogen content in the cladding remains low (<50 ppm);
- At intermediate burnup the pickup fraction drops to values below 0.12, while the hydrogen content increases moderately;
- At high burnup (> 50 MWd/kgU) the pickup fraction may increase rapidly, while the hydrogen content may reach values in the hundreds ppm.

The data presented in the AREVA NP response to RAI# 17d are consistent with the above observation.

In the present version of RODEX4, the hydrogen content is calculated and printed for information only. The H content has no effect on the thermal-mechanical calculation. The value of the pickup fraction in RODEX4 is therefore not significant. If a limit is placed on hydrogen content in the future then a revision to the RODEX4 methodology may be necessary.

Reference 16.1: H. Hayashi et al., "Outside-in Failure of High burnup Fuel Cladding and Evaluation Tests of the Mechanism," 2005 Water Reactor Fuel Performance Meeting, Kyoto, Japan, October 2-6, 2005.

Question 17:

PNNL does not understand how either the cladding creepdown or the strain increment are calculated because the RODEX4 calculated values do not appear to make physical sense. How is the strain increment calculated in Tables 6.2, 6.3, 6.4 and 6.6 of BAW-10247, please provide elastic and plastic strains (or total and plastic)? Figure 17.1 shows the results of the BWR-4 CW-SRA UO₂ Max Strain audit calculation. The attached figures are proprietary and will be removed in the non-proprietary version of RAIs.

[

]

[

]



Figure 17.1 Max power node permanent hoop strain for the BWR-4 CW-SRA UO₂ Max Strain audit calculation



Figure 17.2 Contact pressure for the BWR-4 CW-SRA UO₂ Max Strain audit calculation

Response 17:

The BWR-4 CW-SRA UO₂ Max Strain Calculation involves moderate and strong PCI, as well as trapped stack. In Figures 17.3 through 17.8 the following variables are shown to help the analysis:

Figure 17.3: Local (node 6) LHGR in kW/m versus time

Figure 17.4: Local (node 6) radial gap at mid pellet and pellet end in μm versus time

Figure 17.5: Axial power distribution change at 620 days in kW/m

Figure 17.6: Local (node 6) hoop and axial stresses at the cladding inner surface in MPa versus time

Figure 17.7: Permanent hoop strain at node 6 in % versus time

Figure 17.8: Permanent hoop strain at node 6 in % versus fast fluence



Figure 17.3 Local LHGR at Axial Node 6



Figure 17.4 Pellet-Cladding Radial Gap at Node 6



Figure 17.5 Power Axial Distribution Change at 620 days





Figure 17.6 Stresses in the Cladding at Node 6



Figure 17.7 Permanent Hoop Strain at Node 6 versus Time



Figure 17.8 Permanent Hoop Strain at Node 6 versus Fast Fluence

[

]

[

]

Question 18:

Round 1 RAI #11c stated that RODEX4 has not been compared to creep collapse measurements. In order to approve this model, please provide an example calculation of axial gap formation using both COLAPX and RODEX4.

Response 18:

Background:

RODEX4 was calibrated against creep ovality measurements. This is appropriate as the initial conditions and the performance of the rods measured for creep ovality were well characterized. The range of creep deformation is also directly applicable to the evaluation criteria as it covers the deformation cladding range to the occurrence of pellet-clad radial gap closure. This is the time at which the potential for fuel rod axial gap formation is determined.

The COLAPX code was theoretically developed. It was verified to be conservative for creep collapse relative to the calculation of actual creep collapse in uncharacterized fuel rods with approximate power histories. The criteria for the COLAPX methodology was revised in its most recent approval so that the minimum burnup of radial gap closure was set at a level that would preclude subsequent axial gap formation. This was determined to be 6000 MWD/MTU.

The pellet-clad radial gap closure behavior is better predicted with RODEX4 due to its more accurate calibration than with COLAPX.

Methodologies:

In both the RODEX4 and COLAPX methodologies the potential for axial column gap formation is determined.

In the COLAPX methodology, which consists of both RODEX2 calculations for creepdown and COLAPX calculations for creep ovality, the radial pellet-clad gap status at 6000 MWd/MTU is determined. At this burnup the cold gap must remain open to allow axial densification of the fuel column. This burnup was generically established so that significant axial gaps would not subsequently occur if PCI occurred beyond this burnup. The radial gap closure was for the cold gap without consideration of pellet densification, determined for the design power history. RODEX2/COLAPX calculates the first radial pellet-clad gap closure high in the column due to the symmetric "design" axial power profile.

[

]

Question 19:

Please provide a description of how the RODEX4 methodology will be applied to a plant that undergoes an extended power uprate (EPU). Please provide example audit calculation of rod internal pressure and cladding strain. In addition, please provide a demonstration of how the power histories will be selected for this plant analysis. Perform this example for the maximum expected power uprate.

Response 19:

An extended power uprate means an increase in the core average power. Typically the maximum local power is not increased in a plant uprate due to the local LHGR or MCPR limitations. In this situation the FDL limit remains the same, but more of the assemblies operate at higher average powers. To achieve these core powers more new assemblies are loaded, sometimes a half core, and more assemblies are discharged after only two cycles and at lower burnups.

There is no change in the realistic methodology for this situation. The development and benchmarking of the RODEX4 methodology covers operation with and without EPU. All the power histories are sampled, and the evaluations are performed for the 2995 rod sampling. The rods analyzed will typically run at higher powers to lower burnups. The extreme result will still be required to meet all the same design criteria.

The power uncertainties are established in the same manner as in a non-uprate analysis (see Response 5). The core margin at each exchange interval is used to develop a uniform uncertainty distribution for each rod over each exchange interval.

Tables 6.1 and 6.5 of BAW-10247(P) describe the core parameters for the sample problems. The BWR-4 case (Table 6.5) includes a 20% reactor power uprate. The transition cycle case is for one cycle at 3458 MWt and the two following cycles at 3902 MWt. The equilibrium case for the BWR-4 is for all cycles at EPU conditions of 3902 MWt.

As can be seen from Table 6.5 the batch size increases for the EPU conditions. In response 30c of BAW-10247Q1(P) the distribution of rod powers in the core for the BWR-4 24 month (EPU) transition cycle is shown. The results of the response to question 30c are repeated in tabular form (Table 19.1), for improved clarity. It can be seen that the higher fraction of assemblies loaded, as compared to the standard BWR-6 (Table 19.2), means a higher average distribution of rod powers and earlier fuel discharges.

Note that these power distributions are prior to the application of the reactor core, the power distribution measurement (radial and axial) and operational flexibility (radial and axial) power uncertainties. The maximum planned power in the BWR-4 case was 12.0 kw/ft.

**Table 19.1 Frequency Distribution BWR-4 (EPU) Transition Cycle Case,
Maximum Nodal Power versus Rod Burnup**

**Table 19.1 Frequency Distribution BWR-4 (EPU) Transition Cycle Case,
Maximum Nodal Power versus Rod Burnup (continued)**

**Table 19.2 Frequency Distribution BWR-6 Transition Cycle Case,
Maximum Nodal Power versus Rod Burnup**



**Table 19.2 Frequency Distribution BWR-6 Transition Cycle Case,
Maximum Nodal Power versus Rod Burnup (continued)**



References

- 19.1 Itagaki, N., K. Kakuishi, F. Yasuhiro, and T. Furuya (NFI) and O. Kubota (TEPCO), "Development of New Corrosion Resistance Zr Alloy HIFI," ENS TopFuel Meeting, March 16-19, 2003, Wurzburg, Germany.
- 19.2 K. Ohira, J. Kamimura, N. Otsuka, and S. Yamaguchi, "Recent Experience and Development of BWR Fuel at NFI," Proceedings of Water Reactor Fuel Performance Meeting in Kyoto, Japan, October 2-6, 2005.

Subject: How are Uncertainties Applied??

Page 1 of 5

**eMail dated August 27, 2007
from Michael T. Bunker to Carl E. Beyer**

Subject: How are Uncertainties Applied?

From: BUNKER Michael T (AREVA NP INC)
Sent: Monday, August 27, 2007 2:06 PM
To: 'Beyer, Carl E'; Geelhood, Kenneth J
Cc: HOLM Jerald S (AREVA NP INC); ARIMESCU Ioan (AREVA NP INC); 'Holly Cruz'; 'Shih-Liang Wu'; PRUITT Douglas W (AREVA NP INC)
Subject: RE: HOW ARE UNCERTAINTIES APPLIED??

Carl,

We have put together the following response to your emails from last week with respect to the issue of applying the parameter uncertainties in the bounding analyses.

Issue

The issue is the correct method of combining uncertainties to show bounding predictions of benchmarking cases. The model parameters currently questioned are [

]

Summary

We have reviewed the bounding analyses and agree that a more rigorous bounding analysis would be appropriate. This would entail [

]

We revisited the previous bounding temperature analysis with the more rigorous approach and found both an error in the initial analysis. [

below,

] The discussion of this is provided in detail

With respect to the ramp strain, our analysis indicates that the bounding analysis could be covered almost exclusively with the [

]

With respect to creepdown, the main players are [

]

Discussion

AOO temperature

Our review of the temperature bounding analysis found an error in the analyses which resulted in incorrect power variations being applied at the thermocouple locations. This means that most test results previously shown lacked the effect of power variations. The best estimate analysis was rerun as well as an analysis with [

] The results of these analyses for temperatures above 1300 C are provided in the figures below.

[

]

The statistics of the nominal calculation are: [

]

In conclusion, [

]

Subject: How are Uncertainties Applied??

Page 3 of 5



AOO strain

For the ramp strains, the first sensitivity analysis showed that the [

Because the []



Steady State Creep

Figure 2.5 shows maximum creepdown prediction deviations of [

]

Subject: How are Uncertainties Applied??

Page 5 of 5

Both the measurement and creep uncertainties were applied conservatively. The measurement uncertainty neglects [

]

The creep uncertainty does not include the effect of the [

]

Conservatism in the [void volume verification are in neglecting the new +/-16% swelling uncertainty bound and the 5% power/flux uncertainty. The void volume uncertainty of Figure 11.2 is already conservative. The addition of the solid swelling uncertainty and the increase in the creep uncertainty will be sufficient to bound the data in a combined manner, considering creep, power, swelling and manufacturing uncertainty components.]

Sincerely,

Michael T. Bunker
AREVA NP Inc.
An AREVA and Siemens Company
2101 Horn Rapids Road,
Richland, WA. 99352
(509) 375-8661
michael.bunker@areva.com



September 26, 2007
NRC:07:049

Document Control Desk
U.S. Nuclear Regulatory Commission
Washington, D.C. 20555-0001

Changes to AREVA NP's Topical Report BAW-10247(P), "Realistic Thermal-Mechanical Fuel Rod Methodology for Boiling Water Reactors"

Ref.: 1. Letter, James F. Mallay (AREVA NP Inc.) to Document Control Desk (NRC), "Request for Review and Approval of BAW-10247(P), 'Realistic Thermal-Mechanical Fuel Rod Methodology for Boiling Water Reactors'," NRC:04:047, August 19, 2004.

AREVA NP Inc., (AREVA NP) requested the NRC's review and approval of the topical report BAW-10247P, "Realistic Thermal-Mechanical Fuel Rod Methodology for Boiling Water Reactors" in Reference 1. The purpose of this letter is to propose changes to some of the uncertainties defined in the topical report. The uncertainties used in the methodology are summarized in BAW-10247Q4P, "Response to Request for Additional Information – BAW-10247(P)", Tables C, D, and E. These changes are being proposed based on telephone conversations with the NRC in reaching an agreement to increase uncertainties in specific parameters in order to provide a more conservative bound to the benchmark data.

Attachment A to this letter provides the specific values of the proposed revised uncertainties. A proprietary and a non-proprietary version of Attachment A are provided.

As required by 10 CFR 2.390(b) an affidavit is enclosed to support the withholding of the information from public disclosure.

Sincerely,

A handwritten signature in black ink, appearing to read 'Ronnie L. Gardner', is written over a horizontal line.

Ronnie L. Gardner, Manager
Site Operations and Corporate Regulatory Affairs
AREVA NP Inc.

Enclosures

cc: H. D. Cruz
S. Wu
Project 728

AREVA NP INC.
An AREVA and Siemens company

Attachment A

Revised Uncertainties

AREVA NP proposes to change some of the uncertainties defined in the topical report BAW-10247P. The uncertainties used in the methodology are summarized in the report BAW-10247Q4P, "Response to Request for Additional Information – BAW-10247(P)," tables C, D, and E. These changes are being proposed based on telephone conversations in which the NRC expressed a desire for increased uncertainties in specific parameters in order to provide a more conservative bound to the benchmark data. [

].

The range (number of standard deviations) associated with the pellet thermal expansion, thermal conductivity, and specific heat listed in the summary tables D and E are incorrect. These tables list the ranges as [] was used for these parameters throughout our analyses. The use of the [] range value for pellet thermal expansion and thermal conductivity can be seen in Table 2.12 of BAW-10247Q4P.

requested qualifies under 10 CFR 2.390(a)(4) "Trade secrets and commercial or financial information".

6. The following criteria are customarily applied by AREVA NP to determine whether information should be classified as proprietary:

- (a) The information reveals details of AREVA NP's research and development plans and programs or their results.
- (b) Use of the information by a competitor would permit the competitor to significantly reduce its expenditures, in time or resources, to design, produce, or market a similar product or service.
- (c) The information includes test data or analytical techniques concerning a process, methodology, or component, the application of which results in a competitive advantage for AREVA NP.
- (d) The information reveals certain distinguishing aspects of a process, methodology, or component, the exclusive use of which provides a competitive advantage for AREVA NP in product optimization or marketability.
- (e) The information is vital to a competitive advantage held by AREVA NP, would be helpful to competitors to AREVA NP, and would likely cause substantial harm to the competitive position of AREVA NP.

The information in the Document is considered proprietary for the reasons set forth in paragraphs 6(b) and 6(c) above.

7. In accordance with AREVA NP's policies governing the protection and control of information, proprietary information contained in this Document have been made available, on a limited basis, to others outside AREVA NP only as required and under suitable agreement providing for nondisclosure and limited use of the information.

8. AREVA NP policy requires that proprietary information be kept in a secured file or area and distributed on a need-to-know basis.

9. The foregoing statements are true and correct to the best of my knowledge, information, and belief.

Jerald S Holm

SUBSCRIBED before me this 25th
day of September, 2007.

Susan K McCoy

Susan K. McCoy
NOTARY PUBLIC, STATE OF WASHINGTON
MY COMMISSION EXPIRES: 1/10/2008



eMail dated November 2, 2007
from J. S. Holm to Holly Cruz
with attached file:

Initial RODEX4 Draft SER Comments.doc

From: HOLM Jerald S (AREVA NP INC)
Sent: Friday, November 02, 2007 6:03 AM
To: 'Holly Cruz'
Cc: Shih-Liang Wu (slw2@nrc.gov.); 'Beyer, Carl E'; BUNKER Michael T (AREVA NP INC); ARIMESCU Ioan (AREVA NP INC); PRUITT Douglas W (AREVA NP INC)
Subject: RODEX4

Holly

The attached file contains information relative to three of the conditions in the preliminary SE that you provided on the topical report BAW-10247P. This provides background for our discussion on these conditions next week.

Jerry

Jerald S. Holm
Manager, Product Licensing
AREVA NP Inc.
An AREVA and Siemens company
Tel.: 509-375-8142
Mobile: 434-238-4230
Fax: 509-375-8965
Jerald.Holm@areva.com
AREVA

Initial Restriction 1e, Liner Cladding

The CWSR clad model was purposely generated to model both liner and non-liner CWSR clad. BAW-10247Q4P, Section 2, Part 2 was prepared with both liner and non-liner cladding creep data. The data included 487 span average creep measurements from non-liner clad and 84 from liner clad. This data is shown in figures 1e-1 and 1e-2 below and show that the liner measurements are consistent and in-line with the non-liner measurements. The data from figures 2.3, 2.5, 2.6, and 2.7 of BAW-10247Q4P are re-plotted below with the liner and non-liner data distinguished. The re-plotted figures show that our liner and non-liner clad have similar creep behaviors.

While the RODEX4 methodology [] . Figure 1e-2 shows that this provides a best estimate model for the liner clad with the same or better accuracy than for the non-liner clad.

We feel it would be appropriate either remove this restriction entirely or to revise the wording of the restriction to [] .

Figure 1e-1 Comparison of Liner and non-Liner Creep Behavior



Figure 1e-2 Comparison of Liner and non-Liner Behavior

Initial Restriction 1f, Lower Plenums

As all of our Atrium-10 fuel designs include part length rods (PLRs) with lower plenums, and all of our sample problems included the PLR rods in the analyses, the blanket restriction on all fuel designs with lower plenums needs to be addressed.

A small sub-set of 9 PWR fuel rods with lower plenums was presented which had an over-predictive bias. However, this fuel was fabricated by an old AUC process which is no longer in use and the swelling characteristics of this old fuel type are larger than for the more recent fuel, which forms the bulk of our creepdown database. The excessive swelling of this fuel is considered the major cause of the small over prediction for this sub-set of fuel rods with lower plenums.

It is recognized that a secondary cause is the lack of accounting for the cladding creepdown in the lower plenum region. We feel it would be appropriate to model fuel rods with a lower plenum as having a consolidated upper plenum which includes the free volume of the lower plenum. The temperature and thermally induced creep in the upper plenum would be conservative with respect to gas pressure compared to the lower temperature lower plenum. The irradiation induced creep between the two would be expected to be roughly equivalent for a full length rod and conservative for a part length rod.

As indicted in Section 3.7.2 of the SER, the internal gas pressure is conservatively predicted by RODEX4. Therefore, any small inaccuracies associated with the free void volume prediction for lower plenum fuel rods would be compensated by the conservative FGR calculation.

We would propose that as an alternative to the existing restriction, that for fuel designs with lower plenums, RODEX4 would be required to model the lower plenum free volume in the upper plenum where both thermal and irradiation induced creep would be modeled using the upper plenum conditions.

Initial Restriction 7, Crud Deposition

With respect to initial restriction 7 on including crud deposition which) requires that the RODEX4 calculations must account for a design basis crud thickness.

As our clad oxide measurements [

].

The restriction goes on to specify that specific analyses would be required if an abnormal crud or corrosion layer is observed at any given plant. Where we have plant specific measurements indicating abnormal crud, our analyses for that plant will be based on the plant specific data.

eMail dated November 11, 2007
from J. S. Holm to Holly Cruz
Subject File: RODEX4

From: HOLM Jerald S (AREVA NP INC)
Sent: Sunday, November 11, 2007 6:14 PM
To: 'Holly Cruz'
Cc: BUNKER Michael T (AREVA NP INC); PRUITT Douglas W (AREVA NP INC); ARIMESCU Ioan (AREVA NP INC); BROWN Charles A (AREVA NP INC)
Subject: RODEX4

Holly

Additional information is provided on two of the three RODEX4 SE conditions we are discussing. Please pass this information on to Wu and Clifford. Also, please let me know when the staff would like to discuss the three conditions again.

Thanks

Jerry

Jerald S. Holm
Manager, Product Licensing
AREVA NP Inc.
An AREVA and Siemens company
Tel: 509-375-8142
Mobile: 434-238-4230
Fax: 509-375-8965
Jerald.Holm@areva.com
AREVA

Subject File: RODEX4

Page 2 of 7

eMail dated November 11, 2007
from J. S. Holm to Holly Cruz
Subject File: RODEX4

Liner File

Initial Restriction 1e, Liner Cladding

The CWSR clad model was purposely generated to model [

]

These figures show that our [

]

While the RODEX4 methodology does not [

]

We feel it would be appropriate [

]

Subject File: RODEX4

Page 3 of 7



eMail dated November 11, 2007
from J. S. Holm to Holly Cruz
Subject File: RODEX4

Lower Plenum file

The preliminary SE for the RODEX4 topical report contains a condition that the methodology can not be applied to fuel rods with a lower plenum. Specifically the limitation is:

1. *RODEX4 is approved for modeling BWR fuel rods with the following limitations:*
 - f. *No fuel rod designs containing a lower plenum region.*

This condition appears to be imposed due to the fact that the code over predicts the rod internal free volume for a sub-set of the D24 fuel rods at EOL. This over prediction is, in our opinion, primarily due to the fact that this sub-set of fuel rods [

]

Additional data for 16 fuel rods with lower plenums and irradiated in the D24 reactor has recently been added to our commercial database. These fuel rods include [

]



Figure 1 Benchmarking of lower plenum fuel rods

We believe that another secondary contributor (though with a larger impact than neglecting creep in the plenum regions) to the over prediction of the fuel rod internal free volume is one of the modeling assumptions in RODEX4 related to [

]

In order to investigate the impact of this assumption, the code was modified in order to allow for [

]

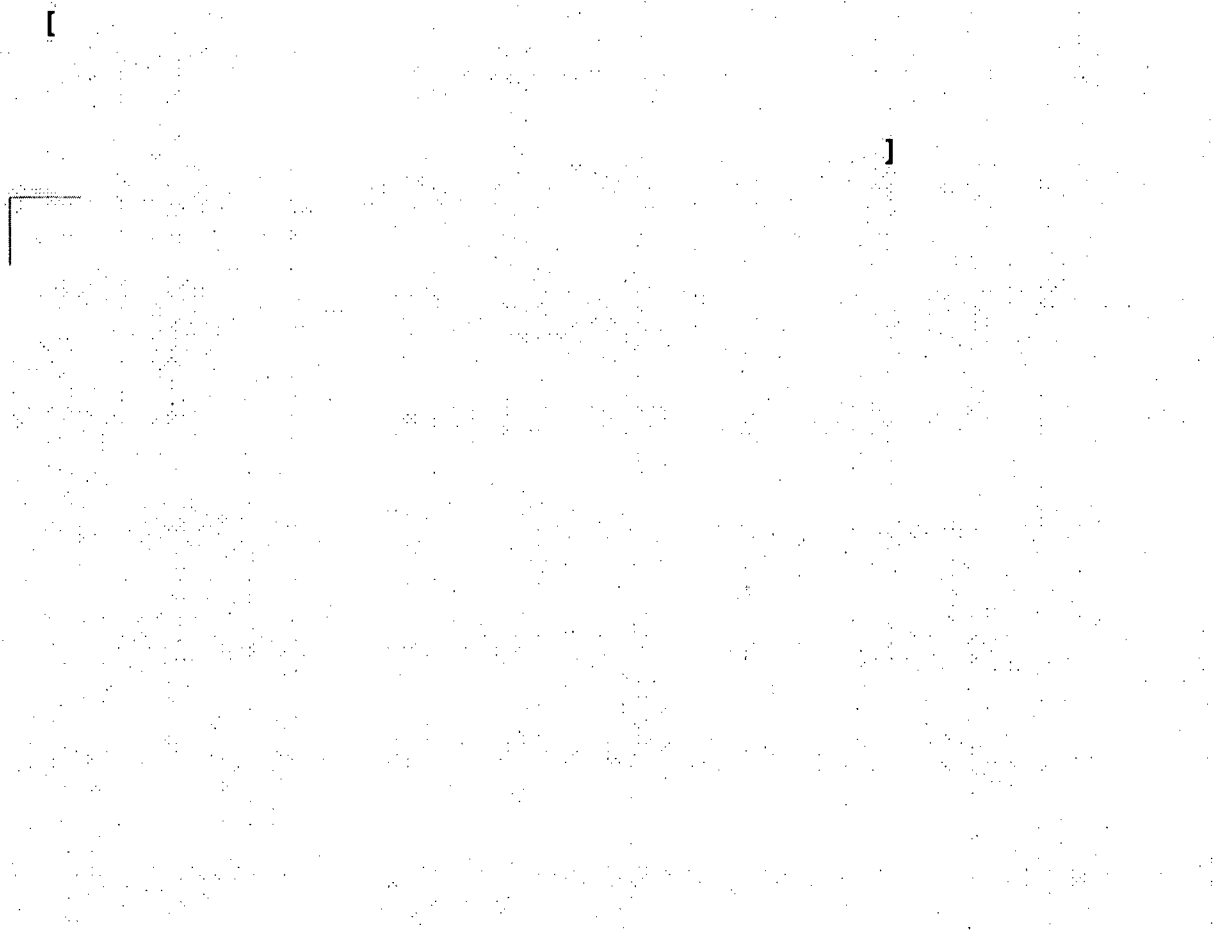


Figure 2 1 Benchmarking of lower plenum fuel rods with the modified code assumption

The results of the modified code are also illustrated below in a figure equivalent to Fig. 11.1 from BAW-10247Q4(P).

Included in this figure are the 16 fuel rods with lower plenums, irradiated in D24, which were recently added to our commercial database. The figure shows best-estimate benchmarking for the whole data set and, in particular, best-estimate and reduced scattering for [

]



Figure 3. Updated Figure 11.1 with the modified code assumption and new D24 DC sub-set

An impact assessment was made in order to determine the effect of this code modification on the licensing application results. The only noticeable change was with respect to the maximum gas pressure, which conservatively increased by about 60 psia.

The above two factors justify the removal of the restriction on the application of the methodology to fuel rods with a lower plenum. The two factors are [

]

BAW-10247(NP)
Revision 0

Realistic Thermal-Mechanical Fuel Rod Methodology for Boiling Water Reactors

August 2004

Nature of Changes

<u>Item</u>	<u>Paragraph or Page(s)</u>	<u>Description and Justification</u>
1.	All	This is a new document.

Contents

Abstract.....	xi
1.0 Introduction	1-1
2.0 Methodology Roadmap	2-1
2.1 Requirements and Capabilities	2-1
2.1.1 Fuel Rod Criteria	2-1
2.1.2 Reactor Operation Scenarios	2-1
2.1.3 RODEX4 Fuel Rod Code	2-2
2.1.4 Fuel Rod Evaluation Methodology	2-3
2.1.5 Documentation	2-4
2.2 RODEX4 Calibration/Validation and Range of Parameters.....	2-4
2.2.1 Fuel Performance Database	2-4
2.2.2 RODEX4 Calibration	2-5
2.2.3 Assessment of Biases	2-6
2.2.4 Validation Ranges	2-6
2.3 Uncertainty Analyses.....	2-7
2.3.1 PIRT Process	2-7
2.3.2 Reactor Operation Uncertainties.....	2-7
2.3.3 Fuel Rod Manufacturing Uncertainties.....	2-8
2.3.4 Model Parameter Uncertainties.....	2-9
2.4 Application Examples	2-10
2.4.1 Normal Operation.....	2-10
2.4.2 Sensitivity Studies	2-11
2.4.3 Slow Transient Anticipated Operational Occurrences.....	2-11
2.4.4 Fast Transient Anticipated Operational Occurrences.....	2-11
3.0 Requirements and Capabilities	3-1
3.1 Fuel Rod Criteria	3-1
3.1.1 Criteria for Normal Operation	3-1
3.1.2 Criteria for Anticipated Operational Occurrences.....	3-2
3.2 Reactor Operation Scenarios	3-2
3.2.1 Scenario for Normal Operation.....	3-2
3.2.2 Scenario for Slow Transient AOOs	3-3
3.2.3 Scenario for Fast Transient AOOs	3-3
3.3 RODEX4 Fuel Rod Code	3-4
3.3.1 Code Requirements	3-4
3.3.2 Code Applicability.....	3-4
3.3.3 RODEX4 Summary	3-5
3.3.3.1 Thermal Processes.....	3-6
3.3.3.2 Mechanical Processes.....	3-7
3.3.3.3 Fission Gas Release Processes.....	3-7
3.3.3.4 Thermal Transient Solution for Fast Transients.....	3-8
3.3.3.5 RODEX4 Documentation.....	3-8
3.4 Fuel Rod Evaluation Methodology	3-8
3.4.1 Evaluation Objectives.....	3-8

3.4.2	Statistical Process	3-9
3.4.3	Methodology for Normal Operation	3-10
3.4.4	Methodology for Slow Transient AOOs	3-11
3.4.5	Methodology for Fast Transient AOOs	3-13
4.0	RODEX4 Calibration/Validation and Range of Parameters	4-1
4.1	Fuel Performance Database	4-2
4.1.1	Separate Effects Tests	4-3
4.1.2	Integral Tests - International Programs	4-3
4.1.3	Commercial Irradiations	4-5
4.2	Calibration/Validation	4-6
4.2.1	Centerline Temperature	4-7
4.2.2	Fission Gas Release	4-13
4.2.3	Clad Creep	4-21
4.2.4	Clad Creep Ovality	4-25
4.2.5	Clad Ramp Strain	4-28
4.2.6	Rod Axial Elongation	4-33
4.2.7	Rod Free Volume	4-35
4.2.8	Clad Oxidation	4-38
4.3	Assessment of Biases	4-41
4.3.1	Centerline Temperature	4-41
4.3.2	Fission Gas Release	4-41
4.3.3	Clad Creep	4-41
4.3.4	Clad Creep Ovality	4-41
4.3.5	Clad Ramp Strain	4-42
4.3.6	Rod Axial Growth	4-42
4.3.7	Rod Free Volume	4-42
4.3.8	Clad Oxidation	4-42
4.4	Validation Ranges	4-42
5.0	Uncertainty Analyses	5-1
5.1	PIRT Process	5-1
5.2	Reactor Operation Uncertainties	5-1
5.2.1	Power Histories	5-2
5.2.2	Variation from Planned Fuel Management	5-2
5.2.3	Core Power Distribution Measurement Uncertainty	5-2
5.2.4	Reactor Power Measurement Uncertainty	5-3
5.2.5	Power Uncertainties for Normal Operation	5-3
5.2.6	Power Uncertainties for Slow Transient AOOs	5-3
5.2.7	Power Uncertainties for Fast Transient AOOs	5-4
5.2.8	PIRT Reactor Operation Uncertainty Summary	5-4
5.3	Fuel Rod Manufacturing Uncertainties	5-8
5.3.1	Cladding Manufacturing Uncertainties	5-8
5.3.2	Pellet Manufacturing Uncertainties	5-10
5.3.3	Rod Manufacturing Uncertainties	5-11
5.3.4	PIRT Manufacturing Uncertainty Summary	5-12
5.4	RODEX4 Model Parameter Uncertainties	5-14
5.4.1	Fission Gas Release Model Parameter Uncertainty	5-16
5.4.1.1	Fission Gas Uncertainty Data Set	5-16

5.4.1.2	Diffusion Coefficient Uncertainty.....	5-17
5.4.2	Irradiation Creep Parameter Uncertainty.....	5-20
5.4.3	Oxidation Parameter Uncertainty	5-22
5.4.4	Creep Ovality Uncertainty	5-23
5.4.5	PIRT Model Parameter Uncertainty Summary.....	5-23
5.5	Thermal Transient Solution Uncertainties	5-28
6.0	Application Examples.....	6-1
6.1	Normal Operation Examples	6-1
6.1.1	BWR-6 Reactor, 18 Month Cycles	6-1
6.1.1.1	Description.....	6-1
6.1.1.2	Example Licensing Analysis	6-2
6.1.1.3	Annealed Clad Material Demonstration	6-3
6.1.1.4	Sensitivity Studies.....	6-3
6.1.2	BWR-4 Reactor, 24 Month Cycles	6-13
6.1.2.1	Description.....	6-13
6.1.2.2	Example Licensing Analysis	6-13
6.2	Slow Transient Example - BWR-4 Control Rod Withdrawal Error.....	6-15
6.2.1	Description	6-15
6.2.2	Control Rod Withdrawal Error Analysis	6-16
6.2.3	Baseline for Control Rod Withdrawal Error Comparison	6-17
6.3	Fast Transient Example – BWR-4 Feedwater Controller Failure	6-18
6.3.1	Description	6-18
6.3.2	FWCF Analyses	6-19
6.4	Comparison of New Realistic with Existing Methodology.....	6-32
7.0	References.....	7-1
Appendix A	Methodology for Varying [.....].....	1

Tables

4.1	International Database	4-4
4.2	Commercial Database.....	4-6
4.3	RODEX4 Temperature Database	4-8
4.4	Cladding Ovality Validation	4-26
4.5	Large Cladding Deformation Database - Ramp Tests	4-29
4.6	Summary of Database for Free Volume Verification	4-37
4.7	RODEX4 Range of Validation	4-43
5.1	PIRT for Reactor Operation, Importance of Uncertainty to Evaluation Result	5-30
5.2	PIRT for Fuel Rod Definition, Importance of Parameter Uncertainty to Evaluation Result	5-31
5.3	PIRT for Fuel Rod RODEX4 Modeling, Importance of Model Uncertainty to Evaluation Result	5-32
5.4	BWR Core Simulator Code Measured Power Distribution Uncertainty	5-34
5.5	Fast Transient Model Uncertainties	5-34
6.1	Parameters for BWR-6 Transition and Equilibrium Batches	6-5
6.2	Normal Operation Results Summary BWR-6 ATRIUM-10 with Standard Clad	6-6
6.3	Normal Operation Results Summary BWR-6, ATRIUM-10 with RX Clad	6-7
6.4	Sensitivity Study Results BWR-6 UO ₂ Rods.....	6-8
6.5	Parameters for BWR-4 Transition and Equilibrium Cores.....	6-14
6.6	Normal Operation Results Summary BWR-4 ATRIUM-10 with Standard Clad	6-15
6.7	CRWE Results Summary BWR-4 Transition and Equilibrium Batches.....	6-17
6.8	Summary of BWR-4 Sample Feedwater Controller Failure, RODEX4 Fast Transients	6-21
6.9	Comparison of Similar Realistic and Deterministic Evaluations	6-33

Figures

4.1	Halden Temperature Database - Fuel Centerline Temperature.....	4-10
4.2	Risø Temperature Database – Fuel Centerline Temperature.....	4-11

4.3	Halden Temperature Database - Temperature Deviation	4-12
4.4	International Fission Gas Release Database	4-16
4.5	International Database - Histogram of FGR Deviation log(C/M)	4-16
4.6	International Database - log(C/M) vs. Measured FGR	4-17
4.7	International Database - log(C/M) vs. Rod Average Exposure	4-17
4.8	Commercial Fission Gas Release Database	4-18
4.9	Commercial Database – Histogram of FGR Deviation log(C/M)	4-18
4.10	Commercial Database - log (C/M) vs. Measured FGR	4-19
4.11	Commercial Database - log (C/M) vs. Rod Average Exposure	4-19
4.12	Commercial Database - FGR of Gadolinia Fuel Rods	4-20
4.13	Rod Inner Pressure at Room Temperature	4-20
4.14	Predicted/Measured Creep Down for BWR 9x9 Cladding	4-23
4.15	Predicted/Measured Creep Down for BWR 9x9 Cladding (Continued)	4-23
4.16	Cladding Creep Down for BWR 10x10 Cladding	4-24
4.17	Predicted/Measured Creep Down of Recrystallized Zircaloy-2 Cladding	4-24
4.18	Validation of Cladding Ovality - HBRP Rods	4-27
4.19	Mark-BEB Rod 65-2 - Rod Diameter at Pellet End	4-30
4.20	Mark-BEB Rod 65-2 - Diameter Increase	4-30
4.21	Mark-BEB Rod 65-4 - Diameter Increase	4-31
4.22	Mark-BEB Rod 66-2 - Diameter Increase	4-31
4.23	Super-Ramp Rod PK2/3 - Diameter Increase	4-32
4.24	Super-Ramp Rod PK2/3 - Rod Diameter at Pellet End	4-32
4.25	Validation of Rod Axial Growth for BWR 10x10 Fuel	4-34
4.26	Validation of Rod Axial Growth for BWR 9x9 Fuel	4-34
4.27	Validation of Rod Axial Growth for BWR RX Clad Fuel	4-35
4.28	Validation of Rod Free Volume	4-38
4.29	Outer Corrosion Layer Thickness in BWR 10x10 Fuel versus Exposure	4-40
4.30	Validation of the Cladding Outer Corrosion	4-40
5.1	Clad Inside Diameter Distribution	5-9
5.2	UO ₂ Fuel Pellet Resinter Density Distribution	5-11
5.3	Fuel Rod Plenum Length Distribution	5-12
5.4	Histogram of the FGR Data Comparisons	5-19
5.5	FGR Data with 95% Upper and Lower Bounds	5-20

5.6	Cladding Creep Down and Fabrication Uncertainty at the 2 σ Bounds of the Outer Diameter.....	5-22
5.7	[] Distribution for BWR-4 Equilibrium Batch Sample Case.....	5-35
6.1	BWR-6 Equilibrium Batch - Maximum Rod Internal Pressure.....	6-9
6.2	BWR-6 Equilibrium Batch - Maximum Rod Internal Pressure Histogram.....	6-9
6.3	BWR-6 Equilibrium Batch - Maximum Clad Strain during Normal Operation	6-10
6.4	BWR-6 Equilibrium Batch - Maximum Clad Strain Increase during Normal Operation	6-10
6.5	BWR-6, Equilibrium Batch - Maximum Remaining Column Densification after Creep Ovality Contact.....	6-11
6.6	BWR-6 Equilibrium Batch - Maximum Fatigue Usage per 1000 Cycles.....	6-11
6.7	BWR-6, Equilibrium Batch - Maximum Clad Oxidation	6-12
6.8	BWR-6, Equilibrium Batch - Maximum Clad Hydrogen Pickup	6-12
6.9	25% Power FWCF	6-22
6.10	30% Power FWCF	6-23
6.11	100% Power FWCF	6-24
6.12	Maximum Strain Results (Case 1) []	6-25
6.13	Maximum Temperature Results (Case 1) []	6-25
6.14	Maximum Strain Results (Case 2) []	6-26
6.15	Maximum Temperature Results (Case 2) []	6-26
6.16	Strain Results vs. Burnup for Limiting Run []	6-27
6.17	Temperature Results vs. Burnup for Limiting Run []	6-27
6.18	Maximum Strain Results (Case 8) []	6-28
6.19	Maximum Temperature Results (Case 8) []	6-28
6.20	Strain Results vs. Burnup for Limiting Run []	6-29
6.21	Temperature Results vs. Burnup for Limiting Run []	6-29

6.22	Maximum Strain Results (Case 10) []	6-30
6.23	Maximum Temperature Results (Case 10) []	6-30
6.24	Strain Results vs. Burnup for Limiting Run []	6-31
6.25	Temperature Results vs. Burnup for Limiting Run []	6-31
A.1	Axial Power Profile Change [Nodal Value]	A-6
A.2	Axial Power Profile Change []	A-6

This document contains a total of 161 pages.

Nomenclature

<u>Acronym</u>	<u>Definition</u>
AOO	Anticipated operational occurrence
ASME	American Society of Mechanical Engineers
BOL	Beginning-of-life
BWR	Boiling water reactor
CHF	Critical Heat Flux
CL	Confidence level
CRWE	Control rod withdrawal error
CSAU	Code Scaling, Applicability and Uncertainty
CWSR	Cold worked stress relieved
DOE EBP	Department of Energy Extended Burnup Program
EFPD	Effective Full Power Days
EOL	End-of-life
FANP	Framatome ANP, Inc.
FDL	Fuel Design Limit, LHGR versus exposure
FGR	Fission gas release
FPIP	Fuel Performance Improvement Program
FWCF	Feedwater controller failure
HBEP	High Burnup Effect Program
HBRP	High Burnup Ramp Program
LHGR	Linear heat generation rate (e.g., kW/ft or kW/m)
LHGRFAC	Core power and/or flow-dependent multiplier on the FDL
LWR	Light water reactor
MATRO	Library of Materials Properties for Light Water Reactor Accident Analysis
NAF	Neutron Absorber Fuel
NMCA	Noble metals chemistry addition
PAPT	Protection Against Power Transient
PCMI	Pellet-clad mechanical interaction
PIE	Post irradiation examination
PIRT	Phenomena identification and ranking table
PWR	Pressurized water reactor
Risø DITP	Danish Irradiation Test Program
Risø DRTP	Danish Ramp Test Program
Risø FGP	Danish Fission Gas Project

Risø TFGP	Transient Fission Gas Project
ROPE	Rod overpressure experiment
RX	Recrystallized annealed
SRP	Standard Review Plan
USNRC	U.S. Nuclear Regulatory Commission
ZRY	Zircaloy

Abstract

This report presents a methodology for the realistic evaluation of the thermal-mechanical performance of fuel rods for Boiling Water Reactors (BWRs), which complies with the USNRC requirements of Section 4.2 of NUREG-800.

The methodology consists of the best-estimate fuel performance code RODEX4 which models the thermal-mechanical behavior of the fuel rods, and an application methodology for determining the behavior of rods in a BWR core, considering normal operation and anticipated operational occurrence scenarios. The objective of the methodology is to quantify the fuel design margins relative to the generic design criteria.

The methodology was developed by Framatome ANP, Inc. and is to be applied to BWR fuel with rod burnups to 62 GWd/MTU.

1.0 Introduction

This report describes the Framatome ANP Inc. (FANP) methodology for the realistic evaluation of the thermal-mechanical performance of fuel rods for Boiling Water Reactors (BWRs). The methodology complies with the USNRC requirements of Section 4.2 of NUREG-800 (Reference 1). As part of this submittal some of the criteria detailed in FANP's Generic Mechanical Criteria for BWR Fuel Designs (Reference 2) have been revised. [

]

The methodology for the realistic evaluation of the thermal-mechanical performance of the fuel rods is developed in two major parts. The first is the best-estimate fuel performance code RODEX4 (Reference 4). The RODEX4 code models the thermal-mechanical behavior of the fuel rods during normal operation and anticipated operational occurrences. This code originated from RODEX3 (Reference 5). The code was structured into a modular architecture, mechanical models were improved, high burnup models were implemented, and validation to an extensive fuel performance database was performed.

The second component of the realistic thermal-mechanical fuel rod performance methodology is the application of the code for determining the behavior of rods in a BWR core. The methodology uses RODEX4 to evaluate scenarios for normal operation and anticipated operational occurrences and to quantify the design margins relative to the generic design criteria in a statistical manner. [

]

* Framatome ANP, Inc. is an AREVA and Siemens Company

[

]

The methodology will be applied to BWR fuel with full length rod design burnups to 62 GWd/MTU. The RODEX4 code is applicable to UO_2 and $UO_2-Gd_2O_3$ (up to 10 w/o Gd_2O_3) fuel rods, with cold worked or annealed Zircaloy-2 or Zircaloy-4 cladding.

2.0 Methodology Roadmap

This section provides an overview of the realistic thermal-mechanical methodology for BWR fuel rod analysis. This [] methodology is described and demonstrated in four elements:

- Requirements and Capabilities
- RODEX4 Calibration and Range of Parameters
- Uncertainty Analyses
- Application Examples

Each of these elements of the methodology is summarized below.

2.1 *Requirements and Capabilities*

2.1.1 Fuel Rod Criteria

The fuel rod thermal-mechanical analyses are performed for the fuel rods of a BWR reactor. The calculations are performed to show compliance with the strain, fatigue, creep collapse, corrosion, rod internal pressure, margin to melt temperature, and ramp strain criteria per the USNRC Standard Review Plan Section 4.2 (Reference 1).

The criteria are grouped as applicable to each evaluation scenario. The analyses for normal operation determine fuel rod pressures, clad strains, creep ovality, fatigue usage and corrosion. Anticipated operational occurrences are evaluated against the transient strain and pellet centerline melt criteria. The fuel rod criteria are detailed in Section 3.1.

2.1.2 Reactor Operation Scenarios

Fuel rod calculations are performed to represent the performance of a fuel design during its life in a BWR core. []

[

]

2.1.3 RODEX4 Fuel Rod Code

The RODEX4 fuel performance code simulates the thermal and mechanical response of a fuel rod in a reactor core as a function of exposure for the local power and flow conditions encountered during reactor operation. Phenomenological rate dependent models evaluate the temperature, strain, and exposure dependent changes in the state of the fuel and cladding materials and the release of the fission gas products. The fuel rod performance code is

calibrated to the observable pellet, clad, and rod behaviors. These are primarily the central pellet temperature, clad circumferential and axial deformation, clad oxidation, rod void volume, and fission gas release fraction.

The RODEX4 fuel performance code was developed to realistically predict the thermal-mechanical behavior of a single fuel rod in a Light Water Reactor (LWR) up to burnups greater than 62 GWd/MTU. It contains a consistent set of physical models for the thermal and mechanical analysis of Pressurized Water Reactor (PWR) and Boiling Water Reactor (BWR) fuel in normal and off-normal conditions. The components modeled are the fuel rod coolant, the pellets, the different zones of the active fuel column, the plenum volumes, the fill and released fission gases, the radial pellet-clad gap, and the cladding.

The RODEX4 code is based on the RODEX2 (Reference 7) and RODEX3 (Reference 5) codes previously approved by the USNRC. RODEX4 has been fully restructured into a modular form. New best-estimate models have been incorporated to model the fuel rod behavior to high burnup and a thermal transient capability was added. The code requirements, applicability, and a summary description are given in Section 3.3.

2.1.4 Fuel Rod Evaluation Methodology

The evaluation process consists of a number of well defined steps. [

[

]

The steps of this analysis processes are described in Section 3.4.

2.1.5 Documentation

A summary of the code is provided in Section 3.3 of this report. The RODEX4 code is also documented in a theory manual (Reference 4). RODEX4 has been validated against fuel rod performance measurement data for test and commercial reactor irradiations as described in Section 4 of this report. The validation of RODEX4 is also described in Reference 8.

Determination of model uncertainties is described in Section 5.

2.2 ***RODEX4 Calibration/Validation and Range of Parameters***

2.2.1 Fuel Performance Database

Calibration and validation of RODEX4 has been performed for BWR and PWR fuel types. The main characteristics of this fuel are annealed or cold worked stress relieved Zircaloy-2 or Zircaloy-4 clad and fuel columns of UO_2 and $\text{UO}_2\text{-Gd}_2\text{O}_3$ fuel pellets. The necessary operating range is steady-state power up to about 15 kW/ft (about 50 kW/m), ramp power up to fuel melt, and rod average burnup to greater than 62 GWd/MTU.

A variety of BWR and PWR fuel rod, pellet, and cladding types in addition to standard FANP BWR fuel are present in the calibration and validation database. These fuel rods are necessary for validation of the code models. They also extend the calibration and validation range beyond the characteristics of the current FANP BWR fuel.

Separate-effects tests are used to independently validate specific models on a stand-alone basis. Integral tests are either power plant irradiations or instrumented tests in research reactors. Instrumented tests provide on-line measurements of pellet centerline temperature and rod inside gas pressure. Post-irradiation exam (PIE) measurements from both test and commercial reactor irradiations, for strain, fission gas release (FGR), void volume and oxidation, are used in the calibration process.

The fuel performance database is summarized in Section 4.1.

2.2.2 RODEX4 Calibration

In order to arrive at the best-estimate condition, the code must undergo a calibration which tunes certain model parameters. The objective of the calibration process is to make the calculated/measured ratio of the important results close to 1.0 with an acceptable minimum variance.

Separate-effects tests are first utilized to establish specific models on a stand-alone basis. These models are primarily for the material properties, which can be determined during out of pile tests.

[

]

[
]

The accuracy of the calibration is demonstrated by the comparison of the measured rod behavior with the best-estimate code predictions for:

- Pellet centerline temperature
- Fuel gas release fraction
- Rod free volume
- Clad creep down and ramp strains
- Clad creep ovality
- Rod growth
- Clad oxidation

See Section 4.0 for a description of the calibration / validation process. The measured / calculated performance comparisons are summarized in Section 4.2.

2.2.3 Assessment of Biases

[

]

2.2.4 Validation Ranges

The validation range varies due to the availability of irradiation measurement data for the various parameters. All the data available to FANP was used for the important parameters to maximize the range of code validation.

[

]

The validation ranges extend to or beyond 62 GWd/MTU rod average exposure, the requested application range of the BWR analysis methodology. The calibrations, generically applicable to the pellets and specifically for the BWR clad, are described in Section 4.4.

2.3 *Uncertainty Analyses*

2.3.1 PIRT Process

[

]

2.3.2 Reactor Operation Uncertainties

The reactor operation establishes the environment experienced by the fuel rods. [

]

[

]

The development of the uncertainties and the disposition of the uncertainties relative to those identified in the PIRT process are described in Section 5.2.

2.3.3 Fuel Rod Manufacturing Uncertainties

Manufactured rod, clad, and pellet characteristics for BWR fuel were determined [

]

[

]

The development of these uncertainties and the disposition of the uncertainties relative to those identified in the PIRT process are described in Section 5.3.

2.3.4 Model Parameter Uncertainties

Model uncertainty distributions were developed, [

]

[

]

2.4 *Application Examples*

The purpose of providing application examples is to demonstrate how the realistic methodology is applied for the analysis scenarios (normal operation, slow transient AOOs, and fast transient AOOs), and to show the sensitivity of results to the power, manufacturing and RODEX4 model parameter uncertainties.

2.4.1 Normal Operation

The normal operation analyses were performed for two different reactor types and fuel management designs using the ATRIUM-10 fuel assembly. [

] Some of the example cases have been performed for conditions similar to existing deterministic calculations to allow the comparison of results.

2.4.2 Sensitivity Studies

Additional analyses are performed to show the predictable nature of the analysis. [

]

2.4.3 Slow Transient Anticipated Operational Occurrences

The example "slow transient" evaluation is for [

] The maximum strains and temperatures during the CRWEs were determined and compared with the design limits.

2.4.4 Fast Transient Anticipated Operational Occurrences

An analysis was also performed to show an example evaluation of some limiting "fast transients" for a BWR-4. [

]

For transients initiated at high core power, the fuel transient limits are generally met without imposing LHGR operational limits. However, for transient initiated from low core powers, it is common to impose power dependent LHGR operational limits so that the transient strain and fuel centerline melt criteria are met (i.e., multipliers to the exposure dependent fuel design limit). Example analyses of both cases are presented.

3.0 Requirements and Capabilities

3.1 Fuel Rod Criteria

The thermal-mechanical analyses are performed for the fuel rods of a BWR batch. The calculations are performed to show compliance with the fatigue, creep collapse, corrosion, rod internal pressure, margin to melt temperature, and strain criteria per the USNRC Standard Review Plan Section 4.2 (Reference 1).

3.1.1 Criteria for Normal Operation

The specific criteria evaluated during normal operation (Reference 2) are as follows:

- The clad tangential uniform strain increment for power increases during normal operation shall not exceed 1%.
- The fatigue usage factor for clad stresses during normal operation and design cyclic maneuvers shall be below 0.67.
- Clad creep collapse shall be prevented. [

- The maximum clad oxidation shall be less than [] to prevent clad corrosion failure. []
Clad hydrogen content at the maximum oxidation shall be calculated.
- The rod internal pressure is limited [] to assure that significant outward clad creep does not occur and unfavorable hydride reorientation on cooldown does not occur.

[

]

The clad stress due to external pressure will continue to be evaluated on a design basis in accordance with Reference 1 and Reference 2 criteria. The fuel rod calculations which interface with the fuel assembly, such as growth, bow, and mechanical fracturing, will continue to be evaluated with the existing approved design methodology (Reference 6).

3.1.2 Criteria for Anticipated Operational Occurrences

The criteria (Reference 1) for anticipated operational occurrences (AOOs) are as follows:

- The clad tangential uniform strain, elastic plus inelastic, shall not exceed 1% for anticipated operational occurrences.
- Pellet temperatures during expected transients shall be maintained below melting to assure that relocation of molten fuel that could come into contact with the cladding or produce local hot spots does not occur.

The margins for anticipated reactor system transients are evaluated for all the FANP fuel rods in the core. The margins for the control rod withdrawal error are evaluated for all the rods in the FANP assemblies adjacent to control rods.

3.2 ***Reactor Operation Scenarios***

3.2.1 Scenario for Normal Operation

Fuel rod calculations are performed to represent the performance of a fuel batch or series of batches of a fuel design type such as ATRIUM-10 in a BWR core. [

]

[

]

3.2.2 Scenario for Slow Transient AOOs

The fuel rods may also experience transient power changes described as anticipated operational occurrences (AOOs). In a BWR, these may be caused by reactor system transients which result in overall core power increases, or by localized transients, such as a control rod withdrawal error which result in fuel rod power increases in the vicinity of the affected control blade. To evaluate these excursions from the normal fuel management histories, analyses are performed to determine transient temperature and strain margins. The analyses are classed as "slow" transients where the event occurs relatively slowly and/or the power is held at the terminal condition.

[

]

3.2.3 Scenario for Fast Transient AOOs

Events are classified as "fast" transients when the excursion occurs quickly and the system returns quickly to normal power or below. The reactor system "fast" transients occur on a relatively short time scale, ranging from about 1 second to about one minute. [

]

[

]

3.3 ***RODEX4 Fuel Rod Code***

3.3.1 Code Requirements

The fuel rod code simulates the thermal and mechanical response of a fuel rod in a coolant channel as a function of exposure for the conditions encountered during normal and anticipated reactor operation. Phenomenological rate dependent models are necessary to evaluate the temperature, stress, and exposure dependent changes in the state of the fuel and cladding materials, and in the release of the fission gas products. The components modeled are the fuel rod coolant, the pellets, the different zones of the active fuel column, the plenum volumes, the fill and released fission gases, the radial pellet-clad gap, and the cladding. The code performance is validated by comparing calculations against experimental values.

- The central pellet temperature, clad circumferential and axial deformation, clad oxidation, fuel rod void volume, and fission gas release are validated over the important variable ranges against an experimental database. This database encompasses the behavior of the major code parameters for the range of intended application.
- The code provides a best-estimate response. The calibration performed during validation shows that little or no bias exists in the code predictions for the range of applicability.
- The code is assessed to determine the dispersion of the difference between calculation and measurement, and the corresponding uncertainty range of important modeling parameters is determined.

3.3.2 Code Applicability

RODEX4 is a best-estimate code specifically developed to predict the thermal-mechanical behavior of a single fuel rod in a Light Water Reactor (LWR) to high burnup. It contains a

consistent set of physical models for the thermal and mechanical analysis of Pressurized Water Reactor (PWR) and Boiling Water Reactor (BWR) fuel in normal and off-normal conditions.

The code has the capability to calculate the behavior of UO_2 and gadolinia bearing fuel rods to beyond 62 GWd/MTU rod burnup. The code includes high burnup effects, such as pellet rim effect, fuel thermal conductivity degradation with burnup, and changes of cladding mechanical properties at high exposure.

Validation of the code is performed for BWR and PWR fuel with Zircaloy clad and UO_2 and UO_2 - Gd_2O_3 fuel pellets. An extensive fuel rod database with various rod, pellet, and clad parameters is used. These fuel rods are used to extend the calibration and validation range beyond the characteristics of the current FANP fuel. For the realistic analysis of BWR fuel, particular model uncertainty distributions are developed for Zircaloy-2 clad.

3.3.3 RODEX4 Summary

The RODEX4 code has a modular structure. It includes a set of stand-alone subprograms, each describing a single physical phenomenon. This enables testing of the individual physical models and facilitates the introduction of new or improved models. The subprograms are called by a driver program that controls overall progress of the analysis. Special numerical subroutines control the time step and accelerate the convergence of the iterative processes. RODEX4 includes a separate library of material properties.

The RODEX4 code evaluates the thermal-mechanical responses of a fuel rod surrounded by coolant. The fuel rod model considers the fuel column, the gap region, the cladding, the gas plena, and the fill and released fission gases. The fuel rod is divided into axial regions with conditions computed for each region. The fuel is also sub-structured into radial regions with the material properties and state variables evaluated for each region. The operational conditions are controlled by the input of rod linear heat generation rate and its axial distribution, fast flux and axial distribution, coolant inlet temperature or enthalpy, the coolant pressure, and the coolant mass velocity.

Thermal boundary conditions for the cladding are calculated with the thermal-hydraulic model for the reactor coolant. The operational conditions are defined at the start and end of an input time period. During the time period, the operational conditions vary linearly, or remain constant. The thermal processes are analyzed based on a finite-difference solution to the steady-state

heat conduction equation. This solution is applicable for events with a time duration down to about a minute.

The evaluation of changes in the physical state of the fuel model components is calculated using incremental calculations based on path dependent solutions of the rate dependent models. The interactions between fuel rod components and evaluation of thermal conditions (intensive variables) are evaluated at the start and end of each time increment. The intensive variables used to evaluate incremental changes in the state of the fuel model components are either calculated or estimated mid-time step values.

The major processes, thermal, mechanical, and fission product release are summarized below.

3.3.3.1 Thermal Processes

The thermal-hydraulic model is a simple steady-state, one-dimensional model of a single coolant channel. The water enthalpy increase in the coolant channel is calculated using an energy balance equation with a heat source coming from the fuel rod. Heat transfer through the film is calculated for forced convection and nucleate boiling regimes.

Radial depression of the thermal neutron flux is taken into account in defining the local volumetric heat generation rate. Plutonium build-up at the pellet periphery is accounted for, as it affects the radial heat generation profile.

The heat conduction in the fuel, and clad is calculated using a general 1-D axi-symmetric geometry. It is implemented with a general variable mesh size to better model regions of steep temperature gradients at the outer pellet edge. [

]

Pellet thermal conductivity includes burnup degradation effects.

The following thermally activated processes are modelled: clad oxidation, thermal expansion, pellet equiaxed grain growth, fission-gas diffusion in grains, and bubble growth on grain boundaries.

3.3.3.2 Mechanical Processes

The stress-state and deformation of the fuel and clad are calculated considering the evolution of:

- 1) The thermal, elastic, creep, and growth deformations of the cladding, under the combined effect of temperature, fast fluence, rod inner and outer pressures, pellet-cladding mechanical interaction, corrosion of the outside of the cladding tube, and the evolution of the physical properties of the Zircaloy.
- 2) The thermal, elastic, densification, swelling, and creep deformations of the cracked pellets under the combined effect of temperature, burnup, pellet-clad mechanical interaction, and the evolution of the physical properties of the uranium oxide.
- 3) The interaction forces between the fuel column and the cladding.

The stress-state and deformation for each axial segment of the fuel is calculated separately based on a generalized plane-strain condition for cladding and a cracked pellet deformation model.

3.3.3.3 Fission Gas Release Processes

The mechanistic fission gas release model provides feedback between fission gas release, the gaseous swelling model, and the other thermal mechanical processes. There are three main stages for the fission gas atoms to reach the free-void space.

The first stage involves gas atom migration to the grain boundary, by both diffusion and grain boundary sweeping. Fission gas bubbles precipitate inside the grain and act as traps for diffusing gas atoms. In competition with this process, fission gas bubbles also act as gas atom sources. This is because of the re-solution process which is caused by interaction of fission fragments with gas bubbles. The intragranular fission gas bubbles can also migrate to the grain boundary under certain conditions of temperature and stress.

The intermediate stage is characterized by the precipitation of grain-face bubbles and the formation of tunnels on the edge of the grains. The intergranular bubbles contribute to gaseous swelling of the pellet.

In the final stage, the porosity created by the grain-edge bubbles forms a network of interconnected tunnels with access to open voidage via the outer surface of the pellet or micro-cracks inside the pellet. This linkage of intergranular bubbles occurs at a certain

fission-gas atom saturation level of the grain boundary, at which time venting of the gas to the free volume is possible.

3.3.3.4 Thermal Transient Solution for Fast Transients

To evaluate the response of the rods to fast transients (AOOs), a thermal transient module is included. This module considers the elastic processes of the pellet and clad during the transient, leaving out creep, gas release, corrosion, etc., but with a thermal solution of the general transient heat conduction equation. [

] The added factors in this solution relative to the steady state solution are the density and specific heat of the pellet and clad. [

] The pellet centerline temperature and clad strain response to a limiting fast (reactor system) transient is the output of interest.

3.3.3.5 RODEX4 Documentation

The RODEX4 code is documented in a theory manual, Reference 4, covering the code structure, the thermal, mechanical, and fission product release processes, and the material properties. It is validated against fuel rod performance measurement data for test and commercial reactor irradiations as described in Section 4 and detailed in the validation report, Reference 8.

3.4 *Fuel Rod Evaluation Methodology*

3.4.1 Evaluation Objectives

The objective of each analysis is to qualify a fuel assembly design for use in a particular reactor for normal operation and anticipated operational occurrences. Each analysis is specific to a particular reactor [

]

Each analysis is also specific to the particular details of the fuel assembly and rod design.

[

]

[

]

3.4.2 Statistical Process

The goal of the methodology is to analyze fuel rod performance during normal operating and anticipated operational occurrence conditions for a given fuel reload and power plant to show that the fuel meets the design criteria with a quantified probability. [

]

[

]

3.4.3 Methodology for Normal Operation

The methodology consists of a number of well defined steps. [

]

[

]

3.4.4 Methodology for Slow Transient AOOs

Relatively slow transients, where the occurrence either extends over a period of many minutes (such as the core flow run-up or loss of feedwater heater), and/or the terminal condition may be held for some period (such as a control rod withdrawal error), are evaluated with essentially the same methodology as that used for the evaluation of normal operation.

[

]

For some transients initiated at off-rated conditions, power-dependent or flow-dependent LHGR operational limits may be defined to assure satisfaction of the fuel transient strain and temperature criteria.

3.4.5 Methodology for Fast Transient AOOs

Relatively fast transients (AOOs), with no hold time (such as those due to core pressurization events), are evaluated using the RODEX4 thermal transient solution capability. [

] A USNRC approved transient licensing analysis methodology (currently Reference 10) is used to produce transient power conditions, and the transient fuel analyses are then performed with the thermal transient module of RODEX4.

[

]

[

]

4.0 RODEX4 Calibration/Validation and Range of Parameters

The RODEX4 code simulates the complex behavior of a fuel rod and assesses a number of different performance measures. The code models, summarized in Section 3.3.3 of this report, are fully described in the RODEX4 Theory Manual, Reference 4. These interacting thermal and mechanical models are dependent on a number of material properties. The material properties and some of the models have been determined by comparison with experimental data to determine a single property or behavior.

Many of the models of the RODEX4 code, however, contain parameters that are not accessible to direct measurement. Those parameters can be indirectly determined by calibration against integrated fuel rod experimental data. A fuel rod experimental database has been built that includes data and experimental results for a large number of fuel rods irradiated in test and commercial reactors. The behavior of these rods is calculated with the code and the results are compared with the experimental data. By using adequate fuel rod performance data it is possible to calibrate the individual physical models.

Since the thermal and mechanical models are strongly coupled by a series of feedback loops, code calibration requires multiple iterations so that the models as an integrated whole are calibrated. The final phase of the calibration is the validation, when the results of the calibrated code are evaluated against the experimental results. The validation demonstrates that all the fuel rod behaviors to be compared with the design criteria are well predicted. The best-estimate prediction of all the primary behaviors is demonstrated over the range of the database.

A crucial aspect of the validation is the use of the same interrelated models to predict all the different behaviors. For example, clad creep affects pellet temperature and subsequent clad ramp strain via its effect in establishing the pellet-clad gap. It also affects fission product release via the gaps effect on the pellet temperature. Pellet conductivity also affects pellet temperature, and thus pellet gas release via the temperature. The temperature in turn affects gaseous swelling and eventually clad strain. Clad oxidation is independent of the other behaviors but does itself affect the temperatures.

The validation is thus dependent on one consistent set of models predicting all the interrelated behaviors in all the different tests and irradiations. This consistent and complete validation of all the codes models provides a cross check between the various sets of experimental data.

[

]

The validation of RODEX4 against the fuel performance database, summarized below, is also described in the RODEX4 Validation Report, Reference 8.

4.1 ***Fuel Performance Database***

RODEX4 has been validated against a database of 323 fuel rods from "International" test programs and about 1000 rods from commercial reactors. For each fuel rod the following information has been compiled:

- the fuel rod characterization data,
- the irradiation history,
- results of measurements recorded in real time and/or post irradiation examination (PIE) results.

In the International programs some experimental results are measured and recorded in real time during irradiation. Other results are obtained from post-irradiation examination (PIE). The real time measurements include the temperature and inner pressure measurement carried out by means of thermocouples located in the fuel column and pressure transducers in the gas plenum. The PIE results include both non-destructive tests (like visual examination, dimensional measurement, rod profilometry, eddy current testing, gamma scanning, alpha-autoradiography, and neutron-radiography) and destructive tests (like ceramography and

metallographic examination, rod puncturing and fission gas analysis, electron probe microanalysis, electron microscopy, X-ray fluorescence, chemical analysis, porosity measurement by image analysis, and density measurement).

By contrast few rods irradiated in commercial reactors go to the hot cell and no measurements are performed during irradiation. The measurements on commercial rods, clad oxide thickness, clad diameter, rod axial growth and Kr-85 fission gas release data are taken primarily at poolside.

4.1.1 Separate Effects Tests

Prior to testing the code against the fuel rod database separate effects tests are used to independently determine specific models on a stand-alone basis. The major models (Reference 4) established by separate-effect tests are:

[

]

4.1.2 Integral Tests - International Programs

Integral tests are either power plant irradiations or instrumented tests in research reactors. For power plant irradiations, PIE measurements for mid-pellet and ridge strain and fission gas release (FGR) can be used for benchmarking. Instrumented tests provide on-line measurements of pellet centerline temperature, and rod inside gas pressure. All the models responsible for these outputs are interrelated, and all participate in the thermal mechanical response of the rod. Therefore, the integral tests are used to validate the models most strongly affecting these behaviors.

Pre- and post-irradiation rod characterization data are available for most integral tests, therefore, the effect of uncertainties in rod dimensions and properties on the results is usually small. Model uncertainties for clad creep and oxidation can also be removed by adjusting

4.1.3 Commercial Irradiations

Commercial irradiations consist of BWR and PWR fuel rods for which post-irradiation measurements have been taken and rod power histories determined. Measurements are available for clad creep strain, fission gas release (FGR) fractions via krypton-85 measurements or rod puncture, oxide thickness, and rod axial elongation. The models responsible for these outputs are interrelated, and all participate in the thermal mechanical response of the rod.

The commercial irradiations are evaluated for rods usually with limited pre- or post-irradiation characterization. The major models being validated by the commercial irradiations are:

[

] The Commercial

Database is summarized in Table 4.2:

[

]

The acceptability of the calibration is demonstrated by the best-estimate behavior of the major code results. These are:

- Pellet centerline temperature
- Pellet gas release fraction
- Clad creep down and ramp strain
- Clad creep ovality
- Clad elongation
- Clad oxidation
- Rod free volume

Any adjustment of parameters during the calibration process requires re-evaluation of the measured/predicted results for all the code behaviors.

4.2.1 Centerline Temperature

The temperature distribution in the fuel pellets controls most of the physical phenomena occurring in a fuel rod during reactor operation including, fuel thermal expansion, and fuel gaseous swelling and creep. These play principal roles in the behavior of the fuel rod.

[

]

The temperature calibration is based on the calculation of 24 Halden rods and 3 Risø rods. The 27 RODEX4 calculations have been performed a number of times adjusting the above parameters to optimize the centerline temperature predictions. These rods are listed in Table 4.3 with their main characteristics, as well as the fuel exposure and maximum LHGR at the thermocouple location.

Table 4.3 RODEX4 Temperature Database

Rod	Cladding diameter mm	Diametral gap μm	Fuel density % TD	Fill gas	Burnup at TC location GWd/MTU	Maximum LHGR kW/m

A global comparison between predictions and measurements for all the rods of the different Halden projects is shown in Figure 4.1. The figure shows the "best-estimate" response of the code over the whole range of temperature between 250 and 2000 °C.

Figure 4.2 shows the global comparison of the predictions versus measurements for the Risø rods. There is a slight underprediction for the xenon rod, but overall there is a best-estimate response.

Figure 4.3 shows the relative predicted-over-measured fuel centerline temperature deviation versus local exposure for the Halden database. The best-estimate response of the code has been established over the whole fuel exposure range between 0 and 101 GWd/MTU.

[

]

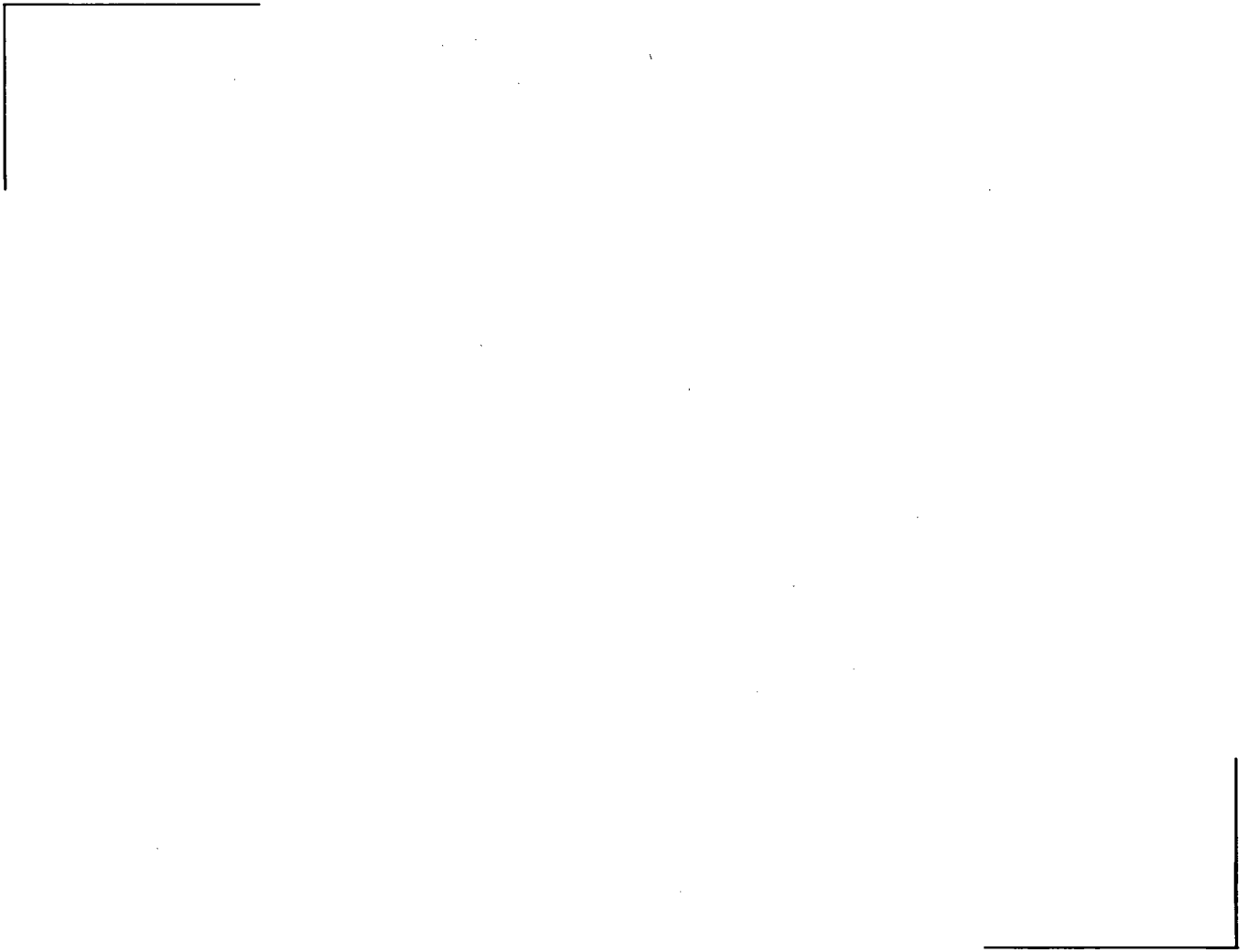
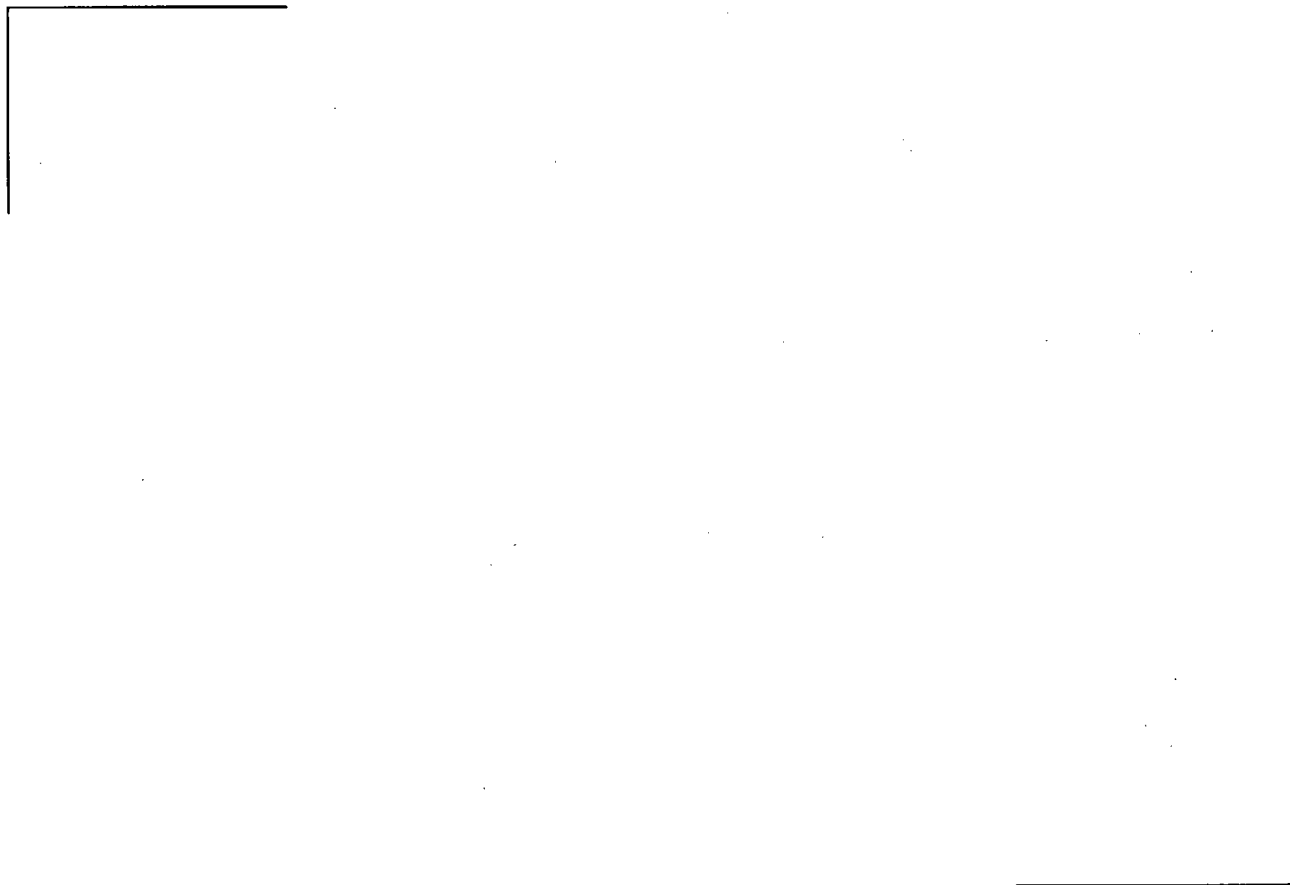


Figure 4.1 Halden Temperature Database - Fuel Centerline Temperature



**Figure 4.2 Risø Temperature Database – Fuel
Centerline Temperature**

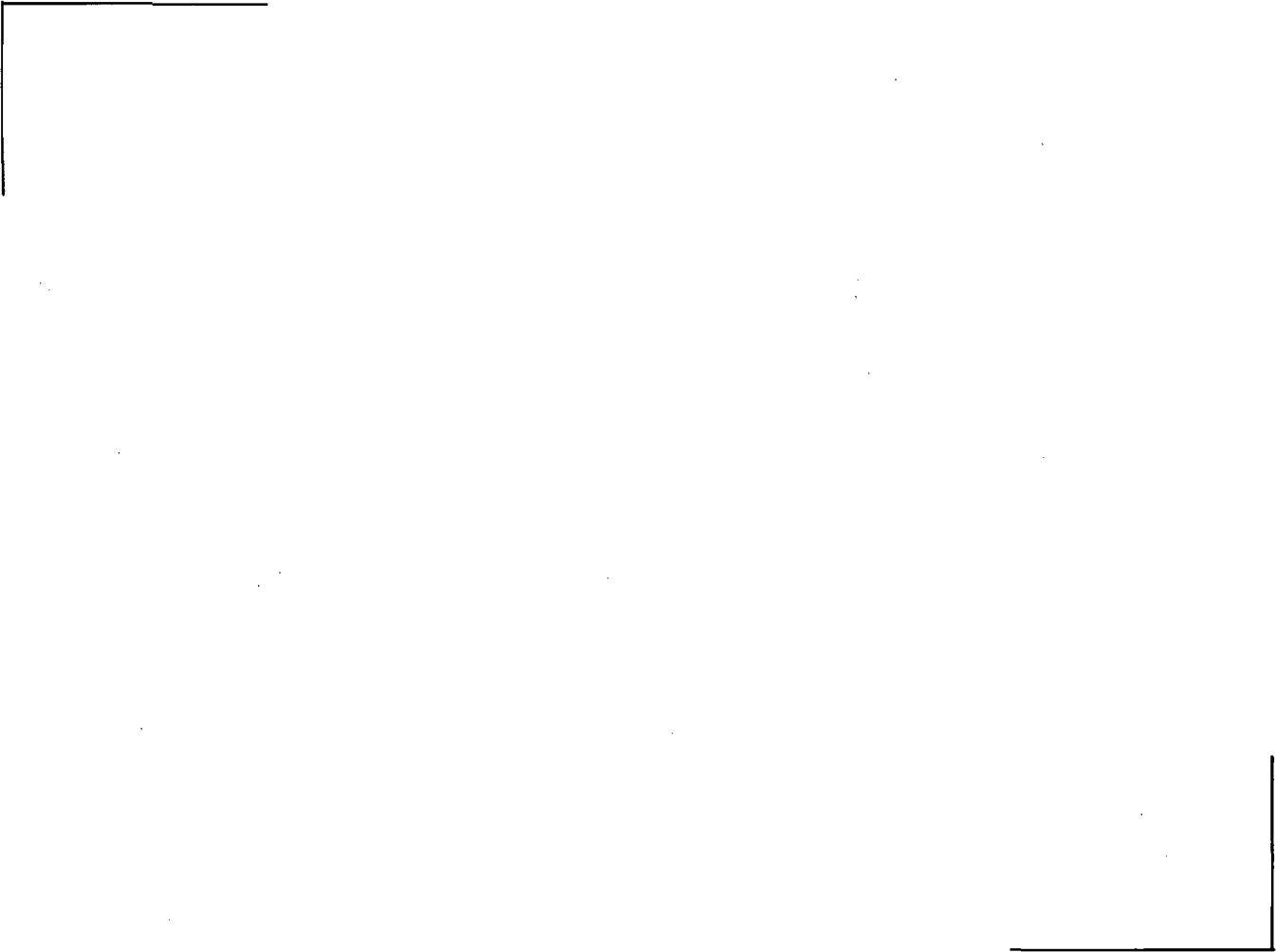


Figure 4.3 Halden Temperature Database - Temperature Deviation

4.2.2 Fission Gas Release

The fission gas release and gaseous swelling calibration was preceded by the thermal calibration since temperature is the major parameter affecting fission gas release. In its turn, gaseous swelling and fission gas release impact the temperature benchmarking by affecting the fuel-to-cladding gap and the gas composition. Several iterations were needed between the thermal, mechanical and fission gas release calibrations to achieve an overall best-estimate calibration.

At the beginning of the gas release calibration process a reduced data set was established consisting of 15 cases which were selected as representative of the burnup and power ranges required for code validation. This reduced data set was used in conjunction with a numerical minimization method to determine the first estimate of the model parameters. Subsequently, the whole database was run and several parameters, the values for activation energy, grain boundary gas bubble fractional coverage and bubble surface concentration, were adjusted in order to achieve a best-estimate code response. During this stage, the gaseous swelling was also calibrated against the ramp strain results because the gaseous swelling is intimately related to fission gas release.

The final fission gas release calibration (validation) is based on the gas release rods in the combined International and Commercial databases. [

]

The International Database for fission gas release consists of 164 fuel rods selected from the following International Fuel Programs.

[

]

The "Commercial Database" contains rods irradiated in commercial reactors [

]

The Commercial Database for fission gas release is made of 365 Framatome ANP rods irradiated in 14 commercial reactors:

[

]

[

]

Figure 4.4 compares predicted to measured gas releases of the International database and shows that an overall best-estimate calibration has been achieved. This is confirmed by Figure 4.5 that shows the histogram of the FGR deviations in log (calculated FGR/measured FGR). Figure 4.6 and Figure 4.7 show log (calculated FGR/measured FGR) as a function of release fraction and burnup respectively. These plots demonstrate that there is no significant local bias of the prediction deviations with power and burnup.

Similar results are presented in Figures 4.8 to 4.11 for the Commercial Database. [

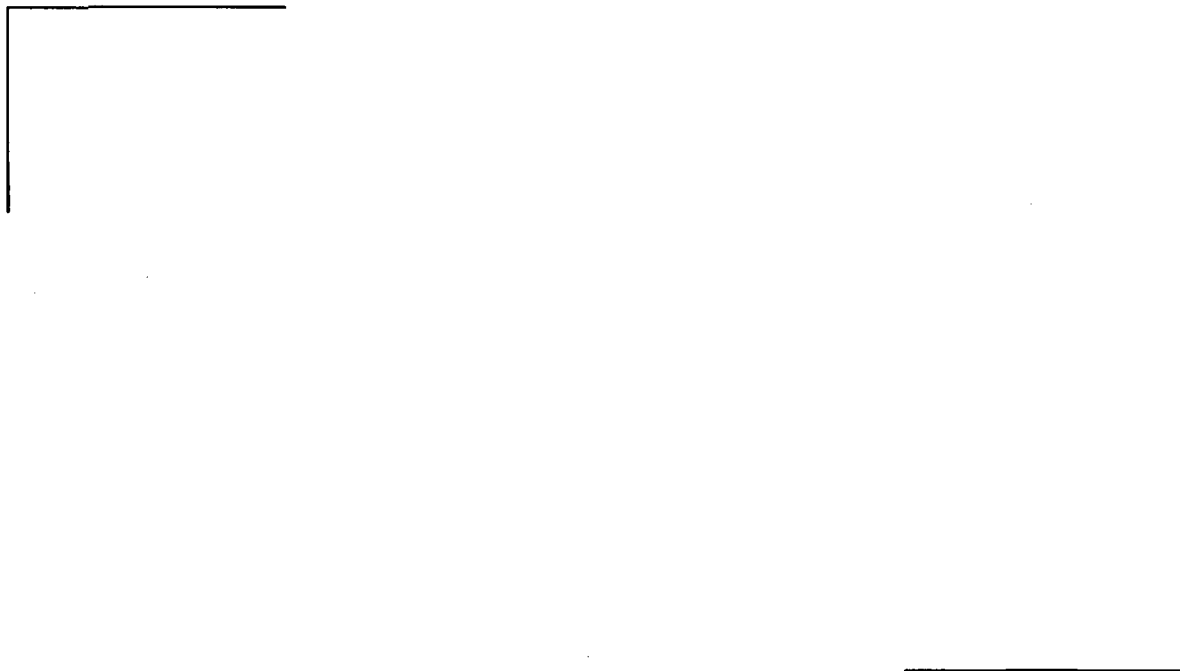
]

Figure 4.12 presents a comparison of the calculated and measured fractional release for the gadolinia rods of the Commercial Database. No significant bias is observed.

The calculated versus measured rod inner pressure at hot cell conditions is summarized in Figure 4.13.



Figure 4.4 International Fission Gas Release Database



**Figure 4.5 International Database - Histogram of
FGR Deviation $\log(C/M)$**

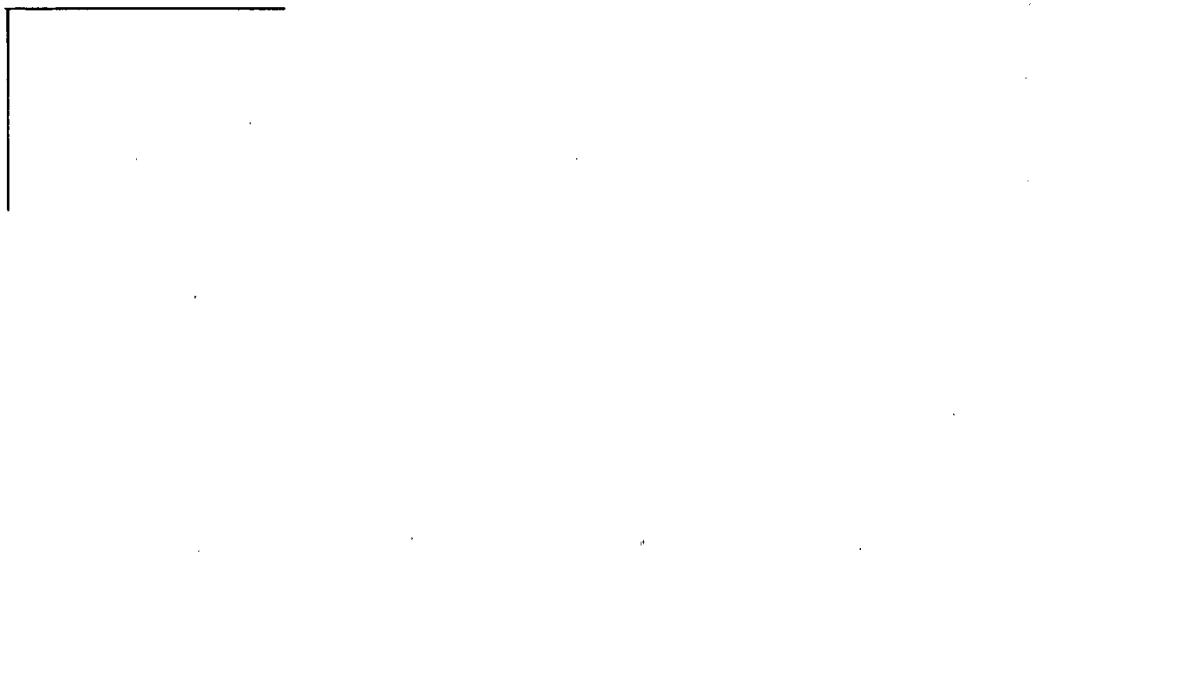
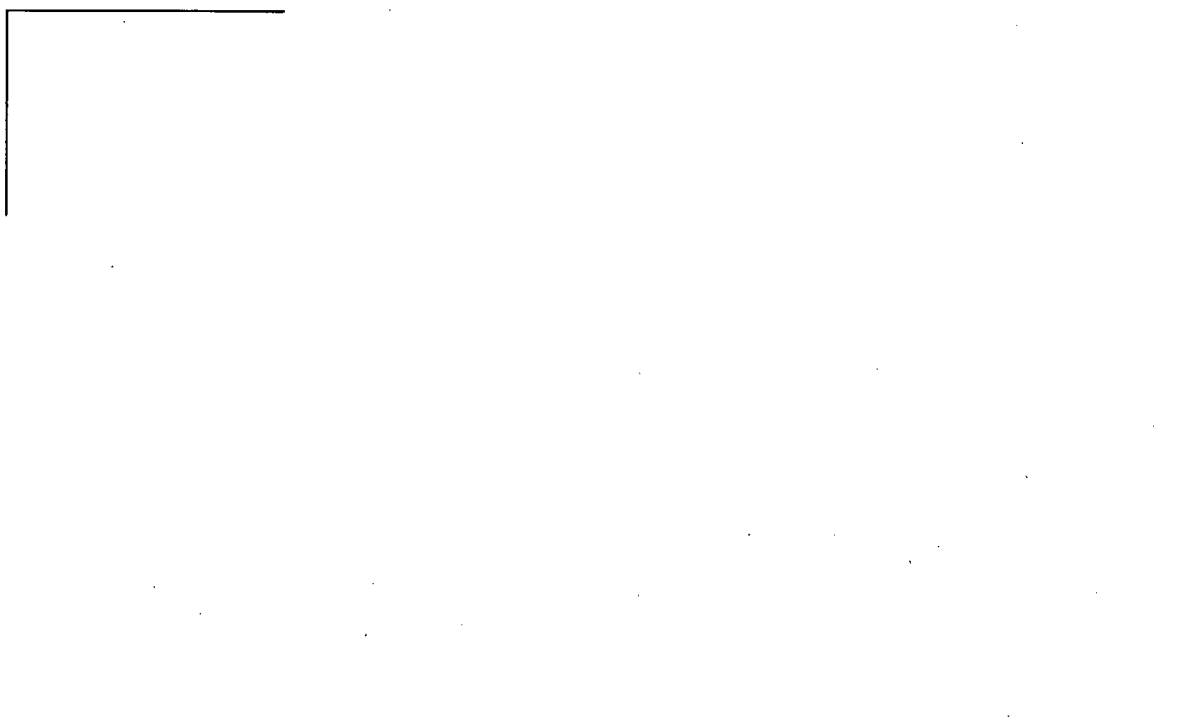


Figure 4.6 International Database - log(C/M) vs. Measured FGR



**Figure 4.7 International Database - log(C/M) vs.
Rod Average Exposure**



Figure 4.8 Commercial Fission Gas Release Database

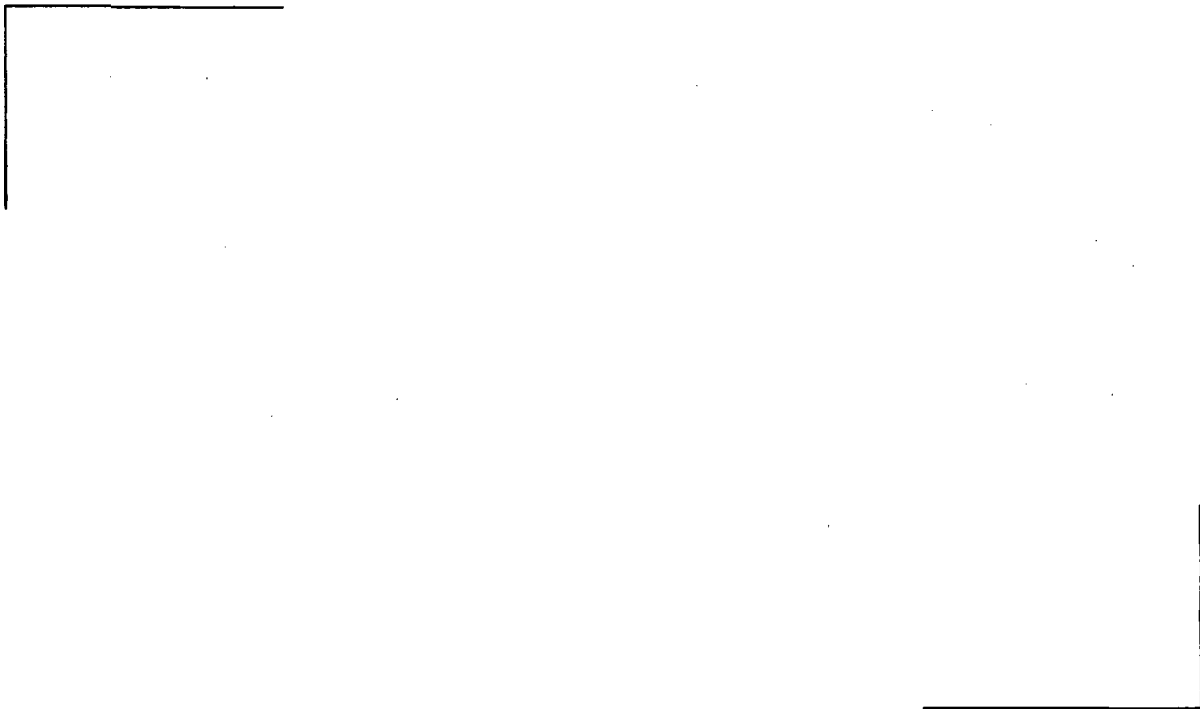


**Figure 4.9 Commercial Database - Histogram of
FGR Deviation $\log(C/M)$**

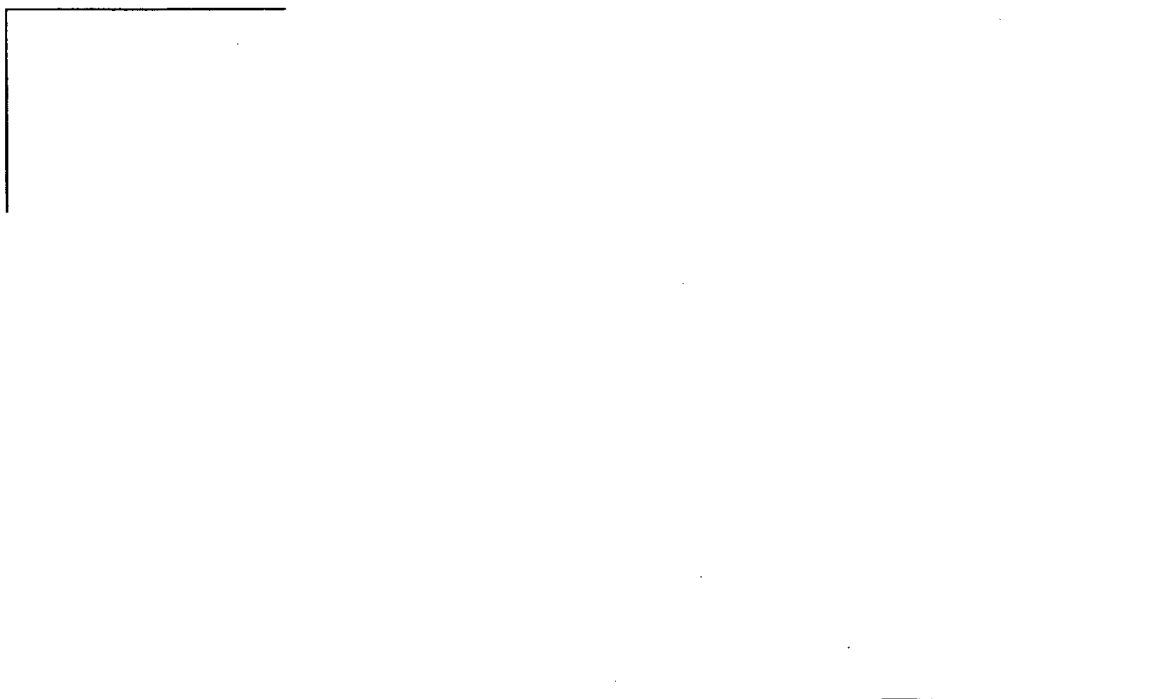
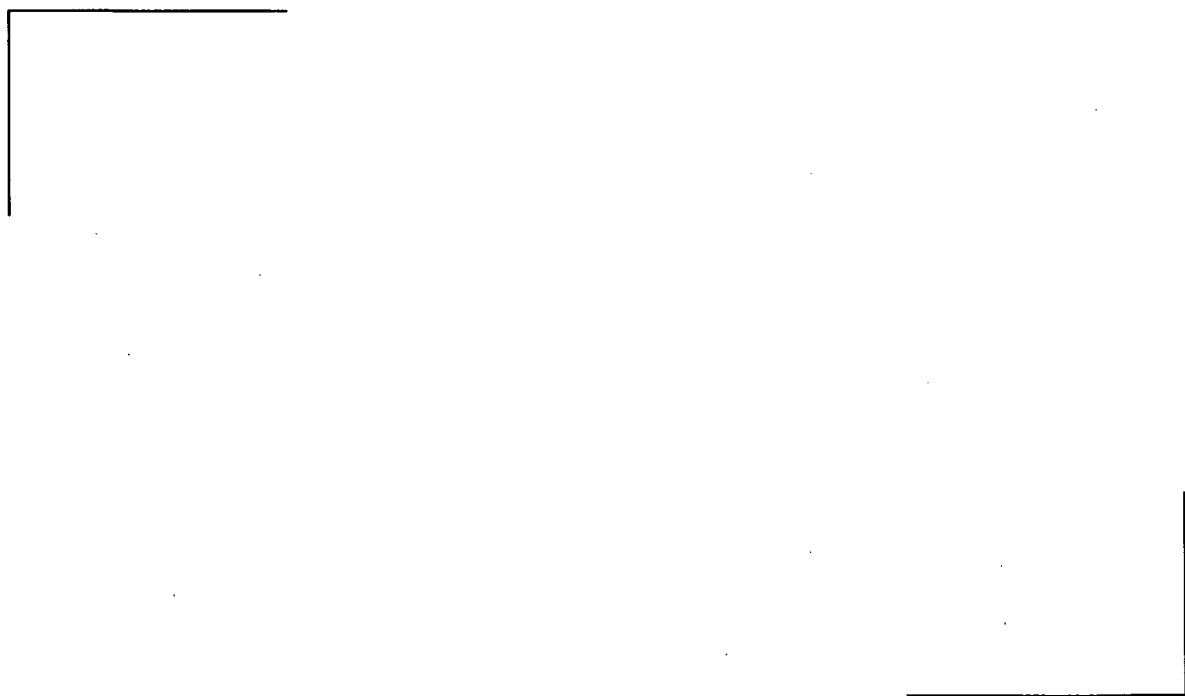


Figure 4.10 Commercial Database - log (C/M) vs. Measured FGR



**Figure 4.11 Commercial Database - log (C/M) vs.
Rod Average Exposure**

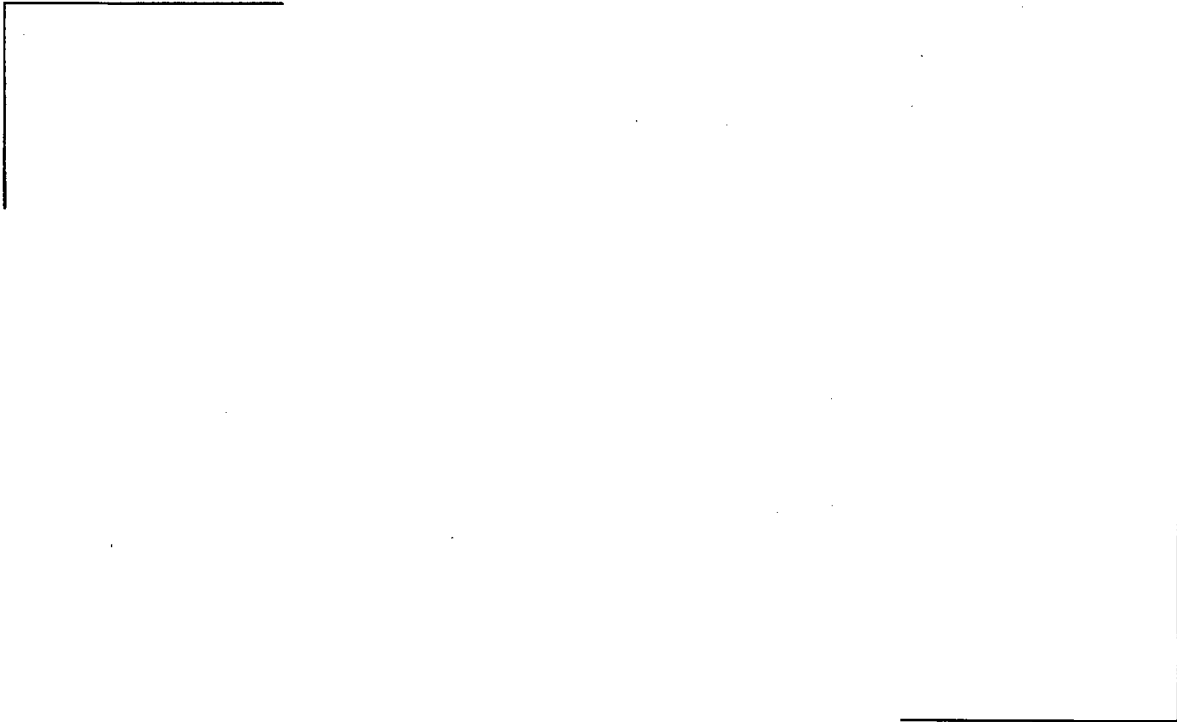


Figure 4.12 Commercial Database - FGR of Gadolinia Fuel Rods

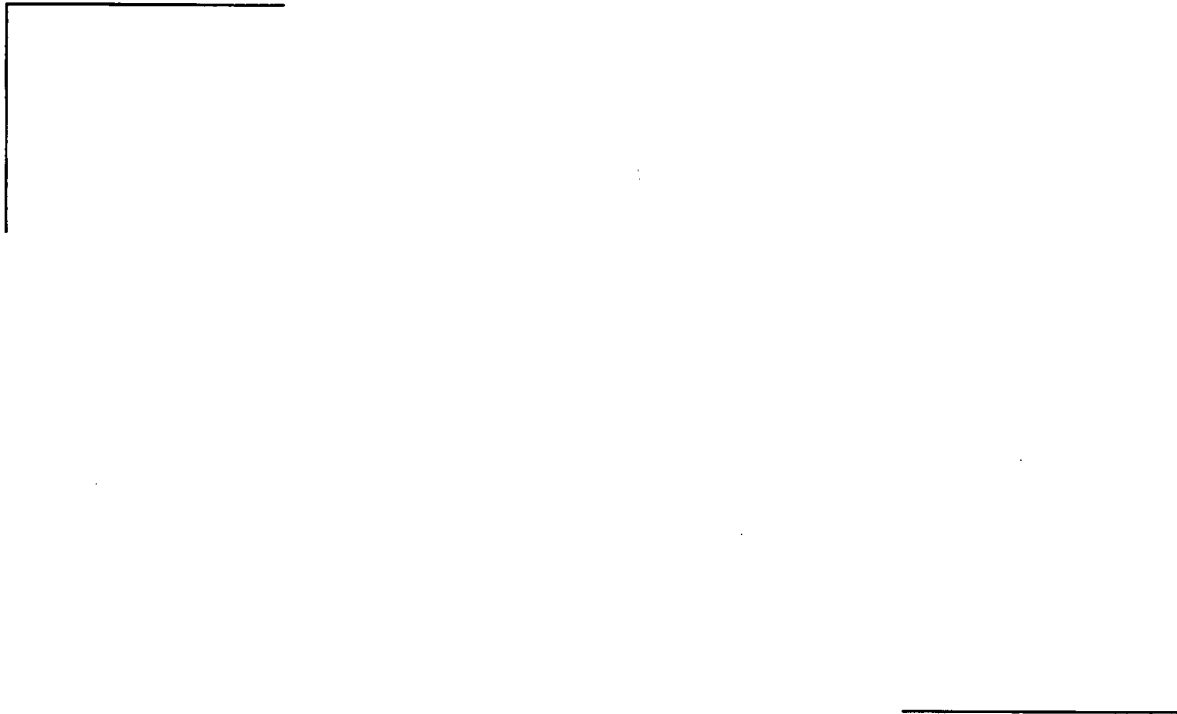


Figure 4.13 Rod Inner Pressure at Room Temperature

4.2.3 Clad Creep

It is important to correctly predict cladding creep down because together with pellet thermal expansion and swelling it controls gap closure. Clad irradiation creep is calibrated primarily to creep down measurements taken after one or two cycles of irradiation, prior to interference with the pellet. The comparison of clad calculated/measured radial deformation is made after correction for the effect of oxidation on the measured clad diameter.

The zircaloy creep correlation of RODEX4 was developed and calibrated on the basis of the ZODIAC Program (not published). ZODIAC is an International program managed by BELGONUCLEAIRE devoted to the study of zircaloy cladding mechanical properties. One of the objectives of the program was the calibration and the validation of the RODEX4 creep model for the Framatome ANP Zircaloy-4 cladding used in PWR reactors. The determination of the creep parameters was based on:

[

]

The BWR creep down database rods with CWSR Zircaloy-2 cladding are from:

[

]

[

]



Figure 4.14 Predicted/Measured Creep Down for BWR 9x9 Cladding

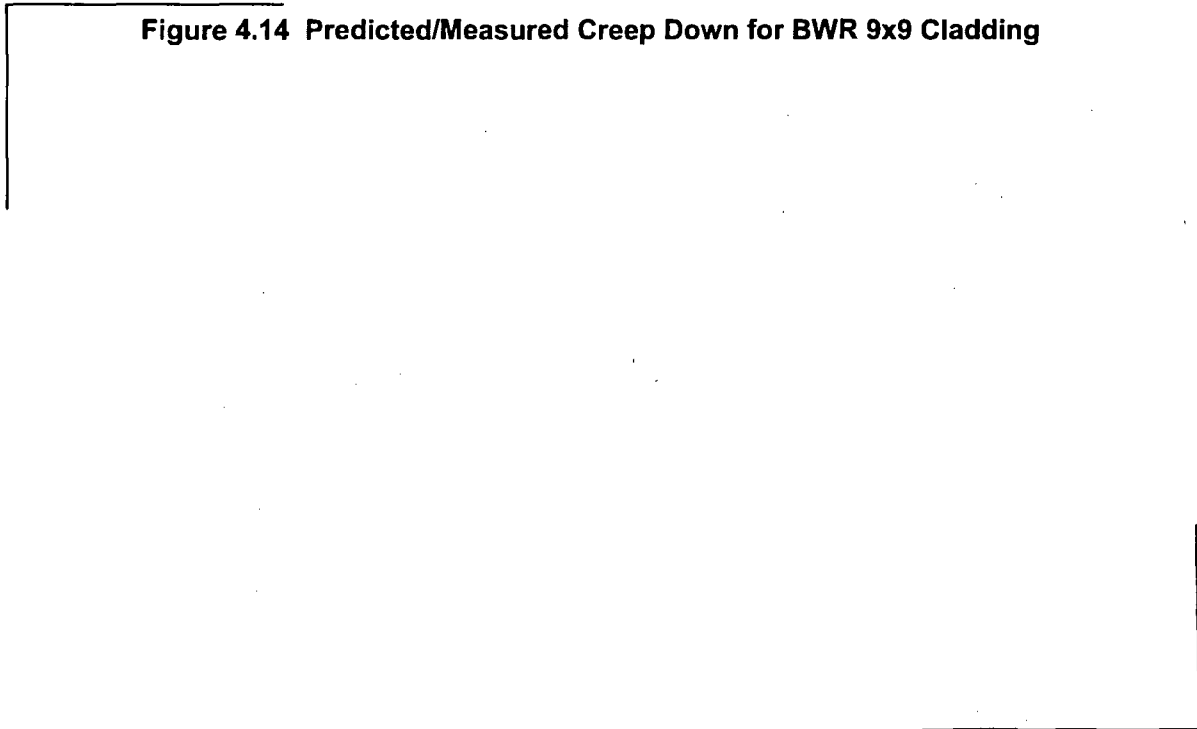


**Figure 4.15 Predicted/Measured Creep Down for BWR 9x9 Cladding
(Continued)**

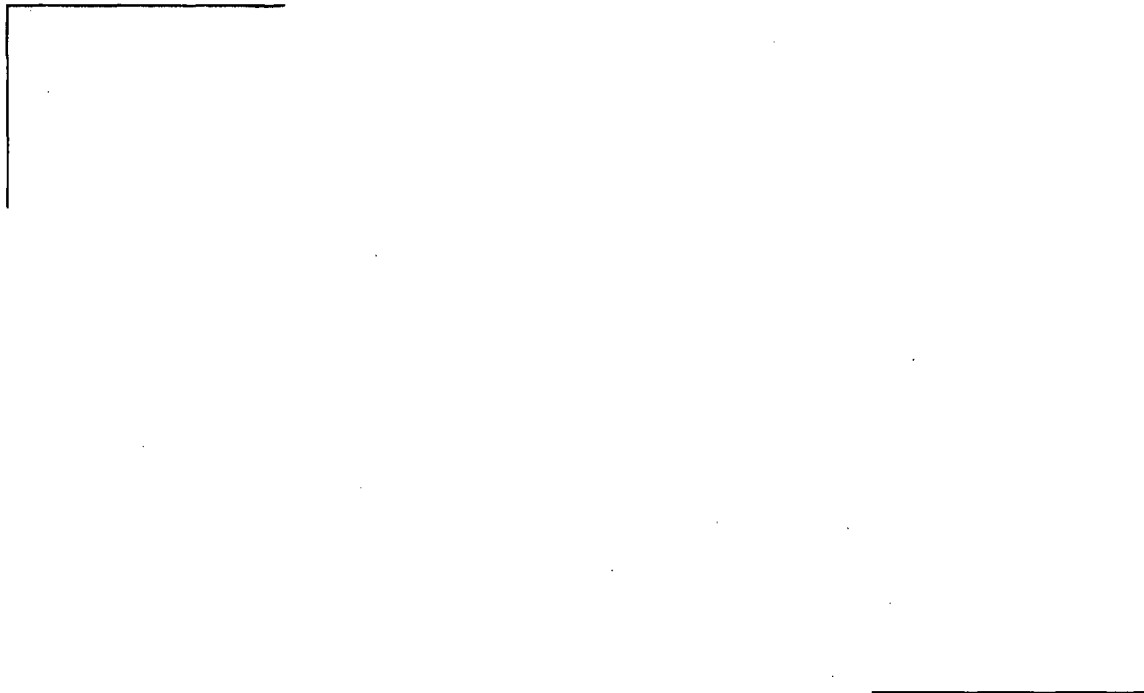
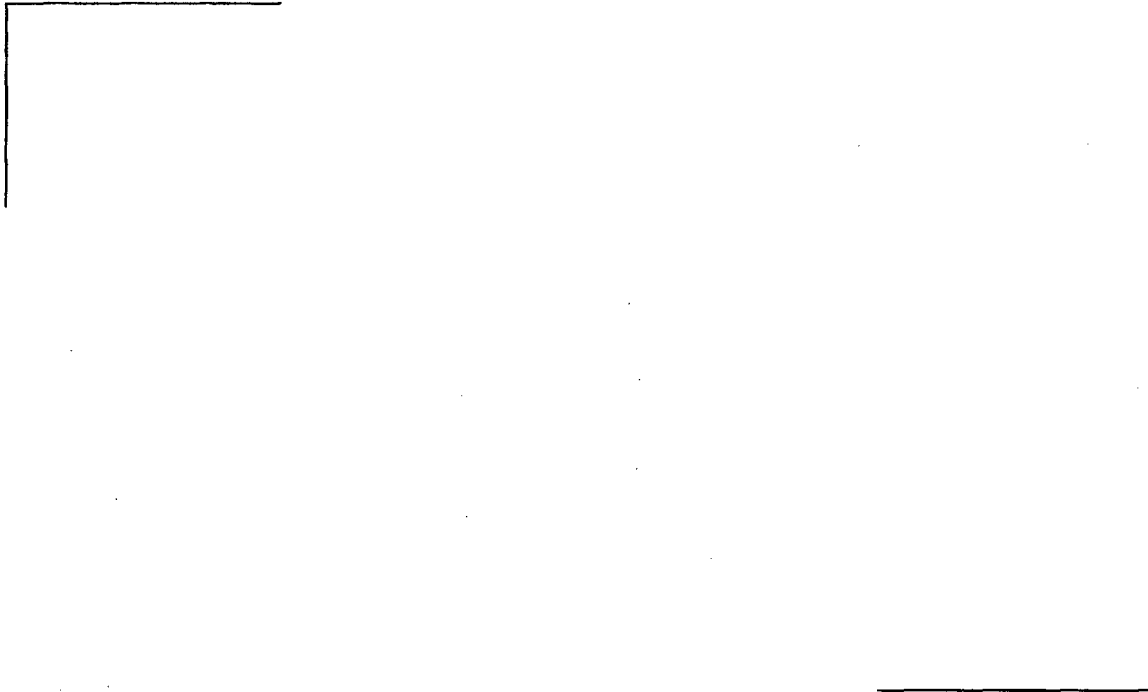


Figure 4.16 Cladding Creep Down for BWR 10x10 Cladding



**Figure 4.17 Predicted/Measured Creep Down of Recrystallized
Zircaloy-2 Cladding**

4.2.4 Clad Creep Ovality

The creep ovality model starts from an initial ovality and predicts the evolution of the ovality as the clad creeps down. The model is dependent on the parameters of the clad creep equation.

The cladding ovality database of RODEX4 is composed of [

]

The cladding type, irradiation parameters and results summary is given in Table 4.4. The comparison between measured and calculated ovality after irradiation, Figure 4.18, shows a best-estimate response.

Table 4.4 Cladding Ovality Validation

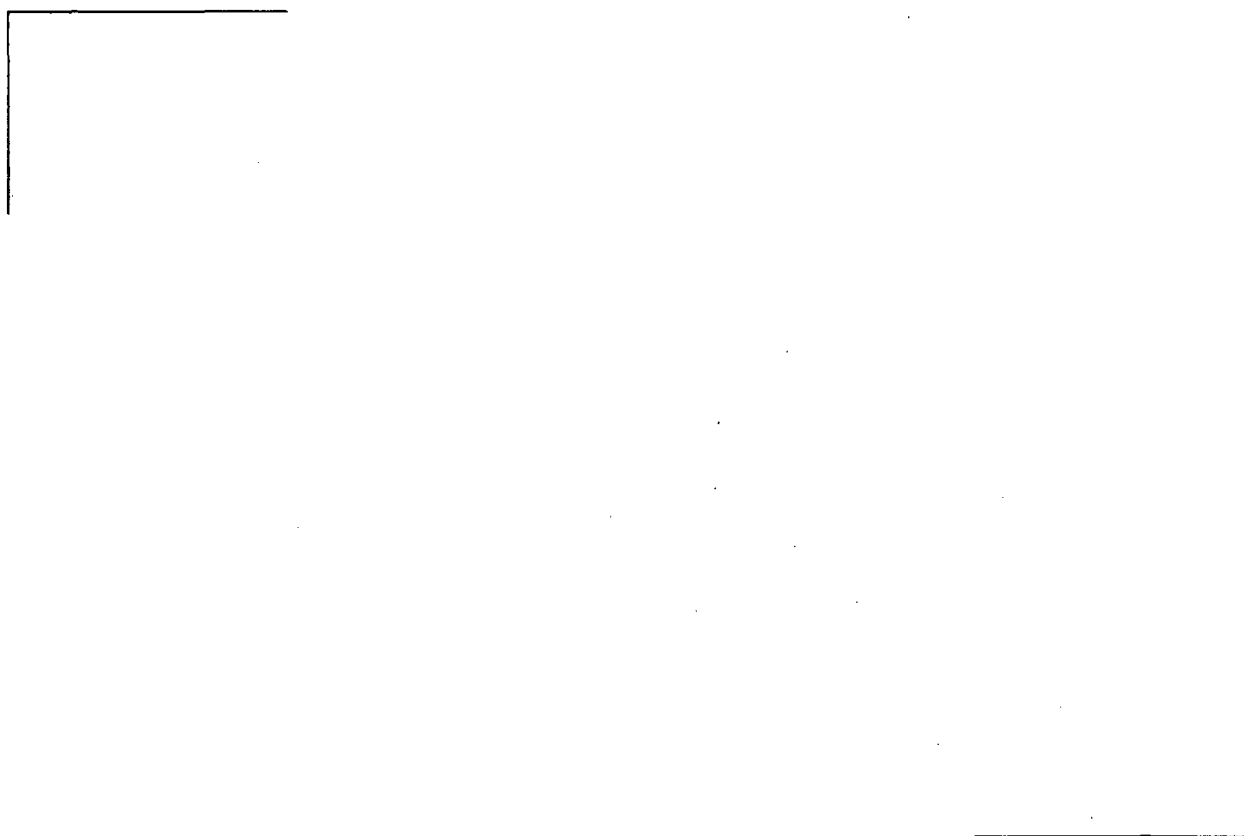


Figure 4.18 Validation of Cladding Ovality - HBRP Rods

4.2.5 Clad Ramp Strain

Important cladding deformation is generally observed after ramp testing of a rod. Fuel thermal expansion and transient gaseous swelling contribute to close the pellet-cladding gap and to load the cladding. Stresses in the cladding reach high values and the cladding deforms by thermal creep.

At LHGRs up to about 40 kW/m fuel thermal expansion is the dominant phenomenon which controls PCMI. At LHGRs above 40 kW/m gaseous swelling may become the dominant phenomenon. The effect of gaseous swelling is often mitigated by fuel hot pressing and fuel creep. Fission gas release also limits gaseous swelling. The interaction between gaseous swelling, fuel hot pressing, fuel creep, and fission gas release has been calibrated together with the thermal conductivity and fission gas release models.

The clad deformation due to these models is validated by confirmation of the clad strain during high power ramp tests. The parameters have been adjusted to get a best-estimate code response for both fission gas release and gaseous swelling. [

]

The clad strain validation is performed for [

]

The RODEX4 code predicts mid-pellet strain and local pellet end strains through the ramp and subsequently at hot cell conditions. The clad diameter increases corrected for corrosion, and the temperature and internal pressure at hot cell conditions, are compared with the results of clad profilometry measurements. The clad mid-pellet and ridge strains are well predicted.

[

]

The ramp test calibration shows that ramp strain increase for rods at 62 GWd/MTU burnup and at strains about equal to the 1% strain limit are well predicted.

Table 4.5 Large Cladding Deformation Database - Ramp Tests



Figure 4.19 Mark-BEB Rod 65-2 - Rod Diameter at Pellet End

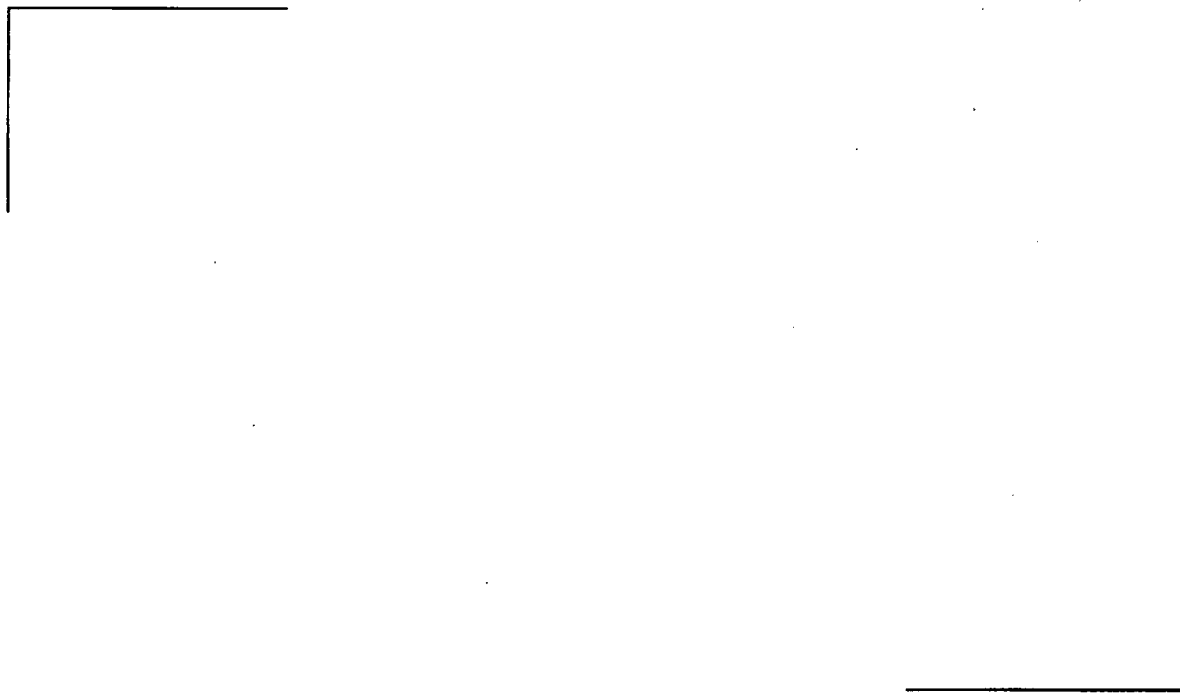


Figure 4.20 Mark-BEB Rod 65-2 - Diameter Increase

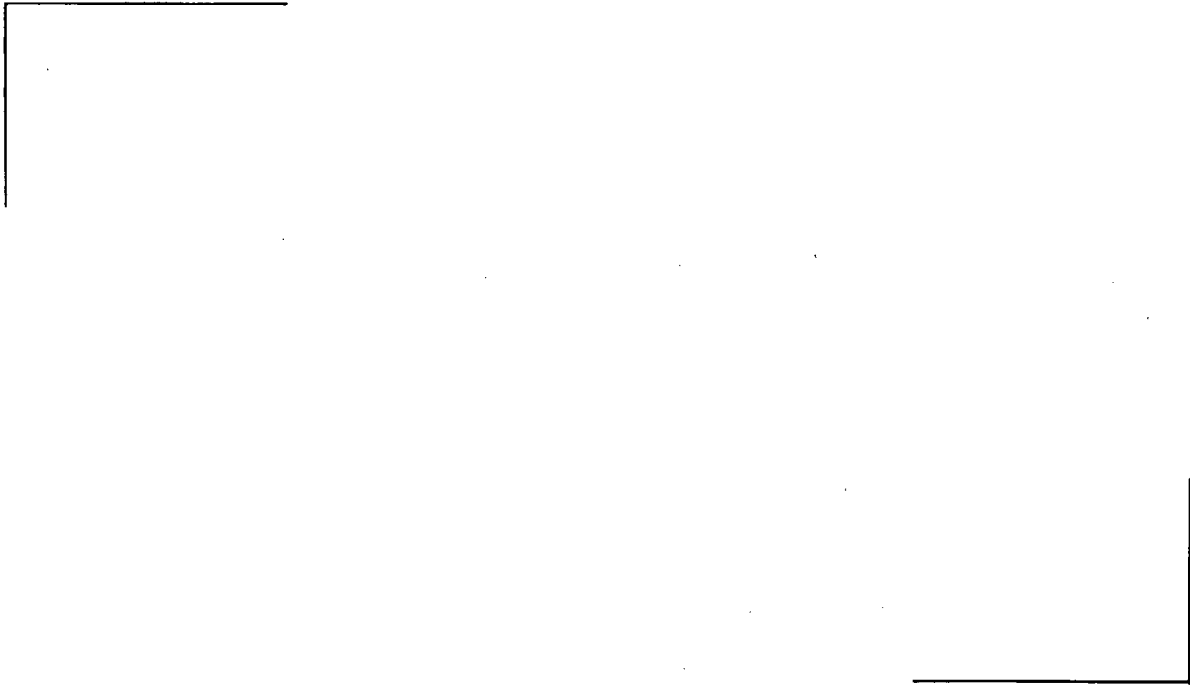


Figure 4.21 Mark-BEB Rod 65-4 - Diameter Increase

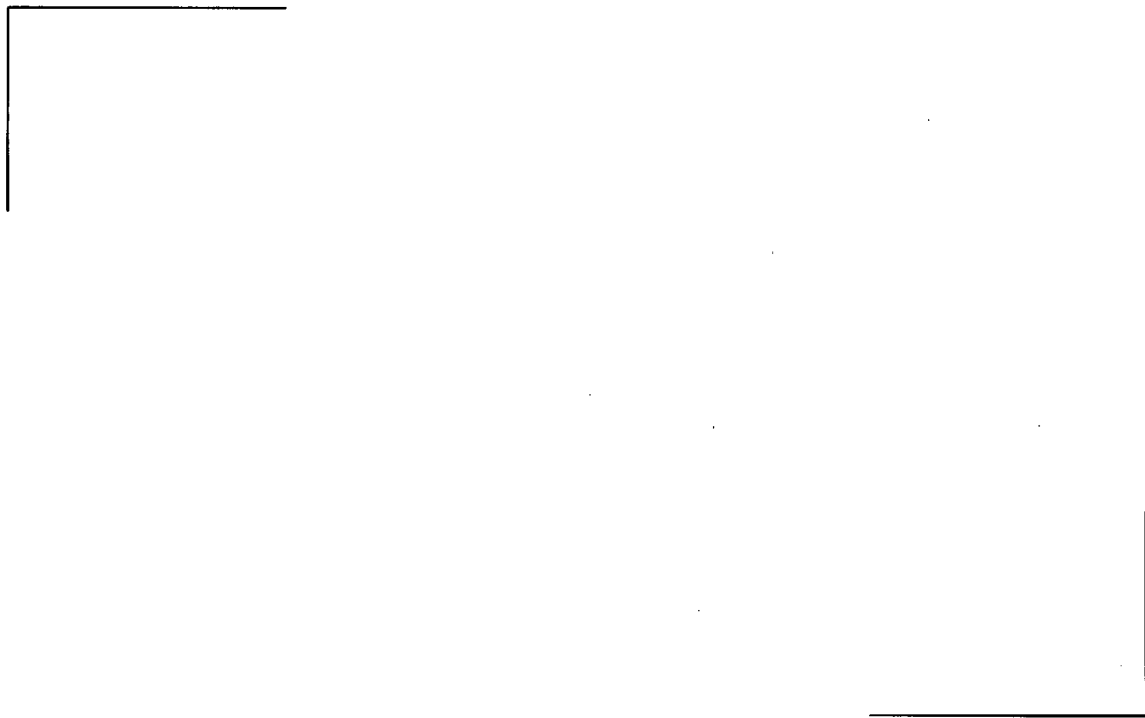


Figure 4.22 Mark-BEB Rod 66-2 - Diameter Increase

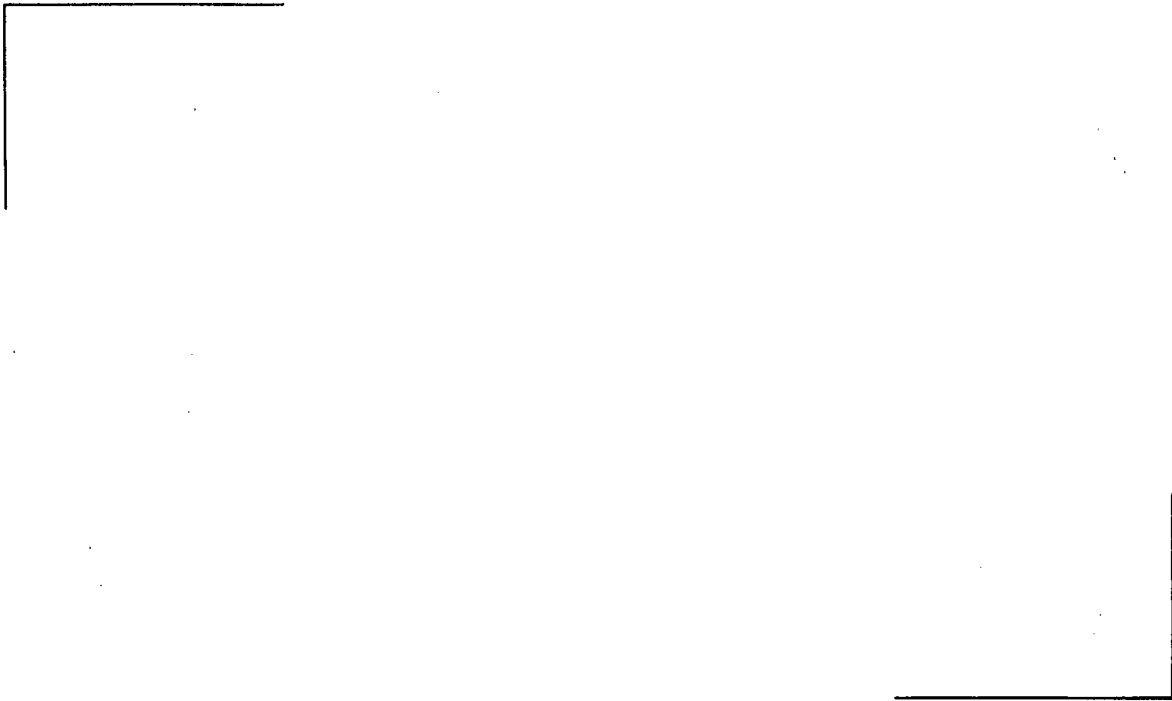


Figure 4.23 Super-Ramp Rod PK2/3 - Diameter Increase

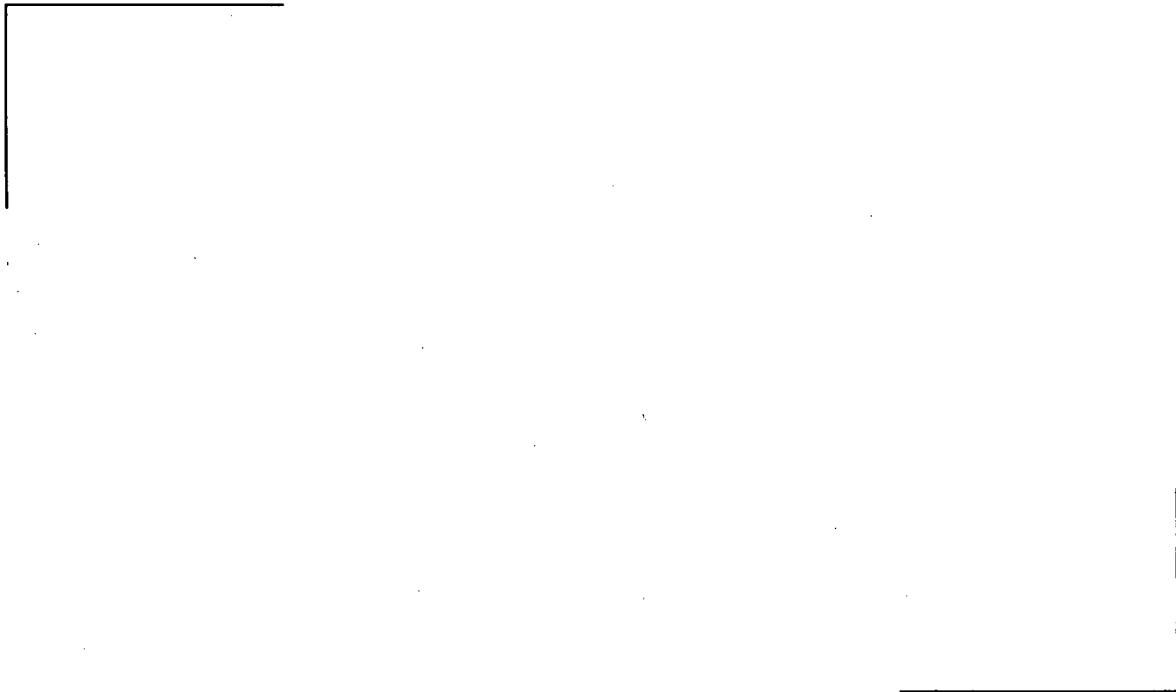


Figure 4.24 Super-Ramp Rod PK2/3 - Rod Diameter at Pellet End

4.2.6 Rod Axial Elongation

Verification of measured/calculated rod axial elongation includes the effects of growth and PCMI induced creep on clad elongation. The growth equation, as just one component of elongation, was calibrated after the pellet temperature, pellet swelling and the clad creep were finalized.

The RODEX4 experimental BWR rod elongation database for CWSR Zircaloy-2 cladding includes rods from:

[

]



Figure 4.25 Validation of Rod Axial Growth for BWR 10x10 Fuel

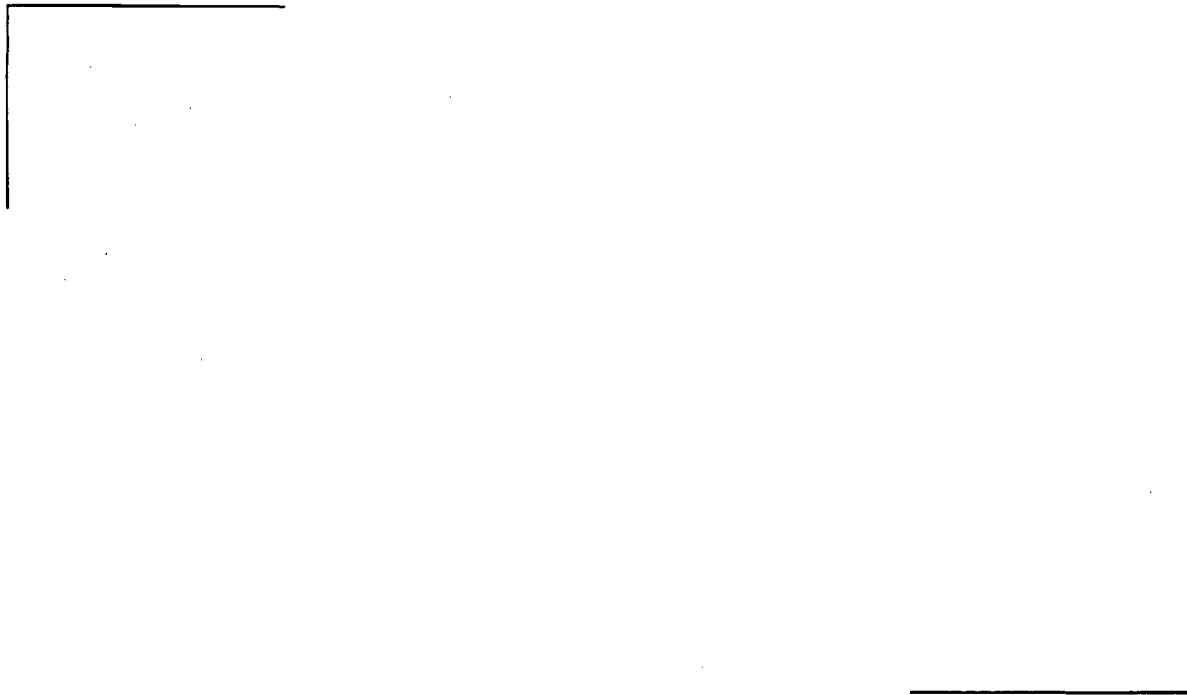


Figure 4.26 Validation of Rod Axial Growth for BWR 9x9 Fuel

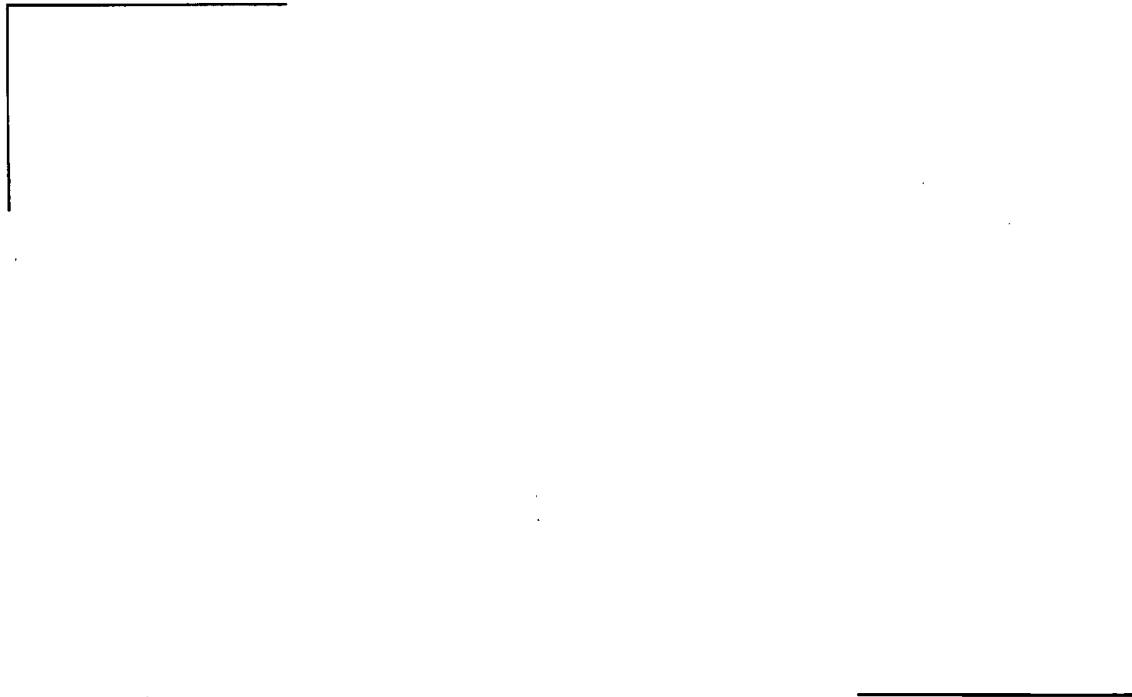


Figure 4.27 Validation of Rod Axial Growth for BWR RX Clad Fuel

4.2.7 Rod Free Volume

The rod inner free volumes are not subjected to any requirement, but they are an important parameter for the correct prediction of the rod inner pressure. The volumes include:

- The upper and lower gas plena
- The pellet-cladding gap along the fuel column
- The open cracks in the pellets
- The fuel open porosity
- The pellet central hole (if any)

Their calculation integrates the effects of:

- Fuel densification
- Fuel swelling
- Fuel thermal expansion
- Pellet cracking

- Cladding creep down
- Cladding axial creep and growth
- Cladding lift-off

i.e., the whole pellet and cladding mechanics.

The "Rod Free Volume" database is summarized in Table 4.6.

[

] The figure shows a best-estimate agreement
between RODEX4 predictions and measurements.

Table 4.6 Summary of Database for Free Volume Verification

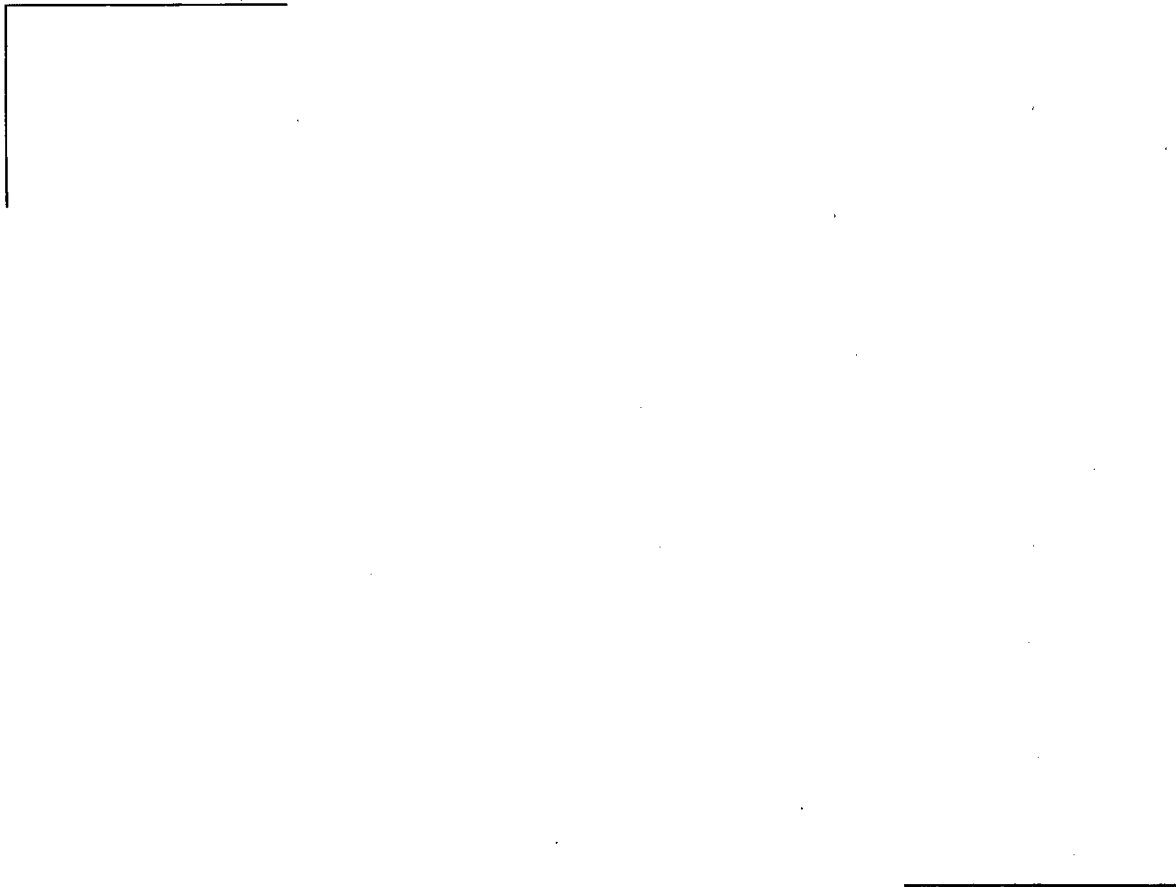


Figure 4.28 Validation of Rod Free Volume

4.2.8 Clad Oxidation

The zircaloy cladding is subjected to external corrosion during irradiation. This results in several concerns. First, if the corrosion thickness becomes too large it may lead to cladding failure.

Secondly, the thermal properties of zirconium oxide are significantly different from the zircaloy properties. The oxidation of the cladding creates a thermal resistance that contributes to increasing the cladding temperature especially at high LHGR. The thermal creep of the cladding during a power transient may consequently be significantly affected by a corrosion layer.

Thirdly, the corrosion contributes to decrease the thickness of metal in the cladding which has an effect on cladding creep down or lift off.

[

]



**Figure 4.29 Outer Corrosion Layer Thickness in
BWR 10x10 Fuel versus Exposure**

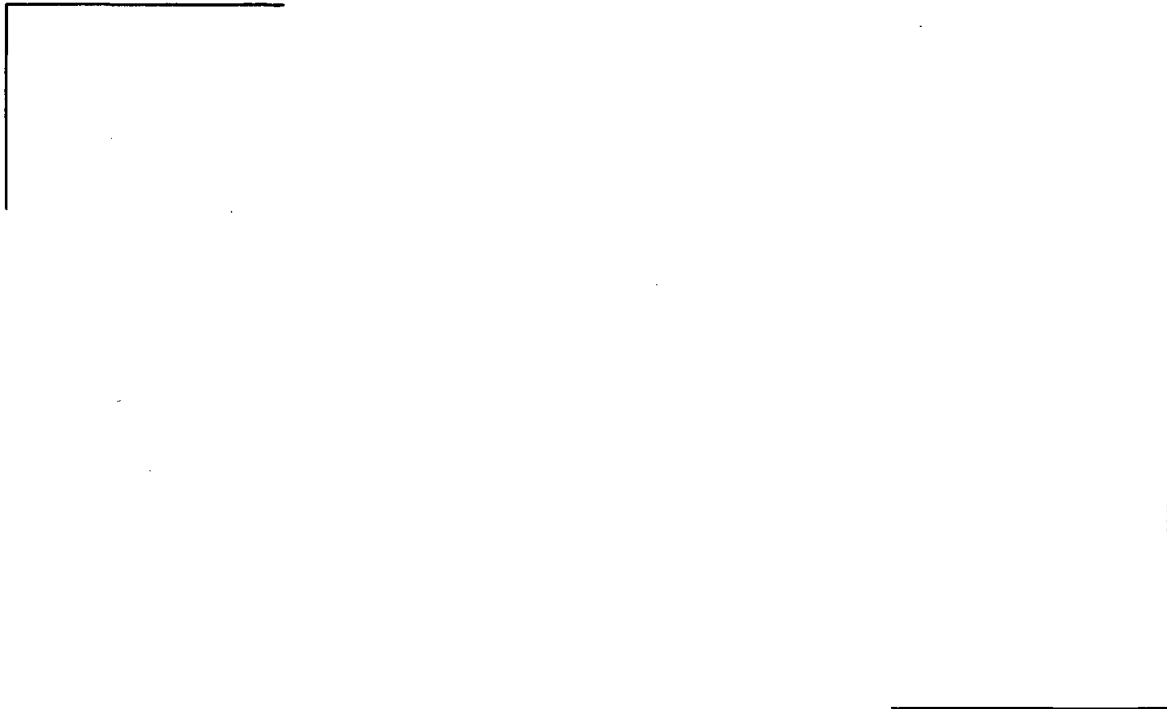


Figure 4.30 Validation of the Cladding Outer Corrosion

4.3 ***Assessment of Biases***

4.3.1 Centerline Temperature

The best-estimate character of the results for both UO₂ and gadolinia fuel is confirmed by the centerline temperature predictions. [

]

4.3.2 Fission Gas Release

The predicted to measured gas releases show that an overall best-estimate benchmarking has been reached. [

]

4.3.3 Clad Creep

Comparisons of 10x10 and 9x9 CWSR fuel rods show that the same value of creep parameter provides a best-estimate code response for both clad designs. [

]

4.3.4 Clad Creep Ovality

The comparison between measured and calculated ovality after irradiation shows close to a best-estimate response. [

]

4.3.5 Clad Ramp Strain

The clad mid-pellet and ridge strains are well predicted with little or no bias. The strain increment during the ramp test both at mid-pellet and pellet end is well predicted [

]

4.3.6 Rod Axial Growth

The growth calibration results confirm a best-estimate elongation response of the code. [

]

4.3.7 Rod Free Volume

A comparison of the calculated to measured rod free volumes, [

]

4.3.8 Clad Oxidation

The clad oxidation is a best-estimate fit [

]

4.4 **Validation Ranges**

The range of data used for final validation is listed in Table 4.7 for each of the important calibration parameters. All high burnup sensitive parameters are validated to an exposure of at least 62 GWd/MTU.

[

]

5.0 **Uncertainty Analyses**

5.1 ***PIRT Process***

[

]

5.2 ***Reactor Operation Uncertainties***

The reactor environment is defined by the fuel rod power and neutron fast flux and by the coolant pressure, temperature, and flow rate. For the realistic thermal-mechanical evaluation of the fuel rods, the power and fast flux are determined with an approved 3D core simulator code (currently MICROBURN-B2) on a rod nodal basis for projected operation. The flow rate is obtained from the simulator calculations on a fuel assembly basis.

5.2.1 Power Histories

[

]

5.2.2 Variation from Planned Fuel Management

[

]

[

]

5.2.4 Reactor Power Measurement Uncertainty

The reactor power measurement uncertainty is obtained from the reactor utility. [

]

5.2.5 Power Uncertainties for Normal Operation

[

]

5.2.6 Power Uncertainties for Slow Transient AOOs

[

]

[

]

5.2.7 Power Uncertainties for Fast Transient AOOs

[

]

5.2.8 PIRT Reactor Operation Uncertainty Summary

The uncertainties in the reactor environment [

]

[

]

[

]

[

]

[

]

5.3 ***Fuel Rod Manufacturing Uncertainties***

5.3.1 Cladding Manufacturing Uncertainties

All of the cladding manufacturing parameters [

]

[

]



Figure 5.1 Clad Inside Diameter Distribution

5.3.2 Pellet Manufacturing Uncertainties

All of the pellet manufacturing parameters of [

]



Figure 5.2 UO₂ Fuel Pellet Resinter Density Distribution

5.3.3 Rod Manufacturing Uncertainties

All of the rod manufacturing parameters [

]

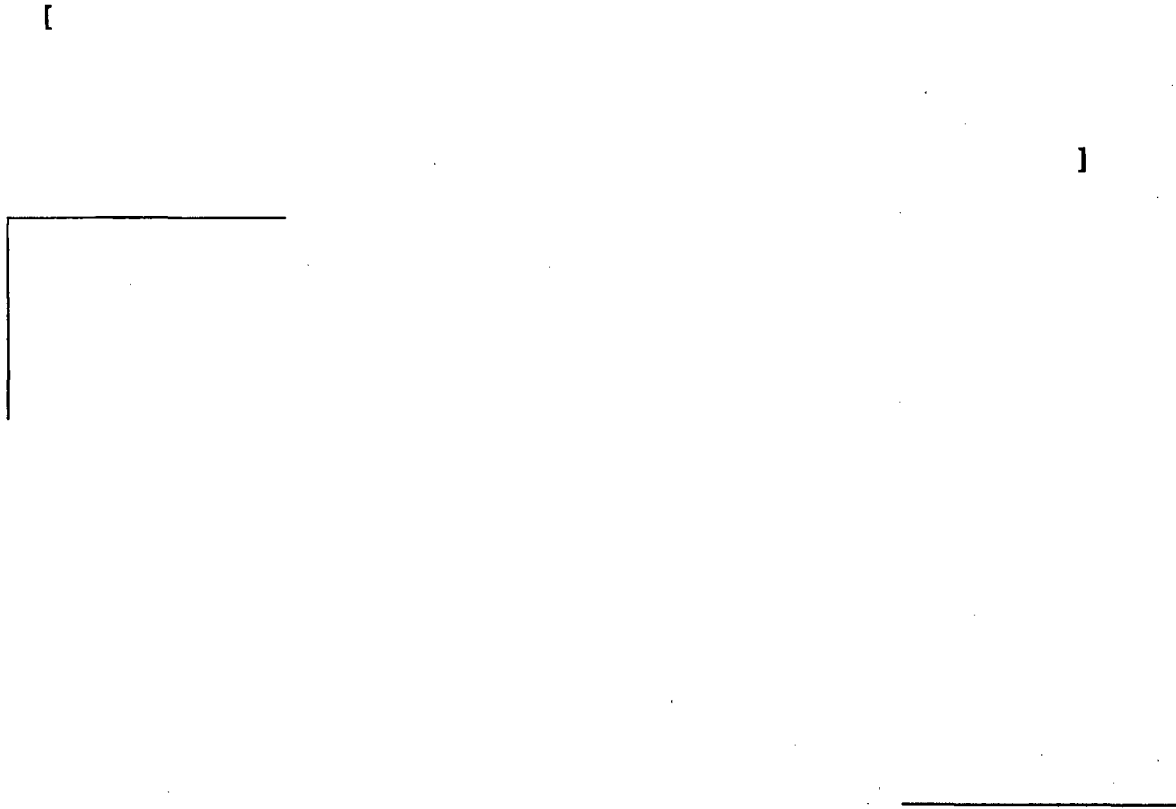


Figure 5.3 Fuel Rod Plenum Length Distribution

5.3.4 PIRT Manufacturing Uncertainty Summary

The disposition and description of the distribution characteristic for each rod manufacturing parameter is listed below as reference in the PIRT

[

]

[

]

5.4 ***RODEX4 Model Parameter Uncertainties***

Model parameter uncertainties were developed by evaluating the measured / calculated results for the calibration and validation database, and by determining the distribution and standard deviation of the applicable model parameter that was needed to bring measured and calculated results into alignment. [

]

[

]

are described below, followed by a section discussing each parameter as referenced to the PIRT and its disposition.

5.4.1 Fission Gas Release Model Parameter Uncertainty

5.4.1.1 Fission Gas Uncertainty Data Set

As described in Section 4.0, the database consists of international program cases [] and commercial cases [] For the calibration of fission product release, a combination of more than 400 international and commercial cases are used.

[

]

5.4.1.2 Diffusion Coefficient Uncertainty

The code response function for a particular output of interest, Y, can be characterized through benchmarking by the following function describing the comparison between calculations and measurements:

[

]

[

]

[

]

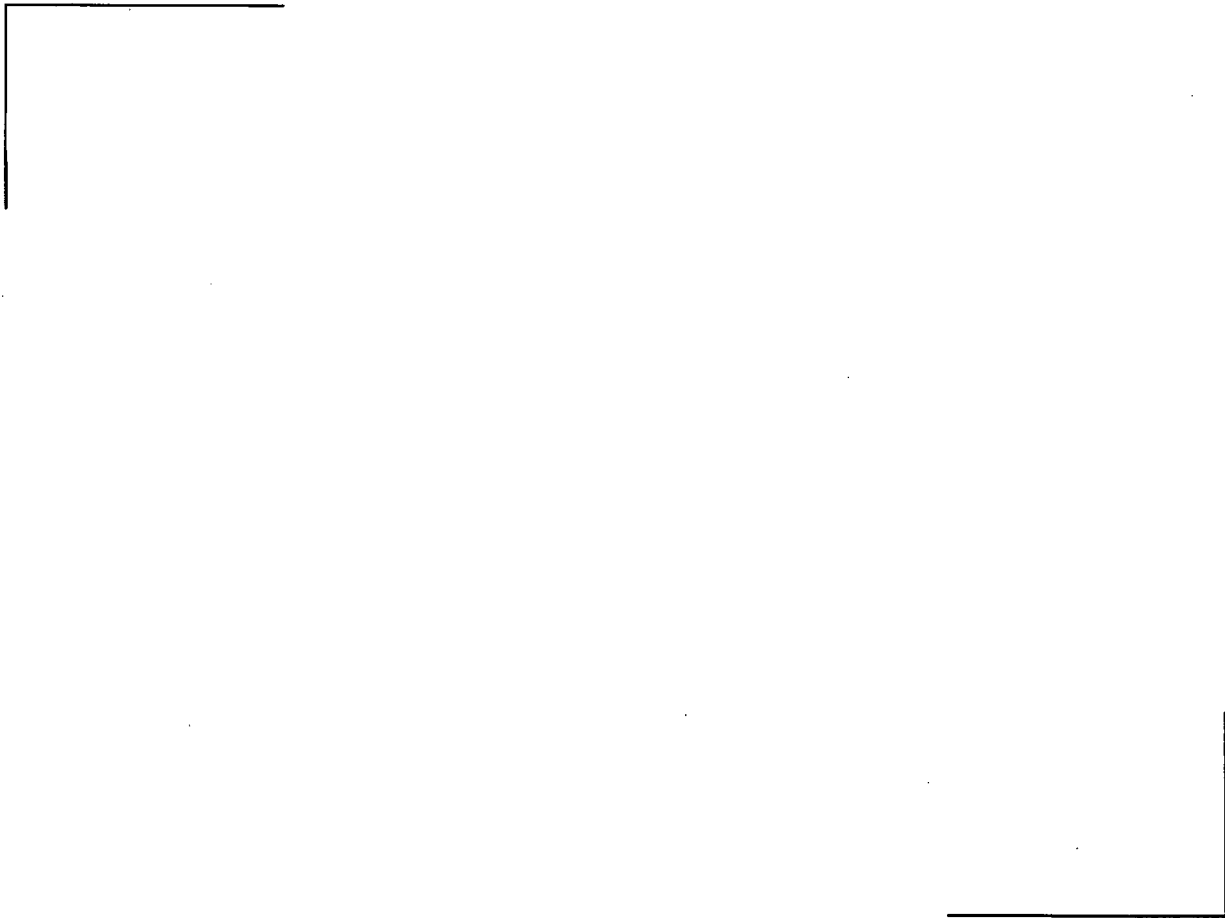


Figure 5.4 Histogram of the FGR Data Comparisons

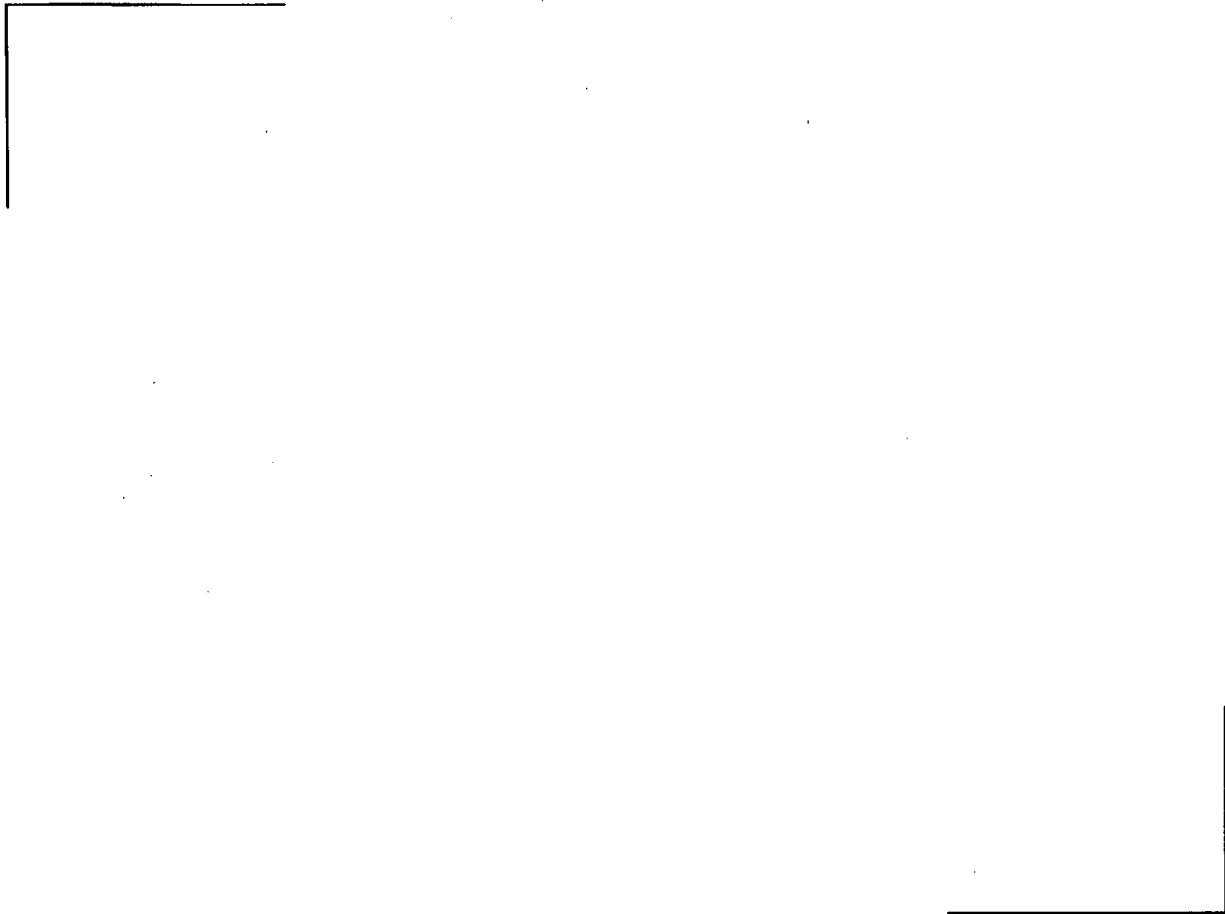


Figure 5.5 FGR Data with 95% Upper and Lower Bounds

5.4.2 Irradiation Creep Parameter Uncertainty

A database of [

]

[

]

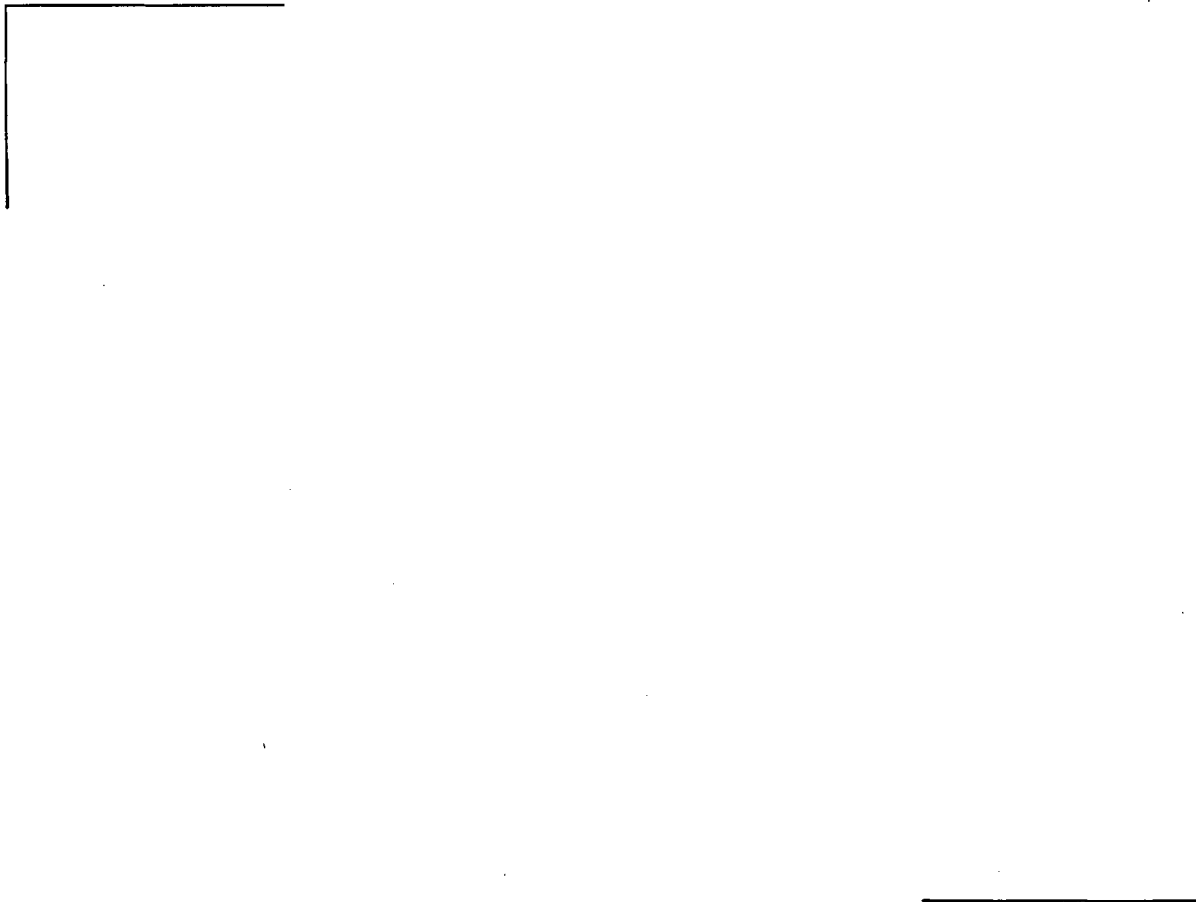


**Figure 5.6 Cladding Creep Down and Fabrication Uncertainty at the
2 σ Bounds of the Outer Diameter**

5.4.3 Oxidation Parameter Uncertainty

The oxidation uncertainty is determined from [

[

]

5.4.4 Creep Ovality Uncertainty

The uncertainty in creep ovality results is due mainly to the clad creep rate uncertainty and to the initial clad ovality. [

]

5.4.5 PIRT Model Parameter Uncertainty Summary

[

]

[

]

[

]

[

]

[

]

[

]

5.5 *Thermal Transient Solution Uncertainties*

[

]

[

]

Table 5.4 BWR Core Simulator Code Measured Power Distribution Uncertainty

Table 5.5 Fast Transient Model Uncertainties

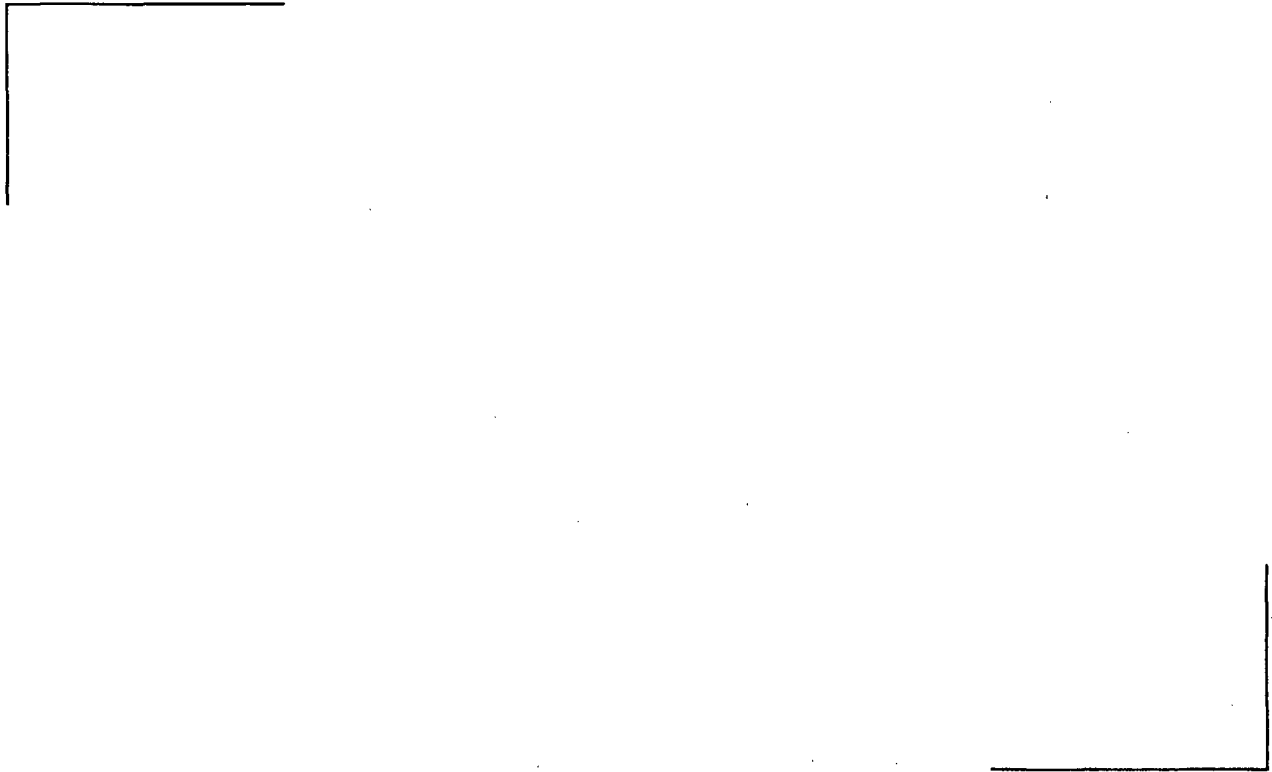


Figure 5.7 [] Distribution for BWR-4 Equilibrium
Batch Sample Case

6.0 Application Examples

The objective of the application examples is to demonstrate the realistic fuel rod analysis for normal reactor operation, slow transients and fast transients.

Normal operation is evaluated for a BWR-6 using 18 month transition and equilibrium cycles, and for a BWR-4 using 24 month transition and equilibrium cycles. The analysis for the BWR-6 transition cycle is repeated with different power and parameter selections to demonstrate the sensitivity of the analyses to the statistical parameters.

The slow transient analysis is demonstrated for a control rod withdrawal error (CRWE) for the BWR-4. This event is important for a BWR-4 where a single rod withdrawal is possible, and not important for a BWR-6 where rod movements are limited to small withdrawals.

The fast transients are evaluated for the BWR-4 transition cycle. Three limiting fast transients from 25%, 30% and 100% reactor power are evaluated.

The input to these examples is meant to be representative. It should not be considered as establishing a frozen set of analysis values. Values used in licensing analyses will be based on the description of the methodology in this report.

6.1 Normal Operation Examples

6.1.1 BWR-6 Reactor, 18 Month Cycles

6.1.1.1 Description

These analyses were performed for transition and equilibrium cores for ATRIUM-10 fuel in a BWR-6 operating 18 month cycles. The transition batch histories were taken for the ATRIUM-10 from a mixed core of ATRIUM-10 and non-FANP fuel assemblies. The equilibrium batch histories are for a full core of ATRIUM-10 fuel. The detailed histories were developed with the MICROBURN-B2 core simulator. Quarter core symmetry was used. [

]

The analysis conditions are summarized in Table 6.1.

6.1.1.2 Example Licensing Analysis

The objective of this set of analyses is to demonstrate the use of this methodology in the qualification of the ATRIUM-10 fuel assembly design for operation to the maximum full length rod average burnup of 62 GWd/MTU. [

]

The maximum result for each of the criteria for the BWR-6 case is summarized in Table 6.2. The results for the equilibrium cycle are plotted as described below:

[

]

[

]

6.1.1.3 Annealed Clad Material Demonstration

The BWR clad model parameters can be selected for the applicable clad condition, CWSR or RX. The UO_2 and $UO_2-Gd_2O_3$ transition and equilibrium sample problems were repeated for the BWR-6 cases to demonstrate the analyses for RX clad properties. The results are summarized in Table 6.3.

6.1.1.4 Sensitivity Studies

The BWR-6 transition cycle for the UO_2 rods was re-evaluated with different analysis conditions to demonstrate the sensitivity of the results to statistical and power parameters. The analyses performed were:

[

]

[

]

These results verify that the code and methodology yield reasonable trends relative to key parameters.



Figure 6.1 BWR-6 Equilibrium Batch - Maximum Rod Internal Pressure



Figure 6.2 BWR-6 Equilibrium Batch - Maximum Rod Internal Pressure Histogram

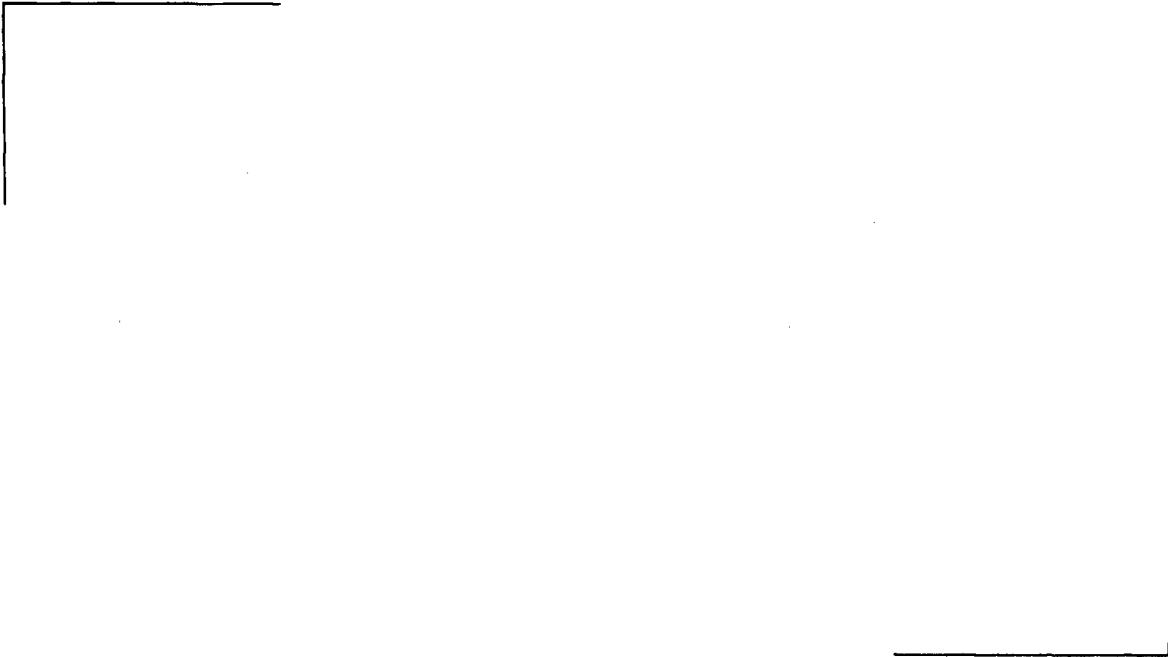


Figure 6.3 BWR-6 Equilibrium Batch - Maximum Clad Strain during Normal Operation

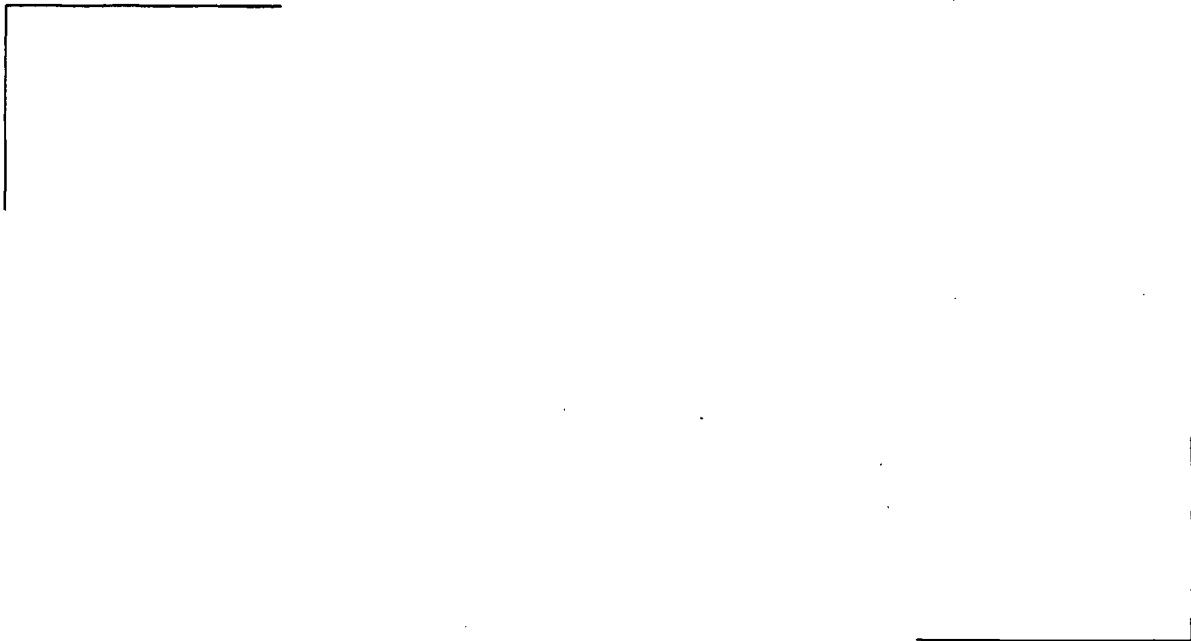


Figure 6.4 BWR-6 Equilibrium Batch - Maximum Clad Strain Increase during Normal Operation



**Figure 6.5 BWR-6, Equilibrium Batch - Maximum Remaining Column
Densification after Creep Ovality Contact**



Figure 6.6 BWR-6 Equilibrium Batch - Maximum Fatigue Usage per 1000 Cycles

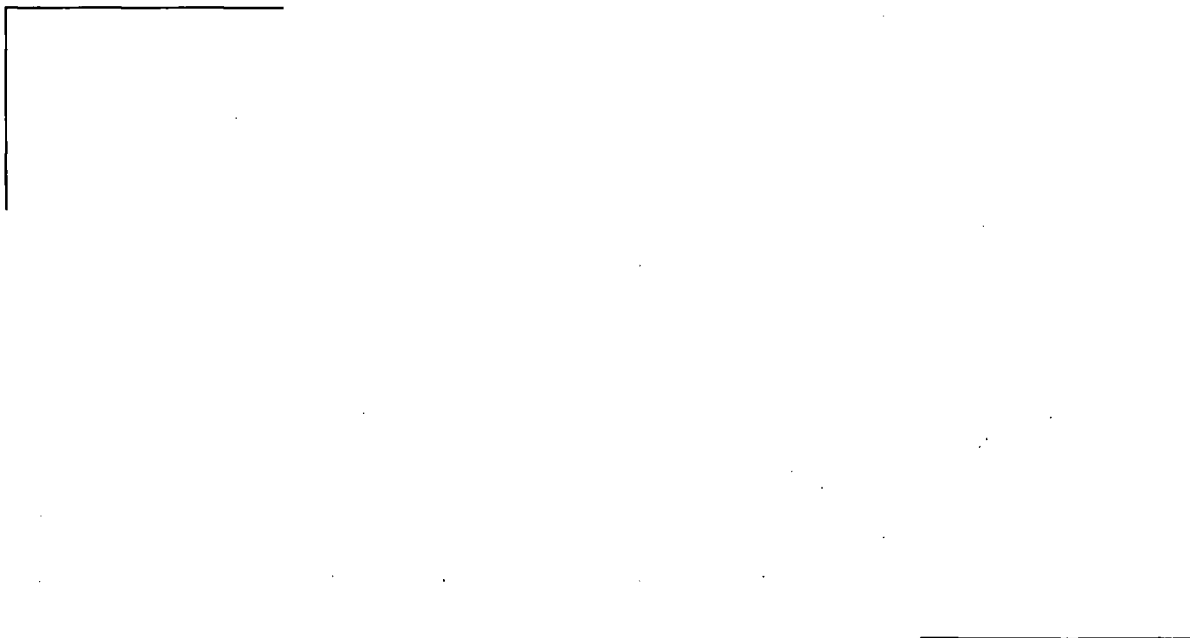


Figure 6.7 BWR-6, Equilibrium Batch - Maximum Clad Oxidation



Figure 6.8 BWR-6, Equilibrium Batch - Maximum Clad Hydrogen Pickup

6.1.2 BWR-4 Reactor, 24 Month Cycles

6.1.2.1 Description

Analyses were performed for transition and equilibrium cores for ATRIUM-10 fuel in a BWR-4 operating 24 month cycles. The transition batch histories were taken for the ATRIUM-10 fuel from a mixed core of ATRIUM-10 and non-FANP fuel assemblies. The equilibrium batch histories were for a full core of ATRIUM-10 fuel. The detailed histories were developed with the MICROBURN-B2 core simulator. Quarter core symmetry was used. [

] The analysis conditions are summarized in Table 6.5.

6.1.2.2 Example Licensing Analysis

[

] The maximum result for each of the criteria for the BWR-4 cases is summarized in Table 6.6.

**Table 6.6 Normal Operation Results Summary
BWR-4 ATRIUM-10 with Standard Clad**

6.2 Slow Transient Example - BWR-4 Control Rod Withdrawal Error

6.2.1 Description

The example slow transient analysis for control rod withdrawal error was performed for the transition and equilibrium batches for ATRIUM-10 fuel in a BWR-4 operating 24 month cycles. The analysis conditions were the same as for the BWR-4 normal operation evaluation as summarized in Table 6.5. The CRWEs are evaluated against the AOO maximum temperature and transient strain criteria.

The BWR-4 has the possibility (albeit remote) of withdrawal errors of individual control rods.

[

]

6.2.2 Control Rod Withdrawal Error Analysis

The example CRWE analysis was performed for the transition and equilibrium cycles for a BWR-4. The analyses were performed separately for each batch and for UO_2 and $UO_2-Gd_2O_3$ fuel rods. In this example, the assemblies adjacent to the control blades are once and twice burned assemblies.

[

]

The maximum result for each of the CRWE analyses is summarized in Table 6.7. The maximum temperature is below melting and the maximum strain increment is below 1%.

6.2.3 Baseline for Control Rod Withdrawal Error Comparison

[

]

**Table 6.7 CRWE Results Summary
BWR-4 Transition and Equilibrium Batches**

6.3 ***Fast Transient Example – BWR-4 Feedwater Controller Failure***

6.3.1 Description

The example fast transient analyses were performed for the transition batch for ATRIUM-10 fuel in a BWR-4 operating 24 month cycles. The analysis initial conditions are determined from the normal operation evaluation. The fast transients are evaluated against the AOO maximum pellet temperature and transient strain criteria.

[

]

[

]

6.3.2 FWCF Analyses

Analyses were performed separately for UO_2 and $\text{UO}_2\text{-Gd}_2\text{O}_3$ fuel rods as their thermal properties are different.

[

]

[

]

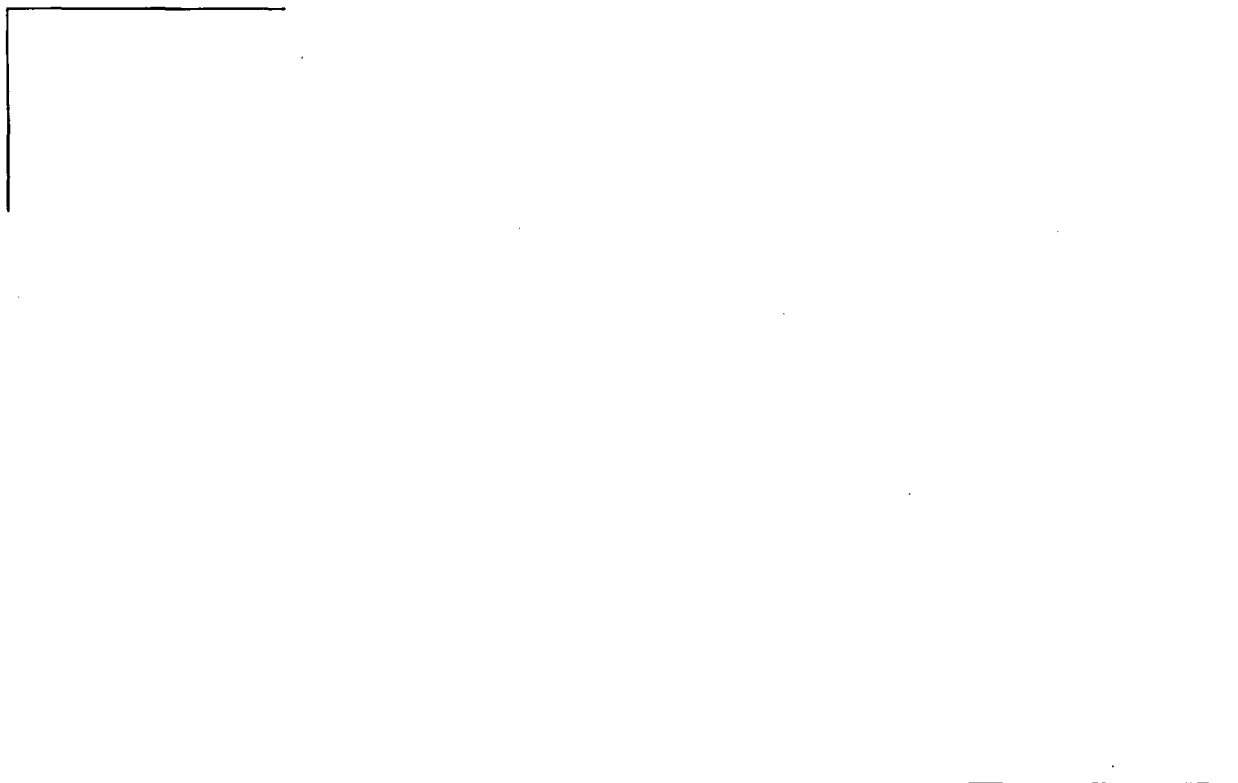


Figure 6.9 25% Power FWCF

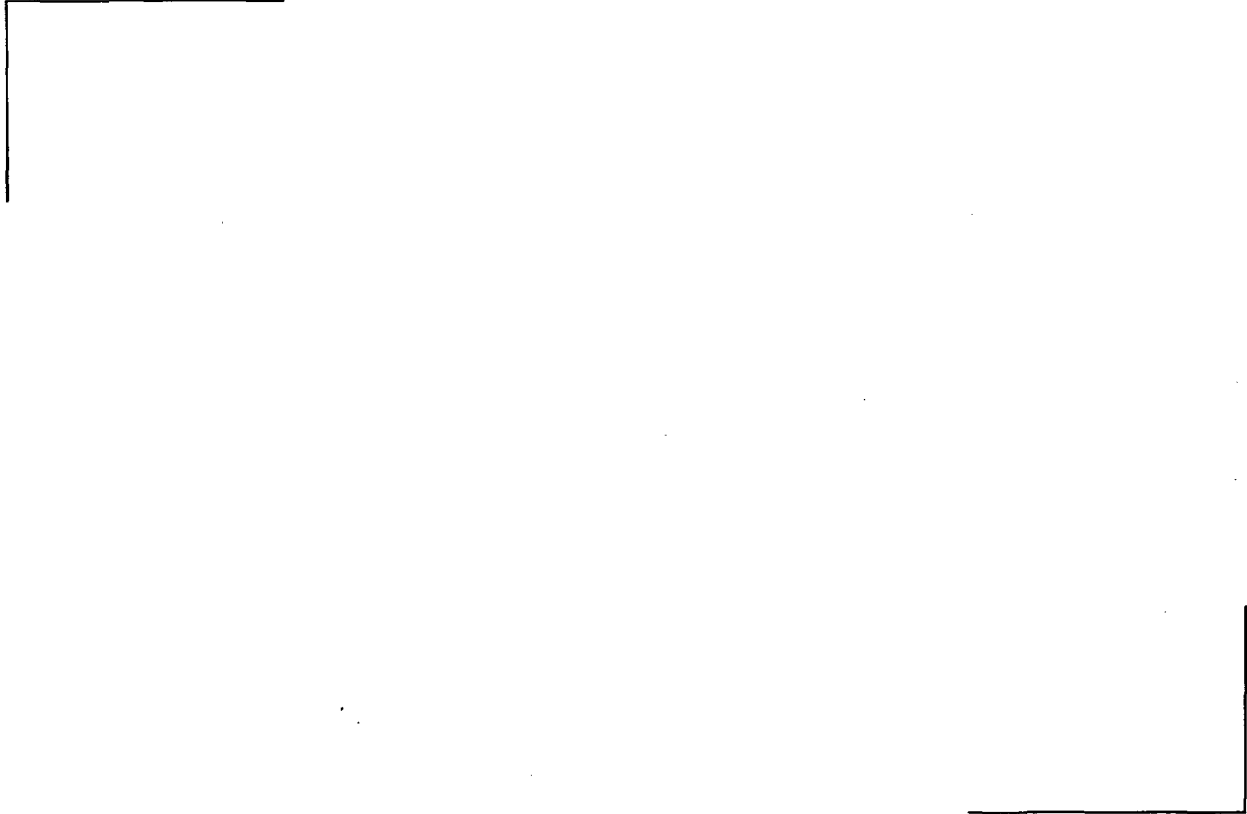


Figure 6.10 30% Power FWCF

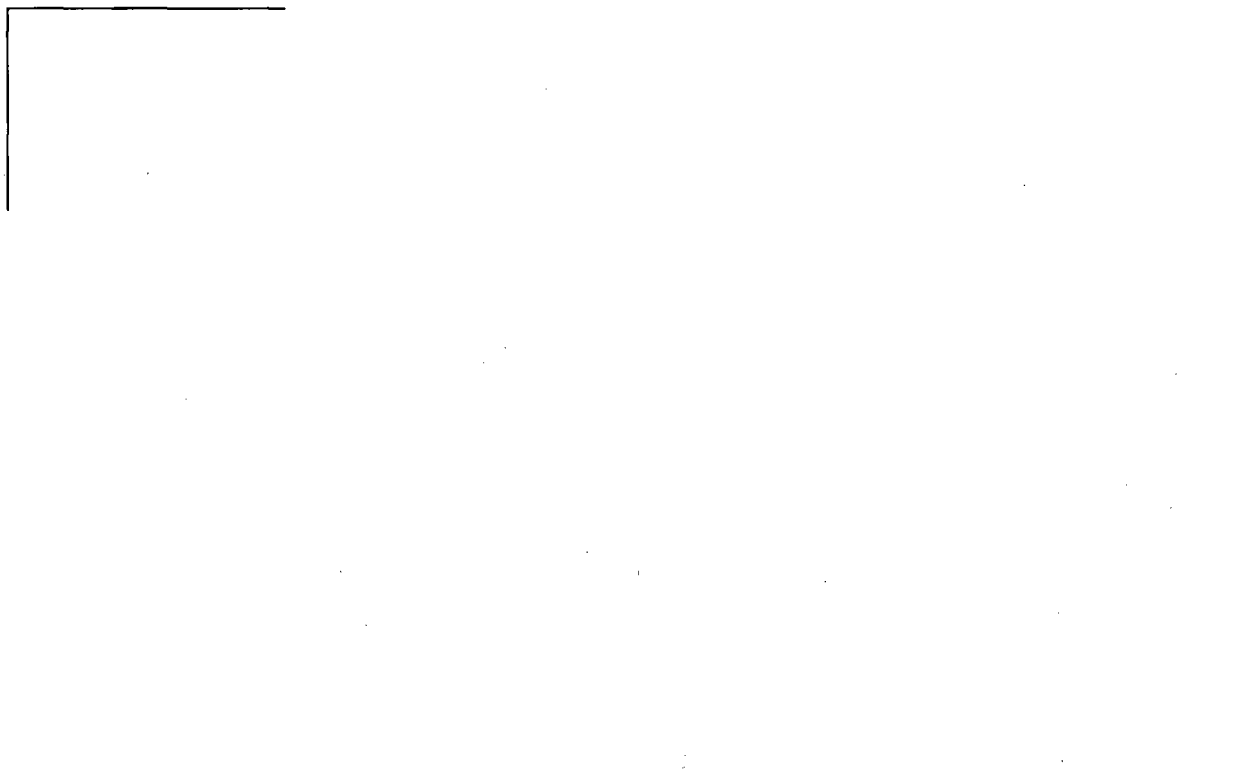


Figure 6.11 100% Power FWCF

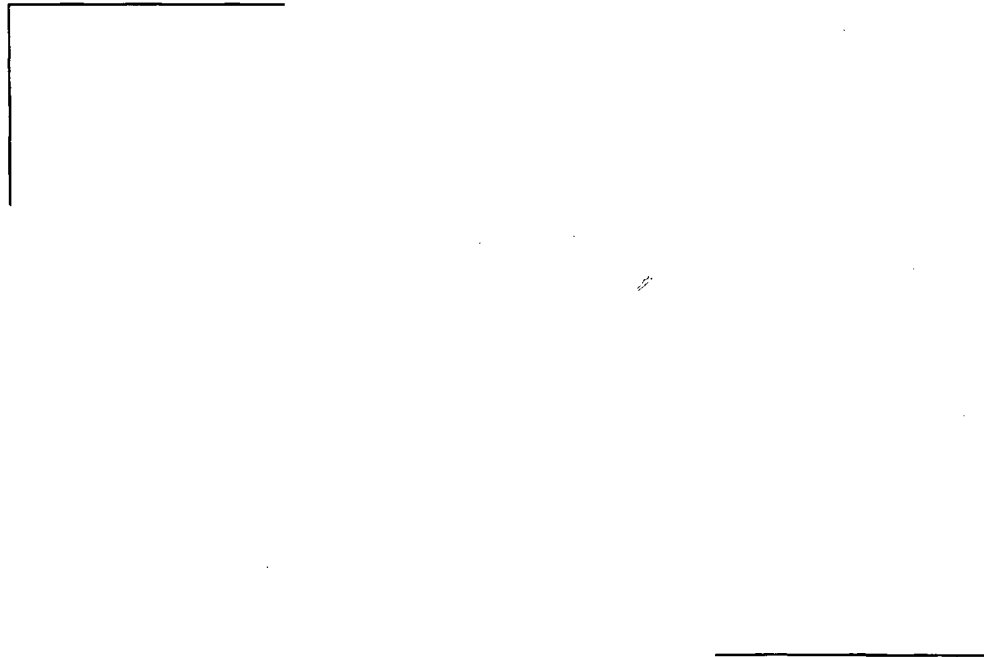


Figure 6.12 Maximum Strain Results (Case 1) [
]

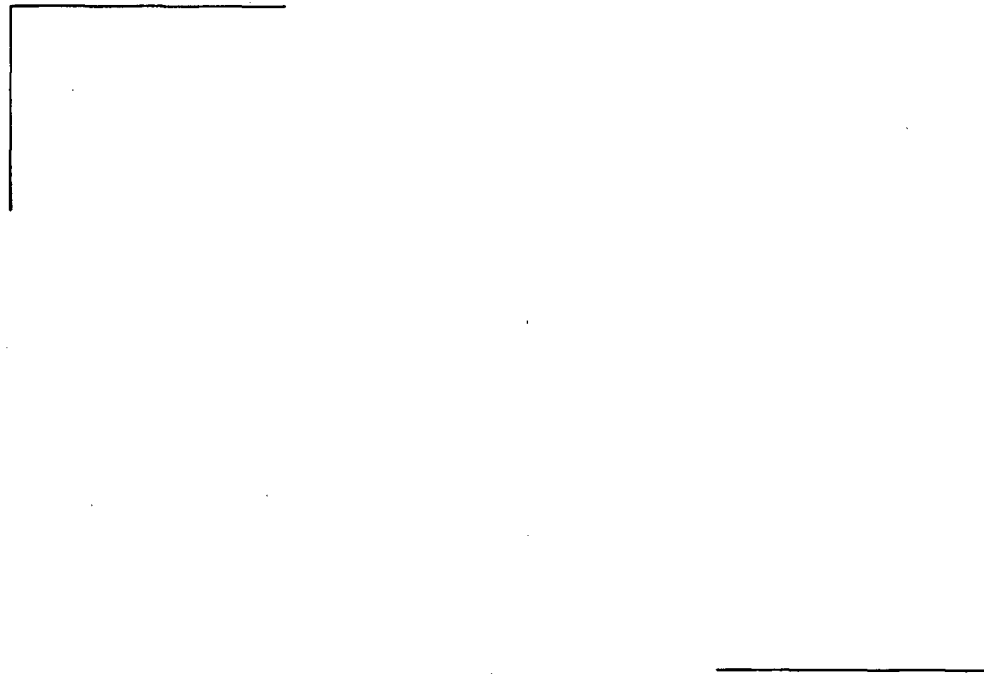


Figure 6.13 Maximum Temperature Results (Case 1) [
]

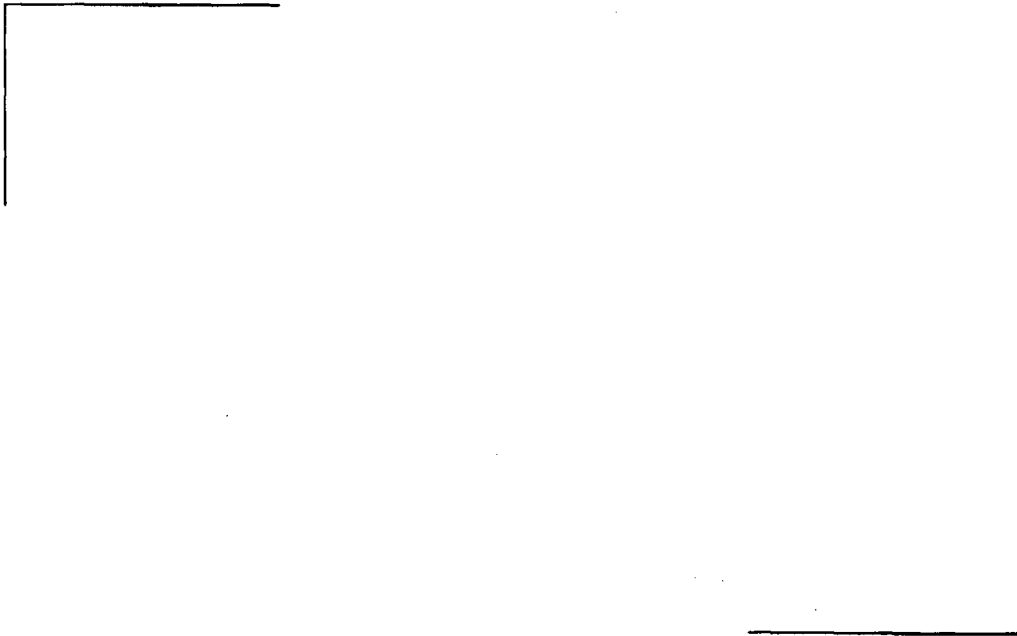


Figure 6.14 Maximum Strain Results (Case 2) [
1

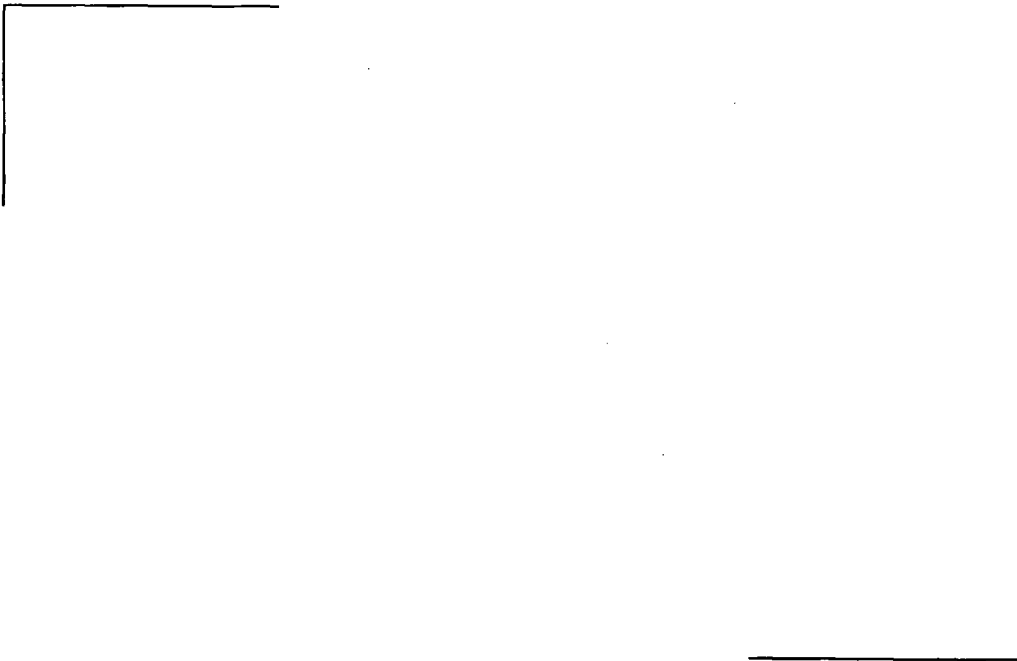


Figure 6.15 Maximum Temperature Results (Case 2) [
1

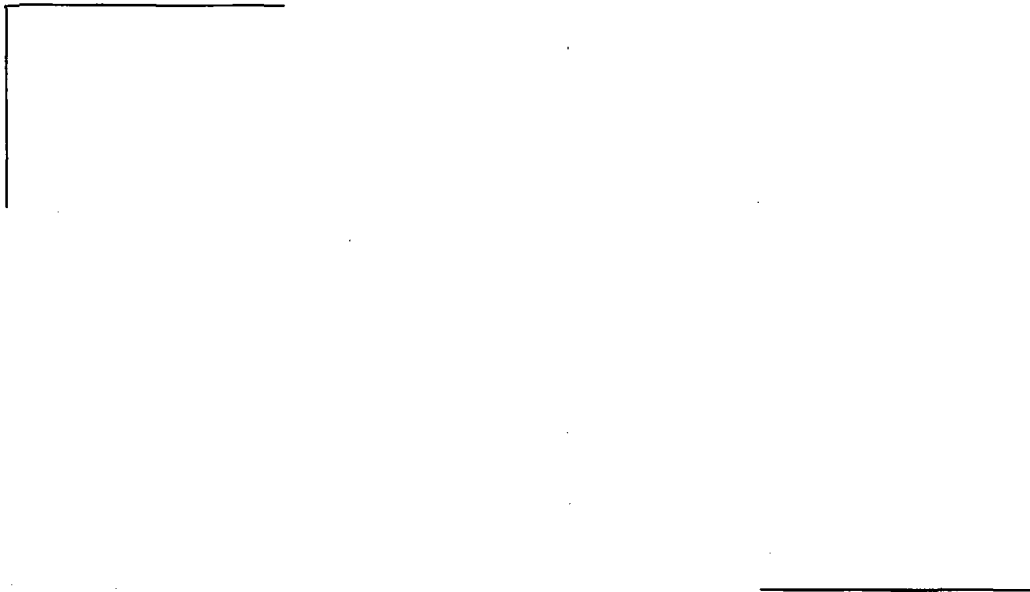


Figure 6.16 Strain Results vs. Burnup for Limiting Run []

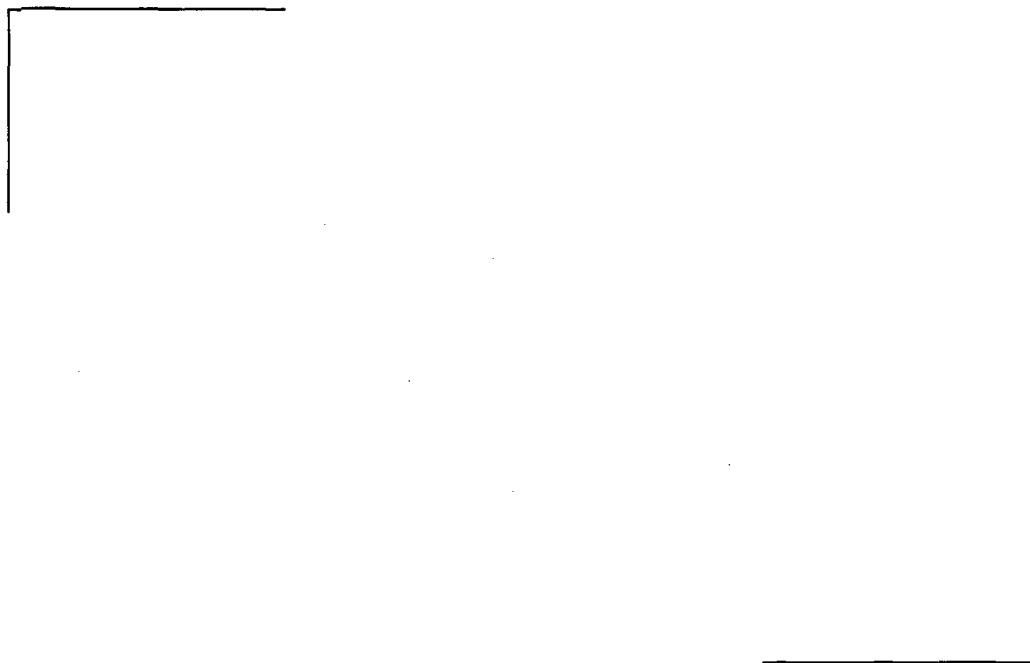


Figure 6.17 Temperature Results vs. Burnup for Limiting Run []

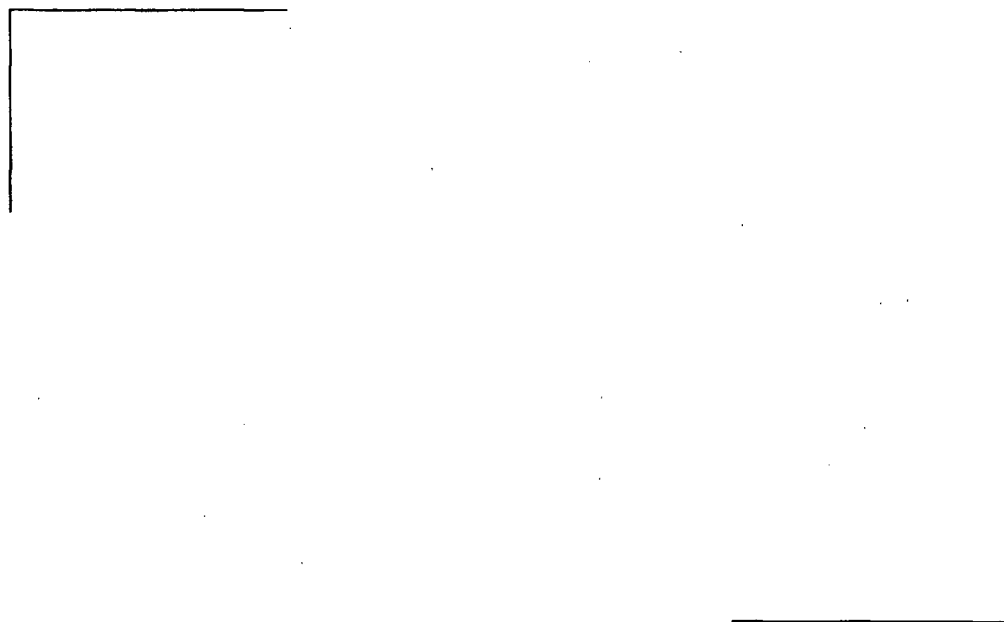


Figure 6.18 Maximum Strain Results (Case 8) [
1

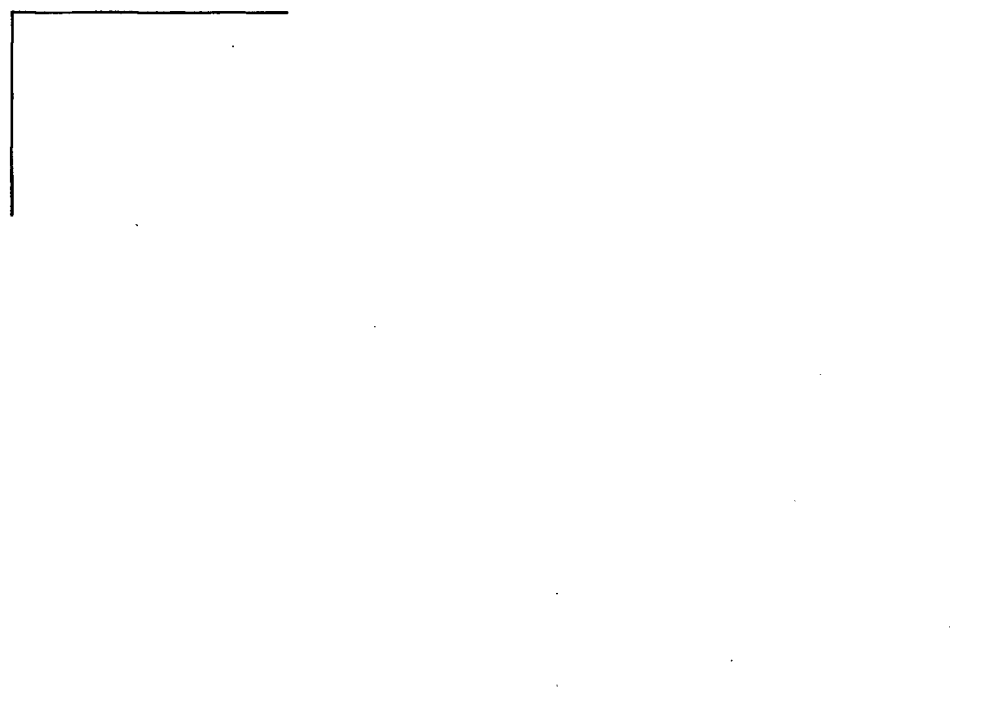


Figure 6.19 Maximum Temperature Results (Case 8) [
1

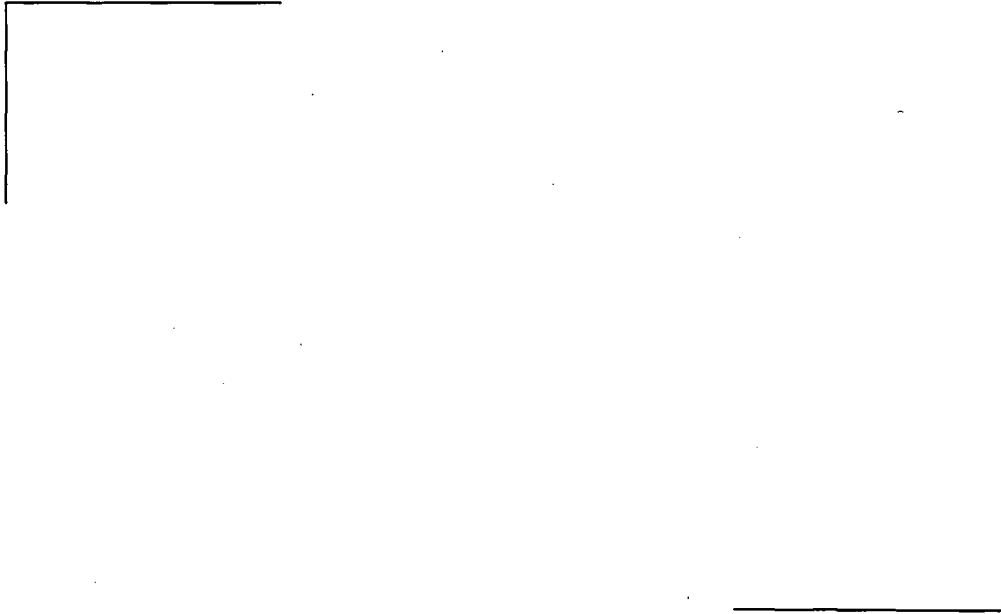


Figure 6.20 Strain Results vs. Burnup for Limiting Run []

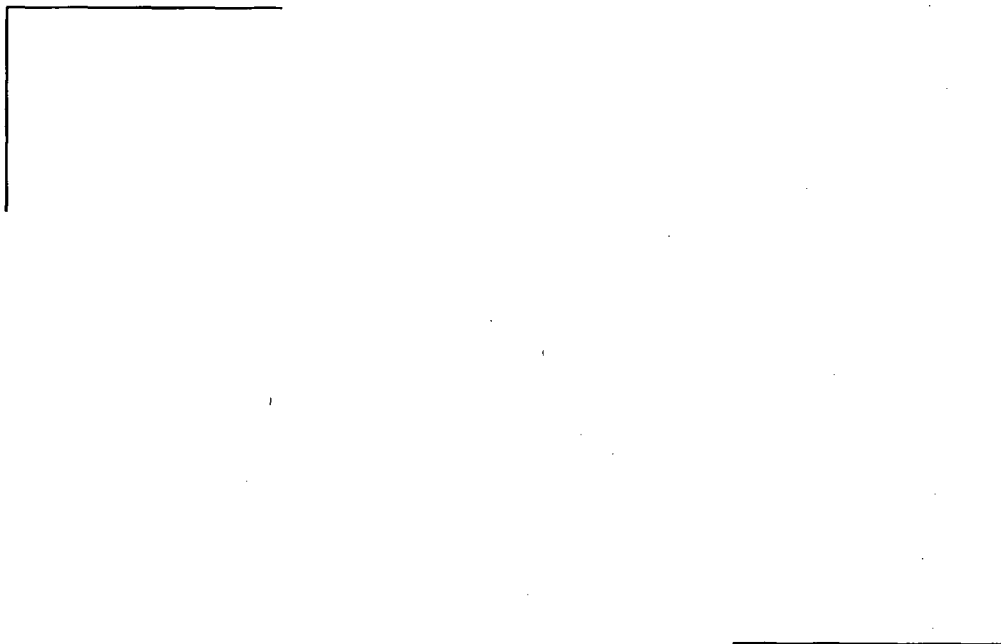


Figure 6.21 Temperature Results vs. Burnup for Limiting Run []

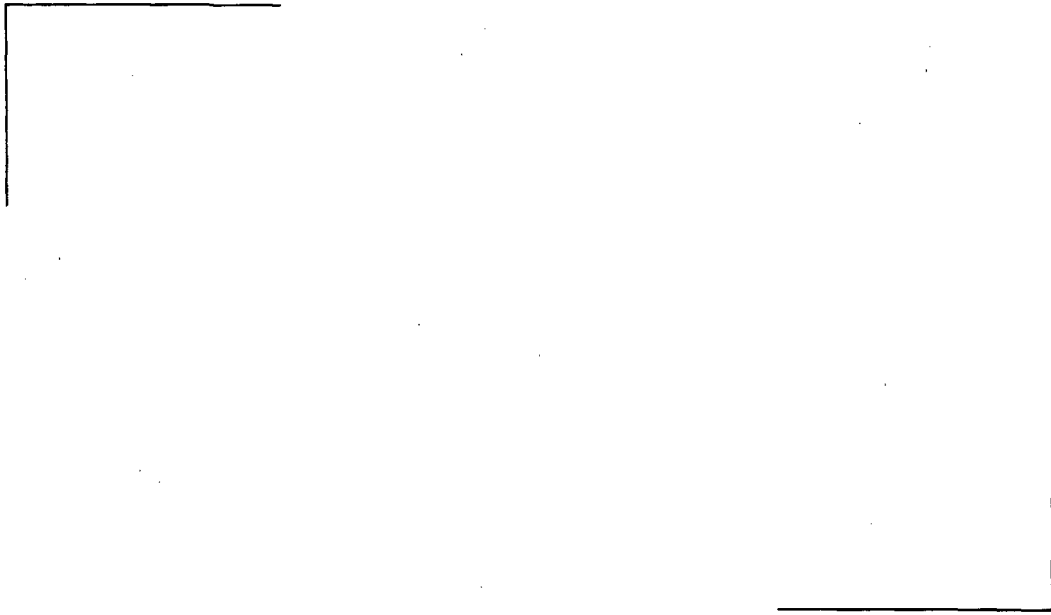


Figure 6.22 Maximum Strain Results (Case 10) []

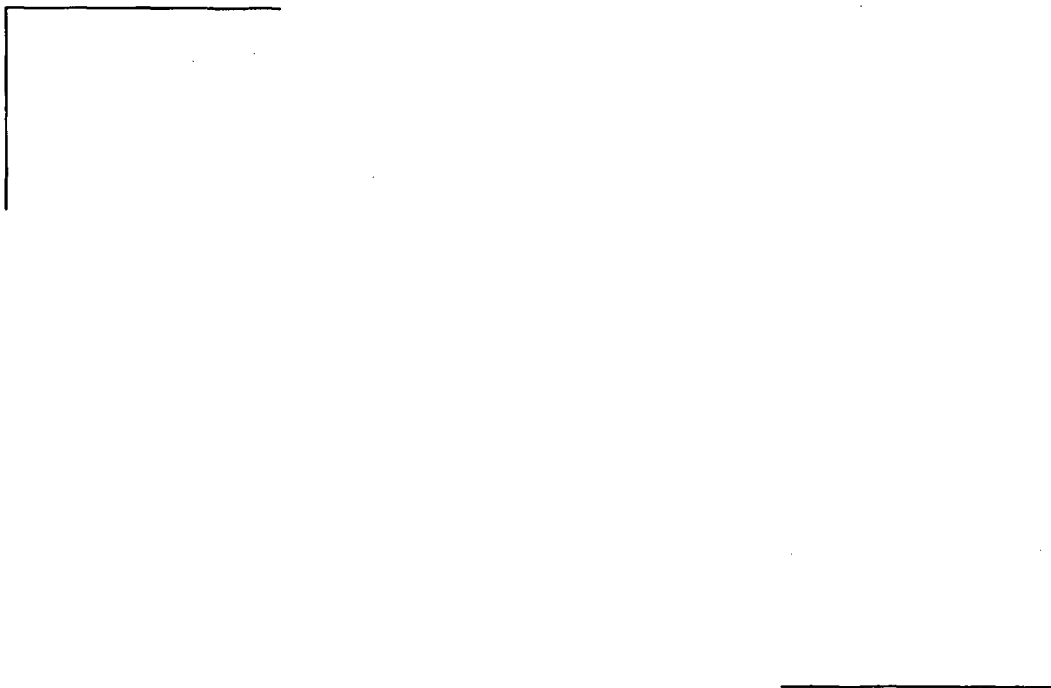


Figure 6.23 Maximum Temperature Results (Case 10) []

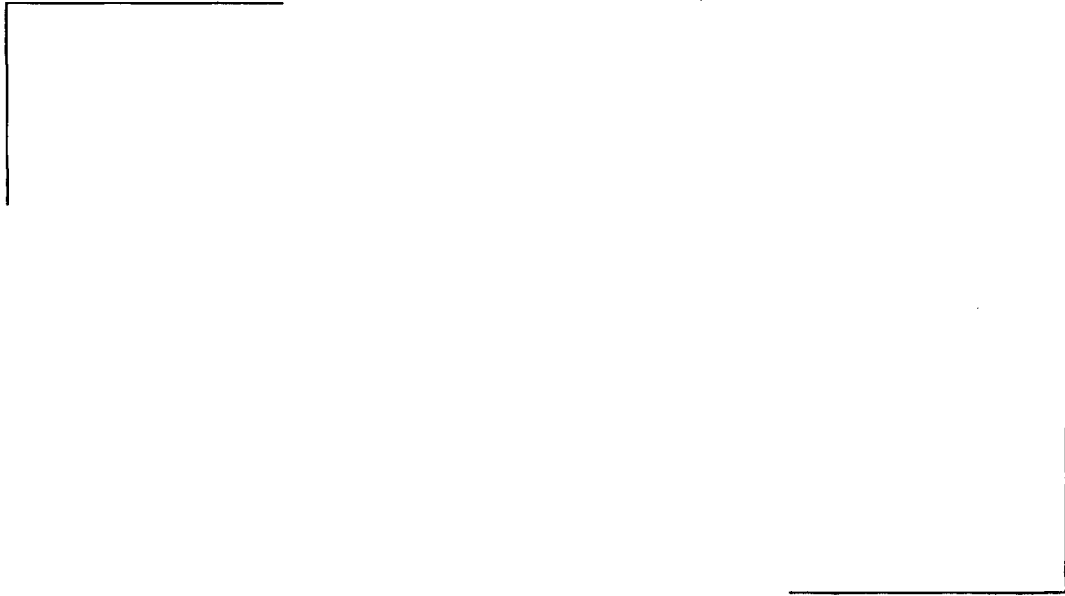


Figure 6.24 Strain Results vs. Burnup for Limiting Run []

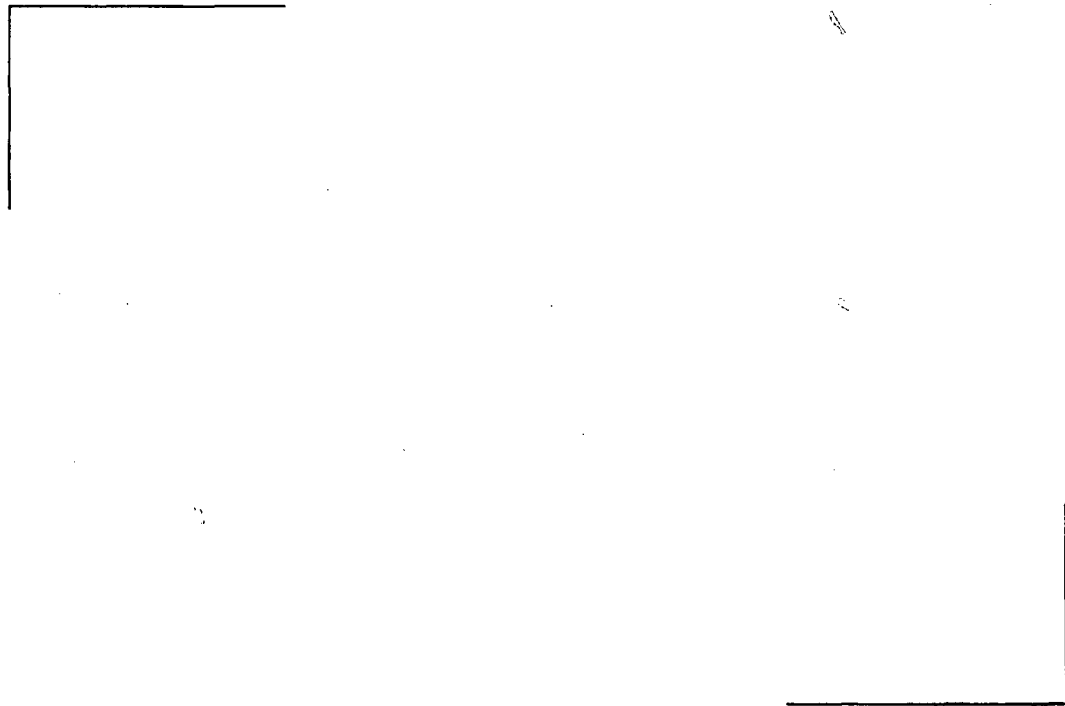


Figure 6.25 Temperature Results vs. Burnup for Limiting Run []

6.4 ***Comparison of New Realistic with Existing Methodology***

Sample problems have been performed with the new (realistic) methodology for cases similar to those for existing ATRIUM-10 designs that are licensed under the current design methodology. The results of the two example problems with the new methodology are compared with the results of two similar deterministic evaluations in Table 6.9.

[

]

7.0 References

1. USNRC Standard Review Plan, *4.2 Fuel System Design*, NUREG-0800, Rev. 2, July 1981.
2. ANF-89-98(P)(A) Revision 1 and Supplement 1, *Generic Mechanical Design Criteria for BWR Fuel Designs*, Advanced Nuclear Fuels Corporation, May 1995.
3. *Quantifying Reactor Safety Margins, Application of Code Scaling, Applicability and Uncertainty Evaluation Methodology to a Large Break, Loss-of-Coolant Accident*, NUREG/CR-5249, December 1989.
4. EMF-2994(P) Revision 0, *RODEX4 Thermal-Mechanical Fuel Rod Performance Code Theory Manual*, Framatome ANP, Inc., August 2004.
5. ANF-99-145(P)(A) Volume I, Volume II, Supplement 1, Revision 0, *RODEX3 Fuel Rod Thermal-Mechanical Response Evaluation Model, Volume I Theoretical Manual, Volume II Thermal and Gas Release Assessments*, Advanced Nuclear Fuels Corporation, April 1996.
6. XN-NF-85-74(P)(A), *RODEX2A (BWR) Fuel Rod Thermal-Mechanical Evaluation Model*, June 1986 and Supplements 1 & 2, Exxon Nuclear Company, February 1998.
7. XN-NF-81-58(P)(A) Revision 2, Supplements 1 & 2(P)(A) Revision 2, *RODEX2 Fuel Rod Thermal Mechanical Response Evaluation Model*, Exxon Nuclear Company, October 1983.
8. EMF-3014(P) Revision 0, *RODEX4 Thermal-Mechanical Fuel Rod Performance Code Verification and Validation Report*, Framatome ANP, Inc., August 2004.
9. EMF-2158(P)(A), *Siemens Power Corporation Methodology for Boiling Water Reactors: Evaluation and Validation of CASMO-4/MICROBURN-B2*, Siemens Power Corporation, October 1999.
10. ANF-913(P)(A) Volume 1 Revision 1 and Volume 1 Supplements 2,3 and 4, *COTRANSA2: A Computer Program for Boiling Water Reactor Transient Analyses*, Advanced Nuclear Fuels Corporation, August 1990.
11. XN-NF-82-06 (P)(A) Revision 1 & Supplements 2,4 and 5, *Qualification of Exxon Nuclear Fuel for Extended Burnup*, Siemens Power Company, October 1986.
12. ANF-88-133(P)(A) and Supplement 1, *Qualification of Advanced Nuclear Fuels PWR Design Methodology for Rod Burnups of 62 GWd/MTU*, Advanced Nuclear Fuels Corporation, December 1991.
13. Conover, W. J., 1971. *Practical Nonparametric Statistics*, John Wiley & Sons, New Your, pp 99-105.

Appendix A Methodology for Varying [

]

Uncertainty Components

[

]

[

]

[

]

[

[

]

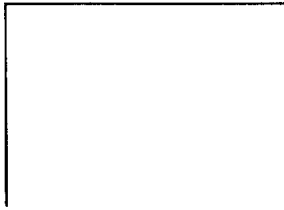


Figure A.1 Axial Power Profile Change [

]

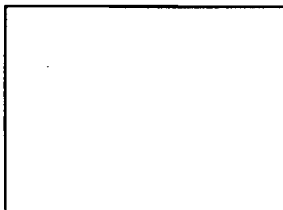


Figure A.2 Axial Power Profile Change [

]